2016

Synthesis and Characterization of Polyhalogenated Boron Dipyrromethenes and Carboranylbisthiophene Oligomers

Ning Zhao
Louisiana State University and Agricultural and Mechanical College, nzhao2@lsu.edu

SYNTHESIS AND CHARACTERIZATION OF POLYHALOGENATED BORON DIPYRROMETHENES AND CARBORANYLBISTHIOPHENE OLIGOMERS

A Dissertation

Submitted to the Graduate Faculty of the
Louisiana State University and
Agricultural and Mechanical College
in partial fulfillment of the
requirements for the degree of
Doctor of Philosophy

in

The Department of Chemistry

by
Ning Zhao
B.S., Lanzhou University, 2010
December 2016

This Dissertation is dedicated to my parents in China for 28 years of care and love, and also for their support and understanding for every important decision that I made.

谨以此文献给我远在中国的父母，感谢他们 28 年的照顾和关爱，以及对我所做的每一个重要决定的支持和理解。

ACKNOWLEDGMENTS

First of all, I would like to thank my advisor, Dr. M. Graça. H. Vicente. She is a great advisor, an amazing person and I would like thank her for affording me the opportunity to work in this wonderful lab. With regard to the research conducted within the group, she possesses a very broad knowledgeable base. The door of her office is always open and she is always happy and willing to talk about the projects and offer advice. She provided me freedom, continuous support and encouragement throughout my Ph.D. studies. I want to thank her for the time she spent on my projects, papers and Dissertation, as well as my job search. As an advisor, she not only cares about the research we conduct, but also about her group members as individuals, not just students. She gave me the tremendous support and help to my life. Without her help, my last five years may be totally different.

My special thanks to Dr. Kevin M. Smith for being my advisor and for the guidance in the last five years. He is very knowledgeable and is always ready to give his suggestions to us. His passion and enthusiasm for chemistry always inspire me to put more efforts on my research. In the meantime, he is truly a "gentleman" with the great personality. I really enjoy working with him.

Many thanks are to my committee members, Dr. David Spivak and Dr. Michal Brylinski for reviewing my dissertation and providing valuable feedback. I also want to give my thanks to Dr. Frank R. Fronczek for his efforts of the X-ray analysis of my 85 crystal structures and Dr. Thomas Weldegheorghis for his help with the NMR facilities in the department. I also thank Ms. Connie David and her undergraduate student for mass spectroscopy determinations of my samples. Thanks also to Ms. Zehua Zhou for the cellular studies of my compounds. I also want to thank Dr. Bruno Fabre (Universite de Rennes, France) for the electrochemical characterization and Dr. Petia Bobadova-Parvanova (Rockhurst University, USA) for the DFT calculations of my compounds.

I have spent so much wonderful time in Vicente and Smith lab with my previous and current lab-mates: Dr. Martha Sibrian-Vasquez, Dr. Timsy Uppal, Dr. Krystal R. Fontenot, Dr. Alecia M. McCall, Dr. Haijun Wang, Dr. Moses I. Ihachi, Dr. R. G. Waruna Jinadasa, Dr. Benson G. Ongarora, Dr. N. V. S. Dinesh Bhupathiraju, Dr. Javoris V. Hollingsworth, Dr. Hui Chen, Dr. Jamie H. Gibbs, Dr. Alex L. Nguyen, Elizabeth Okoth, Daniel J. LaMaster, Qianli Meng, Tyrslai Williams, Maodie Wang, Brandon Byrd, and Guanyu Zhang. Really thank them for the help and suggestions both for my research and life.

My parents Mr. Junke Zhao and Ms. Xihua Hong have been there for me no matter what happens. Thanks for their unconditional love, care, support, encouragement and understanding, and also for providing me the strength and courage to facing all challenges throughout the life.

My last, but not the least, appreciation goes to my wife and my son, Sunting Xuan and Kevin Zhao. Thanks to my wife for her company in the last ten years, which is my best time in my life, and too many precious moments deserve to be remembered forever. Without her, I would not step so far, and my life would not be so colorful and wonderful. Thanks to my son, and I thank him for being in my life. His arrival changed my life, and provided a more clear life goal for me.

TABLE OF CONTENTS

LIST OF ABBREVIATIONS

^{1}H	Proton NMR
^{13}C	Carbon NMR
^{11}B	Boron NMR
δ	Chemical shift
ε	Extinction coefficient
λ_{abs}	Maximum wavelength in the absorption spectra
λ_{em}	Maximum wavelength in the emission spectra
Φ_f	Fluorescent Quantum Yield
BODIPY	Boron Dipyrromethene or 4,4-Difluoro-4-bora-3a,4a-diaza-*s*-indacene
Bn	Benzyl
$CDCl_3$	Deuterated Chloroform
CD_2Cl_2	Deuterated Dichloromethane
d	Doublet
DBU	1,8-Diazabycyclo[5.4.0]-undec-7-ene
DCM	Dichloromethane
DDQ	2, 3-dichloro-5, 6-dicyano-p-benzoquinone
DIEA	N,N-Diisopropylethylamine
DMF	N,N-dimethylformamide
HRMS(ESI-TOF)	High Resolution Mass Spectra (Electrospray Ionization-Time of Flight)
Et	Ethyl
EtOAc	Ethyl acetate
FRET	Förster Resonance Energy Transfer

h	Hours
HOMO	Highest Occupied Molecular Orbital
Hz	Hertz
ICT	Internal Charge Transfer
J	Coupling constant
LUMO	Lowest Occupied Molecular Orbital
M	Molarity
MALDI	Matrix-assisted Laser Desorption/Ionization
Me	Methyl
mg	Milligram
MHz	Mega Hertz
min	Minutes
mL	Milliliter
MO	Molecular Orbitals
MS	Mass Spectrometry
MW	Molecular Weight
m/z	Mass to charge ratio
nm	Nanometer
NIR	Near-infrared
NBS	*N*-Bromosuccinimide
NCS	*N*-Chlorosuccinimide
NMR	Nuclear Magnetic Resonance
Pd/C	Palladium on Carbon

PDT	Photodynamic Therapy
PEG	Polyethylene glycol
PET	Photoinduced Electron Transfer
PET	Positron Emission Tomography
P^{Me}	Methyl propionate
Ph	Phenyl
ppm	Parts per Million
RT	Room Temperature
s	Singlet
t	Triplet
TBCA	Tribromoisocyanuric acid
TCCA	Trichloroisocyanuric acid
TEA	Triethylamine
TFA	Trifluoroacetic Acid
THF	Tetrahydrofuran
TLC	Thin Layer Chromatography
TMS	Trimethylsilane
p-TsOH	*p*-Toluenesulfonic acid
UV	Ultra violet
UV-Vis	Utraviolet-visible spectroscopy

ABSTRACT

Chapter 1 of this dissertation shows a brief overview of fundamental concepts and classic synthetic routes of BODIPY dyes. The synthetic strategies and various application (e.g. PDT sensitizers and fluorescent indicators) of halogenated BODIPYs are also presented in this chapter.

Chapters 2-4 describe the synthesis of three new polyhalogenated BODIPY platforms and their regioselective functionalization. Such new platforms provide new methodologies for producing both symmetric and asymmetric BODIPYs. Pd(0)-catalyzed cross-couplings and aromatic substitution reactions were applied to investigate the reactivity and regioselectivity of different halogen groups on the BODIPY platforms. The studies showed that the reactivity order of the halogens under both these reaction conditions is: 8-Cl $\approx$ 1,7-Br > 3,5-Cl > 2,6-Cl > 4,4-F. This breakthrough in BODIPY chemistry allowed the global stepwise functionalization (up to nona-functionalization) using various organometallic reagents and (or) N-, O-, and S-centered nucleophiles. During the investigation, more than fifty new BODIPYs were prepared via Pd(0)-catalyzed cross-coupling and nucleophilic substitution reactions, which are usually very difficult or impossible to prepare using traditional methods. In summary, the synthetic method developed and the new polyhalogenated BODIPY platforms provide a facile way to introduce special groups for various applications.

Chapter 5 reports the synthesis of a series of 2,2'-(*o*-carboranyl)bisthiophene oligomers with bromo, trimethylsilylethyne, vinyl, N-methylpyrrole or thienyl group by bromination, Sonogashira and Stille cross-coupling reactions. Among those compounds, the di(thienyl-N-methylpyrrole)-*o*-carborane and di(bisthienyl)-*o*-carborane can be successfully electropolymerized on a suitable anode to produce the corresponding conducting polymers. DFT calculations are also performed, which is consistent with the electrochemical data.

CHAPTER 1: INTRODUCTION

1.1 Properties of BODIPY

Over the last several decades, due to their convenience, low cost, high selectivity, and high sensitivity, the probes and sensors that are prepared from fluorescent dyes (e.g. Figure 1) attracted more and more attention in the fields of bio-imaging and environmental-imaging.[1-4] For example, various kinds of fluorescein and rhodamine dyes with rigid structures and high quantum yields have been designed and synthesized for biological applications. However, relatively short λ_{abs} and λ_{ex} and the counter ions of these dyes have hindered the further applications.[5-7] Because in the "biological window" (the 650-1000 nm region), there is minimal interference from the autofluorescence of tissue and cells, and absorption of water, NIR dyes that absorb and emit in the near-infrared (NIR) are always preferred. In addition, the deep penetration of NIR dyes provides the advantages in the clinical applications.[8-12] Therefore, cyanine dyes[13] are often used as alternates because they emit and absorb in the NIR region. However, several challenges in the chemistry of cyanine dyes are still remaining, mainly including poor photostability and low quantum yields resulting from their flexible structures.[13-15]

4,4-Difloro-4-bora-3a,4a-diaza-s-indacenes (BODIPYs) have attracted a lot of attention in both the research and academic fields, since it was first reported in 1968.[16] Due to its remarkable properties (i.e. being a small molecule with a strong fluorescence and high quantum yields, high

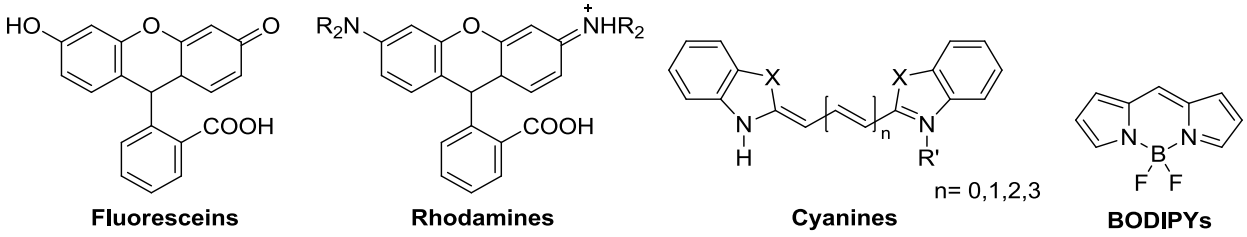

Figure 1-1: The structures of several fluorophores

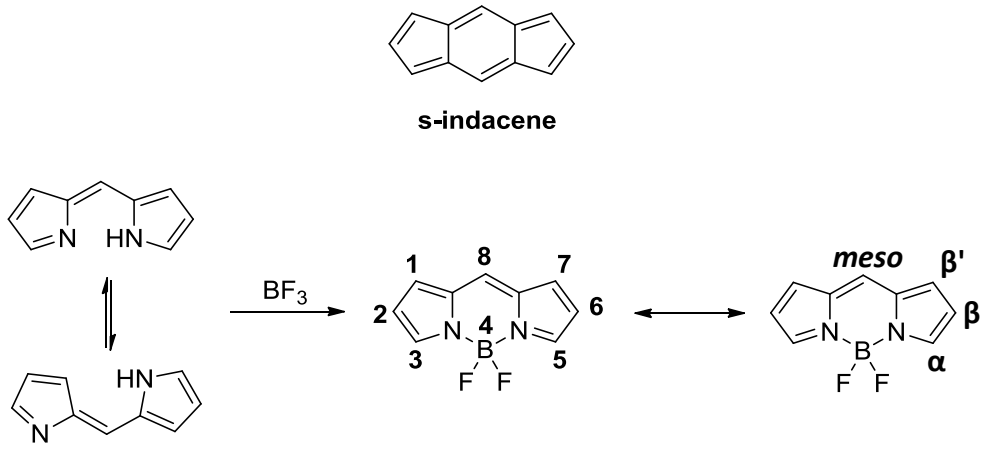

Figure 1-2: Structures of s-indacene and BODIPYs

chemical and physical stabilities, and high tunability[17-19]), BODIPY dyes are now widely used in drug delivery,[20-22] protein[21, 23-24] and DNA[21, 25-26] labeling, light harvesting arrays,[27-28] and fluorescent switches.[29-30]

4,4-Difloro-4-bora-3a,4a-diaza-s-indacenes are also named as boron dypyrromethanes (BODIPYs), due to their structural relationship to as s-indacene, as shown in Figure 1.2. BODIPYs with rigid tricyclic systems are usually prepared from dipyrromethene by complexation with boron trifluoride diethyl etherate. During the complexation, the *cis*/*trans* confirmation of dipyrromethenes is locked as the *cis* confirmation. In addition, the complexation of "BF_2" endow BODIPYs with aromaticity, although it does not fit Huckel's (4n+2) rule.[19] In the nomenclature systems, the 4-position is also referred as the boron position; the 1,7-positions, 2,6-positions, and 3,5-positions at the pyrrolic part of BODIPYs are also named as β', β and α- positions; the 8-position of BODIPY is named as the meso-position, as the labeling systems of porphyrin nomenclature.[17]

Previous results[31] of DFT calculation showed that the HOMO to LUMO transition mainly determines the S_0 to S_1 transition, which is associated with the absorption maxima (λ_{abs}). Thus, it is necessary to understand the distribution of the HOMO and LUMO at the BODIPY cores for the

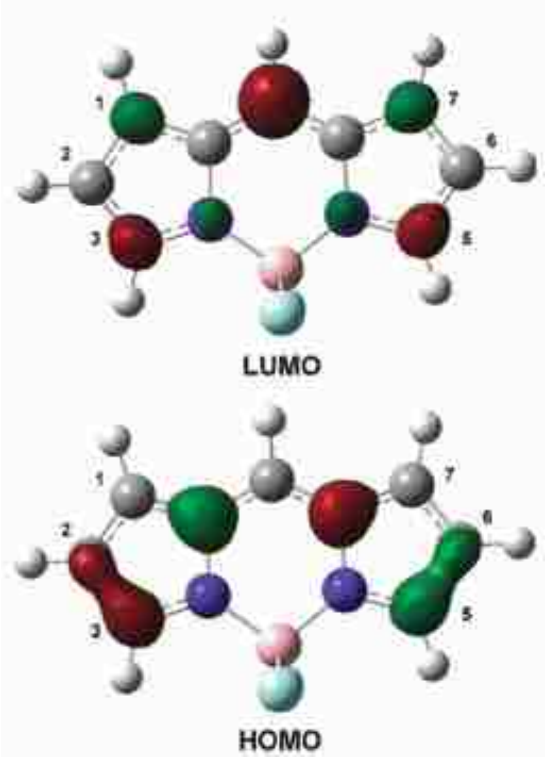

Figure 1-3: Nadal patterns of the LUMO and HOMO of an unsubsituted BODIPY.(Reproduced from Ref. Lu, H.; Mack, J.; Yang, Y.; Shen, Z., Structural modification strategies for the rational design of red/NIR region BODIPYs. *Chem. Soc. Rev.* **2014,** *43* (13), 4778-4823.with permission from the Royal Society of Chemistry, see Appendix E)

modification of λ_{abs}. Figure 1-3 shows the Nadal patterns of the LUMO and HOMO of an unsubsituted BODIPY.[19] In the LUMO, MO coefficients mainly are loacted at the 8, 1,7 and 3,5-positions; the largest MO coefficients is at the 8-position. In the HOMO, MO coefficients are only distributed at the 3,5 and 2,6- positions, while there is larger MO coefficient at the 3,5-positions than that at 2,6- positions. In addition, at the 3,5- positions, there are MO coefficient in both LUMO and HOMO, while there is larger MO coefficient in the HOMO than that in the LUMO.[19] Thus, appropriate functionalizations at the 3, 5, 8-positions could significantly affect the HOMO and LUMO, which then brings a big change in the spectroscopic properties of the BODIPYs.

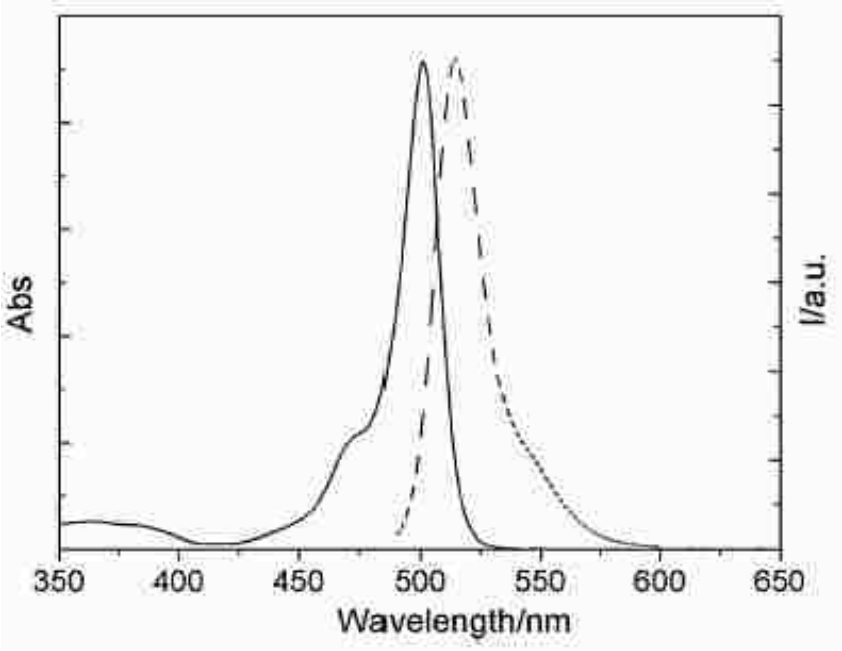

Figure 1-4: Absorption and fluorescence spectra of 1,3,5,7-tetramethyl-8-phenyl BODIPY. (Reproduced from Ref. Lu, H.; Mack, J.; Yang, Y.; Shen, Z., Structural modification strategies for the rational design of red/NIR region BODIPYs. *Chem. Soc. Rev.* **2014,** *43* (13), 4778-4823.with permission from the Royal Society of Chemistry, see Appendix E)

BODIPYs usually absorb strongly and narrowly in the visible region. The classic absorption and fluorescence spectra of 1,3,5,7-tetramethyl-8-phenyl BODIPY are shown in Figure 1-4. The most intense peak around λ= 500 nm is assigned to the S_0 to S_1 transition, and the shoulder around λ= 480 nm is assigned to the 0-1 vibrational transition.[19] In addition, a weaker absorption around λ= 350 nm is usually assigned to the S_0 to S_n ($n \geq 2$) transition.[19] On the other hand, the narrow fluorescence spectra is usually a mirror image of absorption spectra, as shown with dash curve in Figure 1-4.[19] It is widely accepted that the flexible structures of cyanine dyes result in nonradioactive decay, which usually greatly decrease the quantum yields.[32] However, due to complexation of "BF_2", the rigid π-system provides the BODIPYs relatively high quantum yields. Furthermore, the low efficiency of intersystem crossing (ISC) to the triplet state is another widely accepted reason for the high quantum yields.

1.2 Synthesis of BODIPYs

1.2.1 Traditional synthesis of BODIPYs

There are four types of widely-used synthetic methods to approach most of the BODIPY dyes, as shown in Scheme 1-1. The most common approach to BODIPY scaffolds is synthesis via a condensation reaction between a large excess α-free pyrroles and aldehydes,[33-34] in the presence of Lewis acids, to give dipyrromethane (not isolated), followed by oxidation using 2,3-dichloro-5,6-dicyano-1,4-benzoquinone (DDQ), and subsequent treatment with base (usually triethylamine) and boron trifluoride diethyl etherate ($BF_3{\cdot}OEt_2$). An alternative method using α-free pyrroles involves with acid chlorides[35] or anhydrides,[36-37] followed by deprotonation with triethylamine (TEA) and complexation with $BF_3{\cdot}OEt_2$. Besides these routes, a more efficient method to

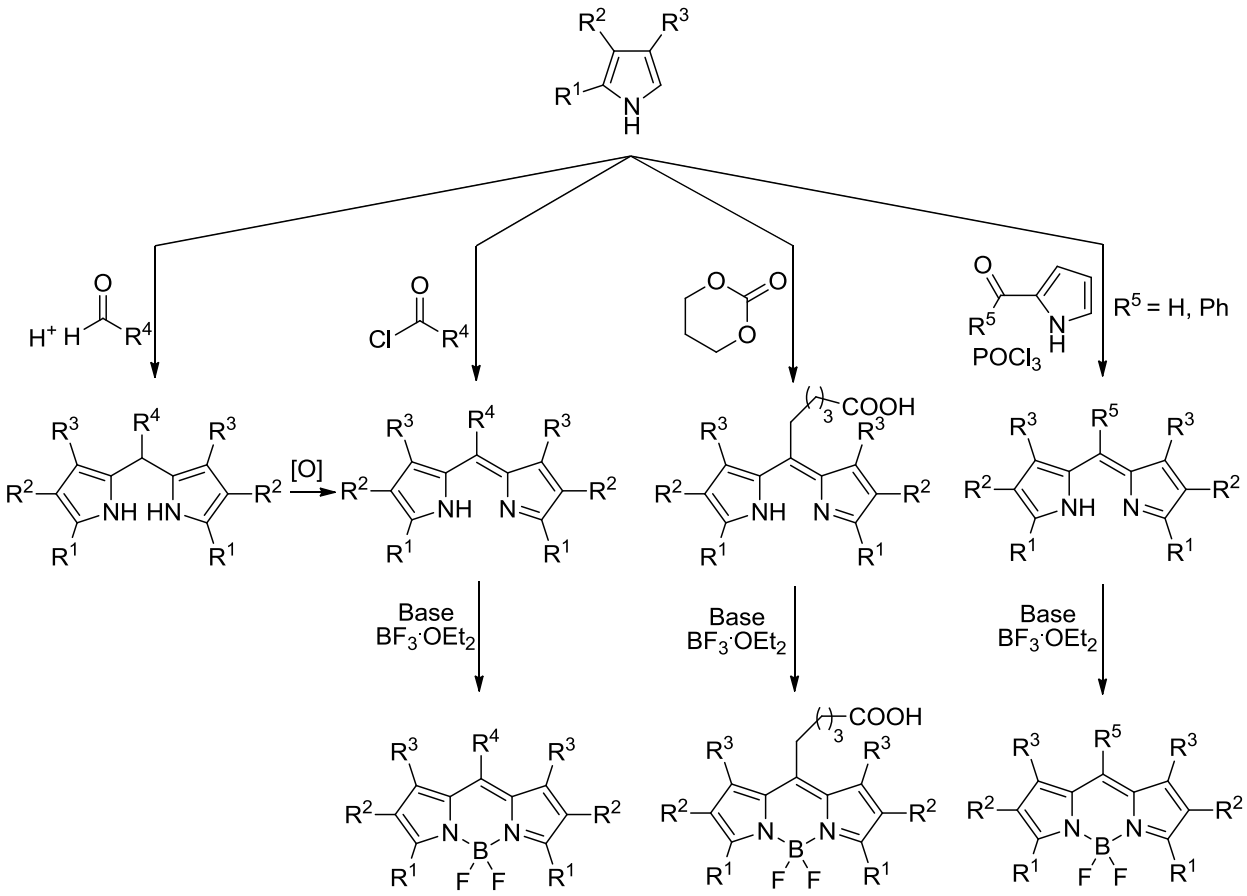

Scheme 1-1: Traditional Approaches to BODIPYs.

synthesize both asymmetrical and symmetrical BODIYs is to employ a condensation between 2-formyl[38] or 2-ketopyrrole[39] and with another (same or different) α-free pyrrole fragment in the presence of phosphorus oxychloride ($POCl_3$) followed by treatment with Et_3N and $BF_3{\cdot}OEt_2$.

1.2.2 Synthesis of BODIPYs from dipyrroketones

Over the last several years, a new synthetic route utilizing dipyrro(thio)ketone to synthesize BODIPYs was developed and investigated. Also, it can provide a functionalizable meso-group, as

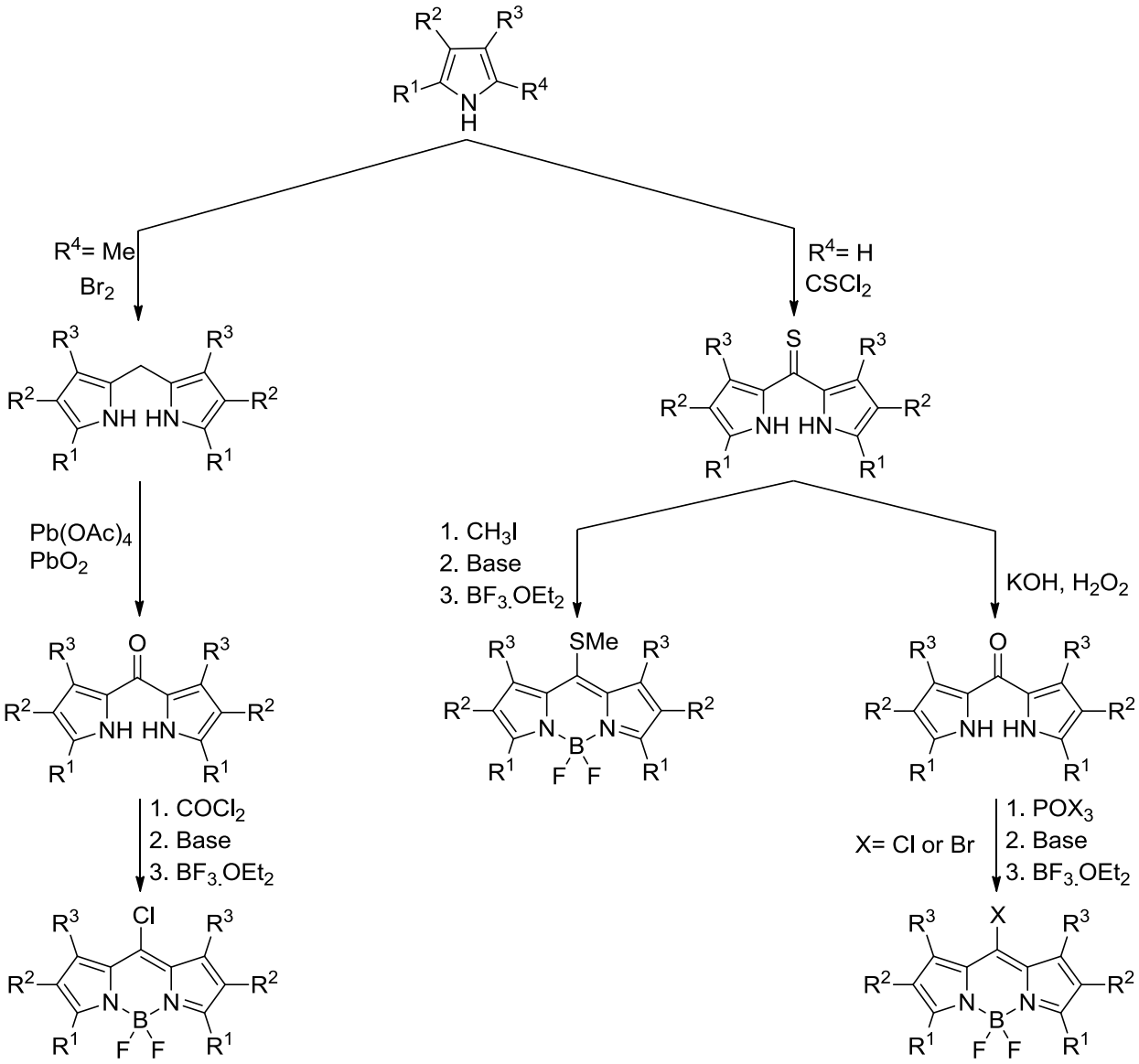

Scheme 1-2: Synthesis of BODIPYs from dipyrro(thio)ketones.

shown in Scheme 1-2.[40-43] The BODIPY synthesis started from the condensation of α-free pyrrole and thiophosgene ($CSCl_2$), which can provide a dipyrrothioketone. Further treatment with iodomethane (CH_3I), organic base, and $BF_3{\cdot}OEt_2$ can afford a meso-thioester BODIPY.[40] The dipyrrothioketone could be converted to a dipyrroketone by employing the oxidation reaction with KOH/H_2O_2 in ethanol using a steam bath. Oxidative halogenation by POX_3 (X = Cl, Br) or phosgene ($COCl_2$), followed by deprotonation and complexation by $BF_3{\cdot}OEt_2$ yielded 8-halo BODIPYs.[41, 43] Besides, Smith and coworkers[42] reported another alternative way to synthesize dipyrroketone from dipyyromethane via the $Pb(OAc)_4/PbO_2$ oxidation. Such dipyrromethanes could be prepared by the condensation of readily available 2-methylpyrrole in the presence of bromine, and followed by heating in the methanol.[42]

1.3 Synthesis of Halogenated BODIPYs

Since the first halo BODIPY[44] was reported in 1990, halogenated BODIPYs, both as synthetic precursors and terminal compounds, continue to attract a lot of attention. As is widely known, most of BODIPYs are non-phototoxic, but some special types of halogenated BODIPYs (usually iodinated or brominated BODIPYs) were suitable for photodynamic therapy. It was resulted from the enhancement of intersystem crossing that is induced by the heavy atom effect.[45-48] On the other hand, due to good reactivity (especially for Pd(0) catalyzed coupling and substitution reactions) of halogenatedgen groups, a large number of functionalized BODIPYs can be achieved from the halogenated BODIPY platforms.[49] Furthermore, previous work[41, 43, 50-51] has been shown that halogen groups can be introduced to all the positions. This allows the sequential functionalizations occurring at all the pyrrolic and meso positions.

1.3.1 Halogenation at 2,6 (α)-positions

2,6-Dihalogenated BODIPYs are the most easily obtained BODIPYs, because the 2,6-

positions are the least positive compared with other positions[17]. There are two different strategies to synthesize 2,6-halogenated BODIPYs. One is exploiting direct electrophilic substitution reactions at the 2,6-positions. 2,(6)-(Di)brominated BODIPYs could be prepared via an electrophilic substitution reaction with bromine,[44, 51] or N-bromosuccinimide (NBS)[52-53] in suitable solvents (DCM or DMF), as shown in Scheme 1-3. $CuBr_2$ also could be an efficient alternate reagent for the bromination at the 2,6-positions of BODIPY, which was reported by Hao and coworkers[54]. In this reaction, the author proposed that the mechanism could be roughly divided by two steps; (1) *in situ*-formation of bromine from $CuBr_{2;}$ (2) electrophilic substitution by bromine that generated from the first step. In 2012, Ortiz[55] reported a chlorination method to access to 2,(6)-(di)chloro BODIPYs from 2,6-free BODIPY using N-chlorosuccinimide (NCS) in THF at the room temperature. Futhermore, 2,(6)-(di)iodo BODPYs can be prepared by the reaction between BODIPYs and ICl,[52] $HNO_3/I_{2,}$[45] and N-iodosuccinimide (NIS)[56] in good yields.

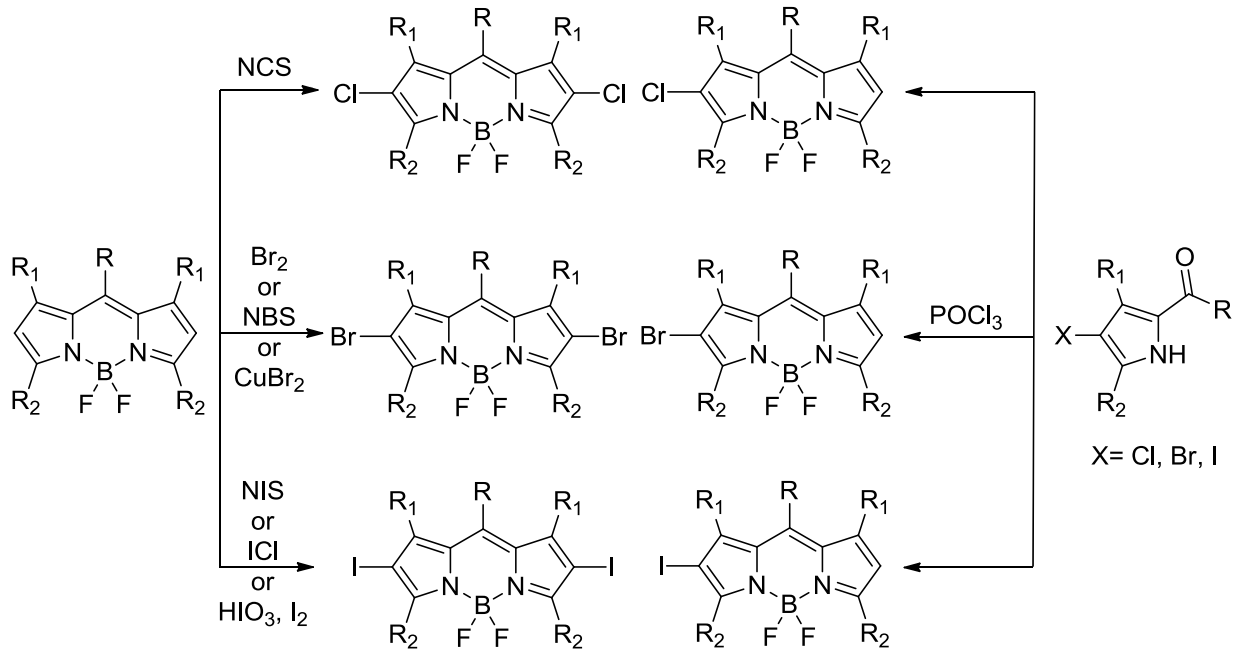

Scheme 1-3: Synthesis of 2,(6)-halogenaed BODIPYs

On the other hand, 2-halogenated BODIPYs could be prepared from halogenated pyrroles. 4-Halo (chloro-, bromo-, and iodo-) 2-acylpyrroles[55, 57-59] could be prepared via a halogenation reaction between 2-acylpyrroles and NXS (X= Cl, Br, I). Such pyrroles could react with another α-free pyrrole fragment and $POCl_3$, followed by a basic complexation with BF_3OEt_2 to produce 2-halogenated BODIPYs.

1.3.2 Halogenation at 3,5-position

In 2005, Boens and coworkers reported the synthesis of 3,5-dichloro BODIPY[60]. In this work, a 1, 9-dichlorodipyrromethane was obtained regioselectively by treating dipyrromethane with 2 equivalent of NCS at -78 °C. Following oxidation by DDQ, deprotonation by triethylamine, and complexation by BF_3OEt_2 yielded the first 3,5-dichloro BODIPY, as shown in Scheme 1-4. By employing the same methods but with NBS (1 or 2 equiv), 3,(5)-(di)bromo BODIPY could be obtained in good yields.[61-62] To conclude, halogenation at the dipyrromethane stage is the preferred synthetic route to avoid the halogenation at the 2,6-positions, instead of direct halogenation at the BODIPY. The reason is that at the dipyrromethane, the 1,9-positions are more reactive compared with 2,8-positions for the aromatic electrophilic substitution reactions, which is opposite from that at the BODIPYs.

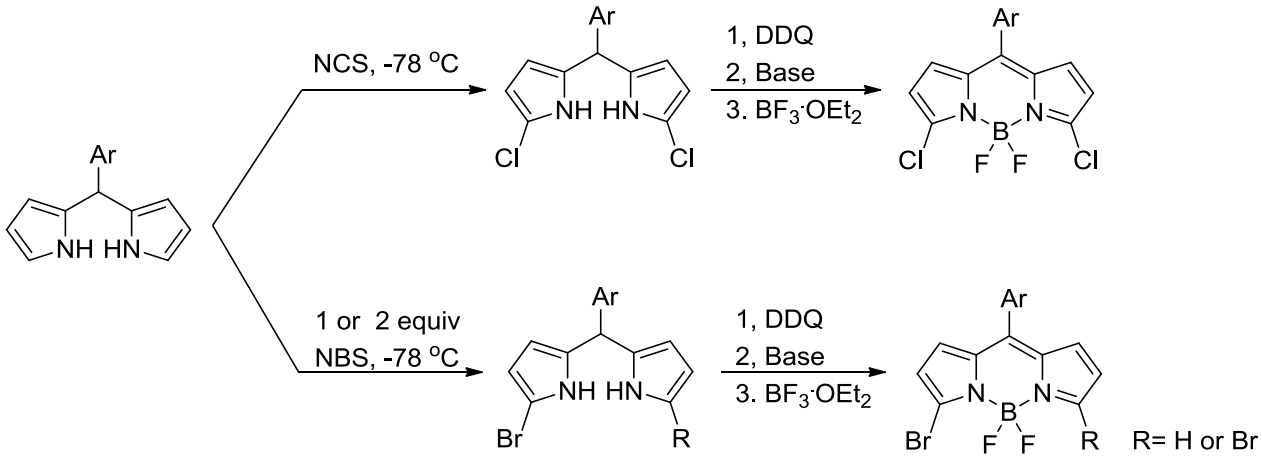

Scheme 1-4: Synthesis of 3,(5)-(di)halogenated BODIPYs

Vicente and coworkers reported an alternate synthetic route to approach the symmetric and asymmetric 3,5-diiodo-BODIPYs[63-65] via the same strategy, as shown in Scheme 1-5. The 1,9-diester dipyyromethane could be prepared by two different synthetic routes; (1) acid-catalyzed condensation of α-free pyrroles with aldehydes, as shown in Section 1.2.1; (2) bromine-induced condensation of α-methylpyrroles, and followed by heating in the methanol, as shown in Section 1.2.2. 1, 9-diiododipyyromethanes were obtained via de-esterification with Pd/I_2 or potassium hydroxide (KOH) followed by HCl (aq), iodination with I_2, and oxidation with DDQ. Subsequent basic complexation with BF_3OEt_2 gave 3,5-diiodo BODIPYs in good overall yields.

Another approach to 3,(5)-(di)halogenated BODIPYs is by utilizing 5-halo 2-acylpyrroles,[58-59, 66] as shown in Scheme 1-6. One of the reported methods is applied to halogenation of α-free pyrroles by NXS (X= Cl, Br, I), followed by trifluoroacetylation and Vilsmeier–Haack reaction, which smoothly provided the desired halogenated pyrroles in fair-good yields. The alternate method to access to this type of halogenated pyrroles involves a Vilsmeier-

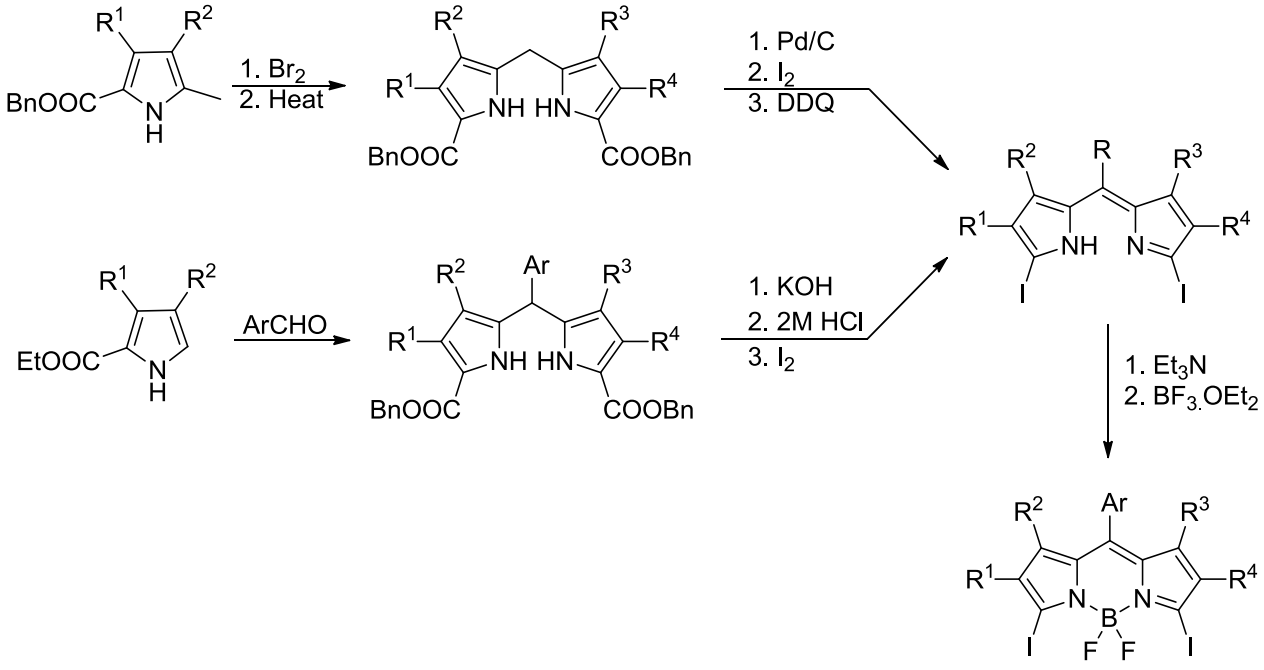

Scheme 1-5: Synthesis of 3,5-diiodo BODIPYs

Haack reaction of isoindolin-1-one followed by basic hydrolysis in ethanol.[66] 3-Halogenated BODIPYs could be obtained from the condensation between 5-halopyrrole and another α-free pyrrole fragment by using the same method as mentioned in the synthesis of 2-halogenated BODIPYs.

Furthermore, Hao and coworkers[54] unprecedentedly developed a new method of regioselective halogenation at 3,5-positions by using $CuCl_2$ as the chlorination reagent, as shown in Scheme 1-7. As is known, a large amount of previous work has already shown the reactivity order of the aromatic electrophilic substitution of BODIPYs: 2,6-positions > 3,5-positions > 1,7-positions[51, 67]. In order to explain this unusual regioselectivity in this reaction, the authors proposed a two-step mechanism: (1) formation the radical-cation (at the 3, 5-positions) BODIPY intermediate in a single electron transfer process; (2) nucleophilic addition reaction of a chloride anion (Cl^-).

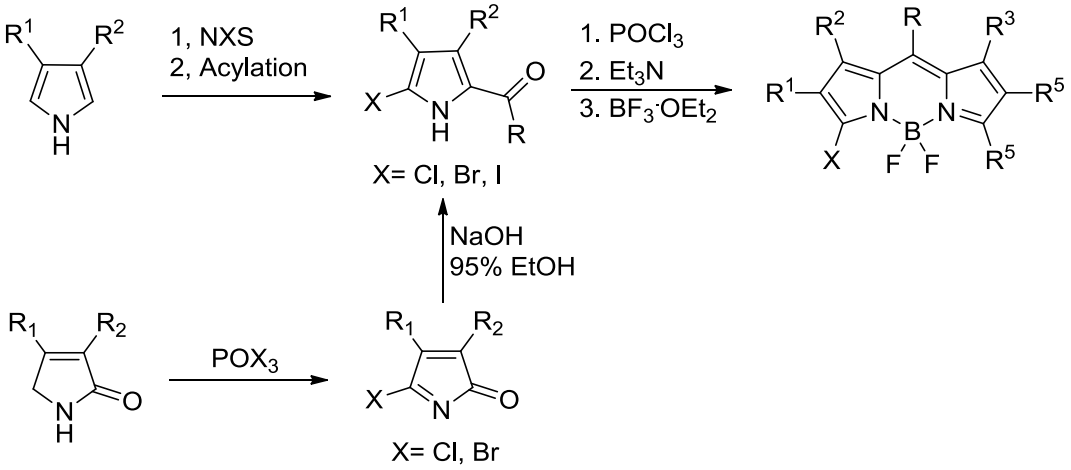

Scheme 1-6: 3,5-halogenated BODIPYs from pyrroles

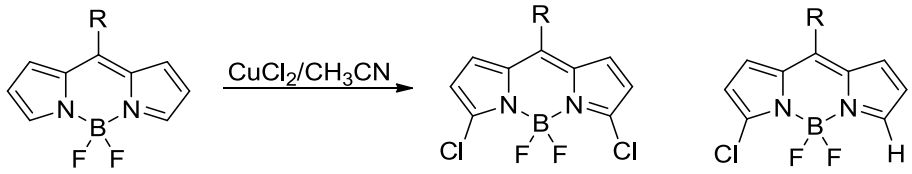

Scheme 1-7: Synthesis of 3, (5)-dichloro BODIPYs

1.3.3 Halogenation at 1,7-positions

The BODIPY 1,7-positions bear the most positive charge, which causes difficulty introduction the halo groups via electrophilic aromatic substitution reactions. The first 1,7-dihalogenated BODIPY was reported by Dehaen and coworkers in 2011[68]. In their work, two different strategies were used for the preparation of 1,7-dihalogenated BODIPYs, as shown in Scheme 1-8. The principle of the first strategy is to block the other positions with methyl groups. Thus, the synthesis was started with the condensation of 2,3-dimethylpyrrole in the presence of acetyl chloride (AcCl), followed by complexation under the basic conditions to provide the 1,7-free BODIPY. Excess bromine in DCM was then used for the bromination of 1,7-free BODIPY yielding the 1,7-dibromo BODIPY in good yield. In the second strategy, the key intermediate--2-formyl-3-halopyrrole was synthesized by the formylation of 2,3-dimethylpyrrole via a Vilsmeier-

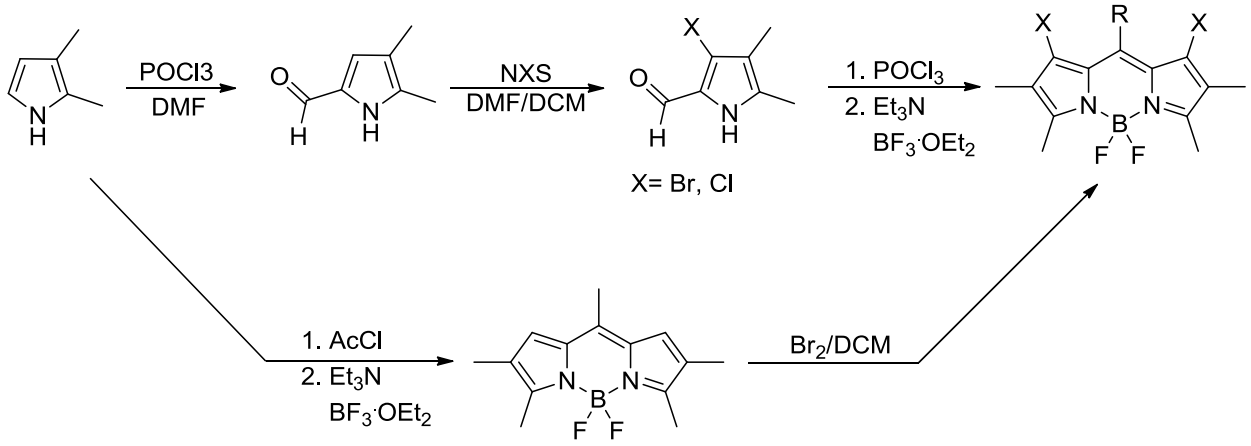

Scheme 1-8: Synthesis of 1,7-dihalogenated BODIPYs

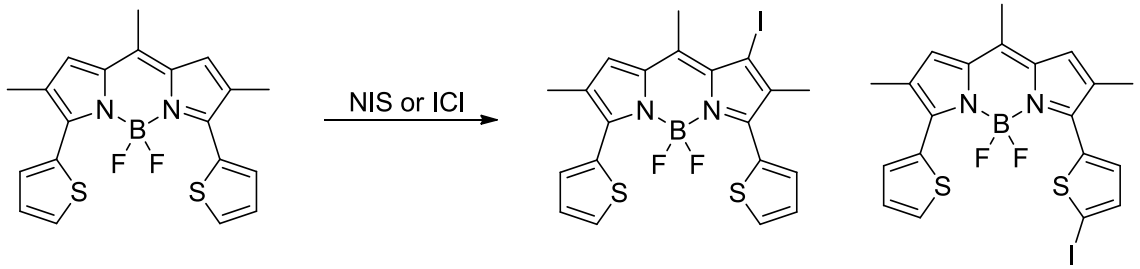

Scheme 1-9: Synthesis of 1-iodo BODIPY

Haack reaction, and followed by bromination at the 3-position using NXS (X= Br or Cl); The generated 2-formyl 3-halo pyrroles were condensed in the presence of $POCl_3$/DCM, followed by complexation in the trimethylamine to provide 1,7-dibromo (chloro) BODIPYs in good yields.

Ziessle and coworkers reported the synthesis of 1-iodo BODIPY as a byproduct in 2012,[69] as shown in Scheme 1-9. In their work, the original plan was to introduce the iodo group at the α-positions of 2,6-thienyl groups. However, this electrophilic substitution reaction lacks regioselectivitity, and produced undesired 1-iodo BODIPY in 32% yield, as well as the desired product in 20% yield.

1.3.4 Halogenation at 8-position

As discussed in Section 1.1, the 8-position is a very important position, with the largest LUMO MO coefficient, the functionalization at this position will greatly affect the spectroscopy properties of BODIPYs. However, there is a lackof methods for functionalization at the 8-position. The most common way (almost the only way) to modify the 8-position is to use modified aldehydes or 2-ketopyrroles for the synthesis of BODIPYs, as discussed in Section 1.2.1. Also, a large amount of work may be needed for the synthesis of modified aldehydes or 2-ketopyrroles. Thus, a functionable group at 8-position was necessary for various applications. Halo groups were excellent candidates and were finally introduced at the 8-position via the dipyyroketone synthetic route,[41, 43] as shown in Section 1.2.2. The dipyrroketone can be prepared in two major steps, as shown in Scheme 1-10: (1) formation of dipyrrothioketone via the condensation of α-free pyrrole in the presence of thiophosgene ($CSCl_2$); (2) basic oxidative hydrolysis by using H_2O_2/KOH in the ethanol. Treatment of dipyrroketones with POX_3 (X= Cl or Br) or phosgene ($COCl_2$) provides the corresponding 5-chloro-dipyrrin salts, followed by complexation under basic conditions, and 8-chloro (bromo) BODIPYs were obtained in high yields. Furthermore, 8-iodo BODIPY could be

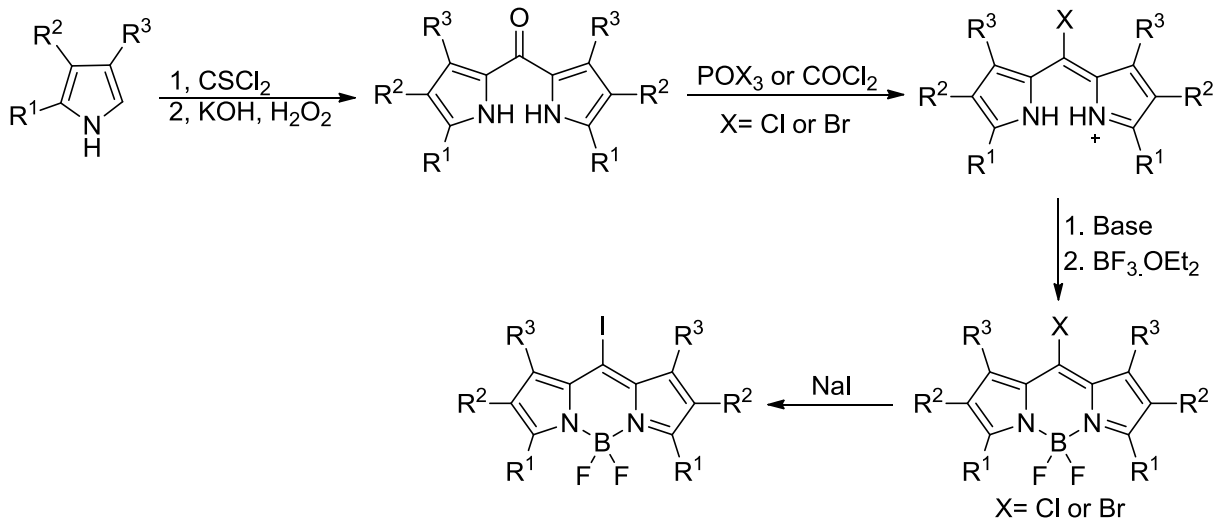

Scheme 1-10: Synthesis of 8-halogen BODIPY

synthesized from the addition/elmination reaction between 8-chloro BODIPY and NaI in refluxing acetone in good yield.

1.3.5 Halogenation at two different positions of BODIPY

1.3.5.1 Halogenation at 2,6(β) and 3,5(α) –positions

Based on the previous results, the 2,6-positons at BODIPYs are the most reactive for the electrophilic aromatic substitution, followed by the 3,5-positions and the 1,7-positions. Thus, halogenation at the both α and β positions can be easily achieved by using an extra amount of halogenation reagents. Over the last several years, many papers have reported that direct chlorination by using NCS[55] or SO_2Cl_2[70], bromination by using bromine,[51] and iodination by using I_2/HIO_3 or ICl[67] at the 2,3,5,6-free BODIPYs can yield the desired 2,3,6-trihalo and 2,3,5,6-tetrahalo BODIPYs in good yields, as shown in Scheme 1-11. One exception among these examples is trihalogenation using a small excess of NCS in THF, which gave the 2,3,5-trichloro BODIPY as the major product with the confirmation of X-ray analysis.[67] Additionally, in the iodination reaction, by increasing the amount of ICl to 4.5 or 8 equiv, 3-chloro 2,5,6-triiodo BODIPY and 3,5-dichloro 2,6-diiodo would be formed and isolated in different yields. However,

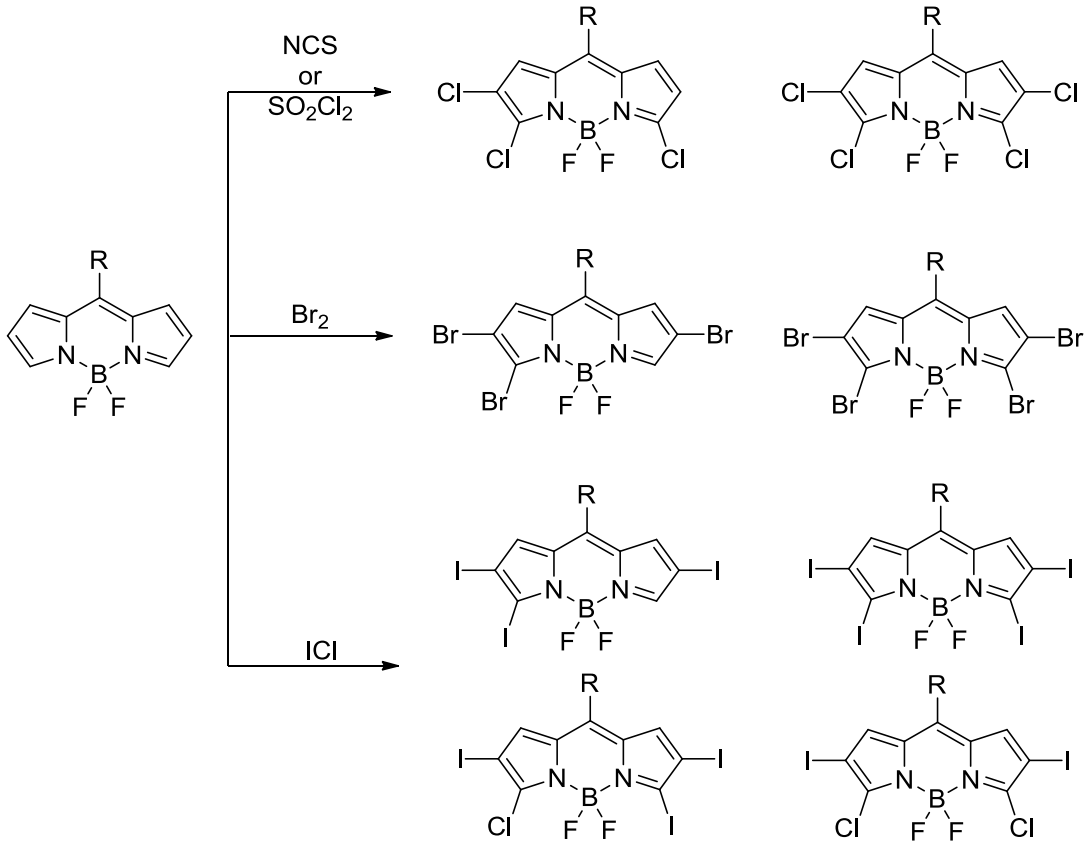

Scheme 1-11: Synthesis of α,β-halogenated BOIDPYs

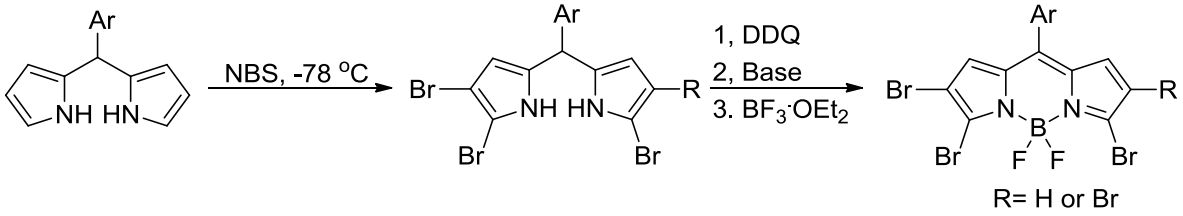

Scheme 1-12: Synthesis of α,β-tribromo and tetrabromo BODIPYs

there was no formation of chlorinated BODIPYs when I_2/HNO_3 was used the iodination reagents.

Ravikanth and coworkers[71] reported the synthesis of 2,3,5,6-tetrabromo-BODIPY by treating a dipyrromethane with 4 equiv of NBS at -78 °C, followed by oxidation withDDQ and basic complexation with BF_3OEt_2, as shown in Scheme 1-12. In this case, regioselectivity of 1,9-positions and 2,8-positions over the 3,7-postions was observed and confirmed.

Utilizing dihalogenated pyrroles to synthesize α,β–polyhalogenated BODIPYs is a

convenient method, as shown in the Scheme 1-13. Treatment of 2-ketopyrrole with 3 equiv of NCS yielded 3,5-dichloro pyrrole and 4,5-dichloropyrrole as a mixture, in moderate isolated yields.[55] Subsequent treatment of 4,5-dichloropyrrole with 3-ethyl-2,4-dimethylpyrrole in the presence of $POCl_3$, followed by complexation with BF_3OEt_2 in basic conditions yielded the asymmetric 2,3-dichloro BODIPY in good yields. Additionality, direct iodination on the asymmetric BODIPY by using 2.5 equiv ICl also provided the 2,3-diiodo-BODIPY with a fair yield, also with 1,2-diiodo BODIPY as a byproduct.[67]

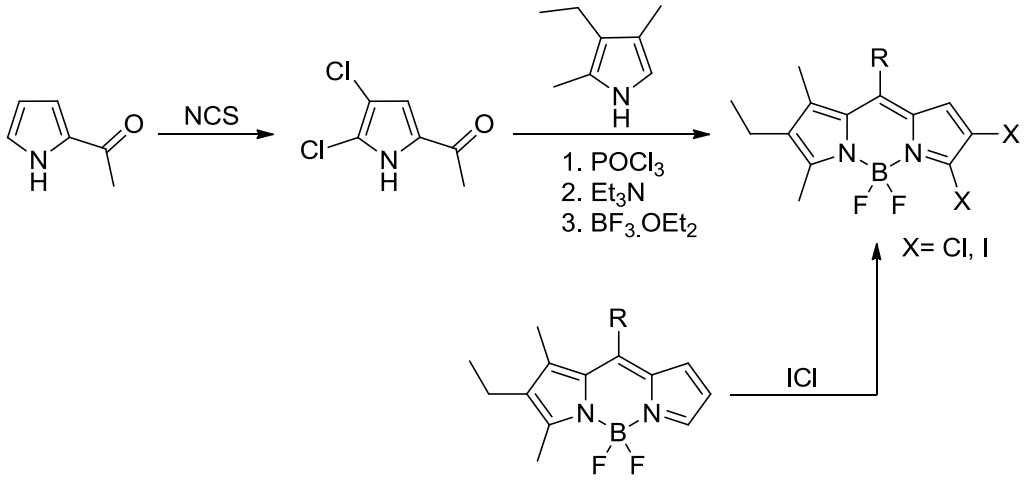

Scheme 1-13: Synthesis of 2,3-dihalogenated BODIPYs

1.3.5.2 Halogenation at 2,6 (β) and 1,7 (β')-positions

Since the 3,5-positions are more reactive than the 2,6-positions toward aromatic electrophilic substitution, β,β'-halogenated BODIPYs are difficultly obtained if 3,5-position is not blocked. Thus, the most reasonable strategy is to exploit the dihalogenated pyrroles, as shown in Scheme 1-14. From Section 1.3.4.1, 4,5-dichloro-2-ketopyrrole could be prepared by the chlorination of a 2-ketopyrrole. Subsequent treatment of such pyrroles with $POCl_3$, and followed by basic complexation with BF_3OEt_2 provides the 1,2-dichloro BODIPY in good yield.[55] On the other hand, 1,2-diiodo-BODIPY was formed as an undesired products from iodination reaction

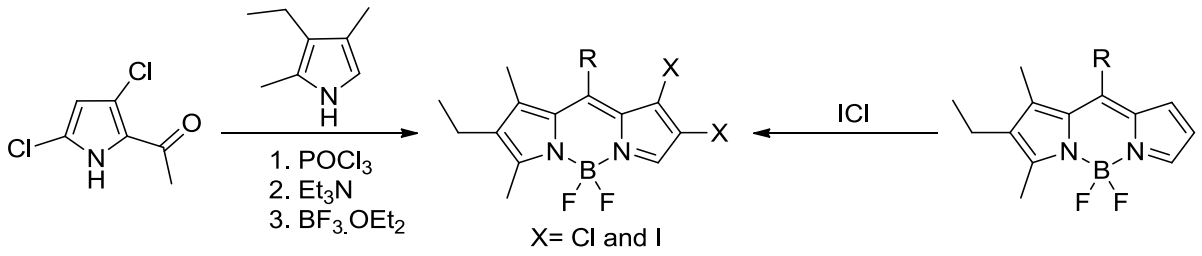

Scheme 1-14: Synthesis of 1,2-dihalo BODIPY

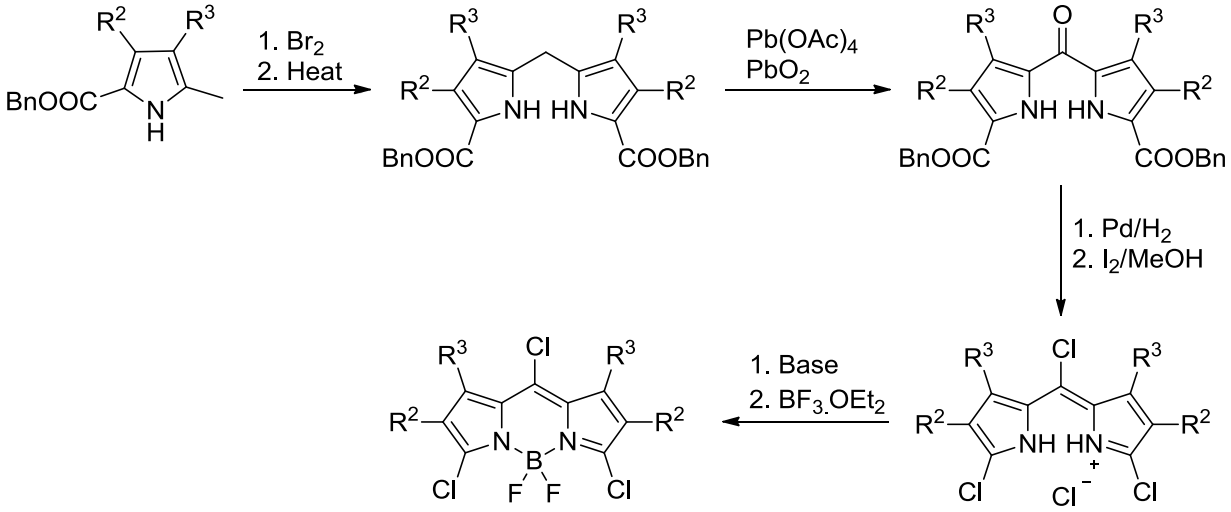

Scheme 1-15: Synthesis of 3,5,8-trichloro BODIPY.

with ICl in moderate yield.[67] As a good leaving group, 3-iodo group is not so stable, which may explain the formation of the 1,2-diiodo BODIPY.

1.3.5.3 Halogenation at 3,5,8-positions

In 2014, Vicente and coworkers reported the synthesis and functionalization of 3,5,8-trichloro BODIPY,[42] which was the first attempt to introduce 8-chloro and 3,5-chloro groups into the same BODIPYs. The key intermediate of total synthesis is a dibenyl 5-dipyrroketone-2,9-dicarboxylate, which was prepared from an oxidation reaction of dipyrromethane by using $Pb(OAc)_4/PbO_2$ in acetic acid. The dipyrromethane precursor was synthesized from the condensation of α-methylpyrrole in the presence of bromine, and followed by heating inmethanol. Debenzylation by Pd/H_2 and iodination with I_2/MeOH yielded the diiododipyrroketone. Such a

compound was subject to excess phosgene in chloroform to give the trichloro dipyrromethene hydrochloride salt. After immediate complexation with $BF_3{\cdot}Et_2O$ in the presence of N,N-diisopropylethylamine, 3,5,8-trichloro BODIPY was obtained in a good overall yield.

1.3.6 Halogenation at three different positions

In these cases, regioselectivity was not an issue to be considered. Thus, 1,2,3,5,6,7-hexachloro (bromo) BODIPY, as well as 1,2,3,5,6-pentabromo BODIPY can be easily obtained in good yields via halogenation of dipyrromethane using excess NCS or NBS,[50, 67, 71] as shown in Scheme 1-16. Additionally, direct electrophilic bromination with (40 equiv or 300 equiv) bromine at pyrrolic-position-free BODPY can directly provide pentabromo- and hexabromo- BODIPYs in good yields.[51]

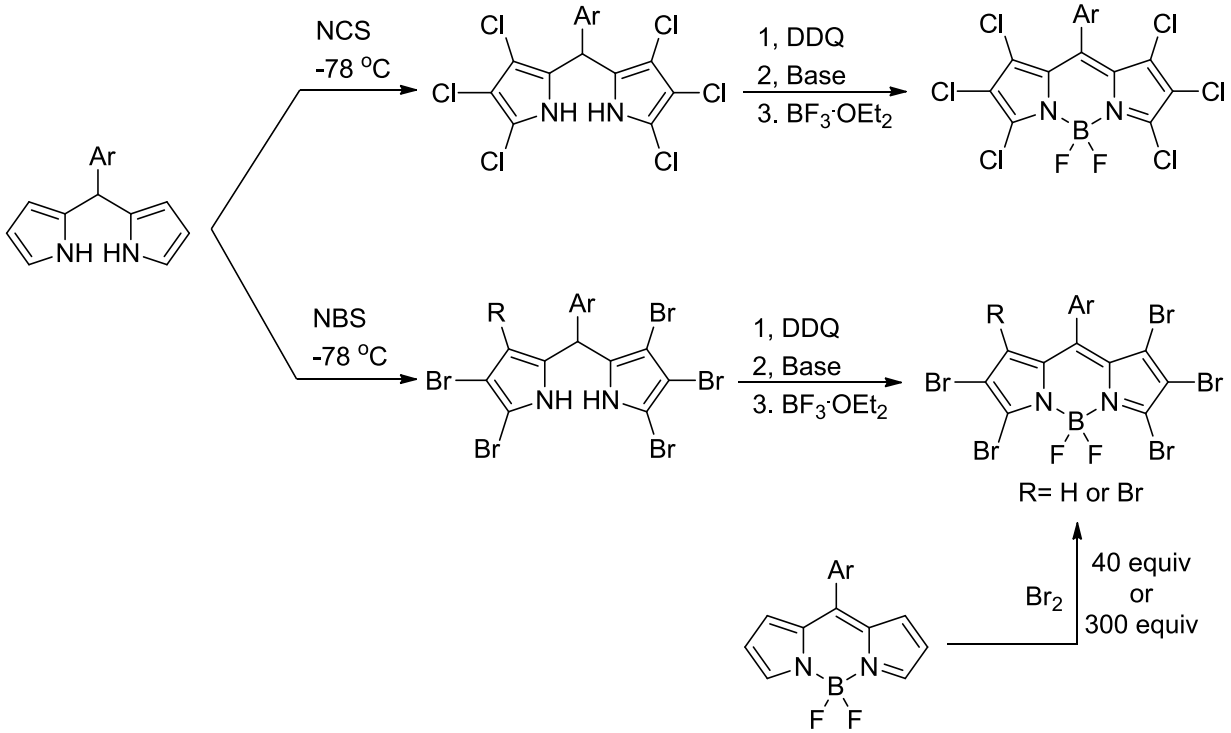

Scheme 1-16: Synthesis of α,β,β'-polyhalogenated BODIPYs.

As shown in Scheme 1-17, asymmetric 1,2,3-triiodo BODIPY could be obtained as the major product when I_2/HNO_3 was used as the iodination reagent.[67] However, the iodination reaction using ICl yielded 1,2,3-triiodo BODIPY, as well as 1,2-diiodo 3-chloro BODIPY as abyproduct in fair isolated yields. The 3-chloro group may be formed from substitution reaction by chloride anion on the 1,2,3-triiodo BODIPY.

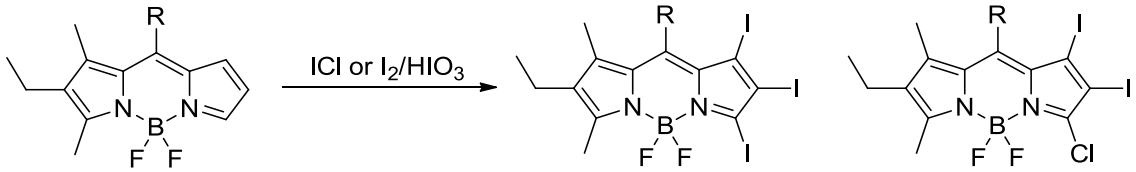

Scheme 1-17: Synthesis of α,β,β'-polyhalo BODIPYs

1.4 Applications of Halogenated BODIPYs

A wide range of reactions, including metal-mediated cross-coupling and substitution reactions, are found to work well with the halogen groups at the BODIPY. The versatility of Suzuki,[41, 56, 68, 72-74] Stille,[41-43, 68, 72] Sonagashira,[41, 56, 64, 68, 72-73] Heck,[41, 68, 72, 75] and Negishi[76] cross-coupling reactions are well investigated on the 1,2,3,5,6,7,8-halo groups at the BODIPYs. Furthermore, C-, O-, N-, S- centered nucleophiles could be introduced into the 3,5-positions of the 3,5-dichloro-BODIPY under basic conditions.[41, 51, 77-78] However, only S-centered nucleophiles works for 1,7-substitution reactions.[51, 68] No publication has shown the successful aromatic substitution reactions at 2,6-dihalo BODIPYs.

1.4.1 Extended Conjugations

Traditional BODIPYs usually absorb and emit in the region of 470-530 nm. Near-infrared (NIR) BODIPYs (e.g. as shown in Figure 1-5) were needed for the various applications. In the last decade, several strategies have been developed to the synthesis for NIR dyes.[19] Among them, aryl fused BODIPYs with rigid structures are particular interesting, due to their high quantum yields and strong π-π interactions. Usually, these types of aryl-fused BODIPYs were prepared by multi-

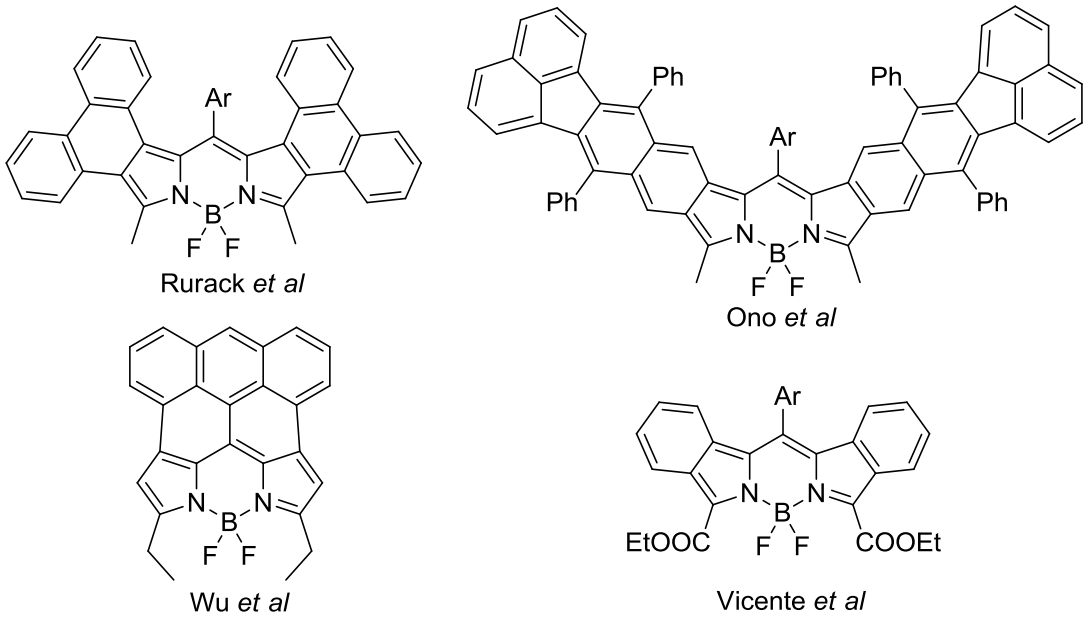

Figure 1-5: Structures of aryl-fused BODIPYs

step synthesis from aryl-fused pyrroles.[79-88] On the other hand, bicyclo[2.2.2]octadiene-fused pyrroles[89-93] or cyclohexane-fused pyrroles[65, 94] are important precursors for the aryl-fused BODIPYs, which usually involved in a retro-Diels-Alder reaction or oxidation reaction using 2,3-dichloro-5,6-dicyano-1,4-benzoquinone (DDQ). Additionally, $FeCl_3$-mediated oxidation at the pre-made BODIPYs[95-98] is also an alternate way to prepare aryl-fused BODIPYs.

It should be noted that halogented BODIPYs[99-103] provided a facile method to synthesized aryl-fused BODIPYs. Dehaen,[99] Hao[102] and their coworkers applied the same strategy to approach the aryl-fused BODIPYs. "N" or "O"-centered nucleophiles were easily introduced at the 2,6-positions of dichloro- or tetrabromo- BODIPYs. Palladium-catalyzed intramolecular coupling (between the bromo-β-position of BODIPY and free-α-position of a phenoxyl group, or the free-β-position of a BODIPY and bromo-α-position of phenoxyl group) was accomplished in good yields, as shown in Scheme 1-18. Another strategy that approach aryl-fused BODIPY is to firstly introduce a suitable aryl groups at the 2,6-positions by using Suzuki-Miyaura coupling reactions

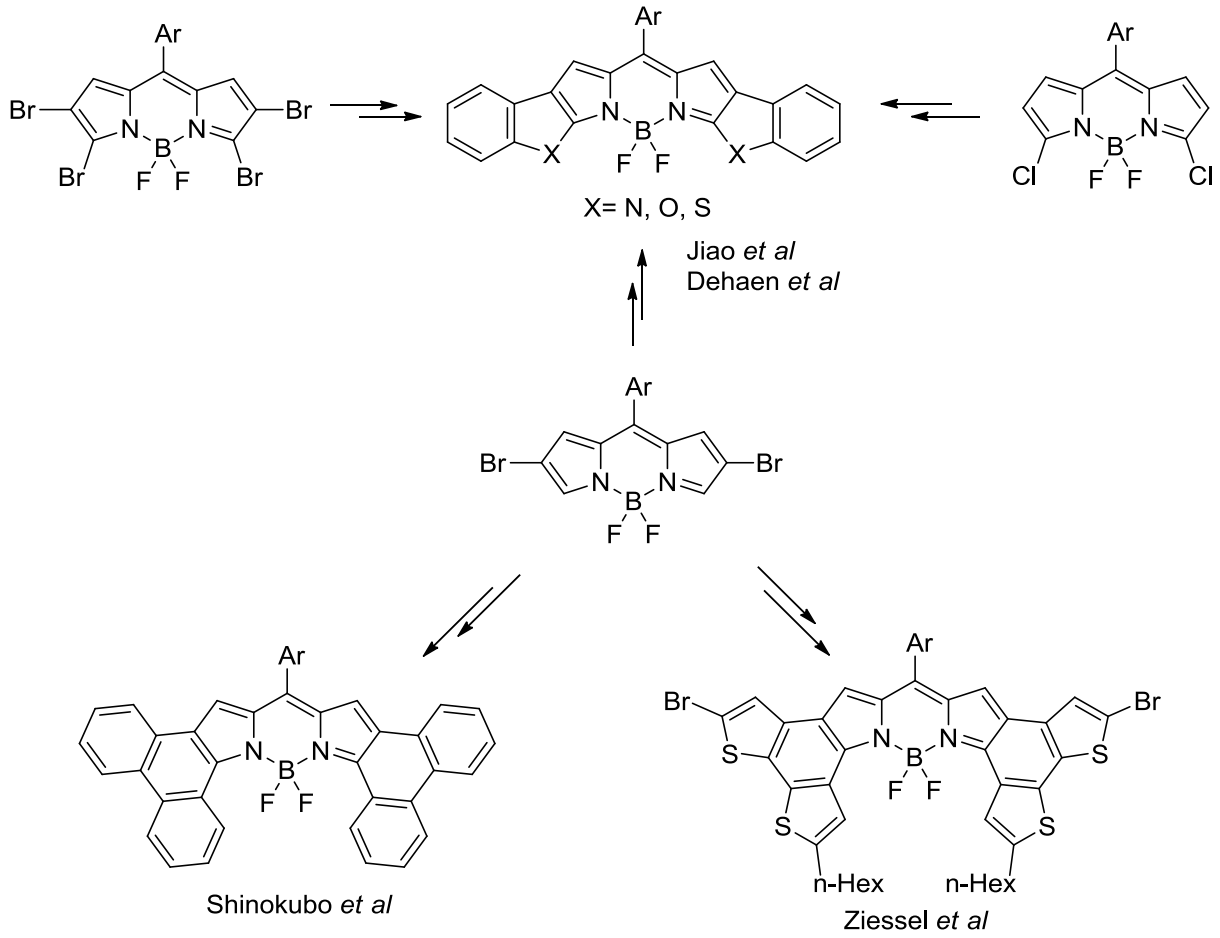

Scheme 1-16: Synthesis of aryl-fused BODIPYs

on 2,6-dibromo BODIPYs. Subsequent $FeCl_3$-mediated or bis(trifluoroacetoxy)iodobenzene oxidation reaction[100-101] or H_2SO_4-induced cyclization[103] will provide the desired aryl-fused BODIPYs in good to excellent yields. π-System extension of aryl-fused BODIPY leads to a significant red-shift both at maximum absorption (up to 673 nm) and emission (692 up to 692 nm) in dichloromethane.

1.4.2 Fluorescent Indicators

Since the first 2,6-dicholo-BODIPY was reported by Dehean and coworkers, halogenated BODIPYs have been widely applied as fluorescent indicators.[104-105] Due to their high tenability, halogenated BODIPY have allowed various functionalizations to approach a wide range of

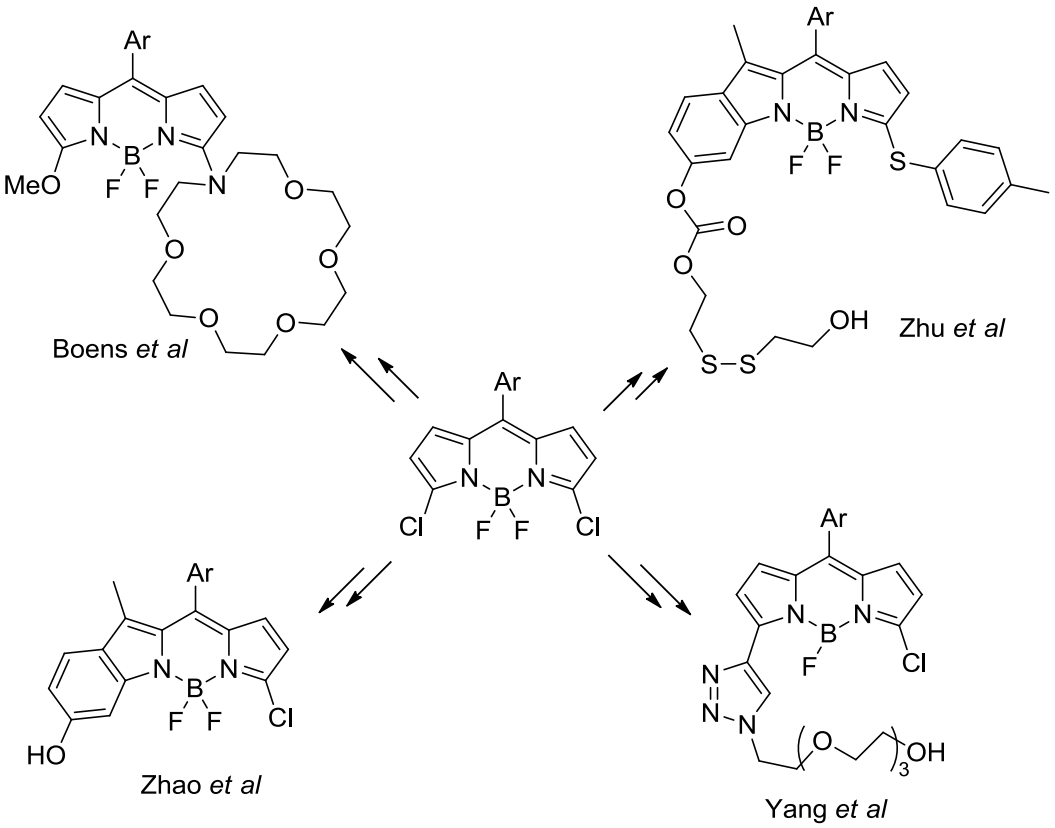

Scheme 1-17: Synthesis of fluorescent indicators from 3,5-dichloro BODIPY.

florescent probes, as shown in Scheme 1-17. Ratiometric fluorescent indicators for Pd^{2+},[106] Ca^{2+},[106] Cu^{2+},[63, 107] Cu^{+},[108] K^{+},[109] Zn^{2+},[110] and some other metal ions[111] could be prepared by substitution reaction between dihalo-BODIPYs with azacrown ether or other nucleophilies in high yields. In 2012, Yang and coworkers reported the ratiometric fluorescent indicators for glutathione detection, which was also synthesized via S_NAr substitution reactions from the dichloro-BODIPY.[112] The working mechanism of this sensors was utilizing the different reactivity of "S" and "N" centered nucleophilies for the S_NAr substitution reactions, as well as the different spectroscopy properties between 5-"S" or "N" substituted BODIPYs. By employing the same strategy and BODIPY platforms, probes for the discrimination of cysteine from homocysteine and glutathione[113-116] and for the discrimination of glutathione from homocysteine and cysteine[117-119] have been prepared in

high yields. Also, several probes[120-123] for the simultaneous detection of glutathione, cysteine and homocysteine have been reported by several research groups in 2014 and 2015. Furthermore, 2,6-dichloro-BODIPYs could also be applied for the probes for detecting γ-glutamyltranspeptidase in the ovarian cancers,[124] as well as nano-materials for imaging[125] with a wide range from blue to near infrared and detection of H_2S[126] from endogenous generation based on Förster resonance energy transfer (FRET) mechanism. Finally, Jeyaraman and coworkers reported several probes for the detection of anions (e.g. N_3^-),[127] NH_3 vapor,[128] and aliphatic amines[129] based on 2,6-dibromo-BODIPYs.

1.4.3 Photodynamic Therapy (PDT)

As a promising class of PDT reagents, BODIPY derivatives possess several characteristics found in a perfect photosensitizer, including strong resistance toward the photobleaching, high extinction coefficients, and low dark-toxicity.[46, 48] As mentioned above, there is very low efficiency of intersystem crossing from singlet states to triplet states for most BODIPY dyes. With development of BODIPY chemistry, 2,6-diiodo-BODIPY,[47] as well as brominated BODIPYs,[130] were firstly reported as efficient photosensitizers in 2005 and 2006. The heavy atom effect that is induced by bromo or iodo atoms was a widely accepted explanation for the enhance quantum yield of singlet oxygen generation. In recent decades, several groups dedicated to the development of ideal BODIPY photosensitizers, which were mainly prepared modified based on 2,6-diiodo-BODIPY platforms, as shown in Scheme 1-18. Knoevenagel condensation could be employed to introduce styryl groups at the 3,5-positions of 2,6-diiodo (bromo) BODIPYs,[130-135] which not only significantly red-shifted the dye to the NIR, but also allowed introduction of the PEG groups to increase their water solubility. Meanwhile, such styryl BODIPYs maintained the same level of the singlet oxygen generation of as 2,6-diido-BODIPs. Borggraeve[136] and Burgess[137] have exploited

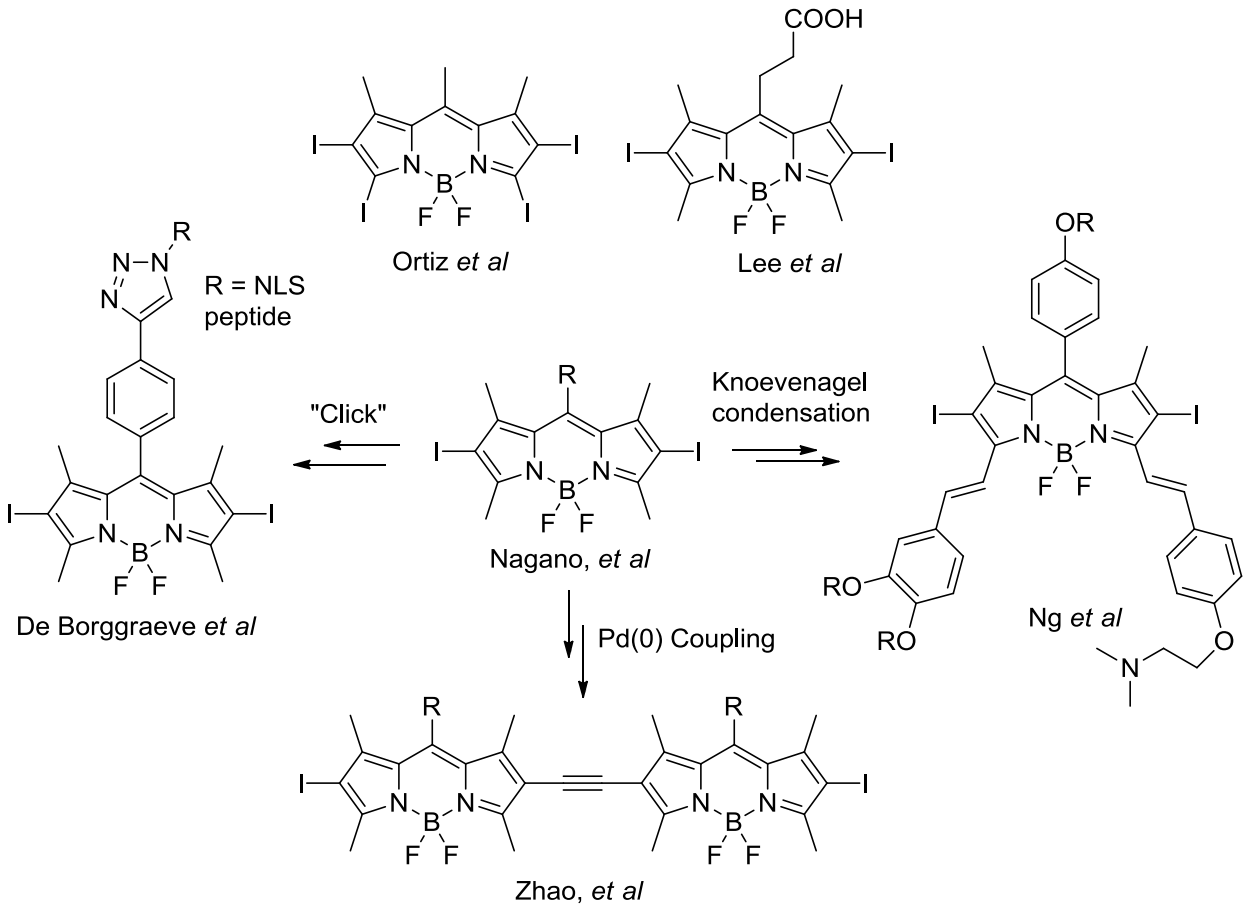

Scheme 1-18: Several types of 2,6-diiodo BODIPY analogues.

the "click" chemistry to introducepeptides at the 8-position of the BODIPY. Conjugated BODIPYs possessto localize lysosomes or target TrkC, respectively. Furthermore, from the diiodo-BODIPY, Zhao and coworkers[56, 73, 88] synthesized a serious of iodo-BOIDYs and BODIPY dimers by using Pd(0) cross-coupling reactions, some of which possessed the long life triplet excited states with. As shown in Scheme 1-12, 2,3,5,6-tetraiodo- and 2,3,6-triiodo-BODIPYs could be synthesized by Ortiz and coworkers.[67] Interestingly, by increasing the numbers of iodo groups at the 3,5-positions, no significant enhancement of singlet oxygen generation was observed. On the other hand, by employing different aldehydes for the BODIPY synthesis, a large number of 2,6-diiodo-BODIPYs could be prepared with different 8-substitutents.[45, 138] For example, a 3-alkylcarboxylic acid

BODIPY was found to localize at the mitochondria of HSC-2 cells, as well as a slightly increasing singlet oxygen generation.[138]

1.5 Research Outlook

Despite a large amount of published BODIPY chemistry research, most of BODIPY-based sensors and probes are prepared based on simple BODIPY platforms, such as dichloro BODIPY. There are several disadvantages of such BODIPY platforms: (1) those BODIPY dyes emit and absorb usually at $\lambda \leq 600$ nm; (2) there are limited functional groups at the BODIPY for further functionalization to improve preperties, such as quantum yields or water solubility. Thus, in order to overcome these problems, novel BODIPY platforms that allows uccessive functionalization are designed, synthesized, characterized, and investigated, as shown in the following Chapters in this Dissertation.

1.6 References

1. Quang, D. T.; Kim, J. S., *Chem. Rev.* **2010,** *110* (10), 6280-6301.

2. Yang, Y.; Zhao, Q.; Feng, W.; Li, F., *Chem. Rev.* **2013,** *113* (1), 192-270.

3. Lee, M. H.; Kim, J. S.; Sessler, J. L., *Chem. Soc. Rev.* **2015,** *44* (13), 4185-4191.

4. de Silva, A. P.; Gunaratne, H. Q. N.; Gunnlaugsson, T.; Huxley, A. J. M.; McCoy, C. P.; Rademacher, J. T.; Rice, T. E., *Chem. Rev.* **1997,** *97* (5), 1515-1566.

5. Magde, D.; Rojas, G. E.; Seybold, P. G., *Photochem. Photobiol.* **1999,** *70* (5), 737-744.

6. Drexhage;, K. H., *J. Res. Natl. Bur. Stand., Sect. A* **1976,** *80* (3), 421-428.

7. Kolmakov, K.; Belov, V. N.; Bierwagen, J.; Ringemann, C.; Müller, V.; Eggeling, C.; Hell, S. W., *Chem. Eur. J.* **2010,** *16* (1), 158-166.

8. Frangioni, J. V., *Curr. Opin. Chem. Biol.* **2003,** *7* (5), 626-634.

9. Cheng, Z.; Wu, Y.; Xiong, Z.; Gambhir, S. S.; Chen, X., *Bioconj. Chem.* **2005,** *16* (6), 1433-1441.

10. Weissleder, R., *Nat Biotech* **2001,** *19* (4), 316-317.

11. Ntziachristos, V., *Nat Meth* **2010,** *7* (8), 603-614.

12. Milstein, A. B.; Stott, J. J.; Oh, S.; Boas, D. A.; Millane, R. P.; Bouman, C. A.; Webb, K. J., *J. Opt. Soc. Am. A* **2004,** *21* (6), 1035-1049.

13. Sun, W.; Guo, S.; Hu, C.; Fan, J.; Peng, X., *Chem. Rev.* **2016,** *116* (14), 7768-7817.

14. Buston, J. E. H.; Young, J. R.; Anderson, H. L., *Chem. Commun.* **2000,** (11), 905-906.

15. Soper, S. A.; Mattingly, Q. L., *J. Am. Chem. Soc.* **1994,** *116* (9), 3744-3752.

16. Treibs, A.; Kreuzer, F.-H., *Justus Liebigs Annalen der Chemie* **1968,** *718* (1), 208-223.

17. Loudet, A.; Burgess, K., *Chem. Rev.* **2007,** *107* (11), 4891-4932.

18. Ulrich, G.; Ziessel, R.; Harriman, A., *Angew. Chem. Int. Ed.* **2008,** *47* (7), 1184-1201.

19. Lu, H.; Mack, J.; Yang, Y.; Shen, Z., *Chem. Soc. Rev.* **2014,** *43* (13), 4778-4823.

20. Peters, C.; Billich, A.; Ghobrial, M.; Högenauer, K.; Ullrich, T.; Nussbaumer, P., *J. Org. Chem.* **2007,** *72* (5), 1842-1845.

21. Kobayashi, H.; Ogawa, M.; Alford, R.; Choyke, P. L.; Urano, Y., *Chem. Rev.* **2010,** *110* (5), 2620-2640.

22. Carten, J. D.; Bradford, M. K.; Farber, S. A., *Dev. Biol.* **2011,** *360* (2), 276-285.

23. Crivellato, E.; Candussio, L.; Rosati, A. M.; Bartoli-Klugmann, F.; Mallardi, F.; Decorti, G., *Journal of Histochemistry & Cytochemistry* **2002,** *50* (5), 731-734.

24. Lee, J.-J.; Lee, S.-C.; Zhai, D.; Ahn, Y.-H.; Yeo, H. Y.; Tan, Y. L.; Chang, Y.-T., *Chem. Commun.* **2011,** *47* (15), 4508-4510.

25. Kurata, S.; Kanagawa, T.; Yamada, K.; Torimura, M.; Yokomaku, T.; Kamagata, Y.; Kurane, R., *Nucleic Acids Res.* **2001,** *29* (6), e34.

26. Jang, H. G.; Park, M.; Wishnok, J. S.; Tannenbaum, S. R.; Wogan, G. N., *Anal. Biochem.* **2006,** *359* (2), 151-160.

27. Yilmaz, M. D.; Bozdemir, O. A.; Akkaya, E. U., *Org. Lett.* **2006,** *8* (13), 2871-2873.

28. Ziessel, R.; Ulrich, G.; Haefele, A.; Harriman, A., *J. Am. Chem. Soc.* **2013,** *135* (30), 11330-11344.

29. Coskun, A.; Deniz, E.; Akkaya, E. U., *Org. Lett.* **2005,** *7* (23), 5187-5189.

30. Golovkova, T. A.; Kozlov, D. V.; Neckers, D. C., *J. Org. Chem.* **2005,** *70* (14), 5545-5549.

31. Liu, H.; Lu, H.; Zhou, Z.; Shimizu, S.; Li, Z.; Kobayashi, N.; Shen, Z., *Chem. Commun.* **2015,** *51* (9), 1713-1716.

32. Karolin, J.; Johansson, L. B. A.; Strandberg, L.; Ny, T., *J. Am. Chem. Soc.* **1994,** *116* (17), 7801-7806.

33. Lee, C.-H.; S. Lindsey, J., *Tetrahedron* **1994,** *50* (39), 11427-11440.

34. Wagner, R. W.; Lindsey, J. S., *Pure Appl. Chem.* **1996,** *68* (7), 1373-1380.

35. Burghart, A.; Kim, H.; Welch, M. B.; Thoresen, L. H.; Reibenspies, J.; Burgess, K., *J. Org. Chem.* **1999,** *64* (21), 7813-7819.

36. Li, Z.; Mintzer, E.; Bittman, R., *J. Org. Chem.* **2006,** *71* (4), 1718-1721.

37. Wang, D.; Fan, J.; Gao, X.; Wang, B.; Sun, S.; Peng, X., *J. Org. Chem.* **2009,** *74* (20), 7675-7683.

38. Wu, L.; Burgess, K., *Chem. Commun.* **2008,** (40), 4933-4935.

39. Tahtaoui, C.; Thomas, C.; Rohmer, F.; Klotz, P.; Duportail, G.; Mély, Y.; Bonnet, D.; Hibert, M., *J. Org. Chem.* **2006,** *72* (1), 269-272.

40. Goud, T. V.; Tutar, A.; Biellmann, J.-F., *Tetrahedron* **2006,** *62* (21), 5084-5091.

41. Leen, V.; Yuan, P.; Wang, L.; Boens, N.; Dehaen, W., *Org. Lett.* **2012,** *14* (24), 6150-6153.

42. Wang, H.; Fronczek, F. R.; Vicente, M. G. H.; Smith, K. M., *J. Org. Chem.* **2014,** *79* (21), 10342-10352.

43. Wang, H.; Vicente, M. G. H.; Fronczek, F. R.; Smith, K. M., *Chem. Eur. J.* **2014,** *20* (17), 5064-5074.

44. Shah, M.; Thangaraj, K.; Soong, M.-L.; Wolford, L. T.; Boyer, J. H.; Politzer, I. R.; Pavlopoulos, T. G., *Heteroat. Chem.* **1990,** *1* (5), 389-399.

45. Gibbs, J. H.; Robins, L. T.; Zhou, Z.; Bobadova-Parvanova, P.; Cottam, M.; McCandless, G. T.; Fronczek, F. R.; Vicente, M. G. H., *Biorg. Med. Chem.* **2013,** *21* (18), 5770-5781.

46. Kamkaew, A.; Lim, S. H.; Lee, H. B.; Kiew, L. V.; Chung, L. Y.; Burgess, K., *Chem. Soc. Rev.* **2013,** *42* (1), 77-88.

47. Yogo, T.; Urano, Y.; Ishitsuka, Y.; Maniwa, F.; Nagano, T., *J. Am. Chem. Soc.* **2005,** *127* (35), 12162-12163.

48. Awuah, S. G.; You, Y., *RSC Adv.* **2012,** *2* (30), 11169-11183.

49. Lakshmi, V.; Rajeswara Rao, M.; Ravikanth, M., *Org. Biomol. Chem.* **2015,** *13* (9), 2501-2517.

50. Lakshmi, V.; Ravikanth, M., *J. Org. Chem.* **2011,** *76* (20), 8466-8471.

51. Jiao, L.; Pang, W.; Zhou, J.; Wei, Y.; Mu, X.; Bai, G.; Hao, E., *J. Org. Chem.* **2011,** *76* (24), 9988-9996.

52. Bonardi, L.; Ulrich, G.; Ziessel, R., *Org. Lett.* **2008,** *10* (11), 2183-2186.

53. Hayashi, Y.; Yamaguchi, S.; Cha, W. Y.; Kim, D.; Shinokubo, H., *Org. Lett.* **2011,** *13* (12), 2992-2995.

54. Zhou, X.; Yu, C.; Feng, Z.; Yu, Y.; Wang, J.; Hao, E.; Wei, Y.; Mu, X.; Jiao, L., *Org. Lett.* **2015,** *17* (18), 4632-4635.

55. Duran-Sampedro, G.; Agarrabeitia, A. R.; Garcia-Moreno, I.; Costela, A.; Bañuelos, J.; Arbeloa, T.; López Arbeloa, I.; Chiara, J. L.; Ortiz, M. J., *Eur. J. Org. Chem.* **2012,** *2012* (32), 6335-6350.

56. Wu, W.; Guo, H.; Wu, W.; Ji, S.; Zhao, J., *J. Org. Chem.* **2011,** *76* (17), 7056-7064.

57. Wan, C.-W.; Burghart, A.; Chen, J.; Bergström, F.; Johansson, L. B. Å.; Wolford, M. F.; Kim, T. G.; Topp, M. R.; Hochstrasser, R. M.; Burgess, K., *Chem. Eur. J.* **2003,** *9* (18), 4430-4441.

58. Leen, V.; Braeken, E.; Luckermans, K.; Jackers, C.; Van der Auweraer, M.; Boens, N.; Dehaen, W., *Chem. Commun.* **2009,** (30), 4515-4517.

59. Leen, V.; Leemans, T.; Boens, N.; Dehaen, W., *Eur. J. Org. Chem.* **2011,** *2011* (23), 4386-4396.

60. Baruah, M.; Qin, W.; Basarić, N.; De Borggraeve, W. M.; Boens, N., *J. Org. Chem.* **2005,** *70* (10), 4152-4157.

61. Rao, M. R.; Mobin, S. M.; Ravikanth, M., *Tetrahedron* **2010,** *66* (9), 1728-1734.

62. Khan, T. K.; Ravikanth, M., *Tetrahedron* **2011,** *67* (32), 5816-5824.

63. Jiao, L.; Li, J.; Zhang, S.; Wei, C.; Hao, E.; Vicente, M. G. H., *New J. Chem.* **2009,** *33* (9), 1888-1893.

64. Jiao, L.; Yu, C.; Uppal, T.; Liu, M.; Li, Y.; Zhou, Y.; Hao, E.; Hu, X.; Vicente, M. G. H., *Org. Biomol. Chem.* **2010,** *8* (11), 2517-2519.

65. Meng, Q.; Fronczek, F. R.; Vicente, M. G. H., *New J. Chem.* **2016,** *40* (7), 5740-5751.

66. Jiao, L.; Yu, C.; Liu, M.; Wu, Y.; Cong, K.; Meng, T.; Wang, Y.; Hao, E., *J. Org. Chem.* **2010,** *75* (17), 6035-6038.

67. Ortiz, M. J.; Agarrabeitia, A. R.; Duran-Sampedro, G.; Bañuelos Prieto, J.; Lopez, T. A.; Massad, W. A.; Montejano, H. A.; García, N. A.; Lopez Arbeloa, I., *Tetrahedron* **2012,** *68* (4), 1153-1162.

68. Leen, V.; Miscoria, D.; Yin, S.; Filarowski, A.; Molisho Ngongo, J.; Van der Auweraer, M.; Boens, N.; Dehaen, W., *J. Org. Chem.* **2011,** *76* (20), 8168-8176.

69. Poirel, A.; De Nicola, A.; Ziessel, R., *Org. Lett.* **2012,** *14* (22), 5696-5699.

70. Wang, L.; Zhang, Y.; Xiao, Y., *RSC Adv.* **2013,** *3* (7), 2203-2206.

71. Lakshmi, V.; Ravikanth, M., *Dalton Trans.* **2012,** *41* (19), 5903-5911.

72. Rohand, T.; Qin, W.; Boens, N.; Dehaen, W., *Eur. J. Org. Chem.* **2006,** *2006* (20), 4658-4663.

73. Chen, Y.; Zhao, J.; Xie, L.; Guo, H.; Li, Q., *RSC Adv.* **2012,** *2* (9), 3942-3953.

74. Lakshmi, V.; Ravikanth, M., *Eur. J. Org. Chem.* **2014,** *2014* (26), 5757-5766.

75. Gai, L.; Mack, J.; Lu, H.; Yamada, H.; Kuzuhara, D.; Lai, G.; Li, Z.; Shen, Z., *Chem. Eur. J.* **2014,** *20* (4), 1091-1102.

76. Palao, E.; Duran-Sampedro, G.; de la Moya, S.; Madrid, M.; García-López, C.; Agarrabeitia, A. R.; Verbelen, B.; Dehaen, W.; Boens, N.; Ortiz, M. J., *J. Org. Chem.* **2016,** *81* (9), 3700-3710.

77. Yu, C.; Wu, Q.; Wang, J.; Wei, Y.; Hao, E.; Jiao, L., *J. Org. Chem.* **2016,** *81* (9), 3761-3770.

78. Rohand, T.; Baruah, M.; Qin, W.; Boens, N.; Dehaen, W., *Chem. Commun.* **2006,** (3), 266-268.

79. Awuah, S. G.; Polreis, J.; Biradar, V.; You, Y., *Org. Lett.* **2011,** *13* (15), 3884-3887.

80. Chen, J.; Burghart, A.; Derecskei-Kovacs, A.; Burgess, K., *J. Org. Chem.* **2000,** *65* (10), 2900-2906.

81. Descalzo, A. B.; Xu, H.-J.; Xue, Z.-L.; Hoffmann, K.; Shen, Z.; Weller, M. G.; You, X.-Z.; Rurack, K., *Org. Lett.* **2008,** *10* (8), 1581-1584.

82. Ni, Y.; Zeng, W.; Huang, K.-W.; Wu, J., *Chem. Commun.* **2013,** *49* (12), 1217-1219.

83. Sarma, T.; Panda, P. K.; Setsune, J.-i., *Chem. Commun.* **2013,** *49* (84), 9806-9808.

84. Umezawa, K.; Matsui, A.; Nakamura, Y.; Citterio, D.; Suzuki, K., *Chem. Eur. J.* **2009,** *15* (5), 1096-1106.

85. Umezawa, K.; Nakamura, Y.; Makino, H.; Citterio, D.; Suzuki, K., *J. Am. Chem. Soc.* **2008,** *130* (5), 1550-1551.

86. Wakamiya, A.; Murakami, T.; Yamaguchi, S., *Chem. Sci.* **2013,** *4* (3), 1002-1007.

87. Yamazawa, S.; Nakashima, M.; Suda, Y.; Nishiyabu, R.; Kubo, Y., *J. Org. Chem.* **2016,** *81* (3), 1310-1315.

88. Yang, Y.; Guo, Q.; Chen, H.; Zhou, Z.; Guo, Z.; Shen, Z., *Chem. Commun.* **2013,** *49* (38), 3940-3942.

89. Wada, M.; Ito, S.; Uno, H.; Murashima, T.; Ono, N.; Urano, T.; Urano, Y., *Tetrahedron Lett.* **2001,** *42* (38), 6711-6713.

90. Shen, Z.; Röhr, H.; Rurack, K.; Uno, H.; Spieles, M.; Schulz, B.; Reck, G.; Ono, N., *Chem. Eur. J.* **2004,** *10* (19), 4853-4871.

91. Okujima, T.; Tomimori, Y.; Nakamura, J.; Yamada, H.; Uno, H.; Ono, N., *Tetrahedron* **2010,** *66* (34), 6895-6900.

92. Nakamura, M.; Tahara, H.; Takahashi, K.; Nagata, T.; Uoyama, H.; Kuzuhara, D.; Mori, S.; Okujima, T.; Yamada, H.; Uno, H., *Org. Biomol. Chem.* **2012,** *10* (34), 6840-6849.

93. Nakamura, M.; Kitatsuka, M.; Takahashi, K.; Nagata, T.; Mori, S.; Kuzuhara, D.; Okujima, T.; Yamada, H.; Nakae, T.; Uno, H., *Org. Biomol. Chem.* **2014,** *12* (8), 1309-1317.

94. Uppal, T.; Hu, X.; Fronczek, F. R.; Maschek, S.; Bobadova-Parvanova, P.; Vicente, M. G. H., *Chem. Eur. J.* **2012,** *18* (13), 3893-3905.

95. Jiao, C.; Huang, K.-W.; Wu, J., *Org. Lett.* **2011,** *13* (4), 632-635.

96. Jiao, C.; Zhu, L.; Wu, J., *Chem. Eur. J.* **2011,** *17* (24), 6610-6614.

97. Zeng, L.; Jiao, C.; Huang, X.; Huang, K.-W.; Chin, W.-S.; Wu, J., *Org. Lett.* **2011,** *13* (22), 6026-6029.

98. Yu, C.; Jiao, L.; Li, T.; Wu, Q.; Miao, W.; Wang, J.; Wei, Y.; Mu, X.; Hao, E., *Chem. Commun.* **2015,** *51* (94), 16852-16855.

99. Leen, V.; Qin, W.; Yang, W.; Cui, J.; Xu, C.; Tang, X.; Liu, W.; Robeyns, K.; Van Meervelt, L.; Beljonne, D.; Lazzaroni, R.; Tonnelé, C.; Boens, N.; Dehaen, W., *Chem. Asian J.* **2010,** *5* (9), 2016-2026.

100. Hayashi, Y.; Obata, N.; Tamaru, M.; Yamaguchi, S.; Matsuo, Y.; Saeki, A.; Seki, S.; Kureishi, Y.; Saito, S.; Yamaguchi, S.; Shinokubo, H., *Org. Lett.* **2012,** *14* (3), 866-869.

101. Heyer, E.; Retailleau, P.; Ziessel, R., *Org. Lett.* **2014,** *16* (9), 2330-2333.

102. Jiao, L.; Zhou, X.; Wu, Q.; Feng, Y.; Yu, Y.; Yu, C.; Hao, E.; Wei, Y.; Mu, X., *Chem. Asian J.* **2015**, n/a-n/a.

103. Sun, Z.-B.; Guo, M.; Zhao, C.-H., *J. Org. Chem.* **2016,** *81* (1), 229-237.

104. Boens, N.; Leen, V.; Dehaen, W., *Chem. Soc. Rev.* **2012,** *41* (3), 1130-1172.

105. Kowada, T.; Maeda, H.; Kikuchi, K., *Chem. Soc. Rev.* **2015,** *44* (14), 4953-4972.

106. Móczár, I.; Huszthy, P.; Maidics, Z.; Kádár, M.; Klára, T., *Tetrahedron* **2009,** *65* (39), 8250-8258.

107. Yang, C.; Gong, D.; Wang, X.; Iqbal, A.; Deng, M.; Guo, Y.; Tang, X.; Liu, W.; Qin, W., *Sensors Actuators B: Chem.* **2016,** *224*, 110-117.

108. Domaille, D. W.; Zeng, L.; Chang, C. J., *J. Am. Chem. Soc.* **2010,** *132* (4), 1194-1195.

109. Baruah, M.; Qin, W.; Vallée, R. A. L.; Beljonne, D.; Rohand, T.; Dehaen, W.; Boens, N., *Org. Lett.* **2005,** *7* (20), 4377-4380.

110. Jia, M.-Y.; Wang, Y.; Liu, Y.; Niu, L.-Y.; Feng, L., *Biosensors Bioelectron.* **2016,** *85*, 515-521.

111. Niu, L.-Y.; Li, H.; Feng, L.; Guan, Y.-S.; Chen, Y.-Z.; Duan, C.-F.; Wu, L.-Z.; Guan, Y.-F.; Tung, C.-H.; Yang, Q.-Z., *Anal. Chim. Acta* **2013,** *775*, 93-99.

112. Niu, L.-Y.; Guan, Y.-S.; Chen, Y.-Z.; Wu, L.-Z.; Tung, C.-H.; Yang, Q.-Z., *J. Am. Chem. Soc.* **2012,** *134* (46), 18928-18931.

113. Niu, L.-Y.; Guan, Y.-S.; Chen, Y.-Z.; Wu, L.-Z.; Tung, C.-H.; Yang, Q.-Z., *Chem. Commun.* **2013,** *49* (13), 1294-1296.

114. Wang, F.; An, J.; Zhang, L.; Zhao, C., *RSC Adv.* **2014,** *4* (96), 53437-53441.

115. Gong, D.; Tian, Y.; Yang, C.; Iqbal, A.; Wang, Z.; Liu, W.; Qin, W.; Zhu, X.; Guo, H., *Biosensors Bioelectron.* **2016,** *85*, 178-183.

116. Zhang, L.; Li, M.; Zhao, C.; Gu, X., *Tetrahedron Lett.* **2016,** *57* (5), 578-581.

117. Wang, F.; Zhou, L.; Zhao, C.; Wang, R.; Fei, Q.; Luo, S.; Guo, Z.; Tian, H.; Zhu, W.-H., *Chem. Sci.* **2015,** *6* (4), 2584-2589.

118. Zhang, Y.; Shao, X.; Wang, Y.; Pan, F.; Kang, R.; Peng, F.; Huang, Z.; Zhang, W.; Zhao, W., *Chem. Commun.* **2015,** *51* (20), 4245-4248.

119. Gao, Y.-G.; Zhang, Y.; Shi, Y.-D.; Hao, H.-J.; Gong, B.; Lu, Z.-L., *Biorg. Med. Chem.* **2016,** *24* (7), 1550-1559.

120. Jia, M.-Y.; Niu, L.-Y.; Zhang, Y.; Yang, Q.-Z.; Tung, C.-H.; Guan, Y.-F.; Feng, L., *ACS Appl. Mater. Interfaces* **2015,** *7* (10), 5907-5914.

121. Niu, L.-Y.; Jia, M.-Y.; Chen, P.-Z.; Chen, Y.-Z.; Zhang, Y.; Wu, L.-Z.; Duan, C.-F.; Tung, C.-H.; Guan, Y.-F.; Feng, L.; Yang, Q.-Z., *RSC Adv.* **2015,** *5* (17), 13042-13045.

122. Niu, L.-Y.; Yang, Q.-Q.; Zheng, H.-R.; Chen, Y.-Z.; Wu, L.-Z.; Tung, C.-H.; Yang, Q.-Z., *RSC Adv.* **2015,** *5* (6), 3959-3964.

123. Wang, F.; Guo, Z.; Li, X.; Li, X.; Zhao, C., *Chem. Eur. J.* **2014,** *20* (36), 11471-11478.

124. Wang, F.; Zhu, Y.; Zhou, L.; Pan, L.; Cui, Z.; Fei, Q.; Luo, S.; Pan, D.; Huang, Q.; Wang, R.; Zhao, C.; Tian, H.; Fan, C., *Angew. Chem. Int. Ed.* **2015,** *54* (25), 7349-7353.

125. Peng, H.-Q.; Sun, C.-L.; Niu, L.-Y.; Chen, Y.-Z.; Wu, L.-Z.; Tung, C.-H.; Yang, Q.-Z., *Adv. Funct. Mater.* **2016,** *26* (30), 5483-5489.

126. Zhao, C.; Zhang, X.; Li, K.; Zhu, S.; Guo, Z.; Zhang, L.; Wang, F.; Fei, Q.; Luo, S.; Shi, P.; Tian, H.; Zhu, W.-H., *J. Am. Chem. Soc.* **2015,** *137* (26), 8490-8498.

127. Raja Sekhar, A.; Kaloo, M. A.; Sankar, J., *Org. Biomol. Chem.* **2015,** *13* (40), 10155-10161.

128. Kaloo, M. A.; Raja Sekhar, A.; Ramana Reddy, R. V.; Raman, R. S.; Sankar, J., *J. Mater. Chem. C* **2016,** *4* (13), 2452-2456.

129. Sekhar, A. R.; Kaloo, M. A.; Sankar, J., *Chem. Asian J.* **2014,** *9* (9), 2422-2426.

130. Atilgan, S.; Ekmekci, Z.; Dogan, A. L.; Guc, D.; Akkaya, E. U., *Chem. Commun.* **2006,** (42), 4398-4400.

131. Ozlem, S.; Akkaya, E. U., *J. Am. Chem. Soc.* **2009,** *131* (1), 48-49.

132. He, H.; Lo, P.-C.; Yeung, S.-L.; Fong, W.-P.; Ng, D. K. P., *Chem. Commun.* **2011,** *47* (16), 4748-4750.

133. Buyukcakir, O.; Bozdemir, O. A.; Kolemen, S.; Erbas, S.; Akkaya, E. U., *Org. Lett.* **2009,** *11* (20), 4644-4647.

134. Gallagher, W. M.; Allen, L. T.; O'Shea, C.; Kenna, T.; Hall, M.; Gorman, A.; Killoran, J.; O'Shea, D. F., *Br. J. Cancer* **2005,** *92* (9), 1702-1710.

135. Gibbs, J. H.; Zhou, Z.; Kessel, D.; Fronczek, F. R.; Pakhomova, S.; Vicente, M. G. H., *J. Photochem. Photobiol. B: Biol.* **2015,** *145*, 35-47.

136. Verwilst, P.; David, C. C.; Leen, V.; Hofkens, J.; de Witte, P. A. M.; De Borggraeve, W. M., *Bioorg. Med. Chem. Lett.* **2013,** *23* (11), 3204-3207.

137. Kamkaew, A.; Burgess, K., *J. Med. Chem.* **2013,** *56* (19), 7608-7614.

138. Lim, S. H.; Thivierge, C.; Nowak-Sliwinska, P.; Han, J.; van den Bergh, H.; Wagnières, G.; Burgess, K.; Lee, H. B., *J. Med. Chem.* **2010,** *53* (7), 2865-2874.

CHAPTER 2: SYNTHESIS OF 3,8-DICHLORO-6-ETHYL-1,2,5,7-TETRAMETHYL-BODIPY AND REACTIVITY STUDIES AT THE 3,5,8,-POSITIONS*

2.1 Introduction

Based on reported methods in Chapter 1, a number of BODIPY platforms, such as those **a-b** in Figure 1, have been prepared and their reactivity investigated.[1-3] BODIPY platform **a** that was reported in 2005 bearing 3,5-dichloro groups undergoes S_NAr and reactive Pd(0)-catalyzed cross-coupling reactions at these positions, which yields a variety of functionalized BODIPYs for various applications,[4-7] as discussed in Chapter 1. On the other hand, Knoevenagel condensations that were widely used to react with the α-methyl groups on BODIPY platform **b** various aldehydes produce the corresponding styryl BODIPYs with significant red shift in both the absorption and emission.[8-12] Such a method is widely applied for the development of various NIR BODIPY probes with the extended conjugation.[1-3, 8, 11, 13-15] In the traditional routes, the lack of functionalizable groups at the meso position made meso-functionalization a challenge, until platform **c**[16-20] with 8-thioester group and platform **d**[21-23] bearing an 8-chloro group were reported. The 8-thioester group at platform **c** was reported to undergo the elimination/addition with N-centered nucleophiles[17-18] and a later reported Liebeskind-Srogl cross coupling reactions with aryl-, alkenyl- bornic acids and

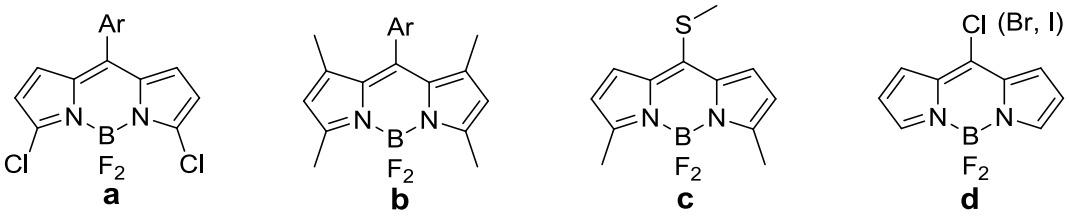

Figure 2-1: Several different BODIPY platforms.

* Reproduced from Ref. Zhao, N.; Vicente, M. G. H.; Fronczek, F. R.; Smith, K. M. Synthesis of 3,8-Dichloro-6-ethyl-1,2,5,7-tetramethyl–BODIPY from an Asymmetric Dipyrroketone and Reactivity Studies at the 3,5,8-Positions. *Chemistry-A European Journal*, 2015, 21, 6181. with the permission of John Wiley and Sons.

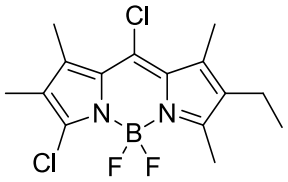

1a

Figure 2-2: Structure of 3,8-dichloro-6-ethyl-1,2,5,7-tetramethyl-BODIPY **1a**.

organostannanes.[16, 20] However, as discussed in Chapter 1, more versatile platform **d** can react with various types of nucleophiles. Also, a wide range of Pd(0)-catalyzed coupling reactions, including Stille, Suzuki, and Sonogashira coupling reactions, work well on the platform **d**.

In order to introduce all there three valuable groups into one BODIPY core, as discussed above, we report the design and synthesis of a versatile, asymmetric BODIPY **1a** bearing 3-chlor and 8-chloro groups, as well as a reactive 5-methyl group. BODIPY **1a** was found to be regioselectively functionalized using four different types of reactions, at all the 3-, 5- and 8-positions, to yield new BODIPYs. The Stille cross-coupling and nucleophilic addition/elimination reactions both occur regioselectively at the 8-position, followed by the 3-position, which allows stepwise functionalization using N-, O-, and S-centered nucleophiles and various commercial available tin reagents. Addtionally, regioselectivity of *meso*- versus α-position toward addition/elimination reactions at the BODIPY was firstly investigated. Furthermore, 5-formyl and styryl BODIPYs can be produced by further functionalization of the Knoevenagel and oxidation reaction at the 5-methyl group of BODIPY **1a**.

2.2 Synthesis of 3,8-Dichloro-6-ethyl-1,2,5,7-tetramethyl-BODIPY

The synthetic route to asymmetric dipyrroketone **5** as a fundamental precursors of BODIPY platefrom **1a** is oulined in Scheme 2-1**,** started with readily available pyrrole **4**, that could be synthesized from commercial available compounds **2** in two steps using published procedure.[24] The conversion of α-methyl group of pyrrole **4**[24] to a carboxylic acid **5**[25-26] is accomplished by

using sulfonyl chloride (SO_2Cl_2) for the chlorination and followed by hydrolysis reaction with sodium acetate in 1,4-dioxane. An acylation reaction with thionyl chloride ($SOCl_2$), followed by an amidation reaction with dimethylamine gas[26] produced 2-amide pyrrole **6** in 85% yield. Asymmetric dipyrroketone **8** was obtained by reactions of pyrrole **6** with phosphoryl chloride ($POCl_3$), followed by addition of 2,4-dimethyl-5-ethyl pyrrole and sequential hydrolysis with aqueous sodium acetate solution[27] in a good overall 86% yield for total 3 steps. The formation of intermediate **7** was confirmed by HRMS. The key dipyyroketone **8** was well characterized by ^{1}H NMR, ^{13}C NMR and HRMS (ESI-TOF).

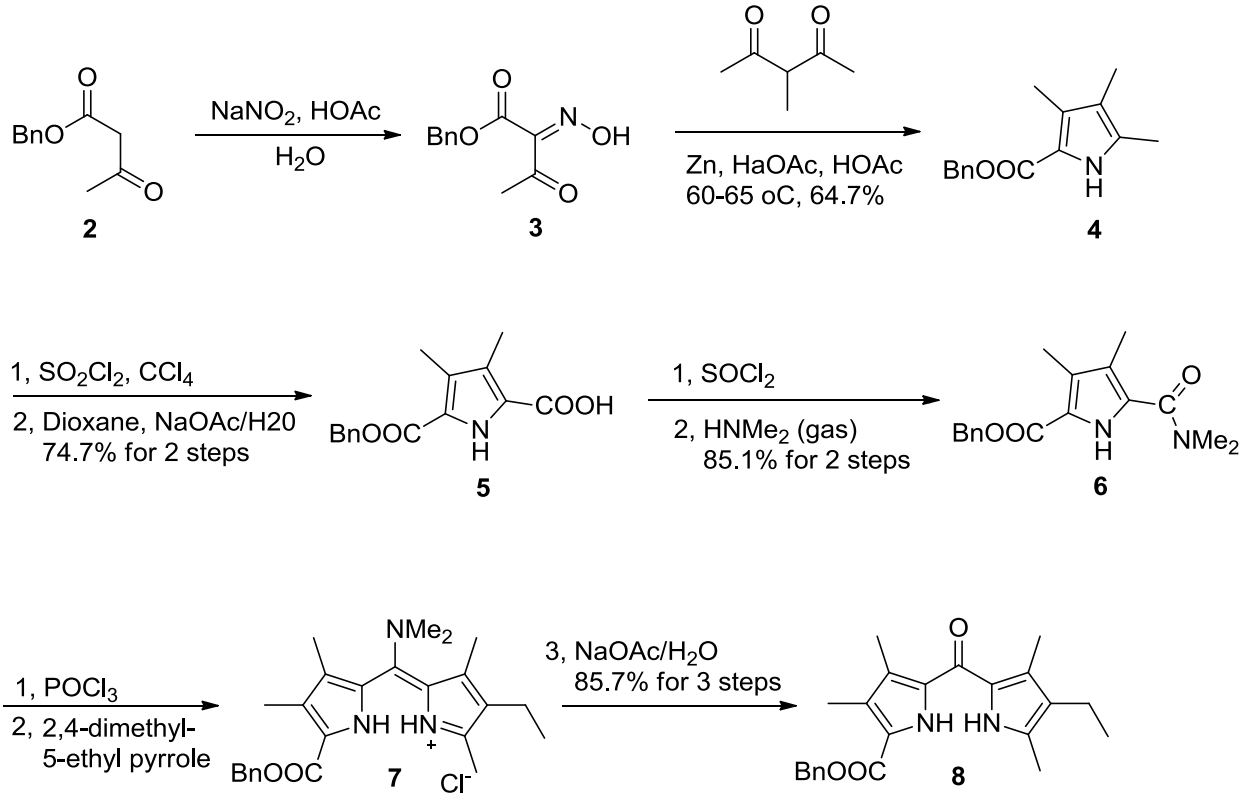

Scheme 2-1: Synthesis of asymmetric dipyrroketone **8**.

As shown in Figure 2-3, the peaks at δ = 8.78 and 9.20 in the ^{1}H NMR spectra can be assigned to NH of the dipyrroketone, showing this asymmetric structures. The structure was also further confirmed by X-ray analysis, as shown in the Figure 2-4. Suitable crystals of **8** was grown

by slow evaporation in $CHCl_3$, the result is shown in Figure 2-4. The NH group of one pyrrole is *syn* to the central carbonyl (N-C-C-O torsion angle 15.5°) in the conformation of dipyrroketone **8**, while the other one is *syn* to benzyl ester carbonyl with a torsion angle of 6.0°.

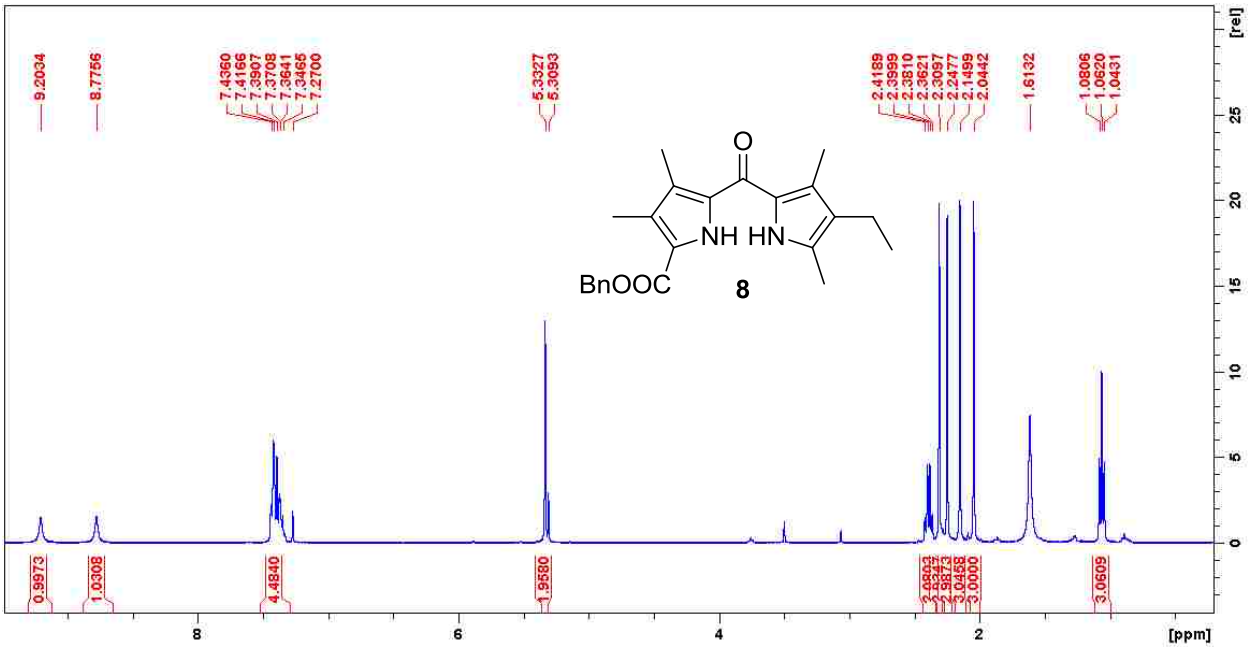

Figure 2-3: ^1H NMR (400 MHz) of dipyrroketone **8** in $CDCl_3$ at room temperature.

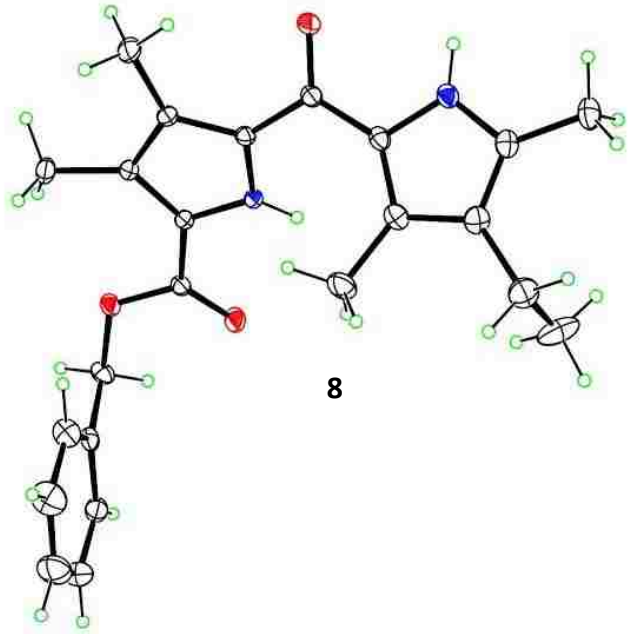

Figure 2-4: X- ray structure of dipyrroketone **8** with 50% probability ellipsoids.

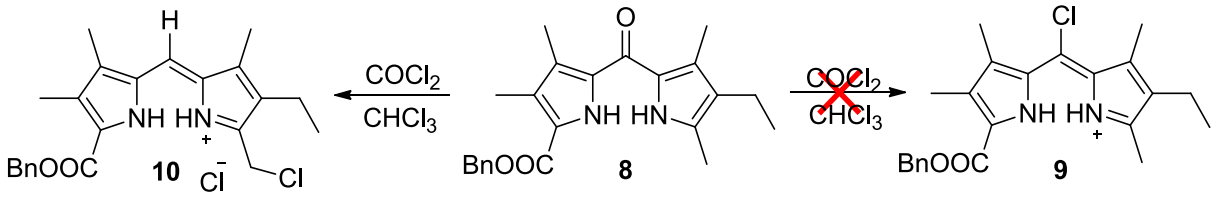

Scheme 2-2: Chlorination of dipyrroketone **8**.

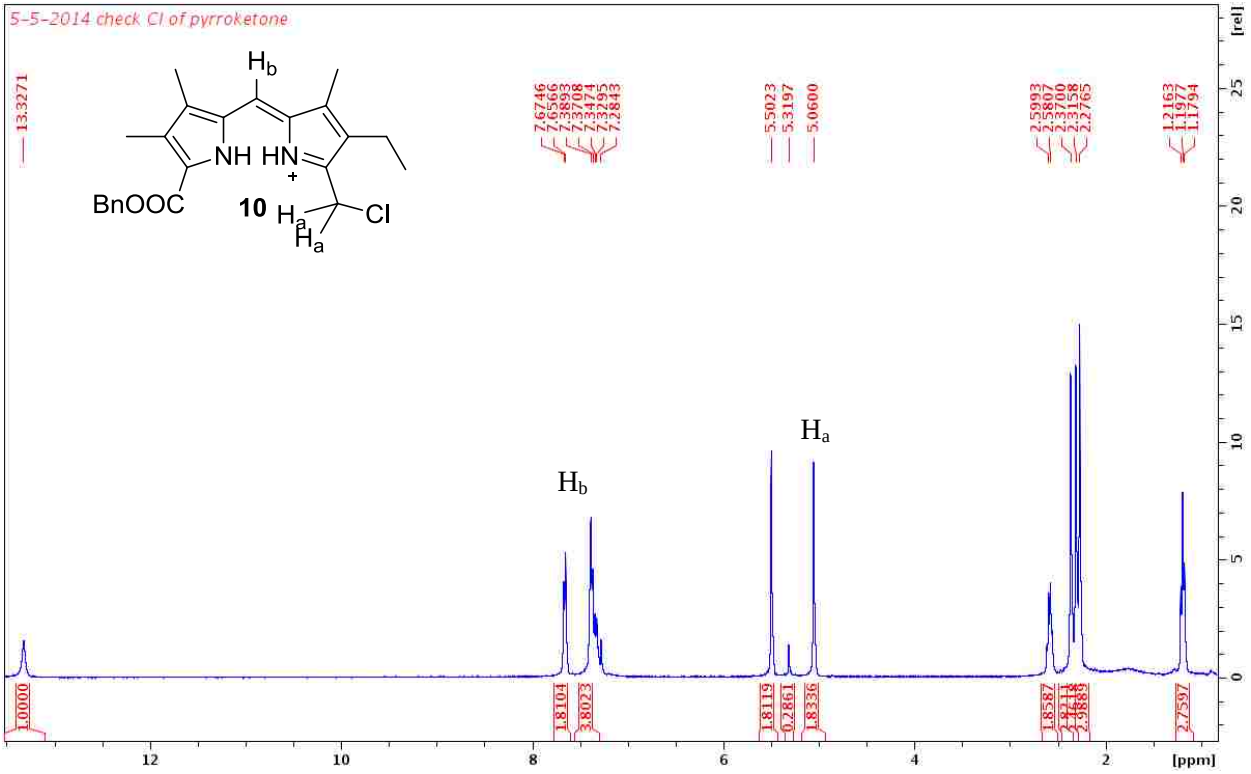

Figure 2-5: ^{1}H NMR of dipyrromethene **10**.

Oxidative chlorination reaction excess phosgene (15% in toluene)[28] with was performed to convert dipyrroketone **8** to dipyrrolmethene **9**, as shown in Scheme 2-2. However, after recrystallization in diethyl ether, the reaction afforded an undesired product 5-chlorodipyrrin salt **10**, instead of **9**. The structure of this compound was determined by ^{1}H NMR (Figure 2-4) spectroscopy and X-ray analysis (Figure 2-5). In ^{1}H NMR spectra of **10**, the NH peak shifted downfield to δ = 13.32 ppm; one signal is missed at δ = 2.0 ppm, while one singlet (integration is 2) was shown at δ = 5.1 ppm, which was attributed to the H_a; the integration between δ = 7.3-7.7

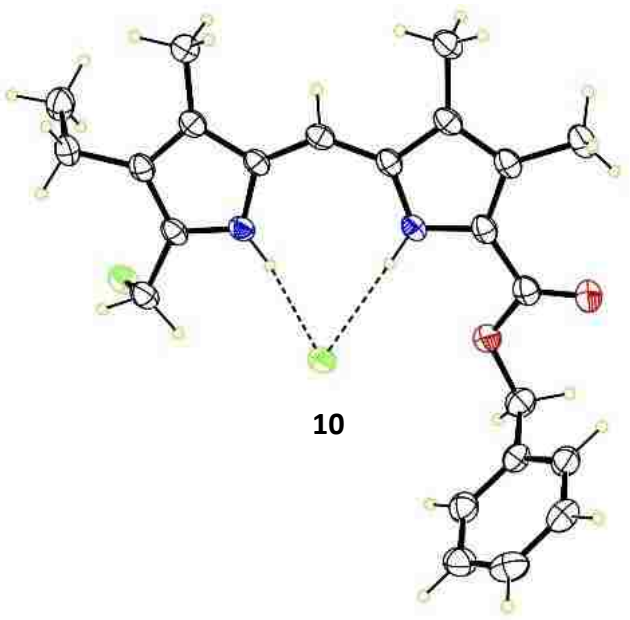

Figure 2-6: X- ray structure dipyyromethene **10** with 50% probability ellipsoids.

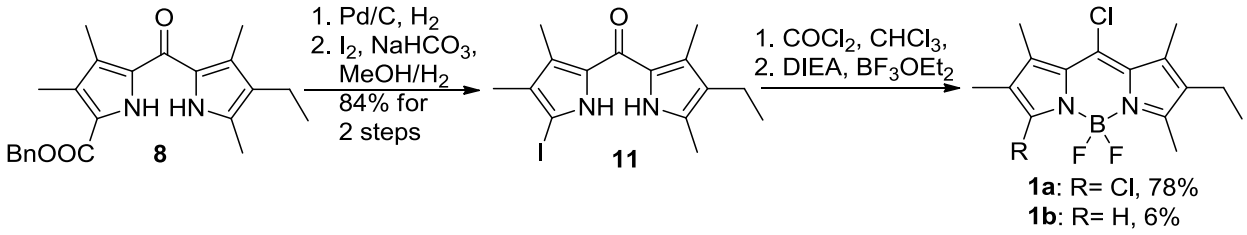

Scheme 2-3: Synthesis of asymmetric BODIPY **1a** and **1b**.

ppm is around 6. I believe the peak of 8-H (H_b) was overlapped with the peaks of the phenyl ring of the 3-COOBn group. In the X-ray analysis, 5-chlorodipyrrin salt **10** is confirmed as the hydrochloride salt with both N atoms protonated. There are hydrogen bonds forming between two "NH" atoms to the chloride ion. The dipyrryl C_9N_2 core is exactly planar to with a mean deviation of 0.017 Å.

We believed that the observed regioselectivity of the chlorination was due to the presence of electron withdrawing group benzyl ester (-COOBn), so an alternative approach was employed, as shown in Scheme 2-3. The benzyl ester group was converted to a much less electron-

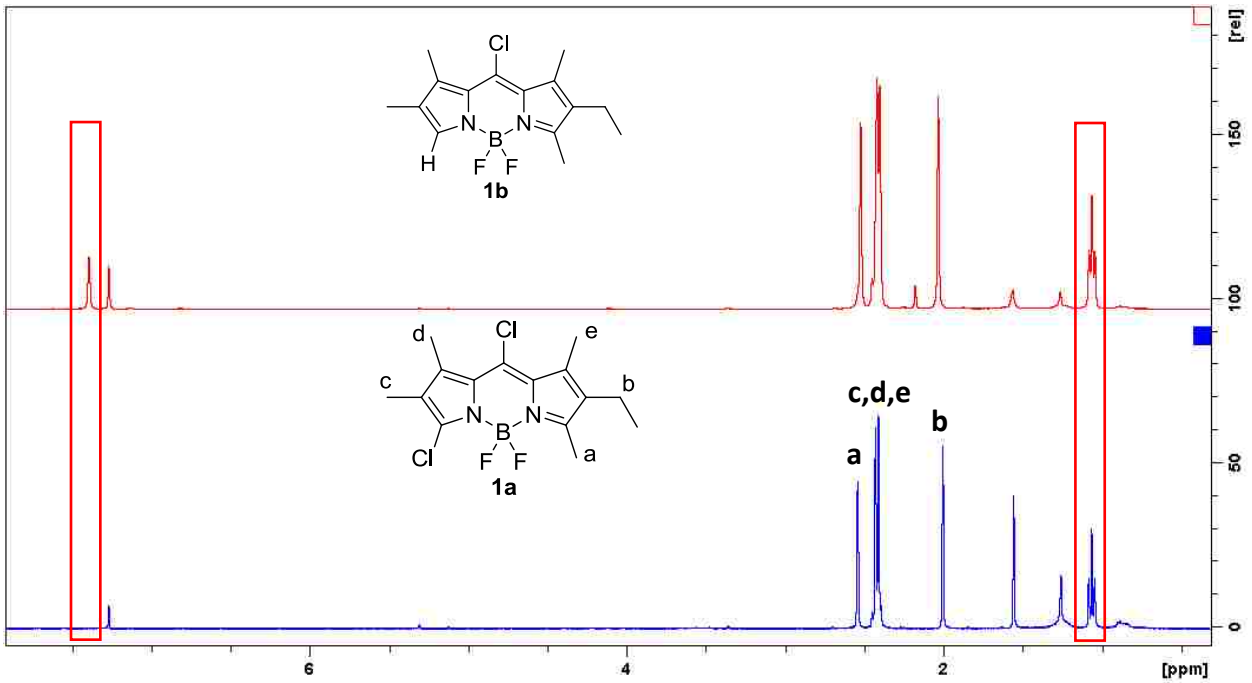

Figure 2-7: ^{1}H NMR spectra of **1a** and **1b**.

withdrawing iodo group via a debenzylation reaction with Pd/H_2, followed by an iodination reaction with I_2/$NaHCO_3$.[29] The newly generated dipyrroketone **11** then reacted with excess phosgene (15% in toluene) for the oxidative chlorination. Several observation suggested a successful reaction: (1) the color of reaction mixture was changed from yellow to dark red; (2) the UV-Vis spectra showed the formation of new peaks of 485/499 nm that belong to dipyrromthene; (3) the "NH" peaks shifted downfield in the ^{1}H-NMR spectra of the crude product. Subsequent deprotonation with *N*,*N*-diisopropylethylamine (DIEA, 7 euqivalents) and complexation with boron trifluoride diethyl etherate (10 equivalents) successfully yielded the fluorescent BODIPY dye **1a** in a 78% isolated yield (over 2 steps), along with a minor monochloro-BODIPY **1b** in 6% yield. BODIPYs **1a** and **1b** were both characterized by ^{1}H NMR, ^{13}C NMR, and HRMS (ESI-TOF), as well as X-ray analysis.

Figure 2-7 shows ^{1}H-NMR spectra of BODIPYs **1a** and **1b**. BODIPY **1a** has almost similar ^{1}H NMR spectra as BODIPY **1b**, and all the peaks in the spectra can be easily assigned. For

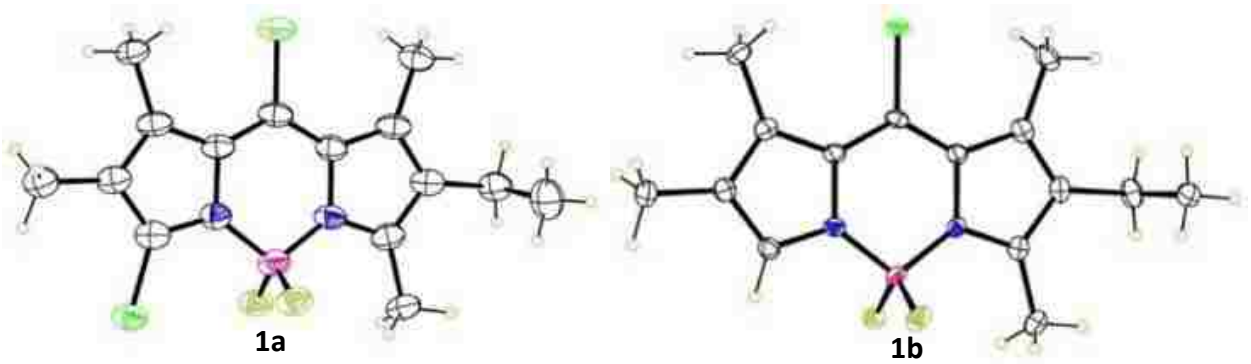

Figure 2-8: X-ray structures of BODIPYs **1a-b**. Only one of the independent molecules is shown for both **1a** and **1b**.

example, the triplet at around δ 1.1 ppm is almost overlap with each other. The difference that distinguish these two BODIPYs is the singlet δ 7.4 ppm, which belongs to the α-H group of **1b** at the unshielding area of aromatic BODIPY core. At the same time, **1a** has one chloro group at 3-position, so no signal is shown at that area.

Suitable crystals of **1a-b** grown by slow evaporation in the chloroform were used for X-ray analysis, and the results are shown in Figure 2-8. There are two independent and almost identical molecules of **1a**, and a disordered molecule of chloroform in the structure of **1a**. In both molecules, there are the mean diviations of 0.027 and 0.036 Å from planarity of their 12-atom BODIPY cores, and a torsional difference (9.8°) in the conformation of 6-ethyl group. On the other hand, there are four independent molecules in the structure of BODIPY **1b**. The mean deviations of their 12-atom BODIPY cores are in the range of 0.023 – 0.054 Å. In such molecules, the conformations of *β*-ethyl group are almost perpendicular to the planes of the BODIPY core, with C-C-C-C torsion angles in the range of 88.3-89.7°.

2.3 Reactivity Studies at the 3,5,8-positions of BODIPY 1a

Previous work from both our group and other groups showed *meso*-chloro or *α*-chloro group of BODIPYs has a high reactivity towards Pd(0)-catalyzed cross-coupling reactions.[23, 28, 30-31] Since base is not required, and the high yielding,[21, 23, 28] Stille cross-coupling[32] reactions are also

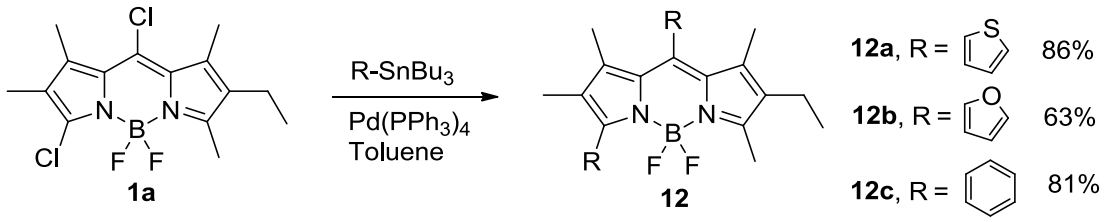

Scheme 2-4: Synthesis of asymmetric BODIPY **12a-c**.

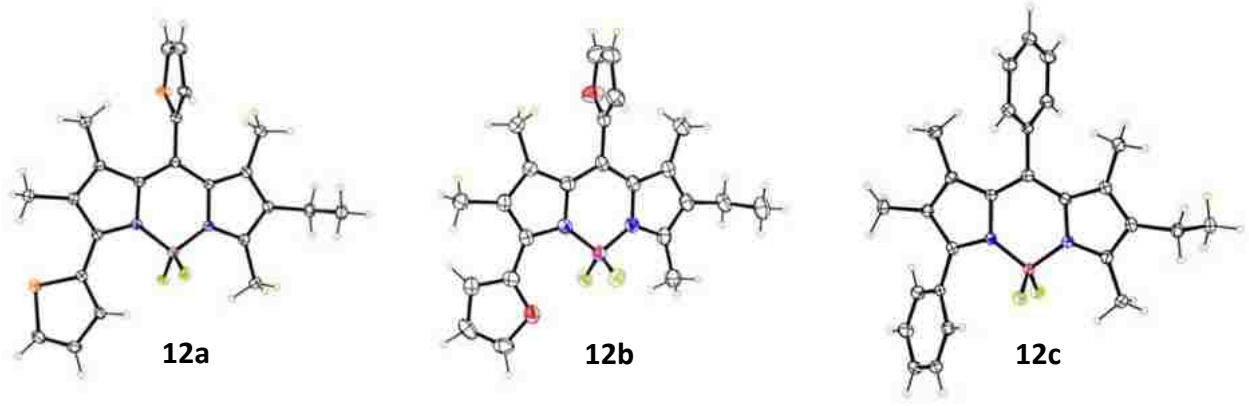

Figure 2-9: X-ray structures of BODIPY **12a-c** (50% probability ellipsoids). Only the major conformer is shown for disordered groups.

very attractive among the Pd(0)-catalyzed cross-coupling reactions. We recently reported that Stille cross-coupling reactions occurring first at the most reactive 8-chloro site, followed by at the 3,5-positions.[28] BODIPY **1a** showed a high reactivity towards Stille coupling reactions in the presence of a small excess amount of tin reagents, and catalyzed by 10 mol% of $Pd(PPh_3)_4$ in toluene and smoothly produced the desired diaryl-BODIPYs **12a-c** in good yields (63% to 86%), as shown in scheme 2-4. Of the three tin reagents used, 2-(tributylstannyl)thiophene showed the highest reactivity that the reaction gave the highest yield after two hours.

Suitable crystals of **12a-c** grown by slow evaporation in the chloroform were used for X-ray analysis, and the results are shown in Figure 2-9. All these three structures show the disorder with the thiophene at 8-position, both furan groups, and 6-ethyl group in BODIPYs **12a**, **12b,** and **12c**. There are the mean deviations of 0.072, 0.087 Å, and 0.054 Å Å from planarity of the 12-atom BODIPY cores for **12a**, **12b**, and **12c**. The 8-aryl substituents forms different dihedral angles

with the cores in the range of 87.78 - 79.78°, to minimize steric interactions with the 1,7-dimethyl groups. On the other hand, dihedral angles between the aryl substituents at the 3-position and the BODIPY core are 41.78° for **12a**, 36.98° for **12b**, and 42.78° for **12c**, respectively.

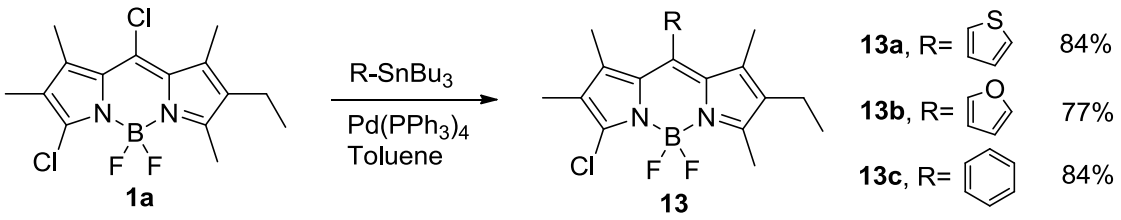

Scheme 2-5: Synthesis of asymmetric BODIPYs **13a-c.**

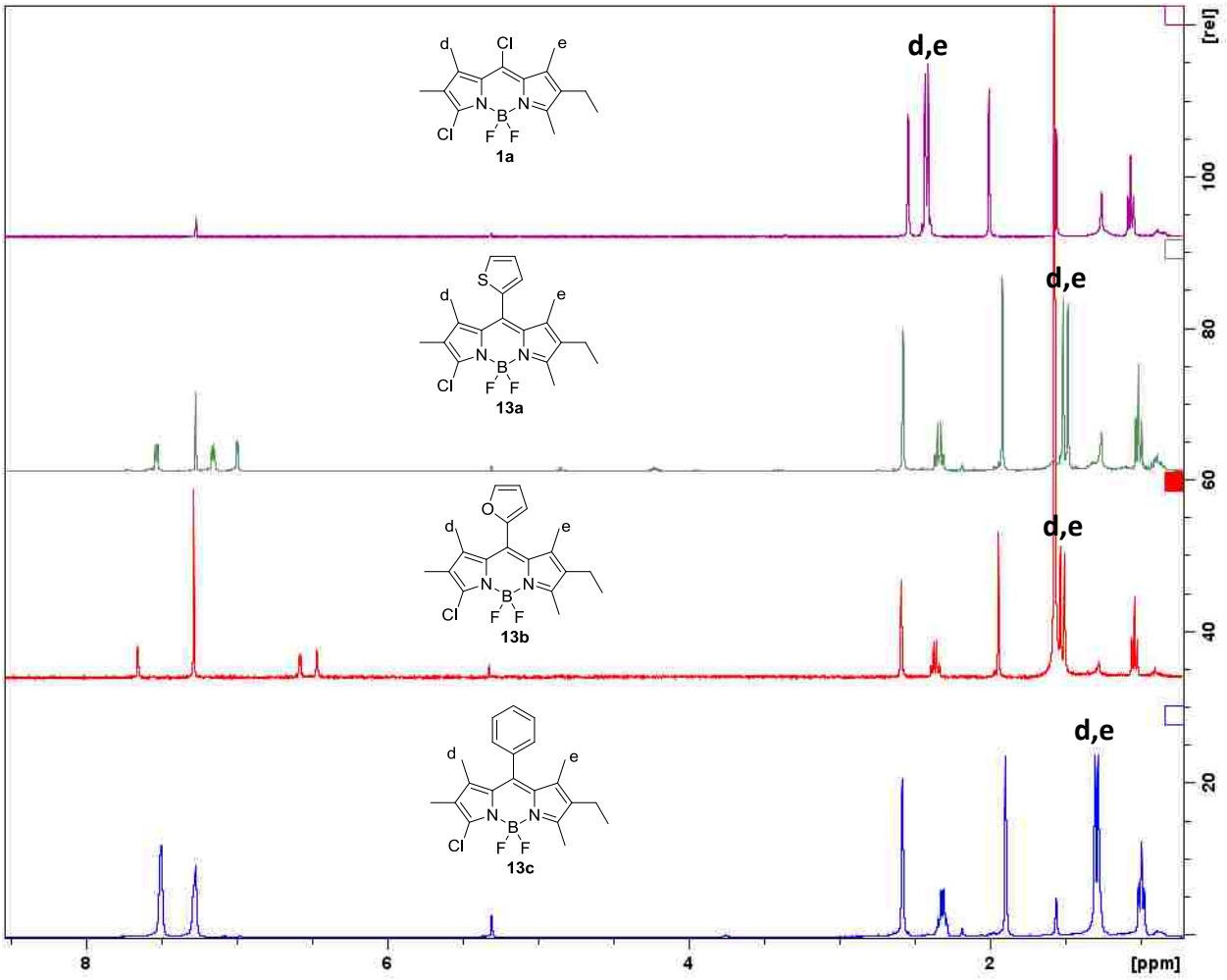

Figure 2-10: NMR spectrum of BODIPY **1a** and **13a-c.**

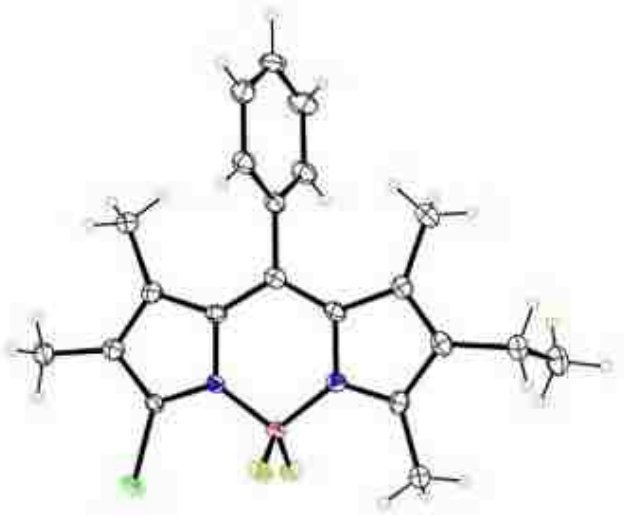

Figure 2-11: X-ray crystal structures of asymmetric BODIPY dyes **13c** (50% probability ellipsoids). Only the major conformer is shown for disordered groups.

On the other hand, using 1 equiv of tin reagents with dilute mixture solutions, the corresponding 8-aryl-BODIPY dyes **13a-c** were obtained in high yields (77-84%), as shown in Scheme 2-5. 8-Chloro group at BODIPY **1a** showed higher reactivity over 3-chloro group towards the Stille cross-coupling reaction, which agrees with previous report.[28]

The mono-coupled products **13a-c** were confirmed by HRMS (see experimental part). ^{1}H NMR spectral comparisons among BODIPYs **1a** and **13a-c** are outlined in Figure 2-10. The singlets of H_d and H_e at the 1,7-positions appear upfield-shift from δ 2.4 ppm (**1a**) to 1.5 ppm (**13a-b**) and 1.3 ppm (**13c**). It can be explained that H_d and H_e both locate in the shielding areas of the 8-aromatic rings, which can verify the regioselectivity of this reactions. A suitable crystal of only **13c** that was grown by slow evaporation in the chloroform was used for X-ray analysis, and the results are shown in Figure 2-11. Mean deviations from planarity of the C_9BN_2 cores of **13c** is 0.013 Å. 8-phenyl group forms dihedral angles of 75.68° for **13c** with the BODIPY cores to minimize steric interactions with the 1,7-methyl groups.

In order to further investigate the regioselectivity observed above, step-wise Stille cross-coupling reactions with two different types of organotin reagents were performed on BODIPY **1a**,

as shown in Scheme 2-6. Therefore, first Stille reaction introduced a thienyl or furanyl group at the 8-position of BODIPY **1a**, followed by a thienyl, furanyl, or trimethylsilylethynyl group that were introduced at the 3-poisiton using a second Stille reactions, to produce BODIPYs **14-16**, in good to excellent yields (58–91%). It should be noted that is 8-furanyl group seemed to deactivate 3-chloro group, which caused the difficulty to introduce aryl group under the same conditions. Extending the reaction time slightly improve the yields, while a large excess amount of tin reagents and higher concentration in the reaction mixture both significantly improved yields, and decreased the reaction time at the same time. Besides, the intermediate compound **13a** with a 8-thienyl group showed a high reactivity with 2-(tributylstannyl)furan with the highest yield.

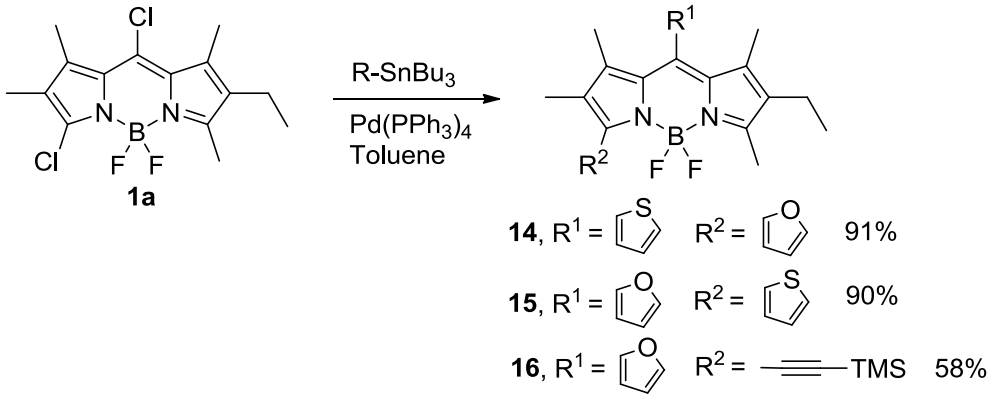

Scheme 2-6: Synthesis of asymmetric BODIPYs **14-16.**

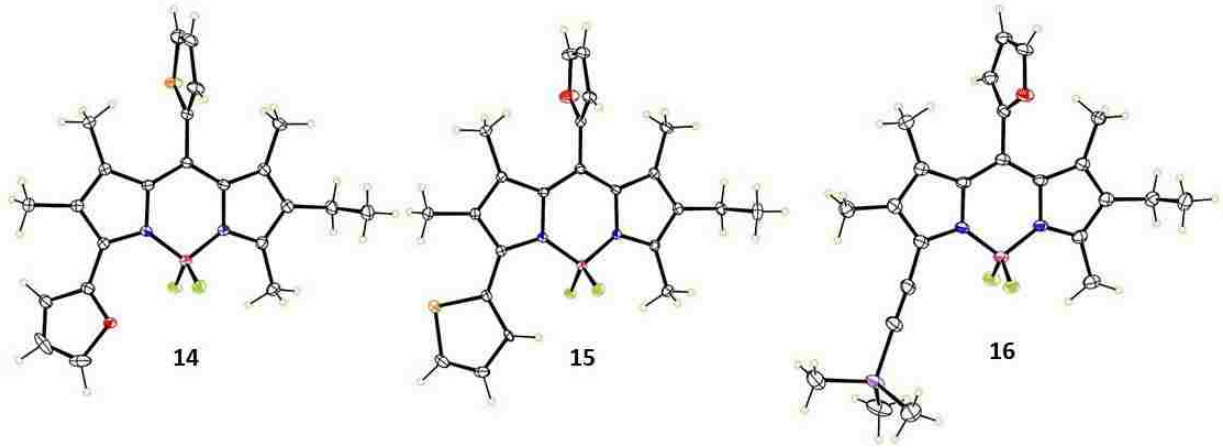

Figure 2-12: X-ray structures of BODIPYs **14-16**, 50% probability ellipsoids.

Suitable crystals of **14-16** that grown by slow evaporation in the chloroform were used for X-ray analysis, and the results are shown in Figure 2-12. In BODIPY **14**, both the 3-furan and 8-thiophene rings displayed rotational disorder. The planarity of the C_9BN_2 core of BODIPYs **14-16** and the dihedral angles formed by 3- and 8- aryl groups are similar to that in the crystal structures of **12a-c** and **13c**.The Mean deviations for the C_9BN_2 cores are 0.082 Å for **14**, 0.071 Å for **15**, and 0.018 Å for **16**. In BODIPY **14**, the 8-thienyl group forms a dihedral angle of 87.2°with the BODIPY core, and the 8-furanyl group form slightly lower angles of 84.8° and 78.0° in BODIPYs **15** and **16**. On the other hand, the 3-furanyl and thienyl groups in the BODIPYs **8** and **9** form dihedral angle of 38.6 and 39.6° with the BODIPY core plane.

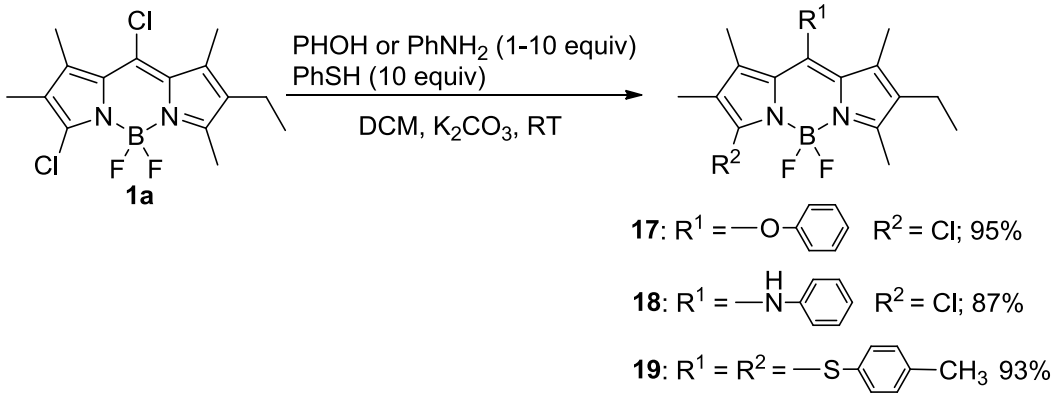

Scheme 2-7: Synthesis of asymmetric BODIPYs **17-19.**

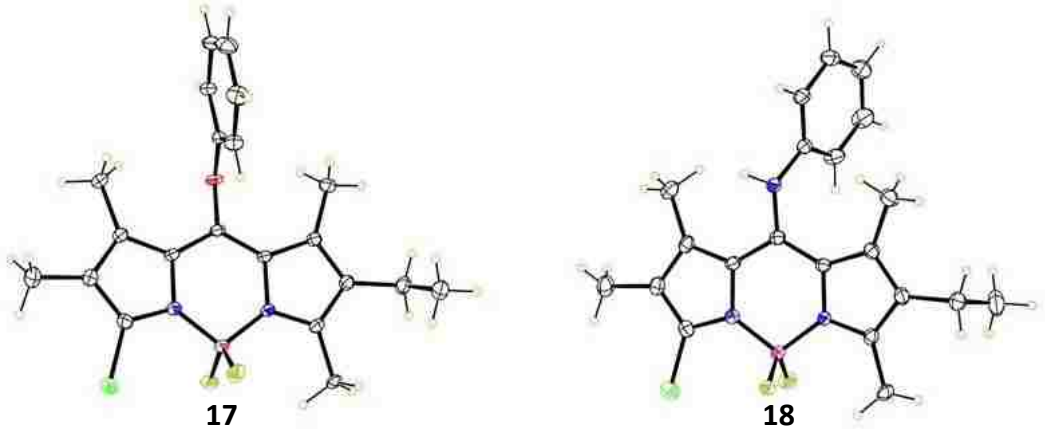

Figure 2-13: X-ray structures of BODIPYs **17** and **18**, 50% probability ellipsoids.

Moreover, the regioselectivity of BODIPY **1a** towards nucleophilic addition/elimination reactions was also investigative three different types of nucleophiles, as shown in Scheme 2-7. Treatment of BODIPY **1** with a large excess amount of phenol or aniline in the presence of potassium carbonate overnight at room temperate yielded only the 8-substituted BODIPYs **17-18** in high yields (87-95%). ^{1}H NMR (see Appendix A) and HRMS spectra (see experimental part) were used to confirm mono-substitution. However, regioselevtivity of these two reactions was not verified until X-ray analysis was conducted, as shown in Figure 2-13. Under similar conditions, stronger nucleophiles *p*-methylthiophenol were used to react with BODIPY **1a** produced 3,8-di-substituted product **19**, isolated in 93% yield.

As mentioned above, X-ray analysis further verifies the regioseletivity of nucleophilic addition/elimination reactions. The structures of BODIPYs **17** and **18** both exhibit a disorder, in which 3-chloro and 5-methyl groups are swapped. In both cases, there is about 8% population of the minor component. There are the mean deviations of 0.033 and 0.061 Å from coplanarity of the C_9BN_2 core for BODIPYs **17** and **18**. Interestingly, 8-aniline plane forms a dihedral angle of 68.6° with BODIPY core, while 8-phenoxy group forms an angle of 86.7°.

Furthermore, in order to investigate the versatility of BODIPY **1a**, step-wise functionalization using both nucleophilic addition/elimination and Stille cross-coupling reactions was performed on such platform, as shown in Scheme 2-8. Therefore, BODIPY **20** could be prepared by a Stille coupling reactions with tributylphenylstannane, followed by a S_NAr reaction with excess amount of SH-carborane in THF in 56% overall yields. On the other hand, under the similar conditions, BODIPY **21** could be obtained in good yield (86% for steps) by a nucleophilic addition/elimination and a subsequent Stille coupling reaction. The crystals of **20** was obtained for the X-ray analysis, as shown in Figure 2-14, which further confirm the regioselectivity of this

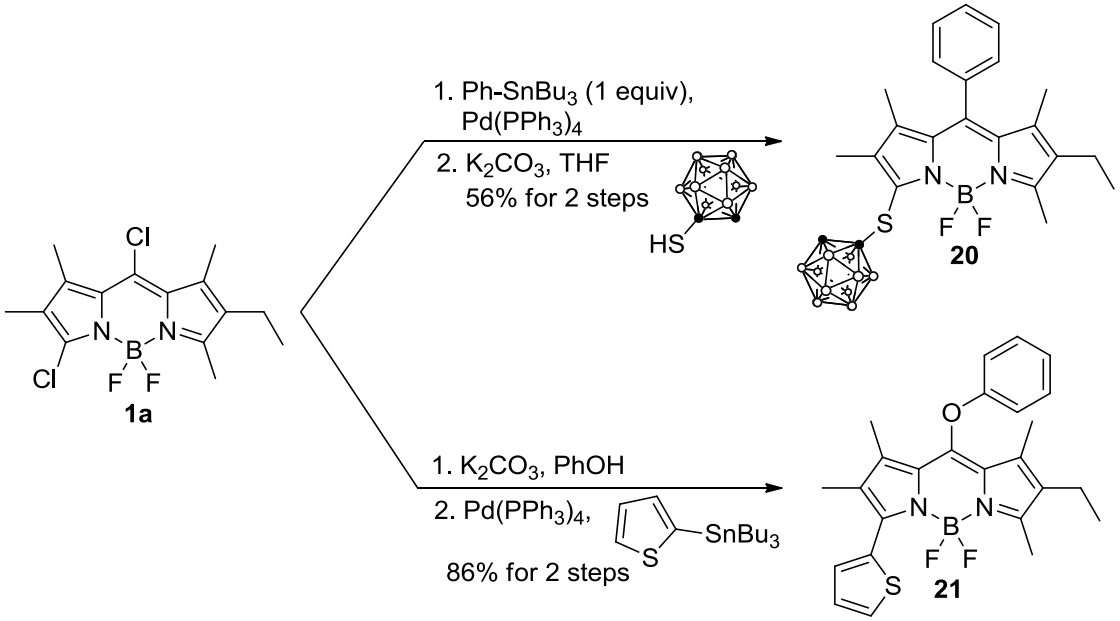

Scheme 2-8: Synthesis of asymmetric BODIPYs **20** and **21**.

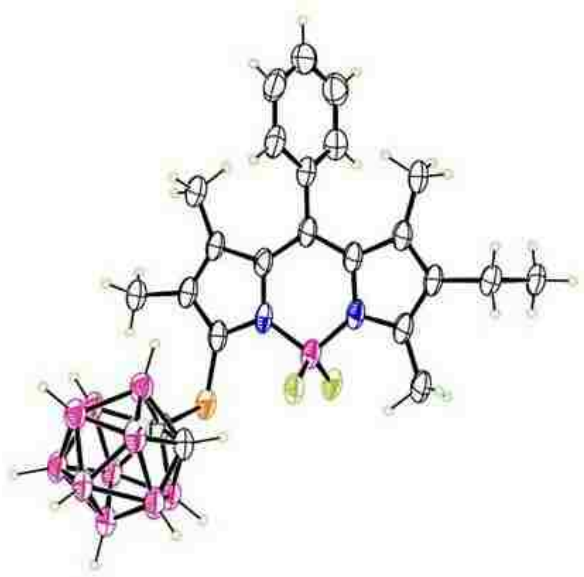

Figure 2-14: X-ray structure of BODIPYs **20,** 50% probability ellipsoids.

reaction. The mean deviation of 0.019 Å of the BODIPY core and a dihedral angle of 77.98 Å between the 8-phenyl group and C_9BN_2 core were observed, respectively.

Finally, the reactivity investigation of 5-methyl group of BODIPY platform **1a** by using classic Knoevenagel condensations and oxidation reactions was conducted, as shown in Scheme

2-9. A reaction between BODIPY **12c** and 10 equivalents of 4-formylbenzoate in the presence of TsOH, piperidine and refluxed toluene for 72 hours afforded a monostyryl-BODIPY dye **22** as the major product, along with a small amount of dipyrromethene **23** as byproduct, maybe due to long time heating in a slightly acidic condition. Treating **23** with TEA, followed by a complexation reaction with $BF_3{\cdot}OEt_2$ reproduced styryl BODOPY **22**. On the other hand, an oxidation reaction of BODIPY **12c** with DDQ in the refluxed toluene produced the desired 5-formyl BODIPY **24** in 26% isolated yield, along with a large amount of unknown byproduct. Besides, longer reaction time and a larger amount of DDQ did not lead to the further oxidization of the α-formyl group to a carboxylic acid group of BODIPY **24**.

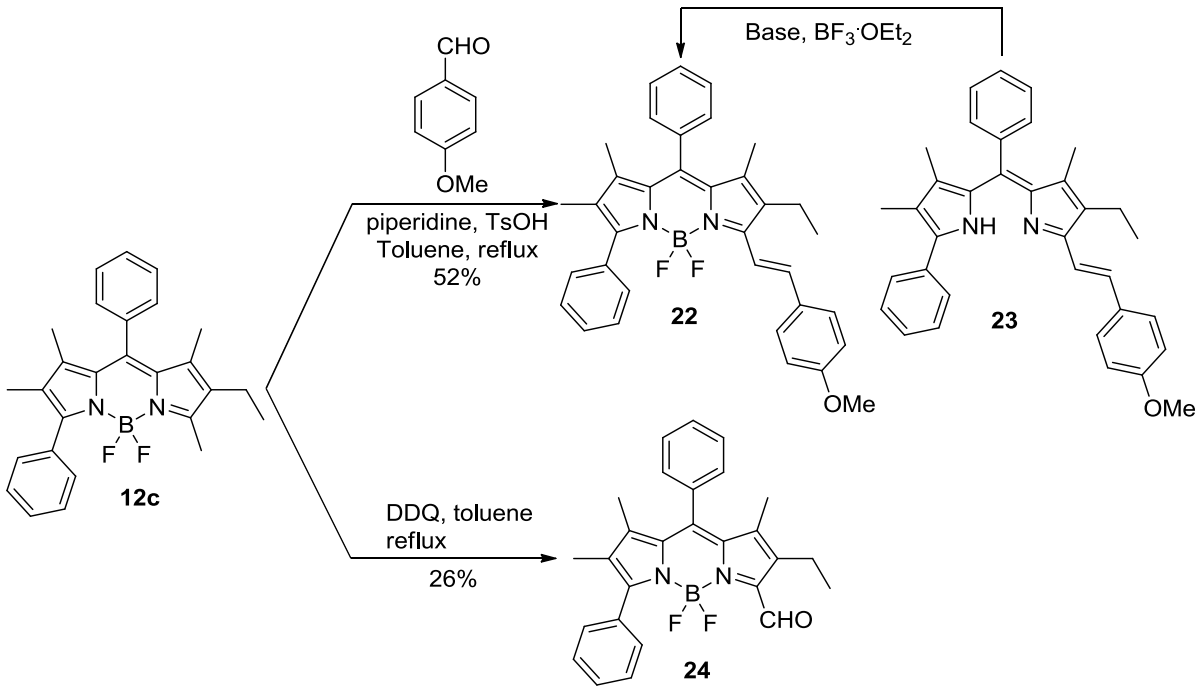

Scheme 2-9: Knoevenagel and oxidation reactions of BODIPY **12c**.

Suitable crystals of BODIPY **22** and **24** that were grown by slow evaporation in the chloroform were used for X-ray analysis, and the results are shown in Figure 2-15. There are two independent molecules and the chloroform solvate presented in the both structures of BODIPY **22**

and **24**. Two independent molecules in BODIPY **22** have the mean deviations of 0.064 and 0.078 Å from coplanarity of BODPY 12-atom core. Additionally, in such two molecules, the 8-phenyl group, the 3-phenyl group, and the 5-styryl group form dihedral angles of 84.0 and 75.08º, 59.8 and 65.98°, and 26.2 and 22.78º with the BODIPY core. In BODIPY **24**, the mean deviation of 0.075 Å from coplanarity is observed. The 8-phenyl group and the formyl C-C=O group form dihedral angles of 72.78 and 6.28º with the BODIPY core.

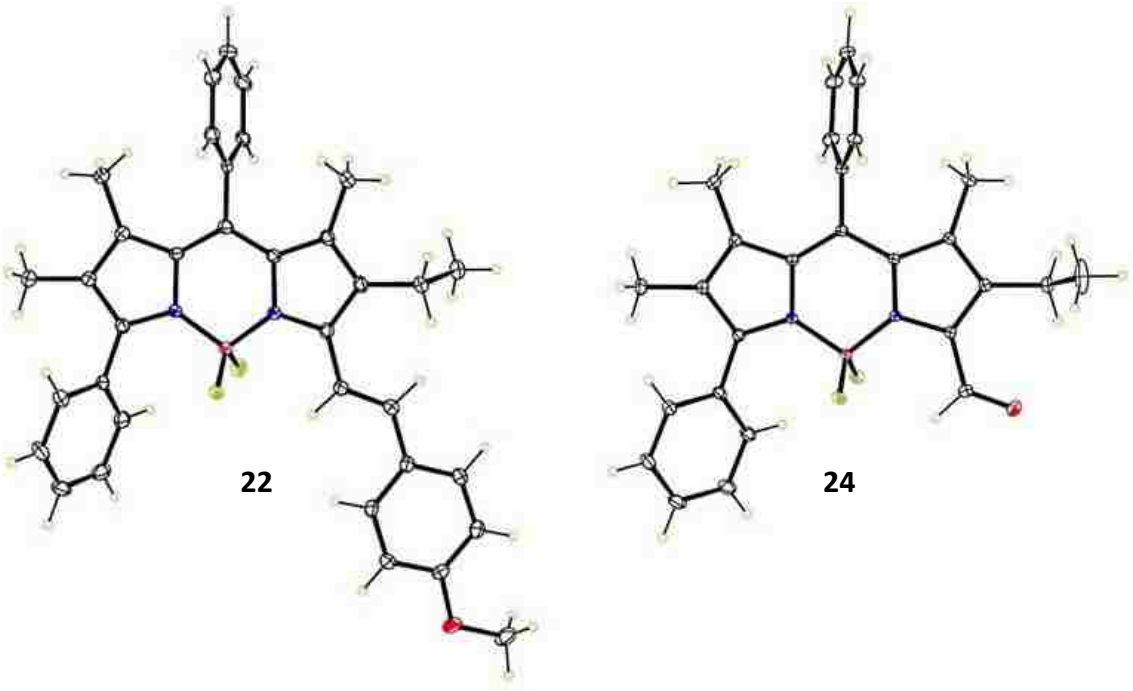

Figure 2-15: X-ray structures of BODIPYs **22** and **24**, 50% probability ellipsoids.

2.4 Spectroscopic Properties

The spectroscopic properties of BODIPYs **1a-b**, **12a–c**, **13a–c**, **14**–**21**, **22** and **24** in dichloromethane namely their maximum absorption (λ_{abs}) and fluorescence wavelengths (λ_{em}), Stokes shifts, molar extinction coefficients (log ε) and fluorescence quantum yields (Φ_f), are summarized in Table 1. Figures 2-16, 2-17 and 2-18 show the normalized absorption and fluorescence spectra of all the new BODIPYs. Such BODIPYs showed the characteristic strong and narrow absorption bands (log ε = 4.22–4.95) and emission bands. Compared to 3,8-chloro-

Table 1: Spectroscopic properties of BODIPYs **1a,b**, **6a-c**, **7a-c** and **8-17** in dichloromethane at room temperature.

BODIPY	Absorption λ_{abs} (nm)	log ε ($M^{-1}cm^{-1}$)	Emission λ_{em} (nm)	Φ_f	Stokes shift (nm)
1a	517	4.80	540	0.52	23
1b	513	4.95	536	0.33	23
12a	547	4.64	591	0.097	44
12b	586	4.78	611	0.022	25
12c	523	4.71	551	0.46	28
13a	529	4.73	548	0.09	19
13b	535	4.78	555	0.0097	20
13c	515	4.71	536	0.48	21
14	577	4.53	592	0.097	15
15	556	4.66	577	0.011	21
16	563	4.84	582	0.022	19
17	505	4.52	521	0.89	16
18	487	4.52	531	0.0017	44
19	582	4.35	610	0.13	28
20	512	4.41	532	0.41	20
21	521	4.62	570	0.94	49
22	587	4.22	617	0.73	30
24	538	4.46	562	0.24	24

*For BODIPYs **1a,b**, **12c, 13a,c**, **17**, **18**, **20** and **21** the calculation of fluorescence quantum yield used rhodamine 6G in ethanol (0.95) as standard; for BODIPYs **12a**, **13b**, and **24**, rhodamine B in ethanol (0.49) was used as a standard; for BODIPYs **12b**, **14-16**, **19** and **22**, crystal violet perchlorate in methanol (0.54) was used as standard.

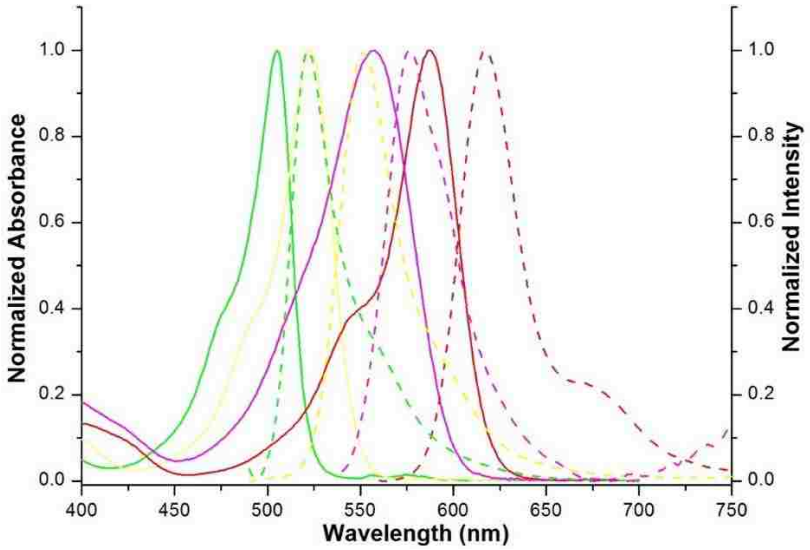

Figure 2-16: Normalized UV-Vis (solid lines) and fluorescence (dash lines) spectra of BODIPYs **12c** (yellow), **15** (magenta), **17** (green) and **22** (red) in dichloromethane at room temperature.

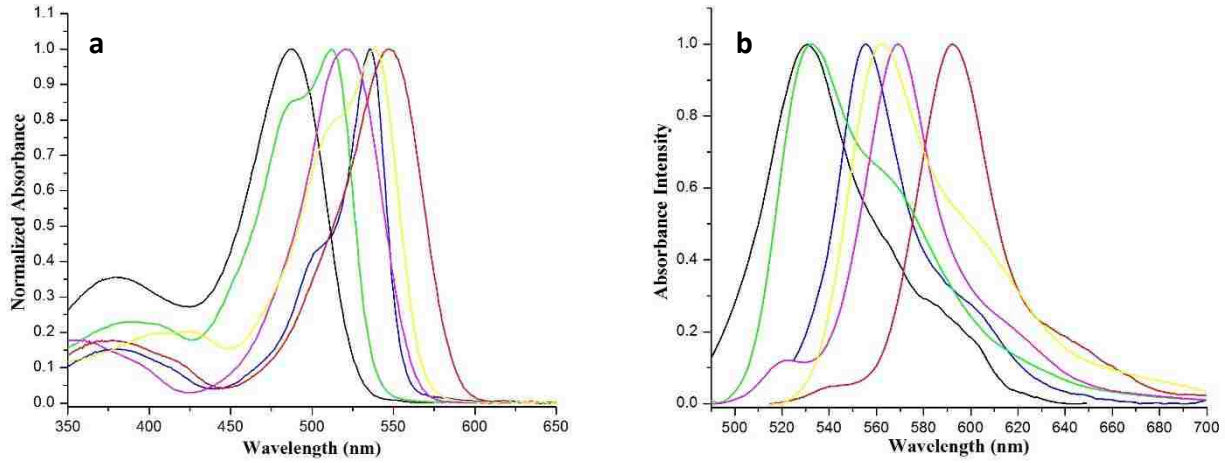

Figure 2-17: Normalized UV-Vis (a) and fluorescence (b) spectra of BODIPY **12a** (red), **13b** (blue), **18** (black), **20** (green), **21** (magenta) and **24** (yellow) in dichloromethane at room temperature.

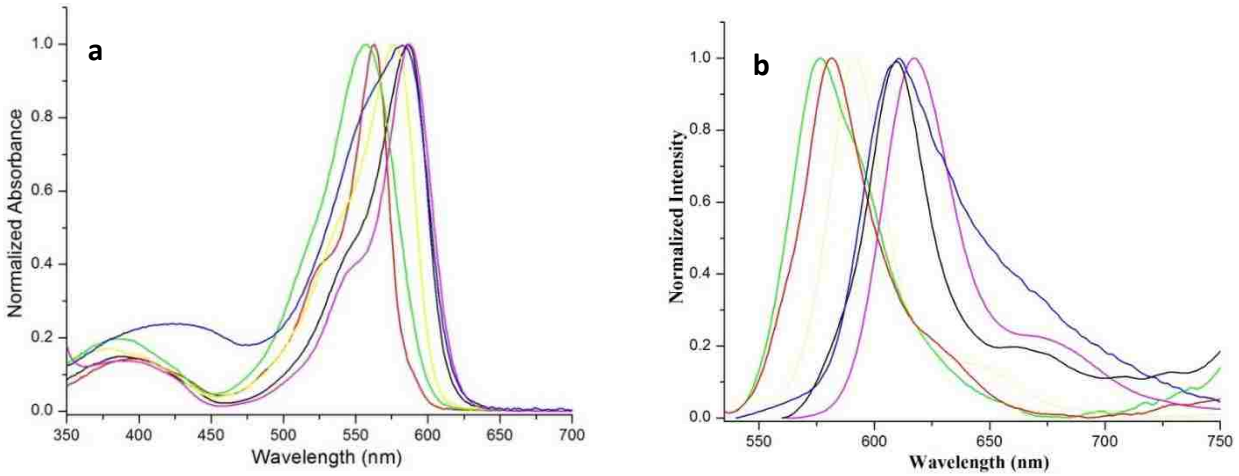

Figure 2-18: Normalized UV-Vis (a) and fluorescence (b) spectra of BODIPY **12b** (black), **14** (yellow), **15** (green), **16** (red), and **19** (Blue), **22** (magenta) in dichloromethane at room temperature.

BODIPY **1a**, 8-phenoxy and 8-phenylamino substitution at the BODIPYs **17** and **18** both led to a blue-shift of 12 nm and 30 nm, as previously reported for 8-aryloxy and 8-arylamino-BODIPYs.[16, 20-23] A widely accepted explanation is that electron-donating groups at the 8-position destabilize the LUMO, which then increases the gap of HOMO–LUMO. Due to the large dihedral angles between their 8-phenyl groups and the BODIP core, **13c** and **20** gave a slight blue-shift in the both absorption and emission.[28] On the other hand, as reported,[28, 33-36] BODIPYs **12a**, **12b**, and **14-16**

with thienyl or furanyl groups at the 3,8-positions provided the largest red-shift, which may be due to the decreased HOMO-LUMO gap. For example, there is a red shift of 60 nm in the absorption of **14**, compared with **1a**. Additionally, compared with **12c,** the 64 nm and 66 nm of red-shift in the absorption and emission were observed for 5-styryl BODIPY **22**, respectively.

The range of Stokes shifts is ranged from by 16-49 nm. As previously reported,[28, 33-35] the largest Stokes shifts were observed for α-thienyl functionalized BODIPYs **21** due to increased geometry relaxation.[37-38] Also, a Stokes shift of 44 nm was observed for 8-phenylamino BODIPY **18**, which is in agreement with previous studies.[17]

The quantum yields vary greatly among different BODIPYs. As reported, 8-phenoxyl BODIPYs **17** and **21** provided the largest quantum yields (0.89 and 0.94) of all BODIPYs synthesized, whereas BODIPY **18** bearing 8-phenylamino was almost nonfluorescent (Φ_f <0.002), probably due to intramolecular charge transfer (ICT) in the excited state, as reported.[17] On the other hand, 3,8-(di)thienyl-, or 3,5-(di)furanyl-functionalized BODIPYs **12a-b**, **13a-b**, and **14-16** possessed the dramatically decreased fluorescence quantum yields (< 0.1), which may be due to increased energy lost that resulting from free motion of all the thienyl or furanyl groups at the 3- or 8-positions.[33-34]

2.5 Conclusion

In conclusion, a versatile BODIPY platform **1a** was designed and successfully synthesized from commercial available compounds in this Chapter. Excellent regioselectivity for the 8-chloro over 3-chloro group on the BODIPY **1a** was studied using Stille cross-coupling reactions with several different organotin reagents and nucleophilic addition/elimination reactions with N-, O-, and S-centered nucleophiles. Additionally, Knoevenagel condensation and DDQ oxidation reactions were used to investigate the reactivity of the 5-methyl group. 16 crystal structures were obtain to

confirm the regioselectivity of those reactions, as well as the structures of the newly obtained asymmetric BODIPYs, which were also fully characterized by ^{1}H NMR, ^{13}C NMR, HRMS (ESI-TOF), and spectroscopy studies in dichloromethane.

2.6 Experimental

2.6.1 Synthesis

General: All reagents and solvents were purchased from Sigma-Aldrich, Fisher Scientifics or Alfa Aesar as reagent grades and used without further purification. Argon was used to protect the air-sensitive reactions. Analytical TLC (polyester backed, 60Å, 0.2 mm, precoated, Sorbent Technologies) was used to monitor the reactions. Column chromatography was performed on silica gel (60Å, 230-400 mesh, Sorbent Technologies). All ^{1}H NMR and ^{13}C NMR spectra were obtained using Bruker AV-400 nanobay or AV-500 spectrometers (400 MHz or 500 MHz for ^{1}H NMR and 100 MHz for ^{13}C NMR) in $CDCl_3$ with trimethylsilane as an internal standard, at 300K. Chemical shifts (δ) are given in parts per million (ppm) with $CDCl_3$ (7.27 ppm for ^{1}H NMR, 77.0 ppm for ^{13}C NMR). All high-resolution mass spectra (ESI-TOF) were obtained using a 6210 ESI-TOF mass spectrometer (Agilent Technologies). All UV-Visible spectra were recorded on a Varian Cary 50 (solutions) spectrophotometer at room temperature. Fluorescence spectra were studied on a PTI QuantaMaster4/2006SE spectrofluorimeter collected emission spectrum. Spectroscopic grade solvents and a 10 mm path length quartz cuvette were used for both measurements. The determination of optical density (ε) was used the solutions with absorbance of λ_{max} between 0.5—1. The dilute solutions with absorbance of particular excitation wavelength between 0.03-0.08 were used for fluorescence quantum yield measurement. Rhodamine 6G (0.95 in ethanol), rhodamine B (0.49 in ethanol) and crystal violet perchlorate (0.54 in methanol) were used as

external standards for calculation of relative fluorescence quantum yields of BODIPYs. All fluorescence quantum yields (Φ_f) were determined using the following equation:[39]

$\Phi_{x=} \Phi_s \times (F_x/F_s) \times (A_s/A_x) \times (n_x/n_s)^2$

where Φ_x and Φ_s are the fluorescence quantum yields of the test samples and standards; F_x and F_s are the areas under the test samples' and standards' emission peaks; A_x *is* the absorbance at which test samples were excited; A_s the absorbance at which stands were excited; n_x *and* n_s are refractive indexes of test sample and standards.

5-((Benzyloxy)carbonyl)-3,4-dimethyl-1H-pyrrole-2-carboxylic acid 5. Benzyl 3,4,5-trimethyl-1H-pyrrole-2-carboxylate **4**[24] (4.34 g, 17.84 mmol) was dissolved in carbon tetrachloride (270 ml). Sulfuryl chloride (7.69 g, 57 mmol) was added dropwise and the resulting solution was stirred overnight at room temperature. The reaction was stopped when the signals for RCH_2Cl ($\delta\approx$ 4.6) and $CHCl_2$ ($\delta\approx$ 6.7 ppm) disappeared from the ^{1}H NMR spectra measured in CCl_4. Organic solvents were removed under reduced pressure to give a red oil residue. The oil residue was dissolved in dioxane (70 ml) and a solution of sodium acetate (11 g) in water (60 ml) was added. The solution was stirred at 60- 65 ^{o}C for 3 h. The solution was then cooled to room temperature and extracted using diethyl ether (2 x 70 ml). The organic layers were combined and washed with 5% Na_2CO_3 solution. All the aqueous layers were then combined and acidified by slowly adding acetic acid (10%). A white precipitate was filtered and washed thoroughly with water. The solid was redissovled in THF and dried over anhydrous Na_2SO_4. The organic solvents were removed under reduced pressure to give the title product (3.64 g) in 74.7% yield. ^{1}H NMR ($CDCl_3$, 400 MHz): 9.48 (1H, s), 7.40-7.44 (5H, m), 5.36 (2H, s), 2.30 (6H, s); ^{13}C NMR ($CDCl_3$, 100 MHz): 165.7, 160.7, 135.7, 129.2, 128.7, 128.4, 128.4, 127.7, 122.5, 120.8, 66.5, 10.1; MS (ESI-TOF) m/z $[M+H]^+$: 274.1076; calculated for $C_{15}H_{16}NO_4$: 274.1074.

Benzyl 5-(N,N-dimethylcarbamoyl)-3,4-dimethyl-1H-pyrrole-2-carboxylate 6. 5-((benzyloxy)carbonyl)-3,4-dimethyl-1H-pyrrole-2-carboxylic acid **5** (4.6 g, 16.8 mol) was added portionwise into thionyl chloride (65 ml) over 20 min. The mixture was stirred for 30 min at 40-45 ^{o}C. The solvent was removed under reduced pressure to give an oily product. The oily residue was redissolved in anhydrous benzene (130 ml). Then, dimethylamine gas was passed into the mixture for 10 min, and the mixture was kept stirring for another 2 h. The reaction was monitored by TLC. After the reaction was completed, the organic solution was washed with water (100 ml), dilute acetic acid (10%) and water again (100 ml), then dried over anhydrous Na_2SO_4. The organic solvents were removed under reduced pressure to give a yellow oil. Further purification by silica gel chromatography with DCM/MeOH as eluents gave the yellow titled product (4.3 g, 85.1%)**.** ^{1}H NMR: ($CDCl_3$, 400 MHz): 9.05 (1H, s), 7.34-7.42 (5H, m), 5.31 (2H, s), 3.06 (6H, s), 2.28 (3H, s), 2.04 (3H, s)**;** ^{13}C NMR ($CDCl_3$, 100 MHz): 164.7, 160.9, 136.1, 128.6, 128.2, 127.2, 126.3, 120.6, 119.8, 66.0, 10.3, 10.3; MS (ESI-TOF) m/z $[M+H]^+$: 301.1548; calculated for $C_{17}H_{21}N_2O_3$: 301.1547.

Benzyl 5-(4-ethyl-3,5-dimethyl-1H-pyrrole-2-carbonyl)-3,4-dimethyl-1H-pyrrole-2-carboxylate 8. Benzyl 5-(N,N-dimethylcarbamoyl)-3,4-dimethyl-1H-pyrrole-2-carboxylate **6** (1.808g, 6.02 mmol) was dissolved in warm $POCl_3$ (9.23g, 60.2 mmol) The mixture was stirred at 50 ^{o}C for 5 h and then cooled to room temperature. Excess $POCl_3$ was removed by evaporation using a CH_2Br_2 chaser under reduced pressure to give a red oily product that was then redissolved in DCM (4 ml). A solution of 3-ethyl-2,4-dimethylpyrrole (0.82 ml, 6.02 mmol) in DCM (4 ml) was added into the mixture under argon. The mixture was then stirred at 30 ^{o}C overnight. The reaction was monitored by UV-Vis (reaction was stopped when extinctions at 351 nm/399 nm reached a maximum). A solution of sodium acetate (10 g) in water (25 ml) added into the mixture,

which was then refluxed for 2-3 h. After the mixture was cooled to room temperature, chloroform (50 ml × 3) was used to extract the organic components which were washed with water, aqueous Na_2CO_3 solution (10%), H_2O again and finally dried over anhydrous $NaSO_4$. The organic solvents were removed under reduced pressure and then the residue was crystallized from Et_2O. Further purification by silica gel chromatography (DCM/MeOH as eluents) gave a pale yellow product (1.95 g), in 85.7% yield. ^{1}H NMR: ($CDCl_3$, 400 MHz): 9.20 (1H, s), 8.78 (1H, s), 7.35-7.44 (5H, m), 5.33 (2H, s), 2.38-2.42 (2H, q), 2.36 (3H, s), 2.31 (3H, s), 2.25 (3H, s), 2.15 (3H, s), 1.04-1.08 (3H, t); ^{13}C NMR ($CDCl_3$, 100 MHz): 175.6, 161.2, 136.0, 133.0, 131.4, 128.6, 128.3, 128.2,127.8, 127.7, 127.4, 125.4, 124.3, 120.4, 66.1, 17.3, 15.0, 11.5, 10.8, 10.3, 9.9; MS (ESI-TOF) m/z $[M+H]^+$: 379.2017; calculated for $C_{23}H_{27}N_2O_3$: 379.2016.

(4-Ethyl-3,5-dimethyl-1H-pyrrol-2-yl)(5-iodo-3,4-dimethyl-1H-pyrrol-2-yl)methanone 11. To a 250 ml flask equipped with a magnetic stirrer was added Pd/C (165 mg, 10%). The flask was evacuated and refilled with THF (10 ml) and then with H_2. The mixture was stirred strongly for 15 min under a H_2 atmosphere. A THF (150 ml) solution of dipyrroketone **8** (1.65 g, 4.36 mmol) was added to the flask under H_2. The mixture was stirred at room temperature for 12 h. The reaction was stopped when starting material had disappeared according to TLC. The palladium catalysts were filtered through a Celite cake and washed with THF (100 ml × 3). The organic solutions were combined and the solvents were removed under reduced pressure to yield a while solid. The solid products then were dissolved in a mixture of $NaHCO_3$ (1.87 g, 22.3 mmol)/H_2O (110 ml) and MeOH (44 ml). A solution of I_2 (1.63 g, 6.42 mmol) in MeOH (26 ml) was added dropwise into the mixture at the room temperature and brown solids were precipitated out immediately. The mixture was stirring for another 2 h at the room temperature after the addition was completed. The precipitates were filtered and washed with water, saturated $NaHCO_3$ (aq), water again and hexanes

to remove excess iodine. The solids were redissolved in DCM and dried over anhydrous Na_2SO_4. The organic solvents were removed under reduced pressure to give a pure pale yellow product (1.36 g, 84.2%). ^{1}H NMR: ($CDCl_3$, 400 MHz): 8.79 (1H, s), 8.64 (1H, s), 2.38-2.43 (2H, q), 2.45 (3H, s), 2.17 (3H, s), 2.13 (3H, s), 2.00 (3H, s), 1.06-1.10 (3H, t); ^{13}C NMR ($CDCl_3$, 100 MHz): 174.5, 133.6, 131.1, 126.9, 126.5, 126.4, 124.9, 124.8, 73.2, 17.3, 15.1, 11.9, 11.5, 11.2, 10.8; MS (ESI-TOF) m/z $[M+H]^+$: 371.0613; calculated for $C_{15}H_{20}IN_2O$: 371.0615.

3,8-Dichloro-6-ethyl-1,5,7-trimethyl-BODIPY 1a-b. Iodo-dipyrroketone **11** (1.36 g, 3.67 mmol) was dissolved in chloroform (300 ml). The flask was evacuated and refilled with argon. Phosgene solution (15% in toluene, 26 ml) was added into the mixture and then it was stirred overnight at room temperature. The reaction was stopped when the starting materials were totally consumed. N_2 was purged into flask to purge extra phosgene into a beaker containing saturated $NaHCO_3$ solution. The organic solvents were removed under reduced pressure to obtain red solids. The red solid was added into another 500 ml round-bottom flask equipped with a stirrer. The flask was evacuated and refilled with argon. Chloroform (300 ml) and N,N-diisopropylethylamine (3.32 g, 25.7 mmol) was added under argon. The mixture was then stirred for 30 min. $BF_3{\cdot}OEt_2$ (5.2 g, 36.7 mmol) was added into the mixture which was stirred for another 10 h. The organic solution was washed with water, saturated $NaHCO_3$ solution and brine. After drying over anhydrous Na_2SO_4, the organic solvents were removed under reduced pressure. Further purification by silica-gel column chromatography with DCM/hexanes as the eluents gave the titled BODIPY **1a** (0.99 g, 78.2%) and its 8-monochloro-BODIPY byproduct (68 mg, 6%). For BODIPY **1a:** ^{1}H NMR ($CDCl_3$, 400 MHz): 2.54 (3H, s), 2.40-2.45 (8H, m), 2.01(3H, s), 1.05-1.09 (3H, t); ^{13}C NMR ($CDCl_3$, 100 MHz): 158.4, 140.4, 138.2, 137.5, 135.4, 135.2, 130.8, 127.6, 124.5, 17.1, 14.5, 14.2, 14.1, 12.9, 8.9; MS (ESI-TOF) m/z $[M+H]^+$ 344.0937; calculated for $C_{15}H_{17}BCl_2F_2N_2$: 344.0939.

For the 8-monochloro-BODIPY byproduct **1b**: ^{1}H NMR ($CDCl_3$, 400 MHz): 7.40 (1H, s), 2.53 (3H, s), 2.40-2.45 (8H, m), 2.04(3H, s), 1.05-1.09 (3H, t); ^{13}C NMR (CDCl3, 400 MHz): 157.8, 140.6, 138.7, 137.5, 137.0, 134.6, 131.0, 129.2, 126.7, 17.1, 14.6, 14.1, 13.4, 12.9, 10.0; MS (ESI-TOF) m/z $[M+H]^+$ 310.1307; calculated for $C_{15}H_{19}BClF_2N_2$: 310.1329.

General procedure for the preparation of BODIPY 12a-c. Into a 50 ml round-bottom flask was added 3,8-dichloro-5-methyl-BODIPY **1a** (34.4 mg, 0.1 mmol) and $Pd(PPh_3)_4$ (10 mol%). The flask was then evacuated and refilled with argon 3 times. Dry toluene (30 ml) and organostannane regents (0.3 mmol) were introduced into the flask. The mixture was refluxed for 6 h under an argon atmosphere. The reaction was stopped when TLC showed the disappearance of starting materials. Toluene was removed under reduced pressure. A flash column (DCM as eluent) was used to separate the crude products. Further purification by using a silica gel column with DCM/hexanes or ethyl acetate/hexanes as the eluents gave the desired disubstituted products.

BODIPY 12a: Yield: 37.7 mg, 85.6%; ^{1}H NMR ($CDCl_3$, 400 MHz): 7.50-7.55 (3H, m), 7.02-7.19 (3H, m), 2.51(3H, s), 2.31-2.36 (2H, q), 1.97 (3H, s), 1.53 (6H, s), 0.99-1.03 (3H, t); ^{13}C NMR ($CDCl_3$, 100 MHz): 158.6, 145.4, 140.4, 138.2, 135.6, 134.9, 133.5, 133.0, 132.8, 132.1, 130.6, 130.5, 128.1, 127.7, 127.7, 127.5, 127.0, 17.1, 14.4, 13.0, 11.3, 11.1, 10.4; MS (ESI-TOF) m/z $[M+H]^+$ 440.1445; calculated for $C_{23}H_{23}BF_2N_2S_2$: 440.1473.

BODIPY 12b: Yield: 25.8 mg, 63.2%; ^{1}H NMR ($CDCl_3$, 400 MHz): 7.49-7.64 (3H, m), 6.44-6.59 (3H, m), 2.57(3H, s), 2.32-2.38 (2H, q), 2.17 (3H, s), 1.52 (3H, s), 1.50 (3H, s), 1.01-1.05 (3H, t); ^{13}C NMR ($CDCl_3$, 400 MHz): 157.9, 147.3, 146.0, 143.6, 142.5, 142.4, 139.2, 138.7, 134.4, 133.8, 133.5, 127.7, 126.3, 115.2(t), 112.3, 111.7, 111.5, 17.1, 14.4, 13.0, 10.9, 10.4; MS (ESI-TOF) m/z $[M+H]^+$ 408.1905; calculated for $C_{23}H_{23}BF_2N_2O_2$: 408.193.

BODIPY 12c: Yield: 34.6 mg, 80.8%; ^{1}H NMR ($CDCl_3$, 400 MHz): 7.35-7.49 (10H, m), 2.46 (3H, s), 2.27-2.33 (2H, q), 1.79 (3H, s), 1.32 (3H, s), 1.35 (3H, s), 0.96-0.99 (3H, t); ^{13}C NMR ($CDCl_3$, 100 MHz): 156.8, 153.2, 141.3, 139.8, 138.2, 135.8, 134.0, 132.9, 131.8, 130.9, 130.0, 129.1, 128.9, 128.4, 128.3, 127.6, 126.4, 17.1, 14.4, 12.8, 12.1, 11.8, 9.7MS (ESI-TOF) m/z $[M-F]^+$ 408.2284; calculated for $C_{27}H_{26}BFN_2$: 408.2282.

General procedure for the preparation of BODIPY 13a-c. Into a 100 ml round-bottom flask was added BODIPY **1a** (34.4 mg, 0.1 mmol) and $Pd(PPh_3)_4$ (10 mol%). The flask was then evacuated and refilled with argon 3 times. Dry toluene (60 ml) and organostannane regents (0.1 mmol) were introduced into the flask. The mixture was refluxing at 80 ^{o}C under Ar. The reaction was stopped when TLC showed the disappearance of starting materials. Toluene was removed under reduced pressure. Silica gel flash column chromatography was used for purification of the products, elution with dichloromethane/hexanes or ethyl acetate/hexanes.

BODIPY 13a: Yield: 33 mg, 84%; ^{1}H NMR ($CDCl_3$, 400 MHz): 6.99-7.52 (3H, m), 2.58(3H, s), 2.31-2.37 (2H, q), 1.92 (3H, s), 1.52 (3H, s), 1.48 (3H, s), 1.00-1.03 (3H, t); ^{13}C NMR ($CDCl_3$, 100 MHz): 159.4, 141.1, 139.0, 138.1, 135.1, 134.8, 133.4, 132.7, 130.2, 128.1, 127.7, 127.6, 124.3, 17.1, 14.3, 13.0, 11.3, 11.1, 8.8; MS (ESI-TOF) m/z $[M+H]^+$ 392.1208; calculated for $C_{19}H_{20}BClF_2N_2S$: 392.1206.

BODIPY 13b: Yield: 29 mg, 77%; ^{1}H NMR ($CDCl_3$, 400 MHz): 6.45-7.64 (3H, m), 2.57(3H, s), 2.32-2.38 (2H, q), 1.93 (3H, s), 1.52 (3H, s), 1.49 (3H, s), 1.01-1.05 (3H, t); ^{13}C NMR ($CDCl_3$, 100 MHz): 160.3, 145.1, 142.8, 140.8, 139.3, 137.7, 135.1, 134.1, 130.6, 126.9, 124.3, 111.8, 111.6, 17.1, 14.3, 13.1, 10.8, 10.6, 8.8; MS (ESI-TOF) m/z $[M+H]^+$ 376.1410; calculated for $C_{19}H_{20}BClF_2N_2O$: 376.1434.

BODIPY 13c: Yield: 32.4 mg, 83. %; ^{1}H NMR ($CDCl_3$, 400 MHz): 7.28-7.50 (5H, m), 2.58(3H, s), 2.29-2.35 (2H, q), 1.90 (3H, s), 1.28 (3H, s), 1.30 (3H, s), 0.98-1.02 (3H, t); ^{13}C NMR ($CDCl_3$, 100 MHz): 158.5, 140.8, 140.5, 138.4, 137.9, 135.1, 134.7, 132.2, 129.4, 129.2, 129.1, 128.1, 124.0, 17.1, 14.4, 12.9, 12.1, 11.9, 8.8; MS (ESI-TOF) m/z $[M-F]^+$ 366.1567; calculated for $C_{21}H_{22}BClFN_2$: 366.1579;

BODIPY 14: Into a 50 ml round-bottom flask was added BODIPY **7a** (19.6 mg, 0.05 mmol) and $Pd(PPh_3)_4$ (10 mol%). The flask was then evacuated and refilled with argon 3 times. Dry toluene (20 ml) and tributyl-(2-furyl)stannane (0.1 mmol) were introduced into the flask. The mixture was refluxed for 6 h under Ar. The reaction was stopped when TLC showed the disappearance of starting materials. Toluene was removed under reduced pressure. A flash column (DCM as eluent) was used to give the crude products. Further purification by silica gel column chromatography with DCM/hexanes or ethyl acetate/hexanes as the eluents gave the desired disubstituted products. Yield: 19.3 mg, 91%; ^{1}H NMR ($CDCl_3$, 400 MHz): 7.46-7.53 (3H, m), 6.59-7.17 (3H, m), 2.57 (3H, s), 2.3-2.37 (2H, q), 2.15 (3H, s), 1.52 (6H, s), 1.00-1.04 (3H, t); ^{13}C NMR ($CDCl_3$, 100 MHz): 157.2, 147.2, 143.5, 141.8, 139.7, 139.0, 135.8, 134.5, 133.1, 132.8, 128.2, 127.8, 127.6, 127.4, 114.9 (t), 112.2, 17.1, 14.4, 12.9, 11.1, 11.0, 10.9; MS (ESI-TOF) m/z $[M+Na]^+$ 446.1517; calculated for $C_{23}H_{23}BF_2N_2NaOS$ 446.1521.

BODIPY 15: Into a 50 ml round bottom flask was added BODIPY **7b** (18.8 mg, 0.05 mmol) and $Pd(PPh_3)_4$ (10 mol%). The flask was then evacuated and refilled with argon for 3 times. Dry toluene (20 mL) and 2-(tributylstannyl)thiophene (0.15 mmol) were introduced into the flask. The mixture was refluxed for 6 h under Ar. The reaction was stopped when TLC showed the disappearance of starting materials. Toluene was removed under reduced pressure. A flash column (DCM as eluent) was used to give the crude products. Further purification by silica gel column

with DCM/hexanes or ethyl acetate/hexanes as the eluents gave the desired disubstituted product. Yield: 19 mg, 89.6%; ^{1}H NMR ($CDCl_3$, 400 MHz): 7.5-7.66 (3H, m), 6.47-7.18 (3H, m), 2.51 (3H, s), 2.32-2.37 (2H, q), 1.99 (3H, s), 1.53 (6H, s), 1.00-1.04 (3H, t); ^{13}C NMR ($CDCl_3$, 100 MHz): 159.4, 146.0, 145.8, 142.6, 140.0, 137.9, 134.8, 134.1, 132.8, 132.6, 130.6 (t), 127.8, 127.6, 127.1, 127.0, 111.7, 112.5, 17.1, 14.4, 13.1, 10.7, 10.5, 10.4; MS (ESI-TOF) m/z $[M+H]^+$ 424.1674; calculated for $C_{23}H_{24}BF_2N_2OS$: 424.1701;

BODIPY 16: Into a 50 ml round-bottom flask was added meso-substituted BODIPY **7b** (18.8 mg, 0.05 mmol) and $Pd(PPh_3)_4$ (10 mol%). The flask was then evacuated and refilled with argon 3 times. Dry toluene (4 ml) and trimethyl[(tributylstannyl)ethynyl]silane (0.06 mmol) were introduced into the flask. The mixture was refluxed for 6 h under an argon atmosphere. The reaction was stopped when TLC showed the disappearance of starting materials. Toluene was removed under reduced pressure. A flash column (DCM as eluent) was used to give the crude products. Further purification by silica gel column chromatography with DCM/hexanes or ethyl acetate/hexanes as the eluents gave the desired disubstituted product. Yield: 12.7 mg, 58%; ^{1}H NMR ($CDCl_3$, 400 MHz): 6.43-7.62 (3H, m), 2.59 (3H, s), 2.32-2.37 (2H, q), 1.99 (3H, s), 1.52 (3H, s), 1.45 (3H, s), 1.00-1.04 (3H, t), 0.31 (9H, s); ^{13}C NMR ($CDCl_3$, 100 MHz): 162.1, 145.8, 143.0, 141.1, 136.3, 135.8, 132.7, 132.6, 132.2, 126.9, 112.0, 111.8, 109.3, 97.3, 17.5, 14.6, 13.7, 10.9, 10.7, 10.0, 0.2; MS (ESI-TOF) m/z $[M+H]^+$ 438.2223; calculated for $C_{24}H_{30}BF_2N_2OSi$: 438.2219;

General procedure for the preparation of BODIPYs 17-19. Into a 5 ml round-bottom flask was added BODIPY **1a** (17.2 mg, 0.05 mmol), nucleophile (1 - 10 equiv) and K_2CO_3 (13.8 mg, 0.1 mmol). DCM (0.5 ml) was added into the flask. The mixture was stirred at room temperature. The reaction was stopped when TLC showed the disappearance of starting materials. The crude product

was subjected to a short flash column (DCM as eluents) to remove polar byproducts. Further purification by silica gel column chromatography with DCM/hexanes or ethyl acetate/hexanes as the eluents gave the desired mono-substituted products.

BODIPY 17: Yield: 19.1 mg, 95%; ^{1}H NMR ($CDCl_3$, 400 MHz): 6.99-7.34 (5H, m), 2.57 (3H, s), 2.34-2.38 (2H, q), 2.01 (3H, s), 1.98 (3H, s), 1.93 (3H, s), 1.01-1.04 (3H, t); ^{13}C NMR ($CDCl_3$, 400 MHz): 158.6, 157.5, 150.5, 138.2, 137.8, 135.2, 133.9, 130.5, 128.3, 125.6, 123.5, 123.0, 114.7, 16.9, 14.4, 13.0, 12.0, 11.7, 8.6; MS (ESI-TOF) m/z $[M+H]^+$ 402.1564; calculated for $C_{21}H_{23}BClF_2N_2O$: 402.1591.

BODIPY 18: Yield: 17.4 mg, 87%; ^{1}H (400 MHz, $CDCl_3$): 6.93-7.25 (5H, m), 6.55 (1H, s), 2.55 (3H, s), 2.31-2.37 (2H, q), 1.98 (3H, s), 1.91 (3H, s), 1.89 (3H, s), 1.00-1.03 (3H, t); ^{13}C (100 MHz, $CDCl_3$): 153.5, 143.5, 140.6, 135.3, 134.9, 133.0, 132.6, 129.8, 127.2, 125.5, 122.8, 118.0, 17.0, 14.7, 12.9, 12.8, 12.64, 8.8; MS (ESI-TOF) m/z $[M+H]^+$: 401.1725; calculated for $C_{21}H_{24}BClF_2N_3$: 401.1751.

BODIPY 19: Yield: 24.2 mg, 93%; ^{1}H (400 MHz, $CDCl_3$): 7.05-7.22 (8H, m), 2.60 (3H, s), 2.36-2.41 (5H, m), 2.31 (6H, s), 2.29 (3H, s), 1.72 (3H, s), 1.01-1.04 (3H, t); ^{13}C (100 MHz, $CDCl_3$): 160.4, 143.6, 141.9, 138.2, 137.2, 136.3, 135.9, 134.3, 133.0, 132.8, 132.1, 131.7, 130.3, 129.8, 129.4, 126.3, 21.1, 21.0, 17.2, 14.5, 14.4, 13.2, 10.1; MS (ESI-TOF) m/z $[M+H]^+$: 520.2085; calculated for $C_{29}H_{32}BF_2N_2S_2$: 520.2099.

BODIPY 20: Into a 5 ml round-bottom flask was added BODIPY **13c** (19.3 mg, 0.05 mmol), SH-carborane (88 mg, 0.5 mmol) and K_2CO_3 (13.8 mg, 0.1 mmol). DCM (1 ml) was added into the flask. The mixture was then refluxed at room temperature. The reaction was quenched with H_2O when TLC showed the disappearance of starting materials. DCM (10 ml × 3) was used to extract the organic components. Organic solvents were combined, dried over anhydrous Na_2SO_4 and

evaporated under reduced pressure to give crude products. Further purification by silica gel column chromatography with ethyl acetate/hexanes as the eluents gave the titled product (17.7 mg, 67.3%). ^{1}H NMR (400 MHz, $CDCl_3$): 7.24-7.5 (5H, m), 1.76-3.34 (11 H, m) 2.63 (3H, s), 2.32-2.38 (2H, q), 2.04 (3H, s), 1.36 (3H, s), 1.29 (3H, s), 0.99-1.03 (3H, t); ^{13}C NMR (100 MHz, $CDCl_3$): 165.0, 143.4, 141.6, 137.3, 135.5, 134.9, 134.7, 134.2, 133.3, 132.5, 129.4(t), 128.0, 127.9, 66.3, 66.2, 17.1, 14.1, 13.6, 12.2, 12.1, 11.1; MS (ESI-TOF) m/z $[M+H]^+$ 527.3512; calculated for $C_{23}H_{24}B_{11}F_2N_2S$: 527.3520.

BODIPY 21: Into a 50 ml round-bottom flask was added meso-substiutued BODIPY **17** (10 mg, 0.025 mmol) and $Pd(PPh_3)_4$ (10 mol%). The flask was then evacuated and refilled with argon 3 times. Dry toluene (20 ml) and 2-(tributylstannyl)thiophene (0.05 mmol) were introduced into the flask. The mixture was refluxed for 6 h under an argon atmosphere. The reaction was stopped when TLC showed the disappearance of starting materials. Toluene was removed under reduced pressure. A flash column (DCM as eluent) was used to obtain the crude products. Further purification by silica gel column chromatography with DCM/hexanes or ethyl acetate/hexanes as the eluents gave the desired products. Yield: 10.2 mg, 90.6%; ^{1}H (400 MHz, $CDCl_3$): 7.50-7.53 (2H, m), 7.32-7.36 (2H, m), 7.17-7.19 (1H, m), 7.05-7.1 (3H, m), 2.50 (3H, s), 2.31-2.37 (2H, q), 2.04 (3H, s), 2.02 (3H, s), 1.99 (3H, s), 0.99-1.03 (3H, t); ^{13}C (100 MHz, $CDCl_3$): 157.8, 157.7, 150.9, 145.4, 137.4, 135.3, 133.6, 132.7, 130.4 (t), 130.1, 128.3, 127.6, 127.0 126.7, 123.0, 122.8, 114.9, 17.0, 14.5, 13.0, 11.9, 11.7, 10.2; MS (ESI-TOF) m/z $[M+H]^+$ 450.1831; calculated for $C_{25}H_{26}BF_2N_2OS$: 450.1858.

BODIPY 22: Into a 50 ml round-bottom flask was added BODIPY **12c** (21.4 mg, 0.05 mmol), some molecular sieves and methyl 4-formylanisole (68 mg, 0.5 mmol) in toluene (10 ml). *p*-TsOH (10 mg) and piperidine (0.1 ml) were added into the mixture**.** The mixture was stirred and refluxed

for 72 h under the argon atmosphere. The reaction was stopped when TLC showed the disappearance of starting materials. The mixture was cooled to room temperature and filtered to remove molecule sieves. The filtrate was poured into water (20 ml), and DCM (20 ml × 3) was used to extract the organic components. The organic solvents were combined, dried over anhydrous Na_2SO_4 and evaporated under reduced pressure to give crude products. Further purification by silica gel column chromatography with ethyl acetate/hexanes as the eluents gave the styryl-BODIPY dye **22** (14.2 mg, 52%). ^{1}H (400Hz, $CDCl_3$): 7.13-7.60 (14H, m), 6.85-6.87 (2H, d), 3.83 (3H, s), 2.56-2.62 (2H, q), 1.80 (3H, s), 1.36 (6H, s), 1.13-1.16 (3H, t); ^{13}C (400Hz, $CDCl_3$): 160.3, 154.1, 152.1, 140.3, 140.1, 138.4, 136.2, 136.1, 133.9, 132.9, 132.8, 131.9, 130.0, 129.1, 128.9, 128.5, 127.7, 127.2, 117.9, 114.1, 55.4, 18.4, 14.0, 12.2, 11.6, 9.8; MS (ESI-TOF) m/z $[M+H]^+$ 545.2687; calculated for $C_{35}H_{33}BF_2N_2O$: 545.2685.

BODIPY 24: Into a 50 ml round-bottom flask was added BODIPY **12c** (21.4 mg, 0.05 mmol). The flask was then evacuated and refilled with argon 3 times. Dry toluene (10 ml) was added**.** The temperature was raised to 110 ^{o}C. A solution of DDQ (56.8 mg, 0.25 mmol) in toluene (10 ml) was added slowly into the mixture which was stirred and refluxed under an argon atmosphere. The reaction was stopped when TLC showed the disappearance of starting materials. Solvents were removed under reduced pressure to give crude products. Further purification by using a silica gel column or preparative TLC plates with ethyl acetate/hexanes as the eluents gave the compound **17** (5.7 mg, 25.8% yield). ^{1}H NMR (400Hz, $CDCl_3$): 10.30 (1H, s), 7.37-7.59 (5H, m), 2.67-2.71 (2H, q), 1.84 (3H, s), 1.44 (3H, s), 1.31 (3H, s), 1.00-1.03 (3H, t); ^{13}C (400Hz, $CDCl_3$): 186.3, 164.5, 144.7, 144.5, 141.2, 137.2, 136.3, 135.8, 134.9, 132.6, 131.5, 130.9, 130.0, 129.6, 129.5, 129.3, 128.1, 127.8, 17.6, 14.3, 12.9, 10.7, 10.0; MS (ESI-TOF) m/z $[M+H]^+$ 442.2145; calculated for $C_{27}H_{26}BF_2N_2O$: 442.2137.

2.6.2 Crystal data

Diffraction data were collected at low temperature (90-105K) on either a Nonius KappaCCD diffractometer equipped with MoKα radiation (λ=0.71073 Å) or a Bruker Kappa Apex-II DUO diffractometer equipped with Mo or CuKα radiation (λ=1.54184 Å). Refinement was by full-matrix least squares using SHELXL, with H atoms in idealized positions, except for those on N in **8**, **10**, and **18**, which were refined. BODIPYS **1a** and **24** have two independent molecules, and **1b** has four. **1a**, **12b** and **22** were nonmerohedral twins, and disorder was present in **1a**, **12a-c**, **14**, **17** and **18**. **1a** and **24** were chloroform solvates. The absolute structures of both noncentrosymmetric crystals **1b** and **13c** were determined. Crystal data: For **1a**: $C_{15}H_{17}BCl_2F_2N_2$. 0.5 $CHCl_3$, triclinic P-1, a=8.4888(3), b=13.9111(6), c=14.8676(6) Å, α=86.609(3), β=88.646(2), γ=89.580(2)°, Z=4, T=90K, R=0.067; **1b**: $C_{15}H_{18}BClF_2N_2$, monoclinic $P2_1$, a=15.4384(5), b=11.5896(4), c=16.8479(5) Å, β=99.215(2)°, Z=8, T=90K, R=0.047; **8**: $C_{23}H_{26}N_2O_3$, monoclinic $P2_1/n$, a=7.7071(6), b=12.3770(9), c=21.4131(17) Å, β=92.673(4)°, Z=4, T=100K, R=0.045; **10**: $[C_{23}H_{26}ClN_2O_2]Cl$, triclinic P-1, a=8.1637(4), b=9.5889(5), c=13.6082(8) Å, α=94.850(3), β=97.737(2), γ=92.855(2)°, Z=2, T=100K, R=0.033; **12a**: $C_{23}H_{23}BF_2N_2S_2$, triclinic P-1, a=9.5771(14), b=10.3269(15), c=11.567(2) Å, α=77.851(8), β=66.885(6), γ=79.384(7)°, Z=2, T=100K, R=0.041; **12b**: $C_{23}H_{23}BF_2N_2O_2$, triclinic P-1, a=9.362(2), b=10.155(2), c=11.682(3) Å, α=76.840(6), β=66.796(6), γ=77.094(6)°, Z=2, T=90K, R=0.089; **12c**: $C_{27}H_{27}BF_2N_2$, monoclinic $P2_1/n$, a=11.4039(6), b=7.9247(4), c=24.2010(12) Å, β=91.650(3)°, Z=4, T=90K, R=0.047; **13c**: $C_{21}H_{22}BClF_2N_2$, monoclinic Pc, a=7.6918(2), b=8.2818(2), c=14.8858(4) Å, β=94.762(2)°, Z=2, T=105K, R=0.035; **14**: $C_{23}H_{23}BF_2N_2OS$, triclinic P-1, a=9.5378(3), b=10.1969(3), c=11.5554(4) Å, α=76.414(2), β=66.800(2), γ=78.800(2)°, Z=2, T=90K, R=0.040; **15**: $C_{23}H_{23}BF_2N_2OS$, triclinic P-1, a=9.4222(2), b=10.2488(2), c=11.6233(3) Å, α=78.492(2), β=66.845(2), γ=77.813(2)°, Z=2,

T=90K, R=0.043; **16**: $C_{24}H_{29}BF_2N_2OSi$, monoclinic $P2_1/c$, a=6.9871(2), b=22.5959(8), c=14.6041(6) Å, β=93.098(2)°, Z=4, T=90K, R=0.041; **17**: $C_{21}H_{22}BClF_2N_2O$, triclinic P-1, a=9.4115(3), b=10.4033(4), c=11.3995(4) Å, α=66.223(2), β=77.459(2), γ=68.527(2)°, Z=2, T=90K, R=0.051; **18**: $C_{21}H_{23}BClF_2N_3$, monoclinic C2/c, a=21.8367(10), b=8.9694(4), c=21.9939(8) Å, β=114.299(2)°, Z=8, T=90K, R=0.050; **20**: $C_{23}H_{33}B_{11}F_2N_2S$, triclinic P-1, a=6.9030(7), b=12.0111(12), c=17.1906(14) Å, α=77.599(7), β=79.990(7), γ=83.195(7)°, Z=2, T=90K, R=0.070; **22**: $C_{35}H_{33}BF_2N_2O$, triclinic P-1, a=11.5598(5), b=13.2476(6), c=19.1537(8) Å, α=85.869(2), β=86.135(2), γ=72.967(2)°, Z=4, T=90K, R=0.048; **24**: $C_{27}H_{25}BF_2N_2O$. $CHCl_3$, triclinic P-1, a=9.6902(5), b=10.7446(6), c=13.9386(8) Å, α=68.727(3), β=75.951(3), γ=73.728(3)°, Z=2, T=90K, R=0.037; CCDC 1038325-1038340 contain the supplementary crystallographic data for this Chapter. These data can be obtained, free of charge, from the Cambridge Crystallographic Data Centre via www.ccdc.cam.ac.uk/data_request/cif.

2.7 Reference

1. Lu, H.; Mack, J.; Yang, Y.; Shen, Z., *Chem. Soc. Rev.* **2014,** *43* (13), 4778-4823.

2. Ulrich, G.; Ziessel, R.; Harriman, A., *Angew. Chem. Int. Ed.* **2008,** *47* (7), 1184-1201.

3. Loudet, A.; Burgess, K., *Chem. Rev.* **2007,** *107* (11), 4891-4932.

4. Rohand, T.; Baruah, M.; Qin, W.; Boens, N.; Dehaen, W., *Chem. Commun.* **2006,** (3), 266-268.

5. Baruah, M.; Qin, W.; Vallée, R. A. L.; Beljonne, D.; Rohand, T.; Dehaen, W.; Boens, N., *Org. Lett.* **2005,** *7* (20), 4377-4380.

6. Baruah, M.; Qin, W.; Basarić, N.; De Borggraeve, W. M.; Boens, N., *J. Org. Chem.* **2005,** *70* (10), 4152-4157.

7. Qin, W.; Rohand, T.; Dehaen, W.; Clifford, J. N.; Driesen, K.; Beljonne, D.; Van Averbeke, B.; Van der Auweraer, M.; Boens, N., *J. Phys. Chem. A* **2007,** *111* (35), 8588-8597.

8. Dost, Z.; Atilgan, S.; Akkaya, E. U., *Tetrahedron* **2006,** *62* (36), 8484-8488.

9. Gibbs, J. H.; Zhou, Z.; Kessel, D.; Fronczek, F. R.; Pakhomova, S.; Vicente, M. G. H., *J. Photochem. Photobiol. B: Biol.* **2015,** *145*, 35-47.

10. He, H.; Lo, P.-C.; Yeung, S.-L.; Fong, W.-P.; Ng, D. K. P., *J. Med. Chem.* **2011,** *54* (8), 3097-3102.

11. Rurack, K.; Kollmannsberger, M.; Daub, J., *Angew. Chem. Int. Ed.* **2001,** *40* (2), 385-387.

12. Uppal, T.; Bhupathiraju, N. V. S. D. K.; Vicente, M. G. H., *Tetrahedron* **2013,** *69* (23), 4687-4693.

13. Peng, X.; Du, J.; Fan, J.; Wang, J.; Wu, Y.; Zhao, J.; Sun, S.; Xu, T., *J. Am. Chem. Soc.* **2007,** *129* (6), 1500-1501.

14. Lee, J.-J.; Lee, S.-C.; Zhai, D.; Ahn, Y.-H.; Yeo, H. Y.; Tan, Y. L.; Chang, Y.-T., *Chem. Commun.* **2011,** *47* (15), 4508-4510.

15. Kamkaew, A.; Lim, S. H.; Lee, H. B.; Kiew, L. V.; Chung, L. Y.; Burgess, K., *Chem. Soc. Rev.* **2013,** *42* (1), 77-88.

16. Arroyo, I. J.; Hu, R.; Tang, B. Z.; López, F. I.; Peña-Cabrera, E., *Tetrahedron* **2011,** *67* (38), 7244-7250.

17. Bañuelos, J.; Martín, V.; Gómez-Durán, C. F. A.; Córdoba, I. J. A.; Peña-Cabrera, E.; García-Moreno, I.; Costela, Á.; Pérez-Ojeda, M. E.; Arbeloa, T.; Arbeloa, Í. L., *Chem. Eur. J.* **2011,** *17* (26), 7261-7270.

18. Gomez-Duran, C. F. A.; Garcia-Moreno, I.; Costela, A.; Martin, V.; Sastre, R.; Banuelos, J.; Lopez Arbeloa, F.; Lopez Arbeloa, I.; Pena-Cabrera, E., *Chem. Commun.* **2010,** *46* (28), 5103-5105.

19. Goud, T. V.; Tutar, A.; Biellmann, J.-F., *Tetrahedron* **2006,** *62* (21), 5084-5091.

20. Peña-Cabrera, E.; Aguilar-Aguilar, A.; González-Domínguez, M.; Lager, E.; Zamudio-Vázquez, R.; Godoy-Vargas, J.; Villanueva-García, F., *Org. Lett.* **2007,** *9* (20), 3985-3988.

21. Leen, V.; Yuan, P.; Wang, L.; Boens, N.; Dehaen, W., *Org. Lett.* **2012,** *14* (24), 6150-6153.

22. Misra, R.; Dhokale, B.; Jadhav, T.; Mobin, S. M., *Dalton Trans.* **2013,** *42* (37), 13658-13666.

23. Wang, H.; Vicente, M. G. H.; Fronczek, F. R.; Smith, K. M., *Chem. Eur. J.* **2014,** *20* (17), 5064-5074.

24. Johnson, A. W.; Markham, E.; Price, R.; Shaw, K. B., *Journal of the Chemical Society (Resumed)* **1958,** (0), 4254-4257.

25. Smith, K. M.; Craig, G. W.; Eivazi, F.; Martynenko, Z., *Synthesis* **1980,** *1980* (06), 493-495.

26. Jackson, A. H.; Supphayen, D., *J. Chem. Soc., Perkin Trans. 1* **1987,** (0), 277-286.

27. Ballantine, J. A.; Jackson, A. H.; Kenner, G. W.; McGillivray, G., *Tetrahedron* **1966,** *22, Supplement 7* (0), 241-259.

28. Wang, H.; Fronczek, F. R.; Vicente, M. G. H.; Smith, K. M., *J. Org. Chem.* **2014,** *79* (21), 10342-10352.

29. Jiao, L.; Yu, C.; Uppal, T.; Liu, M.; Li, Y.; Zhou, Y.; Hao, E.; Hu, X.; Vicente, M. G. H., *Org. Biomol. Chem.* **2010,** *8* (11), 2517-2519.

30. Leen, V.; Braeken, E.; Luckermans, K.; Jackers, C.; Van der Auweraer, M.; Boens, N.; Dehaen, W., *Chem. Commun.* **2009,** (30), 4515-4517.

31. Rohand, T.; Qin, W.; Boens, N.; Dehaen, W., *Eur. J. Org. Chem.* **2006,** *2006* (20), 4658-4663.

32. Espinet, P.; Echavarren, A. M., *Angew. Chem. Int. Ed.* **2004,** *43* (36), 4704-4734.

33. Chen, Y.; Zhao, J.; Guo, H.; Xie, L., *J. Org. Chem.* **2012,** *77* (5), 2192-2206.

34. Chen, Y.; Zhao, J.; Xie, L.; Guo, H.; Li, Q., *RSC Adv.* **2012,** *2* (9), 3942-3953.

35. Zhao, N.; Vicente, M. G. H.; Fronczek, F. R.; Smith, K. M., *Chem. Eur. J.* **2015,** *21*, 6181-6192.

36. Rihn, S.; Retailleau, P.; Bugsaliewicz, N.; Nicola, A. D.; Ziessel, R., *Tetrahedron Lett.* **2009,** *50* (50), 7008-7013.

37. Brizet, B.; Desbois, N.; Bonnot, A.; Langlois, A.; Dubois, A.; Barbe, J.-M.; Gros, C. P.; Goze, C.; Denat, F.; Harvey, P. D., *Inorg. Chem.* **2014,** *53* (7), 3392-3403.

38. Xu, H.-J.; Bonnot, A.; Karsenti, P.-L.; Langlois, A.; Abdelhameed, M.; Barbe, J.-M.; Gros, C. P.; Harvey, P. D., *Dalton Trans.* **2014,** *43* (22), 8219-8229.

39. Didier, P.; Ulrich, G.; Mely, Y.; Ziessel, R., *Org. Biomol. Chem.* **2009,** *7* (18), 3639-3642.

CHAPTER 3: STEPWISE POLYCHLORINATION OF 8-CHLORO-BODIPY AND REGIOSELECTIVE FUNCTIONALIZATION OF 2,3,5,6,8-PENTACHLORO-BODIPY*

3.1 Introduction

As described in the Chapter 1, halogenated BODIPYs are particularly attractive targets, which allow the introduction of a variety of functional groups to all seven carbon positions on the BODIPY core, via both nucleophilic metal-catalyzed cross-coupling and substitutions reactions.[1] On the other hand, halogenated BODIPYs were also widely applied to the synthesis of aryl-fused BODIPYs, preparation of fluorescent indicators, and photodynamic therapy (PDT) sensitizers, as shown in Chapter 1. In the last two decades, various halogenated BODIPY platforms has been reported, as shown in Figure 1.[2-9] For example, BODIPY **1** is the first halogenated BODIPY that was reported in 1990;[2] 3,5-dichloro-BODIPY **2**[3] were prepared by Dehean and coworkers in 2005

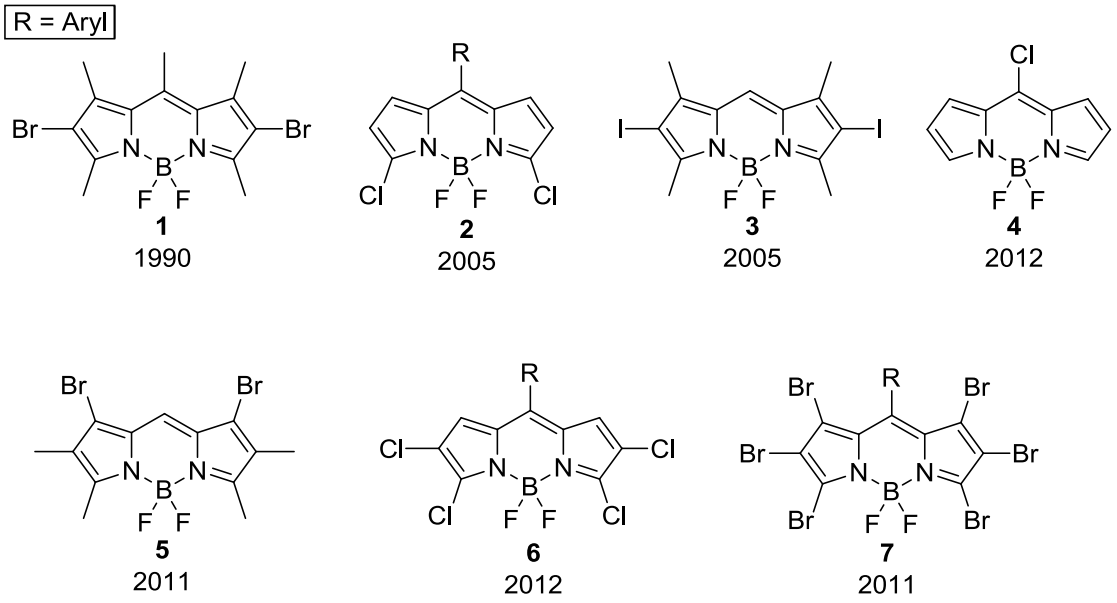

Figure 3-1: Several halogenated BODIPYs

* Reprinted (adpated) with permission from (Zhao, N.; Xuan, S.; Fronczek, F. R.; Smith, K. M.; Vicente, M. G. H., Stepwise Polychlorination of 8-Chloro-BODIPY and Regioselective Functionalization of 2,3,5,6,8-Pentachloro-BODIPY. *J. Org. Chem.* **2015,** *80* (16), 8377-8383). Copyright (2016) American Chemical Society.

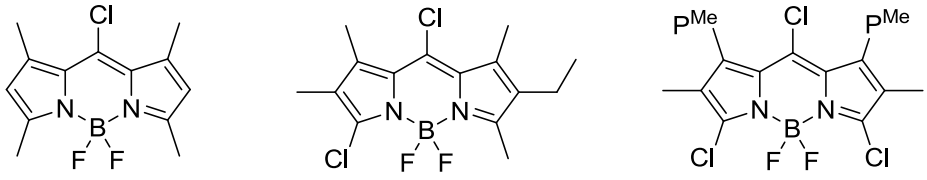

Figure 3-2: Halogenated BODIPYs prepared in Vicente group.

and widely applied as fluorescent indicators (see Chapter 1); hexabromo-BODIPY **7**[5-6] allowed for the full functionalization at all the pyrrolic positions. Generally, there are three main strategies to approach the synthesis of halogenated BODIPYs: (1) direct halogenation at the BODIPY core with suitable halogenation reagents; (2) halogenation at the dipyrromethane stage, and followed by oxidation and boron complexation; (3) halogenation at the pyrrole stage, followed by condensation, oxidation and a boron complexation.

In our group, we are particular interested in the halogenated BODIPYs bearing an 8-chloro group. As described in the recent paper,[10] there is the largest MO coefficients in the LUMO at the 8-position. Thus, the introduction of functional groups at the 8-position will greatly affect the spectroscopic properties, such as the fluorescent quantum yields. Based on this strategy, our group reported the synthesis of the BODIPYs **8**[11], **9**[12] and **10**[13] were all containing an 8-chloro group, and Pd(0) catalyzed coupling reactions and substitution reactions were used to investigated the reactivity and regioselectivity of the chloro groups at the BODIPY periphery. The decreased reactivity order for both nucleophilic addition-elimination and Stille cross coupling reactions was observed to be: 8-Cl >> 3,5-Cl, which allowed for regioselective functionalizations at the 8 and 3,5-positions of the BODIPYs. However, new synthesis of higher halogenated BODIPYs were needed to further investigate the reactivity of the 1,2,6,7-positions. Herein, in this chapter, I focused on developing a convenient and quick method to afford polycholorinated (up to five halo groups) BODIPY dyes with a short reaction time.

3.2 Synthesis of Polychlorinated BODPYs

This work started with the preparation of 8-chloro BODIPY **4** in three steps, as previous reported,[9, 14-16] as shown in Scheme 3-1. The synthesis procedure involved condensation of pyrrole **11** with thiophosgene, followed by oxidative hydrolysis, chlorination by phosgene, and boron complexation under the basic condition in a good overall yield. Treating BODIPY **4** with 10 equiv of NCS in THF at room temperature for up to 24 hours did notyield the desired pentachloro BODIPY **13**, as shown in Scheme 3-2. Separation via prep. TLC provided the mono-chlorinated BODIPY **14** as the major product with a 52% isolated yield. Increasing the temperature, reaction time, or the amount of NCS only provided complex mixtures of chlorinated products, probably as a result of the low reactivity of **4** under these chlorinating conditions, compared with 8-phenyl BODIPY.[8] Therefore, we investigatedalternative methodologies for the regioselective polychlorination of BODIPY **4** using more reactive sources of Cl^+, in particular trichloroisocyanuric acid (TCCA), inspired by the work reported by Mattos et al.[17] In his work, we

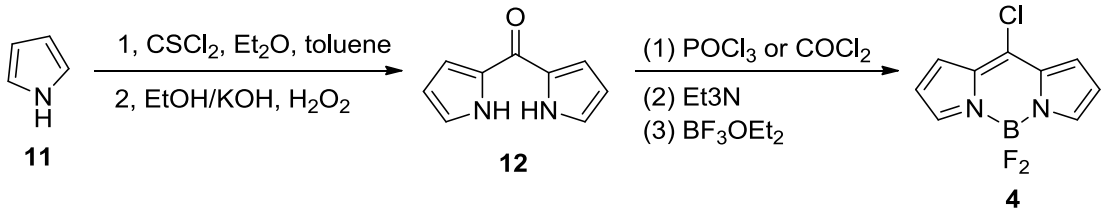

Scheme 3-1: Synthesis of 8-chloro BODIPY **4**

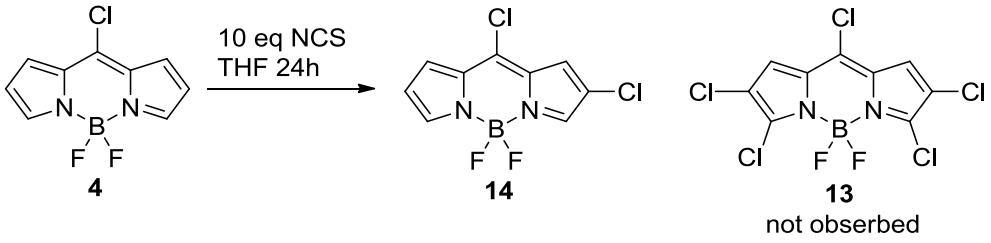

Scheme 3-2: Chlorination of 8-chloro BODIPY **4 using NCS.**

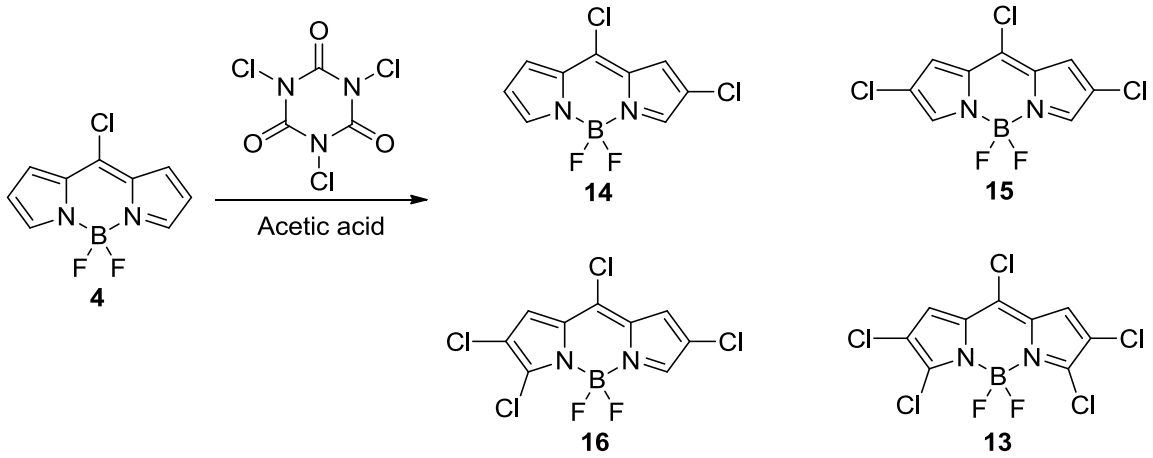

Scheme 3-3: Step-wise chlorination of 8-chloro BODIPY **4** using TCCA

noticed deactived benzenes could be quickly brominated using tribromoisocyanuric acid (TBCA) under strong acid conditions, in 2 minutes. Therefore, we chose trichloroisocyanuric acid (TCCA) as the source of electrophilic Cl^+ and acetic acid as the protic solvent to activate the TCCA.

By treating BODIPY **4** with 1.33 equiv of TCCA (portion-wise) in acetic acid, monochlorination was achieved, yielding the dichloro product **14** in 10 min, in 83% yield, as shown in Scheme 3-3. The monochlorination only occurred at the 2,(6)-position and no other monochlorinated products were detected. By increasing the amount of TCCA to 2.33 equiv, the dichlorinated BODIPY **15** was formed as the major product in 83% isolated yield. By increasing the amount of TCCA to 3 equiv, the formation of the BODIPY **13** and **16** was clearly noticed, although BODIPY **15** was still the major product. However, further increasing the amount of TCCA, produced both BODIPYs **13** and **16** were generated at the same time, as seen by TLC It should be noted that it was difficult to separate **16** from **13** and **15** due to their very similar polarities. A long column eluted with CH_2Cl_2/hexanes provided pure compound **16** in only about 15% yield. The trichlorination was first confirmed by HRMS (ESI-TOF) with a $[M]^-$ peak 329.9094 (calcd. 329.9082). By increasing the amount of TCCA to 5 equiv, TLC showed BODIPY **13** was formed and became the major product. Interestingly, we noticed that BODIPY

13 could be obtained in 81% yield after only 10 min by using 10 equiv TCCA. However, further increasing the amount of TCCA, even to the point of saturation did not provide a fully-chlorinated products. Also, extending the reacting time to 24 or up to 72 h, increasing the temperature to reflux for longer time, or using a more protic solvent (H_2SO_4) all led to the decomposition of the BODIPYs.

The ^{1}H NMR spectra of **4** and **13-16** were used to confirm the regioselectivity of the chlorination reactions, as shown in the Figure 3-3. As reported,[8, 18] the hydrogens at 3,5 positions appear the most downfield chemical shift while the protons at the 2,6 positions appear the most upfield chemical shift chemical shift. In addition, 2,6-positions are known to bear least positive charge,[18] therefore electrophilic chlorination is expected to occur at 2,6-positions first. A comparison of the ^{1}H NMR spectra of **4** and **14** showed the disappearance of a single proton δ at 6.6 ppm in **14,** both two protons in **15**. The crystal structure of **15** (Figure 3-4) further confirmed that the two chloro groups were located at the 2,6-positions. In the ^{1}H NMR spectra, the

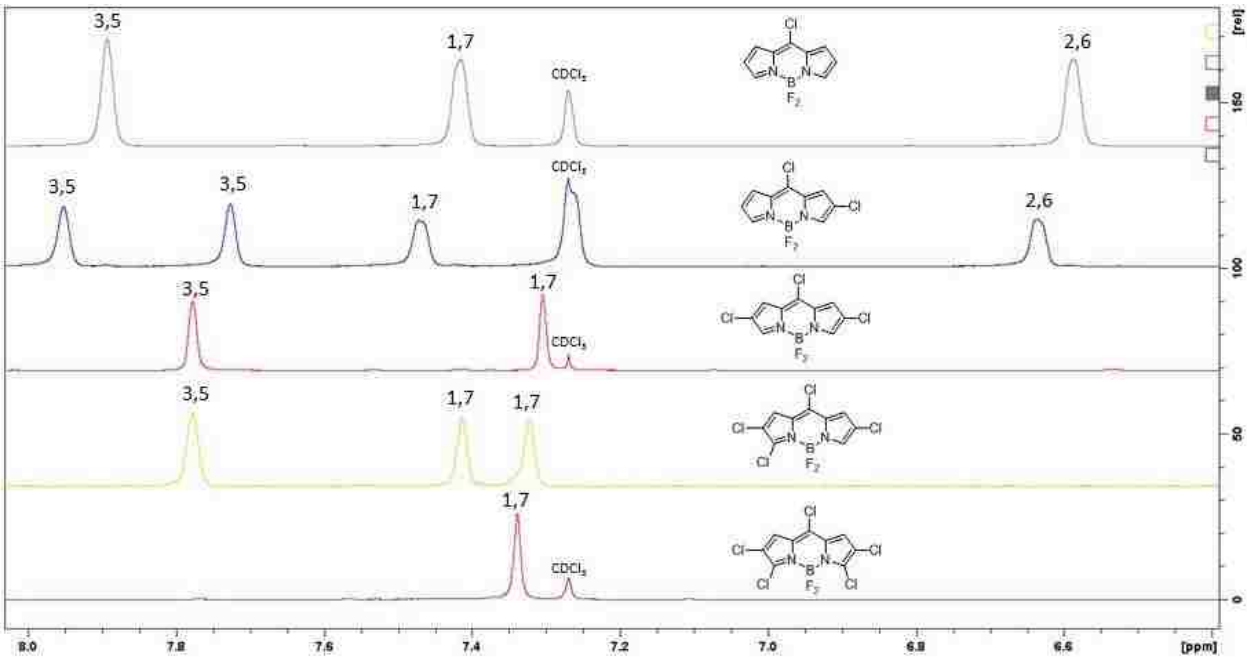

Figure 3-3: ^{1}H NMR (400 MHz) of BODIPYs **4** and **13-16** in $CDCl_3$ at room temperature.

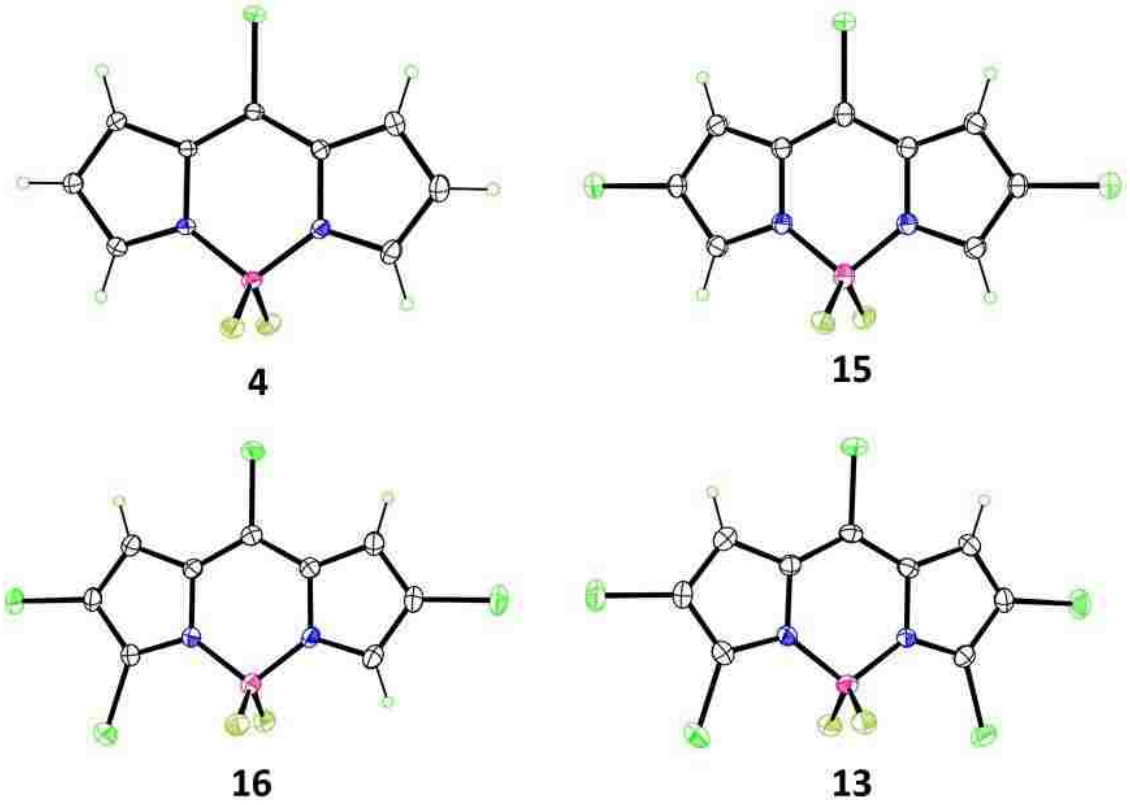

Figure 3-4: X-ray structures of BODIPYs **4**, **13**, **15** and **16**.

characteristic peaks at 3,5- positions (δ ≈ 7.9 ppm) gradually disappeared from **14** to **13** and **16**. It is should be noticed that the only singlets in the spectrum of **13** at δ ≈ 7.3 ppm belong to the hydrogens at 1,7-positions.

The suitable crystals of BODIPYs **4**, **13**, **15** and **16** are grown by slow evaporation in $CHCl_3$, which provided the direct evidence of the regioselectivity of the chlorination reactions. The results obtained are shown in Figure 3-4. The X-ray structure of **4** is in good agreement with the published 150K structure,[19] with the 12 atoms of the C_9BN_2 BODIPY core having a mean deviation of only 0.008 Å from coplanarity. BODIPY **15** is disordered on a C2h site, which requires the C_9BN_2 core to be exactly planar in the crystal. In BODIPY **16**, the mean deviation from coplanarity is only a little larger (≈ 0.015 Å). The two independent molecules of **13** are less

planar. One has a slightly bowed conformation with mean deviation (≈ 0.064 Å), and the B atom of the other one lies 0.110 Å out of the plane of the other eleven atoms.

3.3 Reactivity of 2,3,5,6,8-Chloro Groups of BODIPY 13

3.3.1 Suzuki Catalyzed Coupling Reactions of BODIPY 13

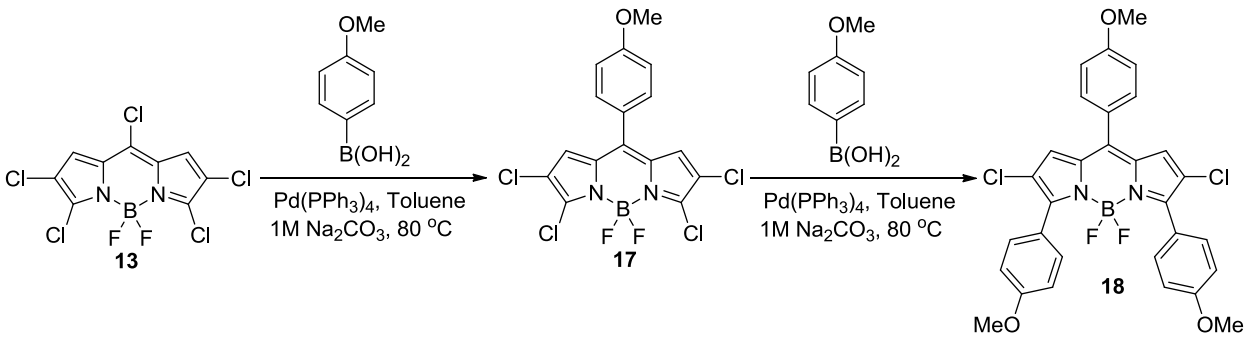

Scheme 3-4: Suzuki coupling reactions of BODIPY **13**.

Due to various types of commercial available boronic acids and the mild reaction conditions, Suzuki cross-coupling[20] reactions are particularly attractive for the functionalization of BODIPYs. Thus in this work, the Suzuki cross-coupling reaction was utilized to investigated the reactivity and regioseletivity of the different types of chloro groups of BODIPY **13**. A Suzuki type coupling reaction between 2.2 equiv of 4-methoxyphenylboronic acid and BODIPY **13** in the presence of $Pd(PPh_3)_4$, toluene, and 1M Na_2CO_3(aq) with carefully monitoring the reaction by TLC, afforded only the mono-coupled BODIPY dye **17** in a 82% isolated yield. Interestingly, instead of increasing the efficiency, a larger amount of $Pd(PPh_3)_4$ (>20%) in the reaction led to decomposition of starting material, this may be due to the oxidation and reduction reactions between the electron deficient BODIPY **13** and the electron rich catalyst at high temperature. In the ^{1}H NMR spectra, the singlet at δ ≈ 7.34 ppm assigned to the hydrogens at 1,7-positions showed the symmetric structure of BODIPY **17**, as shown in Figure 3-5. In addition, compared with **13**, this singlet upfieldly shifted from δ 7.34 to 6.94 ppm, due to 1,7-protons located in the shielding

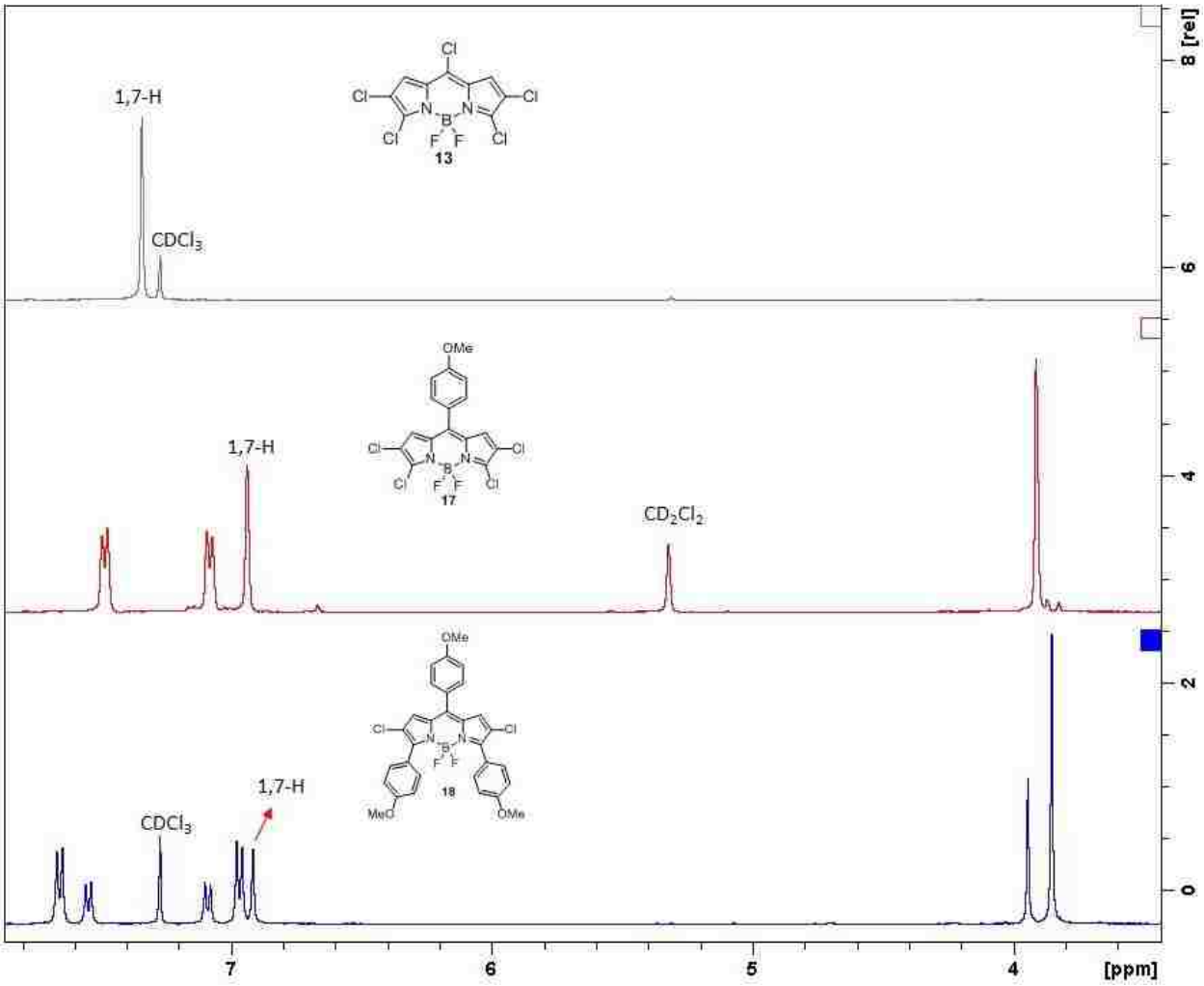

Figure 3-5: ^{1}H NMR (400 MHz) spectra of BODIPY **13**, **17** and **18** in $CDCl_3$ or CD_2Cl_2 at room temperature.

area of the 8-aryl group. The same type of reaction was used to investigated the regioselectivity between the α-(3,5)- and β-(2,6)- chloro groups. By treating BODIPY **17** with 10 equiv boronic acid (portion-wise) and monitoring by TLC, BOIDPY **18** could be obtained in 74% isolated yield. The regioselectivity of the cross-coupling reactions was further confirmed by X-ray analysis, as shown in Figure 3-6. In BODIPY **17**, the B atom of the central ring lies 0.220 Å out of the C_3N_2 plane, and the 8-phenyl ring forms a dihedral angle of 49.6° with it. BODIPY **18** has two independent molecules, both of which have the central C_2N_2B ring fairly planar, with the B atoms lying 0.102 and 0.123 Å out of the planes of the other 5 atoms. The 8-phenyl planes forms dihedral

angles of 49.5 and 50.2° with the central core planes, while the 3,5-phenyl groups form dihedral angles in the range 57.1-87.6° with them.

However, under the same conditions, the global coupled product **19** could not be formed (Scheme 3-5). Several different conditions were investigated for the coupling reactions at the 2,6-chloro groups, which are summarized in Table 1. A larger amount of boronic acids, up to 50 equivalents, or longer reaction times, up to 48 hours, and stronger bases did not yielded the desired

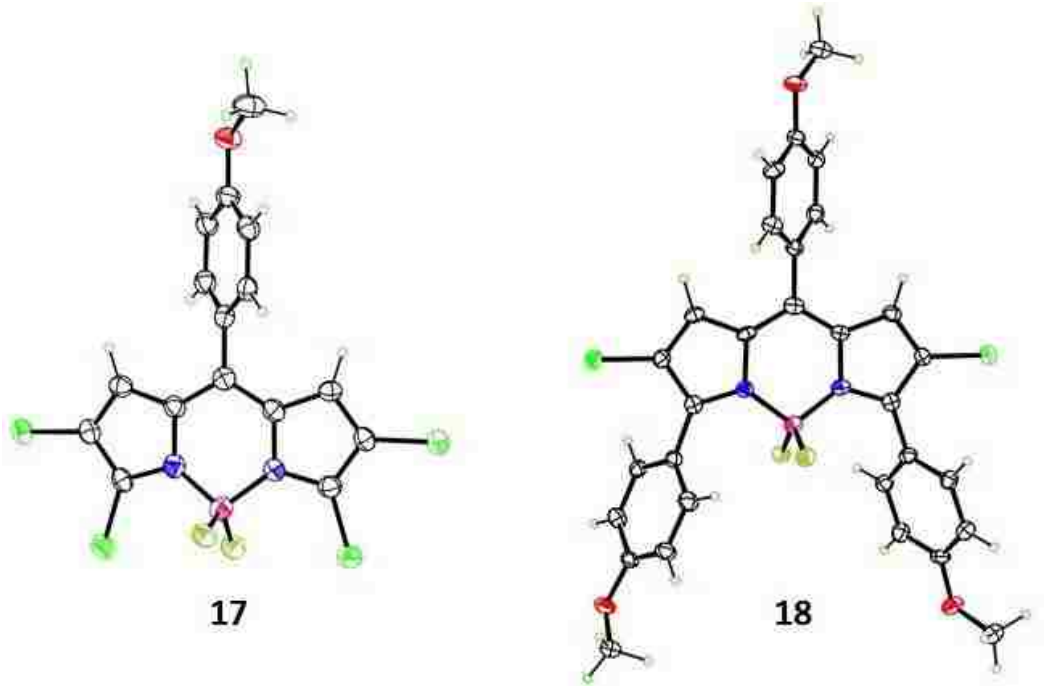

Figure **3-6**: X-ray structures of **17** and **18**.

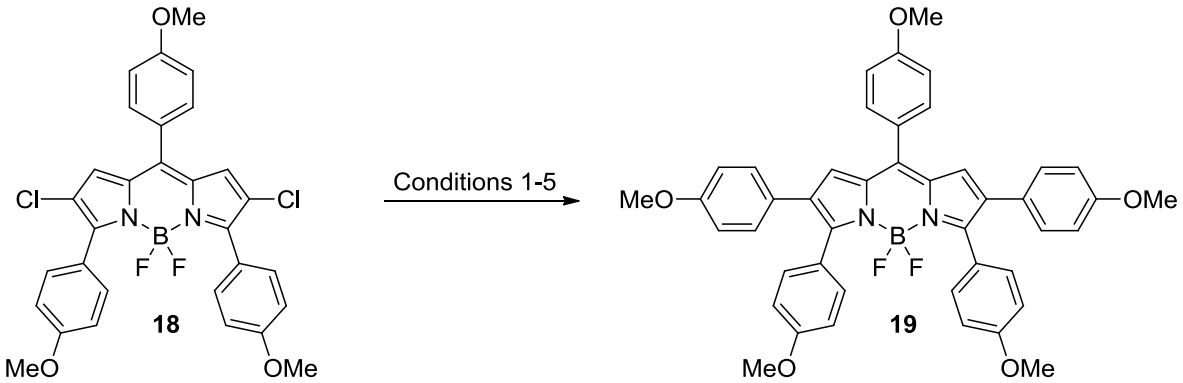

Scheme 3-5: Suzuki coupling reactions of BODPY **18**.

Table 1: Optimized conditions of Suzuki coupling reactions of BODPY **18**.

	Solvent	Catalyst	Base	Equiv of boronic acid	Temp. (°C)	Yield
1	Toluene	$Pd(PPh_3)_4$	1M Na_2CO_3	10-50	80-120	0
2	Toluene	$Pd(PPh_3)_4$	1M K_2CO_3	10-50	80-120	0
3	Toluene/THF	$Pd(PPh_3)_4$	1M Na_2CO_3	10-50	80-120	0
4	Toluene	$Pd(dppf)Cl_2$	1M Na_2CO_3	10-50	80-120	0
5	Toluene	$Pd(PCy_3)G2$	1M Na_2CO_3	10	Reflux	57

2,6-dicoupled products. It may be due to the relative strong 2,6 "C-Cl" bonds, which lead to a more difficult oxidative addition to palladium(0) complex. In the paper reported by Miyaura 2001,[21] ligand PCy_3 can greatly increase the efficiency of the oxidative addition between Pd(0) and chlorobenzene. Inspired by their work, the globally coupled BODIPY **19** was synthesized as the major product in 57% yield from BODIPY **18**, using commercial available chloro[(tricyclohexylphosphine-2-(2'-aminobiphenyl)palladium [$Pd(PCy_3)G2$] as the catalyst, in the presence of 10 equiv of 4-methoxyphenylboronic acid, refluxing toluene.

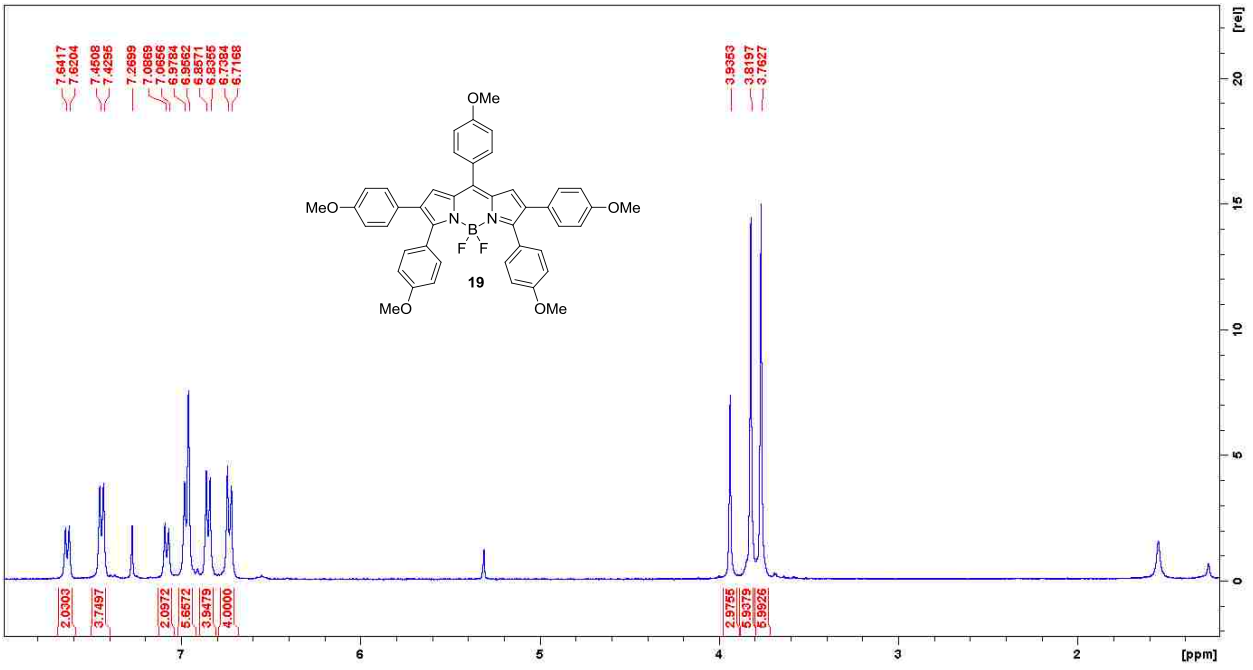

Figure 3-7: ^1H NMR (400 MHz) of BODIPY **19** in $CDCl_3$ at room temperature

The structure of the global coupled product **19** was confirmed by HRMS (ESI-TOF) with a $[M]^-$ peak 577.1182 (calcd. 577.1183). In the ^1H NMR spectra, a slightly downfield shift of the 1,7-hydrogens (from δ 6.9 to 7.0 ppm) was observed, as shown in Figure 3-8. It may be due to the 1,7-hydrogens closely located by the unshielding area of the 2,6-phenyl groups. A suitable crystal was obtained by slow evaporation in the $CHCl_3$, as shown in Figure 3-9. In BODIPY **19**, the 8-phenyl group forms a dihedral angle of 50.1° with the BODIPY core plane, while 2,6-phenyl groups and 3,5-phenyl groups form dihedral angles of 20.7 and 33.5°, and 59.4 and 69.8° with it.

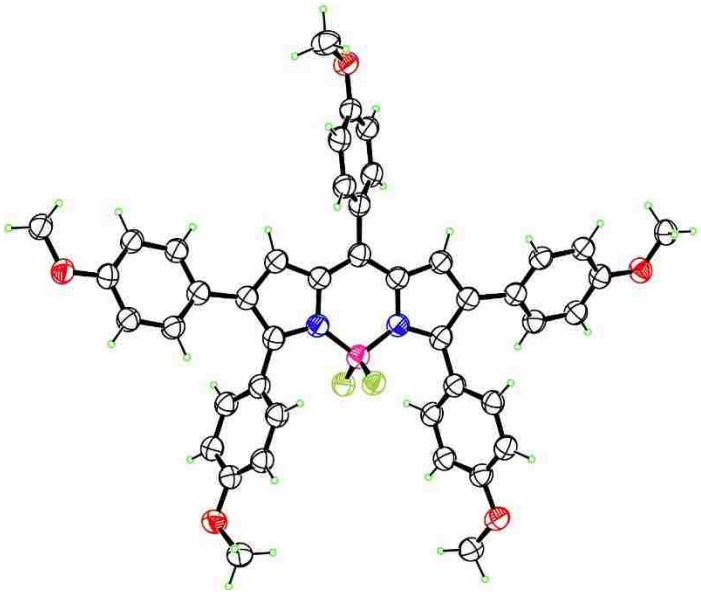

Figure 3-8: X-ray structure of BODIPY **19**.

3.3.2 Suzuki Catalyzed Coupling Reactions of BODIPY 13

Since base is not required, and the usual high yields,[9, 11, 13] Stille cross-coupling[22] reactions, these are also very attractive among the Pd(0)-catalyzed cross-coupling reactions. We recently reported that Stille cross-coupling reactions occur first at the most reactive 8-chloro site, followed by the 3(5)- (di)chloro groups.[12-13] Therefore, Stille coupling reactions are also used to investigate the reactivity and regioselectivity of different chloro groups at the periphery of BODIPY **13**.

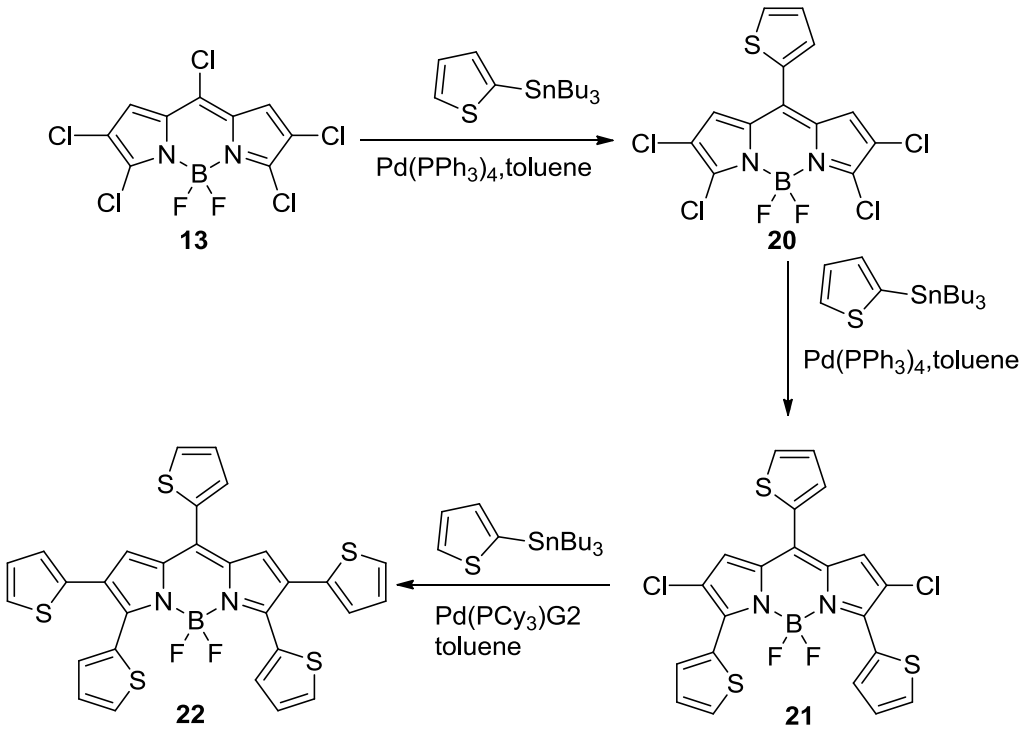

Scheme 3-6: Stille cross-coupling reactions of BODIPY **13**.

Treatment of BODIPY **13** with 2.2 equiv of 2-(tributylstannyl)thiophene in the presence of $Pd(PPh_3)_4$ in refluxing toluene yielded only the 8-thienyl product **20** in high yield (87%), as shown in Scheme 3-6. Increasing the amount of 2-(tributylstannyl)thiophene to 10 equiv gave exclusively the 2,6-dichloro-BODIPY **21** in 77% yield. Further increasing the amount of 2-(tributylstannyl)thiophene, up to 300 equiv, the reaction temperature, up to 130 °C), and the reaction time, up to 72 h, did not produce the pentathienyl-BODIPY **22**, only a trace amount of mono-2-coupled product, which was confirmed by HRMS. However, using $Pd(PCy_3)G_2$ as the catalyst, the globally coupled BODIPY **22** was successfully obtained as the major product in 57% yield.

In the ^{1}H NMR spectra, the singlet at δ 7.34 ppm of BODIPY **13** assigned to the hydrogens at the 1,7-positions appeared upfield shifted to 7.19 ppm for BODIPY **20** and at 7.21 ppm for BODIPY **21**, due to 1,7-hydrogens located at the shielded area of the 8-thienyl group.

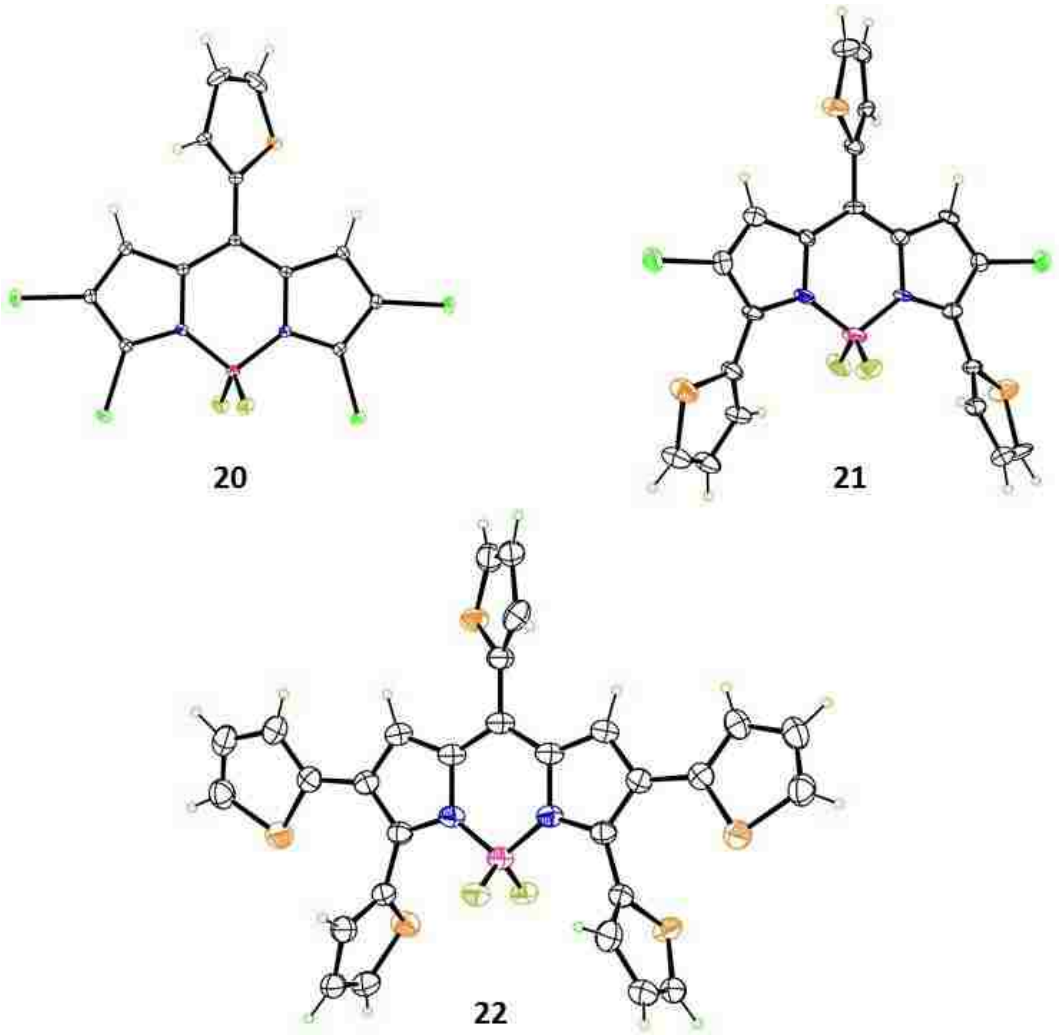

Figure 3-9: X-ray structure of BODIPYs **20-22**.

Suitable crystals for X-ray analysis were obtained by slow evaporation in the $CHCl_3$, as shown in Figure 3-9. BODIPY **20** lies on a twofold axis in the crystal, necessitating disorder of the 8-thienyl group. The BODIPY core is in a slightly twisted conformation, with the C and N atoms of the C_2N_2B ring lying 0.038 Å out of the plane. The thiophene plane forms a dihedral angle of 37.7° with the C_2N_2B ring. BODIPY **21**, as the hemi-toluene solvate, has four independent molecules, and five of the 12 thiophenes are disordered. The conformations of the four molecules are similar, with the planes of the 8-thienyl groups forming dihedral angles in the range 47.1-52.9° with the central C_2N_2B ring. Thienyl groups at the other positions form more variable dihedral

angles with the core, in the range 38.6-55.1°. BODIPY **22** also lies on a twofold axis in the crystal as **20**, with two of the three independent thiophenes disordered. Similar to **20** and **21**, the 8-thienyl forms a dihedral angle of 40.9° with the core. However, in contrast to **21**, the 3,5-thienyl groups in BODIPY **22** are nearly orthogonal to the BODIPY core (84.0° of dihedral angle), while those at the 2,6-positions are nearly coplanar (18.5° of dihedral angle) to the core.

3.3.3 Nucleophilic Substitution reactions of BODIPY 13

Previous investigations showed the substitution reactions first occurs at the most reactive 8-chloro site followed by the 3(5)-chloro site.[12] Thus, in this work, nucleophilic substitution reactions were used to investigate the regioselectivity of pentachloro BODIPY **13**. At room

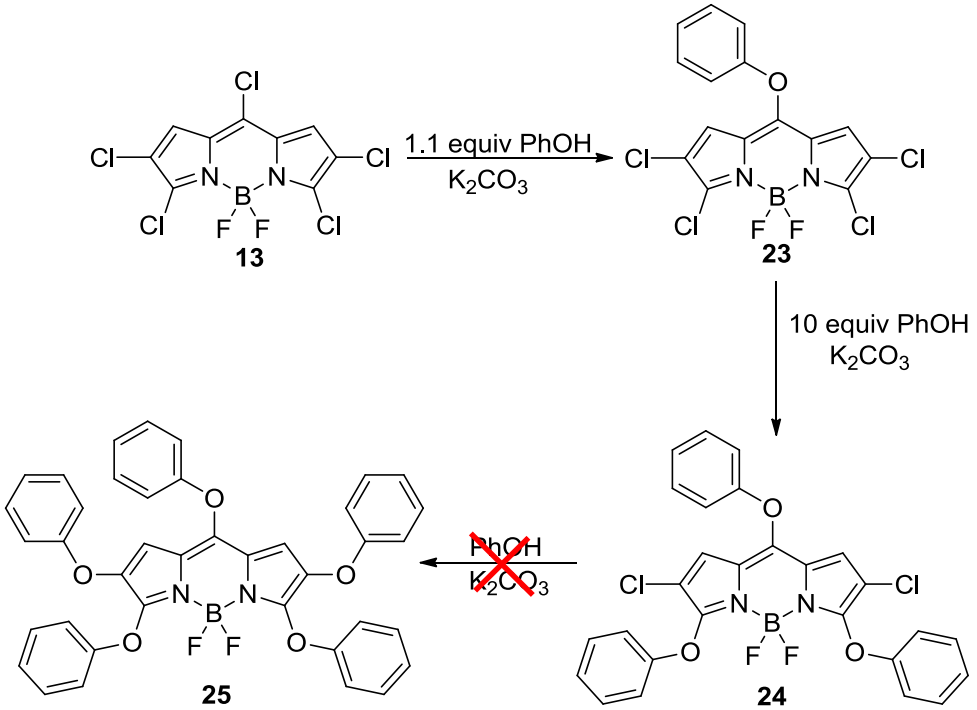

Scheme 3-7: Nucleophilic substitution reactions of **13**.

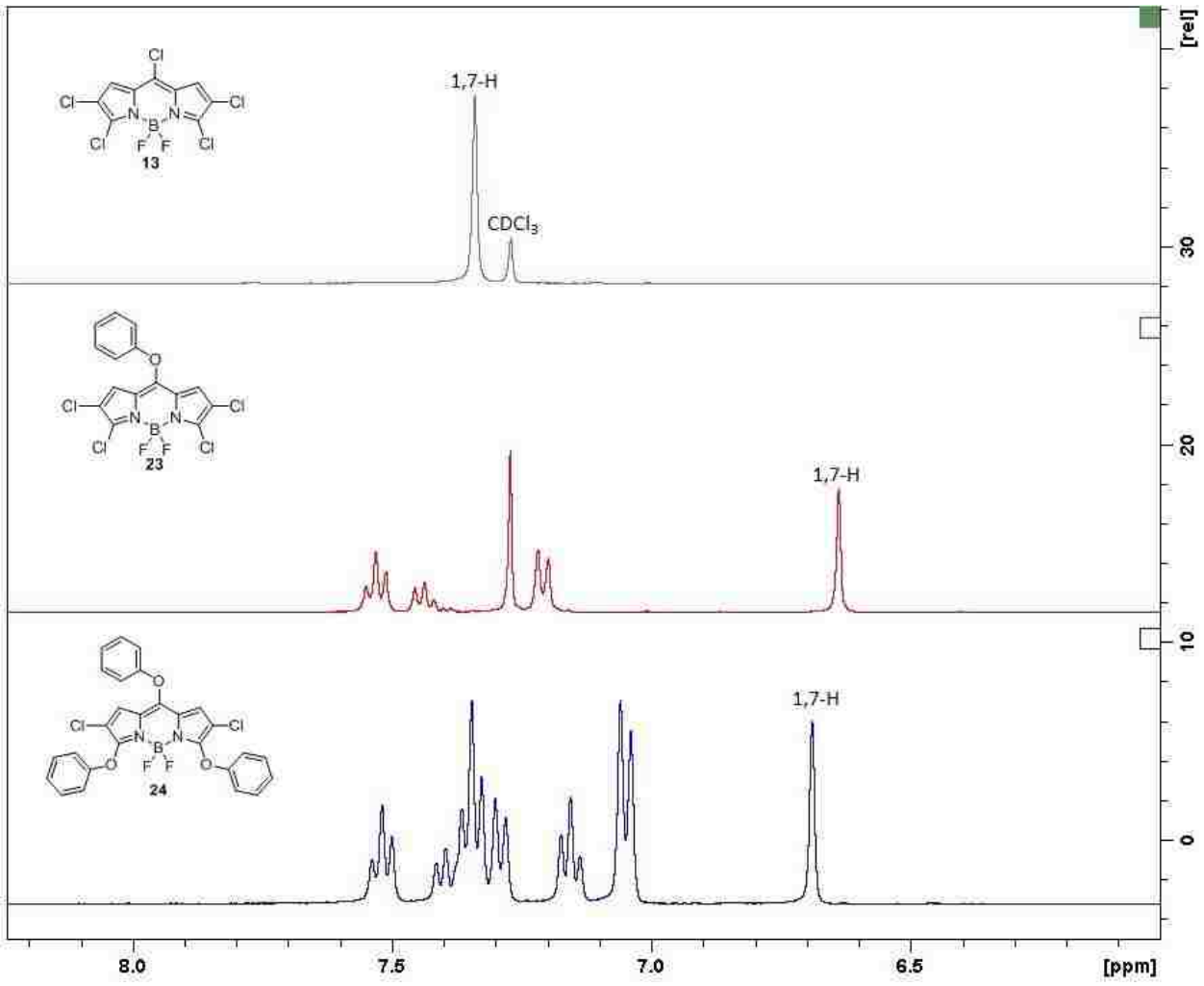

Figure 3-10: ^{1}H NMR (400 MHz) spectra of **13**, **23** and **24** in CDCl3 at room temperature.

temperature, BODIPY **13** reacted with phenol (1.1 equiv) in the presence of K_2CO_3 to yield the 8-phenoxy-BODIPY **23** in 85% yield, as shown in Scheme 3-7. Increasing the amount of phenol to 10 equiv gave the 3,5,8-triphenoxy-BODIPY **24** in 91% yield, which was confirmed by ^{1}H-NMR (see Figure 3-9) and HRMS. Further increasing the reaction time, the amount of phenol, or temperature did not produce the penta-substituted product **25**, as reported.[5] As shown in Figure 3-10, the singlet at δ ≈ 7.34 ppm of BODIPY **13** assigned to the hydrogens at the 1,7-positions upfieldly shifted to δ 6.64 ppm for BODIPY **23** and δ 6.69 ppm BODIPY **24**, due to the 1,7-protons located at the shield area of 8-phenoxyl group. A suitable crystal of **23** for X-ray analysis was

obtained by slow evaporation in the $CHCl_3$, as shown in Figure 3-11. BODIPY **23** has a similar conformation as BODIPY **17**, with the B atom lying 0.163 Å out of the C_3N_2 plane. The 8-phenyl ring forms a dihedral angle of 75.9° with the C_3N_2 plane.

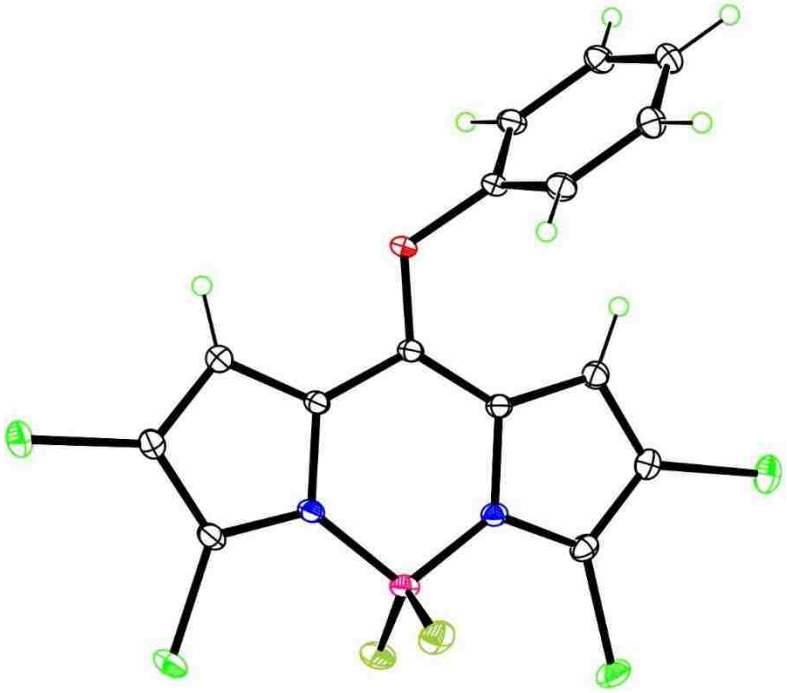

Figure 3-11: X-ray structure of BODIPY **23**.

3.3.4 Multifunctionalization of BODIPY 13

The multi-functionalization of BODIPY **13** via Stille and Suzuki cross-coupling reactions was performed, which is used to illustrate the versatility of **13**, as shown in Scheme 3-8. First, a Suzuki cross-coupling reaction with 2.2 equiv of 4-methoxyphenylboronic acid and **13** yielded BDOIPY **17** in 82% yield. Second, the 3,5,8-tri-coupled BODIPY **26** was obtained via a Stille cross coupling reaction with 10 equiv of tributyl(phenylethynyl)tin, in 77% yield. Finally, Treatment of **26** with 10 equiv of 2-(tributylstannyl)thiophene, catalysed by $Pd(PCy_3)G2$, provided fully-coupled BODIPY **27** in 49% yield. ^{1}H, ^{13}C NMR, and HRMS were used to confirm the structures of BODIPY **26** and **27**. In addition, the crystal structure of BODIPY **26** was obtained, as shown in Figure 3-12. The C_3N_2B core of **26** has the B atom 0.227 Å lying out of the plane with

the other 5 atoms, while there is a dihedral angle of 52.0° between the C_3N_2B core and the 8-phenyl group, dihedral angles of 13.7° and 48.7° between 3,5-substituents and the C_3N_2B core.

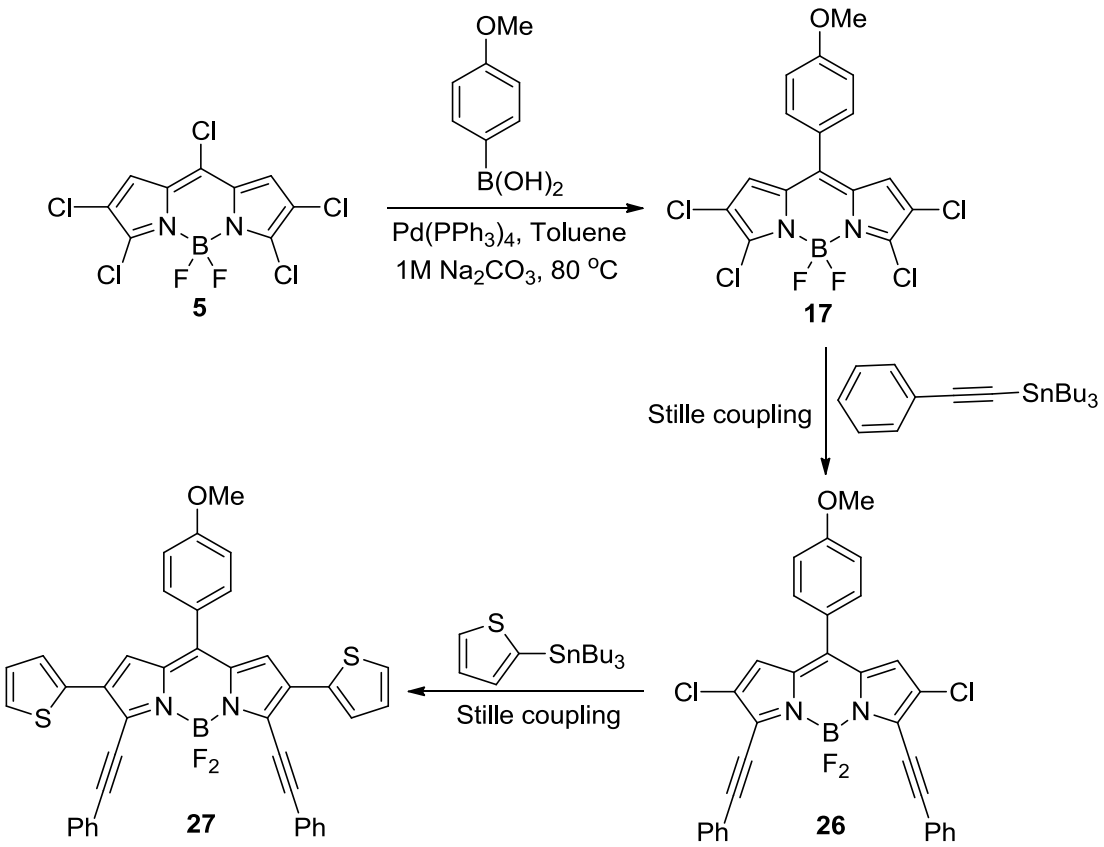

Scheme 3-8: The multi-functionalization of BODIPY **13**.

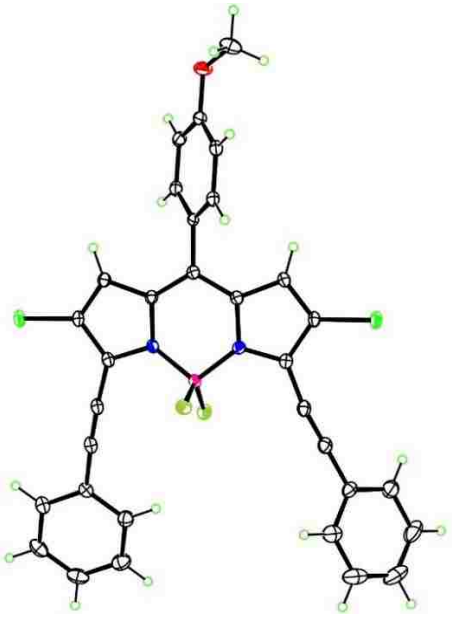

Figure 3-12: X-ray structure of BODIPY **26**.

3.4 Photophysical Properties

The spectroscopic properties of BODIPYs **13-21, 23-24** and **26-27** in THF, and **22** in CH_2Cl_2, namely their maximum absorption (λ_{abs}) and fluorescence wavelengths (λ_{em}), Stokes shifts, molar extinction coefficients (log ε) and fluorescence quantum yields (Φ_f), are summarized in Table 2. Figures 3-13, 3-14, 3-15, and 3-16 show the normalized absorption and fluorescence spectra of all the new BODIPYs. Such BODIPYs showed the characteristic strong and narrow absorption bands (log ε = 3.9-4.9) and emission bands. The introduction of (1-4) chloro groups into the BODIPY core led to the moderate red-shifts (8-38 nm) in both the absorption and emission bands of **4**,[8] while the introduction of phenyl, thienyl or ethynylphenyl groups at the 2,3,5,6,-positions causes the big red-shifts in both the absorption (up to 160 nm) and the emission bands (up to 176 nm) of BODIPY **13**, due to significant decreased the HOMO-LUMO gap.[10, 12-13] On the other hand,

Table 2. Spectroscopic properties of BODIPYs in THF at room temperature.

BODIPY	Absorption λ_{abs} (nm)	Log ε ($M^{-i}cm^{-i}$)	Emission λ_{em} (nm)	Φ_f	Stokes Shift (nm)
14	510	4.73	538	0.71	28
15	530	4.10	558	0.80	28
16	535	4.47	561	0.51	26
13	540	4.56	562	0.94	22
20	543	4.29	571	0.07	28
17	529	4.50	554	0.57	25
23	496	4.25	542	0.94	46
21	622	4.06	673	0.03	51
18	574	4.35	622	0.09	48
24	500	4.68	541	0.64	41
22[b]	638[b]	3.89[b]	704[b]	0.003[b]	66[b]
19	615	4.78	647	0.33	32
26	637	4.88	648	0.68	11
27	700	4.53	738	0.03	38

[a]Rhodamine 6G (0.88 in ethanol) was used as standard for **14**, **23**, and **24**, rhodamine B (0.49 in ethanol) for **13, 15** and 1**6**, crystal violet perchlorate (0.54 in methanol) for **18**, and methylene blue (0.04 in ethanol) for **19**, **21**, **22**, and **26-27**;[23] [b]data obtained in CH_2Cl_2.

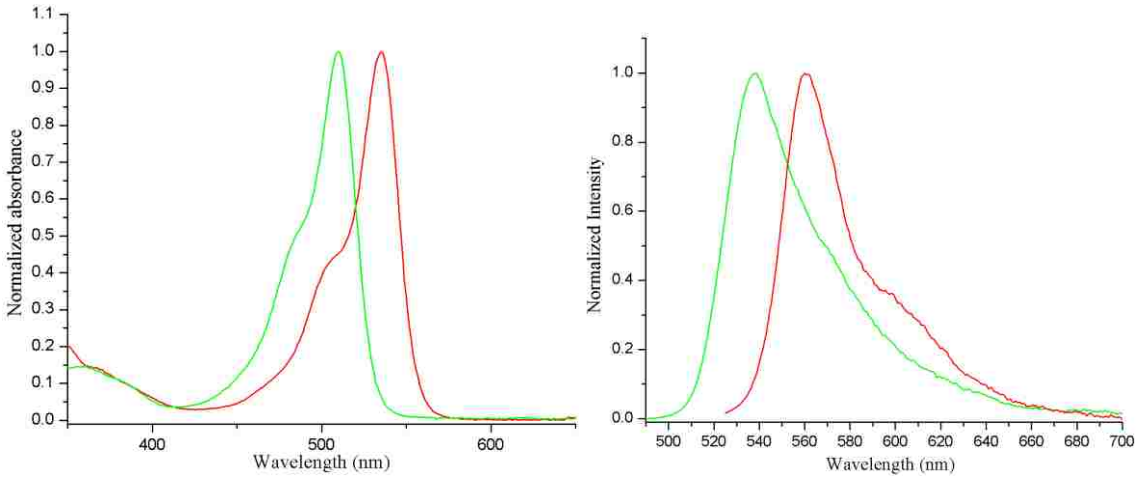

Figure 3-13: Normalized UV-Vis spectra (**a**) and fluorescence spectra (**b**) of BODIPYs **14** (green) and **16** (red) in THF at room temperature.

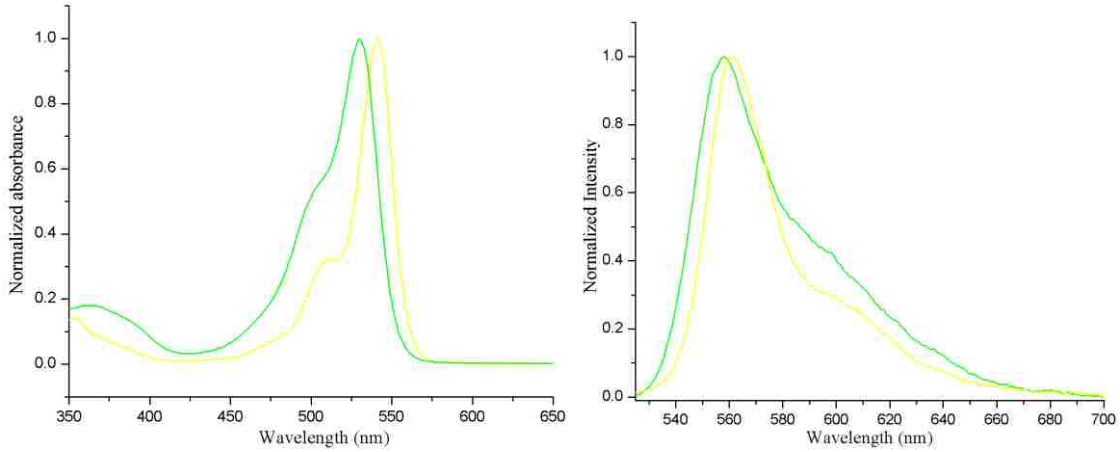

Figure 3-14: Normalized UV-Vis spectra (**a**) and fluorescence spectra (**b**) of BODIPYs **13** (yellow) and **15** (green) in THF at room temperature.

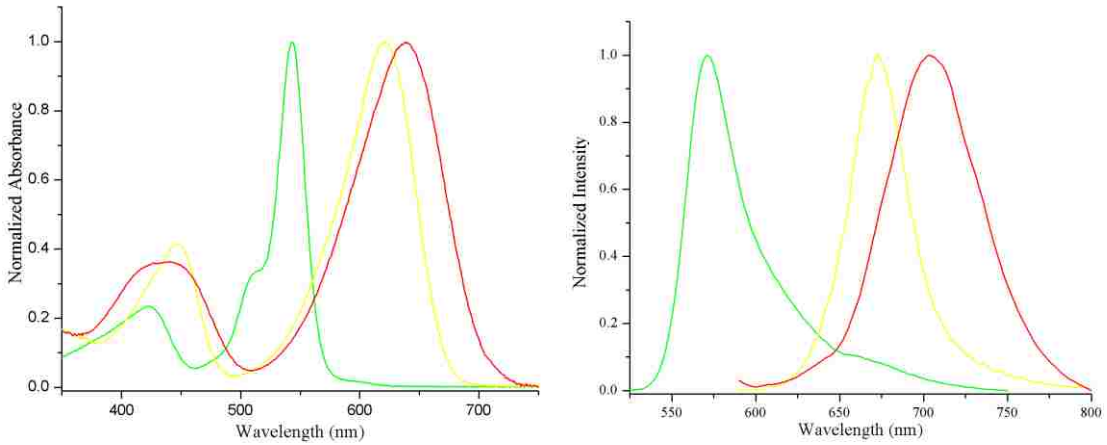

Figure 3-15: Normalized UV-Vis spectra (**a**) and fluorescence spectra (**b**) of BODIPYs **20** (green) and **21** (yellow) in THF and **22** (red) in DCM at room temperature.

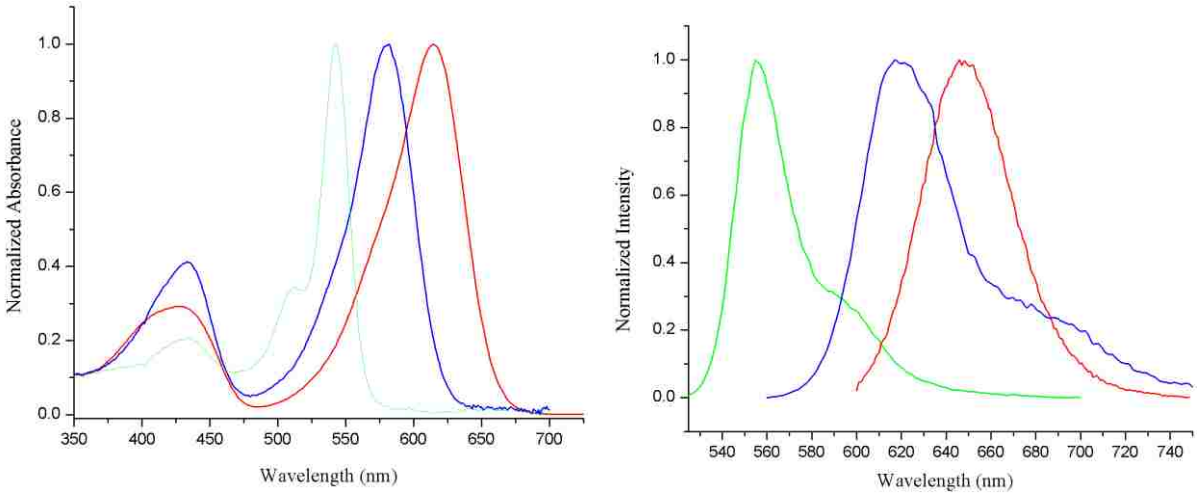

Figure 3-16: Normalized UV-Vis spectra (**a**) and fluorescence spectra (**b**) of BODIPYs **17** (green) **18** (blue) and **19** (red) in THF at room temperature.

substitution with phenoxyl groups at the 8-position of BODIPY **13** caused pronounced slight blue-shifts due to increase in the HOMO-LUMO gap, as reported.[9, 11-12, 19, 24] I believe that there is largest MO coefficient in the LUMO at the 8-position, electron-donating group at this position cause blue-shift the BODIPY spectra.

The range of Stokes shifts is in the range of 22-66 nm. As previously reported,[12-13, 25-26] the largest Stokes shifts were observed for the 3,5- and 2,3,5,6-thienyl functionalized BODIPYs **21**, **22** and **27** due to increased geometry relaxation.[27-28] BODIPY **26** with di-phenylethynyl groups at the 3,5-positions has the largest bathochromic shifts (112 nm) from BODIPY **17**, which also gave the smallest Stokes shift (11 nm), as reported.[29]

The quantum yields vary greatly among the different BODIPYs (0.003 – 0.94). The8-phnoxyl BODIPY **23-24** provided the largest quantum yields (0.94) of all BODIPYs synthesized, while thienyl-functionalized BODIPYs **20-22** and **27** showed dramatically decreased the fluorescence quantum yields (< 0.1), which may be due to increased energy lost that resulting from free motion of all the thienyl groups.[25-26]

3.5 Conclusions

A convenient stepwise chlorination method of "deactivated" BODIPYs was developed; this method used TCCA/AcOH at room temperature. Via this method, a versatile platform pentachloro BODIPY **13** was prepared, which was shown to undergo regioselective Stille and Suzuki cross-coupling reactions, first at the most reactive *meso*-8-, followed by the α-(3,5)-, and finally at the β-(2,6)-chloro groups. In addition, nucleophilic substitutions by use phenol as the nucleophiles took place first at the 8-position, followed by the 3,5-positions. Under the same condition, however, the 2,6-chloro groups were unreactive.

The regioselectivity of all the chlorination, Stille and Suzuki cross-coupling and nucleophilic substitution reactions was confirmed by X-ray crystallography analysis. Major conclusion from these studies showed pentathienyl-BODIPY **22** with the smallest dihedral angles (18.5°) for the 2,6-thienyls and the largest dihedral angles (84.0°) for the 3,5-thienyl. BODIPY **27** was prepared by applying the methodologies developed via three-step synthesis. Such BODIPY absorbed (λ_{max} = 700 nm) and emitted (λ_{max} = 738 nm) both in the NIR region of the optical spectrum. We also noticed thienyl coupled at the 3,5- and/or 2,6-positions of BODIPYs gave the largest Stokes shifts, up to 100 nm, while thephenoxyl-subsitutued at the 8-position of BODIPY induced the highest fluorescence quantum yields .

3.6 Experimental

3.6.1 Synthesis

General: All reagents and solvents were purchased from Sigma-Aldrich, Fisher Scientifics or Alfa Aesar as reagent grades and used without further purification. Argon was used to protect the air-sensitive reactions. Analytical TLC (polyester backed, 60Å, 0.2 mm, precoated, Sorbent Technologies) was used to monitor the reactions. Column chromatography was performed on silica

gel (60Å, 230-400 mesh, Sorbent Technologies). All ^{1}H NMR and ^{13}C NMR spectra were obtained using Bruker AV-400 nanobay or AV-500 spectrometers (400 or 500 MHz for ^{1}H NMR and 100 or 125 MHz for ^{13}C NMR) in $CDCl_3$ or CD_2Cl_2 with trimethylsilane as an internal standard, at room temperature. Chemical shifts (δ) are given in parts per million (ppm) with $CDCl_3$ (7.27 ppm for ^{1}H NMR, 77.0 ppm for ^{13}C NMR) and CD_2Cl_2 (5.32 ppm for 1H NMR, 53.4 ppm for 13C NMR). All high-resolution mass spectra (ESI-TOF) were obtained using a 6210 ESI-TOF mass spectrometer (Agilent Technologies). All UV-Visible spectra were recorded on a Varian Cary 50 (solutions) spectrophotometer at room temperature. Fluorescence spectra were studied on a PTI QuantaMaster4/2006SE spectrofluorimeter corrected emission spectrum. A 10 mm path length quartz cuvette and spectroscopic grade solvents were used for the measurements. The determination of optical density (ε) was used the solutions with absorbance of λ_{max} between 0.5—1. The dilute solutions with absorbance of particular excitation wavelength between 0.02-0.05 were used for fluorescence quantum yield measurement. Rhodamine 6G (0.95 in ethanol), rhodamine B (0.49 in ethanol) and crystal violet perchlorate (0.54 in methanol) were used as external standards for calculation of relative fluorescence quantum yields of BODIPYs. All fluorescence quantum yields (Φ_f) were determined using the following equation:[30]

$$\Phi_{x=} \Phi_s \times (F_x/F_s) \times (A_s/A_x) \times (n_x/n_s)^2$$

where Φ_x and Φ_s are the fluorescence quantum yields of the test samples and standards; F_x and F_s are the areas under the test samples' and standards' emission peaks; A_x *is* the absorbance at which test samples were excited; A_s the absorbance at which stands were excited; n_x *and* n_s are refractive indexes of test sample and standards.

General procedure for chlorination of BODIPY 4

8-Chloro BODIPY **4** (22.6 mg, 0.1 mmol) was dissolved in acetic acid (2 mL). TCCA was added portion-wise to the solution and the final mixture was stirred at room temperature for 10 min. TLC was used to monitor the reactions. The mixture was poured into water (200 mL) and extracted with CH_2Cl_2 (15 mL × 3). The organic layers were combined, washed with aqueous saturated $NaHCO_3$ and water, and then dried over anhydrous Na_2SO_4. The solvents were removed under reduced pressure and the resulting residue was purified by preparative TLC and column chromatography, using CH_2Cl_2/hexanes or ethyl acetate/hexanes for elution.

2,8-Dichloro BODIPY 14: This compound was prepared using TCCA (31 mg, 0.133 mmol), yielding 21.6 mg, 83% of **14** (yellow solid), mp (°C) 143−144; ^{1}H NMR ($CDCl_3$, 400 MHz): δ = 7.95 (s, 1H), 7.73 (s, 1H), 7.47 (s, 1H), 7.26 (s, 1H), 6.64 (s, 1H); ^{13}C NMR ($CDCl_3$, 125 MHz): δ = 147.1, 141.1, 141.0, 134.6, 132.3, 130.6, 125.1, 122.4, 120.0; HRMS (ESI-TOF) *m/z* 258.9919 $[M]^-$, calculated for $C_9H_5BCl_2F_2N_2$: 258.9927.

2,6,8-Trichloro BODIPY 15: This compound was prepared using TCCA (54 mg, 0.233 mmol), yielding 21.6 mg, 73% of **15** (red solid), mp (°C) 212-213; ^{1}H NMR ($CDCl_3$, 400 MHz): δ = 7.78 (s, 2H), 7.31 (s, 2H); ^{13}C NMR ($CDCl_3$, 125 MHz): δ = 143.2, 140.9, 132.9, 126.2, 123.5; HRMS (ESI-TOF) *m/z* 293.9502 $[M]^-$, calculated for $C_9H_5BCl_3F_2N_2$: 293.9501.

2,3,6,8-Tetrachloro BODIPY 16: This compound was prepared using TCCA (93 mg, 0.4 mmol), yielding 4.9 mg, 15% of **16** (red solid), mp (°C) 208-209; ^{1}H NMR (CD_2Cl_2, 400 MHz): δ = 7.78 (s, 1H), 7.41 (s, 1H); 7.32 (s, 1H); ^{13}C NMR (CD_2Cl_2, 125 MHz): δ = 143.7, 143.1, 139.4, 132.7, 131.0, 126.5, 126.0, 123.7, 122.3; HRMS (ESI-TOF) *m/z* 329.9094 $[M]^-$, calculated for $C_9H_3BCl_4F_2N_2$: 329.9082.

2,3,5,6,8-Pentachloro BODIPY 13: This compound was prepared using TCCA (0.23 g, 1 mmol) yielding 27.3 mg, 81% of **13** (red solid). mp (°C) 218-219; ^{1}H NMR ($CDCl_3$, 400 MHz): δ = 7.34

(s, 2H); ^{13}C NMR ($CDCl_3$, 125 MHz): δ = 144.0, 136.7, 130.4, 125.8, 122.7; HRMS (ESI-TOF) *m/z* 360.8754 $[M]^-$, calculated for $C_9H_2BCl_5F_2N_2$: 360.8758.

General procedure for Stille cross-couplings of BODIPYs

To a 15 mL round-bottomed flask were added the starting BODIPY, organotin reagent and 3% mol of either $Pd(PPh_3)_4$ (for **20, 21, 26**) or $Pd(PCy_3)G2$ (for **22**, **27**). The flask was evacuated and refilled with nitrogen 4 times. Toluene (5 mL) was added and the final mixture was stirred and refluxed under N_2. TLC was used to monitor the reactions. The toluene was removed under reduced pressure and the resulting residue was purified by preparative TLC and column chromatography using CH_2Cl_2/hexanes or ethyl acetate/hexanes for elution.

8-Thienyl-2,3,5,6-tetrachloro BODIPY 20: This compound was prepared from BODIPY **13** (18.2 mg, 0.05 mmol) and 2-(tributylstannyl)thiophene (37.3 mg, 0.1 mmol), yielding 17.2 mg, 87% of **20** (red solid). mp (°C) 298-300; ^{1}H NMR ($CDCl_3$, 400 MHz): δ = 7.77-7.79 (q, 1H, $^3J_{(H,H)}$= 4.0 Hz, $^4J_{(H,H)}$= 1.1 Hz), 7.51-7.52 (q, 1H, $^3J_{(H,H)}$= 2.6 Hz, $^4J_{(H,H)}$= 1.1 Hz), 7.30-7.32 (q, 1H, $^3J_{(H,H)}$= 3.7 Hz, $^4J_{(H,H)}$= 1.3 Hz), 7.19 (s, 2H); ^{13}C NMR ($CDCl_3$, 125 MHz): δ = 142.7, 136.2, 133.5, 132.4, 132.3, 130.9, 128.7, 128.2, 121.8; HRMS (ESI-TOF) *m/z* 411.8959 $[M]^-$, calculated for $C_{13}H_5BCl_4F_2N_2S$: 411.8959.

3,5,8-Trithienyl-2,6-dichloro BODIPY 21: This compound was prepared from BODIPY **20** (20.5 mg, 0.05 mmol) and 2-(tributylstannyl)thiophene (187 mg, 0.5 mmol), yielding 19.1 mg, 77% of **21** (dark blue solid). mp (°C) 255-257; ^{1}H NMR ($CDCl_3$, 400 MHz): δ = 7.94-7.95 (m, 2H), 7.71-7.72 (m, 1H), 7.63-7.64 (m, 2H), 7.51-7.52 (m, 1H), 7.28-7.30 (m, 1H), 7.19-7.21 (m, overlap, 4H); ^{13}C NMR ($CDCl_3$, 125 MHz): δ = 147.4, 134.4, 134.0, 133.5(t), 133.1, 132.7, 131.0, 130.8, 129.5, 128.5, 128.3, 127.6, 123.4; HRMS (ESI-TOF) *m/z* 504.9540 $[M]^-$, calculated for $C_{21}H_{11}BCl_2F_2N_2S_3$: 504.9559.

2,3,5,6,8-Pentathienyl-BODIPY 22: This compound was prepared from BODIPY **21** (15.2 mg, 0.03 mmol) and 2-(tributylstannyl)thiophene (112 mg, 0.3 mmol), yielding 10.3 mg, 57% of **22** (dark green solid). mp (°C) 255-257; ^{1}H NMR ($CDCl_3$, 500 MHz): δ = 7.73-7.74 (m, 1H), 7.60-7.61 (m, 1H), 7.54-7.55 (m, 2H), 7.51-7.52 (m, 2H), 7.30-7.32 (m, overlap, 3H), 7.23-7.24 (m, 2H), 7.10-7.12 (m, 2H), 6.94-6.96 (m, 2H), 6.80-6.81 (m, 2H); ^{13}C NMR ($CDCl_3$, 125 MHz): δ = 149.0, 135.6, 135.2, 134.7, 134.6, 132.6, 132.4, 130.9, 130.8, 129.7, 129.1, 128.2, 128.1, 127.3, 127.2, 126.4, 125.6; HRMS (ESI-TOF) *m/z* 601.0086 $[M]^-$, calculated for $C_{29}H_{17}BF_2N_2S_5$: 601.0093.

General procedure for Suzuki cross-couplings of BODIPYs

To a 15 mL round-bottomed flask were added the starting BODIPY and either 3 mol% of $Pd(PPh_3)_4$ (for **17**, **18**) or 3 mol% of $Pd(PCy_3)G2$ (for **19**). Toluene (4 mL) and 1M Na_2CO_3 (aq) (1 mL) were added under N_2. 4-Methoxyphenylboronic acid was added portion-wise and the final mixture was stirred and refluxed under N_2. TLC was used to monitor the reactions. The mixture was poured into water (20 mL) and extracted with CH_2Cl_2 (10 mL × 3). The organic layers were combined, washed with aqueous saturated brine, water and dried over anhydrous Na_2SO_4. The solvents were removed under reduced pressure and the resulting residue was purified by column chromatography using CH_2Cl_2/hexanes or ethyl acetate/hexanes for elution.

8-(*p*-Methoxyphenyl)-2,3,5,6-tetrachloro-BODIPY 17: This compound was prepared from BODIPY **13** (18.2 mg, 0.05 mmol) and 4-methoxyphenylboronic acid (16.7 mg, 0.11 mmol), yielding 17.7 mg, 82% of **17** (orange-red solid). mp (°C) 234-236; ^{1}H NMR ($CDCl_3$, 400 MHz): δ = 7.64-7.67 (d, 2H, $^{3}J_{(H,H)}$= 8.1 Hz), 7.07-7.09 (d, 2H, $^{3}J_{(H,H)}$= 8.1 Hz), 6.94 (s, 2H), 3.91 (s, 3H); ^{13}C NMR ($CDCl_3$, 100 MHz): δ = 162.9, 144.7, 141.5, 132.6, 131.4, 128.3, 124.0, 121.2, 114.5, 55.7; HRMS (ESI-TOF) *m/z* 432.9574 $[M-H]^-$; calculated for $C_{16}H_9BCl_4F_2N_2O$: 432.9572.

3,5,8-tri(*p*-Methoxyphenyl)-2,6-dichloro-BODIPY 18: This compound was prepared from BODIPY **17** (21.7 mg, 0.05 mmol) and 4-methoxyphenylboronic acid (76 mg, 0.5 mmol), yielding 21.4 mg, 74% of **18** (dark blue), mp (°C) 315-316; ^{1}H NMR ($CDCl_3$, 400 MHz): δ = 7.64-7.67 (d, 4H, $^{3}J_{(H,H)}$= 8.6 Hz), 7.53-7.56 (d, 2H, $^{3}J_{(H,H)}$= 8.6 Hz), 7.08-7.10 (d, 2H, $^{3}J_{(H,H)}$= 8.5 Hz), 6.95-6.98 (d, 4H, $^{3}J_{(H,H)}$= 8.7 Hz), 6.91 (s, 2H), 3.94 (s, 3H), 3.85 (s, 6H); ^{13}C NMR ($CDCl_3$, 125 MHz): δ = 161.9, 160.8, 154.0, 143.3, 132.8, 132.3, 131.9, 128.1, 126.0, 122.5, 121.7, 114.2, 113.5, 55.6, 55.2; HRMS (ESI-TOF) m/z 577.1182 $[M]^-$; calculated for $C_{30}H_{23}BCl_2F_2N_2O_3$: 577.1183.

2,3,5,6,8-Penta(*p*-Methoxyphenyl)-BODIPY 19: This compound was prepared from BODIPY **18** (17.4 mg, 0.03 mmol) and 4-methoxyphenylboronic acid (45 mg, 0.3 mmol) yielding 12.1 mg, 56% of **19** (dark blue solid), mp (°C) 252-254; ^{1}H NMR ($CDCl_3$, 400 MHz): δ = 7.62-7.64 (d, 2H, $^{3}J_{(H,H)}$= 8.5 Hz), 7.43-7.45 (d, 4H, $^{3}J_{(H,H)}$= 8.5 Hz), 7.07-7.09 (d, 2H, $^{3}J_{(H,H)}$= 8.5 Hz), 6.96-6.98 (overlap, 6H), 6.84-6.86 (d, 4H, $^{3}J_{(H,H)}$= 8.6 Hz), 6.72-6.74 (d, 4H, $^{3}J_{(H,H)}$= 8.6 Hz), 3.93 (s, 3H), 3.82 (s, 6H), 3.76 (s, 6H); ^{13}C NMR ($CDCl_3$, 125 MHz): δ = 161.4, 160.1, 158.5, 155.5, 142.3, 134.5, 133.9, 132.4, 132.0, 129.5, 127.7, 127.1, 126.8, 124.4, 113.9, 113.7, 113.4, 55.5, 55.2, 55.1; HRMS (ESI-TOF) m/z 721.2802 $[M]^+$; calculated for $C_{44}H_{37}BF_2N_2O_5$: 721.2800.

General procedure for nucleophilic substitution of BODIPYs

The starting BODIPY was dissolved in CH_2Cl_2 (1 mL) and CH_3CN (1 mL). Phenol and Na_2CO_3 (1 equivalents) were added and the solution stirred at room temperature. TLC was used to monitor the reactions. The mixture was poured into water (10 mL) and extracted with CH_2Cl_2 (10 ml × 3). The organic layers were combined, washed with aqueous saturated brine, water and dried over anhydrous Na_2SO_4. The solvents were removed under reduced pressure and the resulting residue was purified by column chromatography using CH_2Cl_2/hexanes or ethyl acetate/hexanes for elution.

8-Phenoxy-2,3,5,6-tetrachloro-BODIPY 23: This compound was prepared from BODIPY **13** (18.2 mg, 0.05 mmol) and phenol (5 mg, 0.055 mmol), yielding 17.9 mg, 85% of **23** (orange-red solid). mp (°C) 198-199; ^{1}H NMR ($CDCl_3$, 400 MHz): δ = 7.51-7.55 (m, 2H), 7.42-7.45 (m, 1H), 7.20-7.22 (d, 2H, $^{3}J_{(H,H)}$= 8.4 Hz), 6.64 (s, 2H); ^{13}C NMR ($CDCl_3$, 100 MHz): δ = 155.5, 155.4, 139.2, 130.9, 127.5, 123.9, 123.6, 120.0, 119.4; HRMS (ESI-TOF) m/z 418.9413 $[M]^-$; calculated for $C_{15}H_7BCl_4F_2N_2O$: 418.9410.

BODIPY 24: This compound was prepared from BODIPY **23** (12.6 mg, 0.03 mmol) and phenol (27 mg, 0.3 mmol), yielding 14.7, 91% of **24** (orange-red solid), mp (°C) 180-181; ^{1}H NMR (CD_2Cl_2, 400 MHz): δ = 7.50-7.54 (t, 2H, $^{3}J_{(H,H)}$= 7.4 Hz), 7.33-7.41 (m, overlap, 6H), 7.28-7.30 (d, 2H, $^{3}J_{(H,H)}$= 7.9 Hz), 7.14-7.17 (t, 2H, $^{3}J_{(H,H)}$= 7.5 Hz), 7.04-7.06 (d, 4H, $^{3}J_{(H,H)}$= 8.0 Hz), 6.60 (s, 2H); ^{13}C NMR (CD_2Cl_2, 100 MHz): δ = 156.1, 155.8, 154.4, 153.8, 130.7, 129.7, 126.8, 124.3, 119.4, 118.7, 117.0, 109.4; HRMS (ESI-TOF) m/z 535.0713 $[M]^-$; calculated for $C_{27}H_{17}BCl_2F_2N_2O_3$: 535.0714.

BODIPY 26: This compound was prepared from BODIPY **18** (21.7 mg, 0.05 mmol) and tributyl(phenylethynyl)tin (196 mg, 0.5 mmol), yielding 21.8 mg, 77% of **9** (dark-green solid), mp (°C) 248-250; ^{1}H NMR ($CDCl_3$, 400 MHz): δ = 7.74-7.76 (q, 4H, $^{3}J_{(H,H)}$= 5.7 Hz, $^{3}J_{(H,H)}$= 1.6 Hz), 7.48-7.50 (d, 2H, $^{3}J_{(H,H)}$= 8.7 Hz), 7.40-7.45 (m, overlap, 6H), 7.06-7.08 (d, 2H, $^{3}J_{(H,H)}$= 8.7 Hz), 6.86 (s, 2H), 3.93 (s, 3H); ^{13}C NMR ($CDCl_3$, 125 MHz): δ = 162.3, 141.9, 135.7, 134.4, 132.6, 132.4, 130.0, 128.5, 126.9, 126.7, 125.6, 121.9, 114.4, 107.2, 80.7, 55.6; HRMS (ESI-TOF) m/z 565.0969 $[M]^-$; calculated for $C_{32}H_{19}BCl_2F_2N_2O$: 565.0972.

BODIPY 27: This compound was prepared from BODIPY **26** (17 mg, 0.03 mmol) and 2-(tributylstannyl)thiophene (112 mg, 0.3 mmol), yielding 9.7 mg, 49% of **27** (dark-green solid), mp (°C) 292-293; ^{1}H NMR ($CDCl_3$, 400 MHz): δ = 7.78-7.81 (m, 4H), 7.59-7.61 (m, 4H), 7.44-7.46

(m, overlap, 6H), 7.31-7.33 (m, 2H) 7.10-7.14 (m, 4H), 7.00 (s, 2H), 3.96 (s, 3H); ^{13}C NMR ($CDCl_3$, 125 MHz): δ = 162.0, 141.3, 136.3, 135.1, 134.7, 132.5, 132.2, 131.2, 129.8, 128.5, 127.5, 126.3, 125.1, 125.0, 124.7, 122.5, 114.3, 106.4, 83.6, 55.6; HRMS (ESI-TOF) m/z 661.1493 $[M]^-$; calculated for $C_{40}H_{25}BF_2N_2OS_2$: 661.1506.

3.6.2 Crystal data

Crystal structures were determined at low-temperature (90K except for **13**) with MoKα data from either a Bruker Kappa APEX-II DUO (for **4**, **15**, **16**, **13**, **20**, **23**, **26**) or a Nonius KappaCCD (for **17**, **18**, **21**, **22**) diffractometer. Data for **19** were collected on a Bruker Kappa APEX-II DUO diffractometer with CuKα radiation. For all structures, H atoms were located from difference maps but constrained in calculated positions during refinement. Refinement was by SHELX-97.[17] For **15**, the molecule is disordered on a 2/m (C_{2h}) site. For **13**, Z'=2, and the data were collected at T=160K, since a crystal-destroying phase change occurs around 150K. For **20**, Z'=1/2 with the molecule on a twofold axis and the thiophene disordered. For **21**, Z'=4, 5 of the 12 independent thiophenes are disordered, as is one of the two independent toluene solvent molecules. For **18**, Z'=2. In **22**, Z'=1/2 with the molecule on a twofold axis and two of the three independent thiophenes disordered. CCDC 1053715-1053721 and CCDC 1401007-1401011 contain the supplementary X-ray data for this work.

3.7 Reference

1. Lakshmi, V.; Rajeswara Rao, M.; Ravikanth, M., *Org. Biomol. Chem.* **2015,** *13* (9), 2501-2517.

2. Lee, C.-H.; S. Lindsey, J., *Tetrahedron* **1994,** *50* (39), 11427-11440.

3. Baruah, M.; Qin, W.; Basarić, N.; De Borggraeve, W. M.; Boens, N., *J. Org. Chem.* **2005,** *70* (10), 4152-4157.

4. Yogo, T.; Urano, Y.; Ishitsuka, Y.; Maniwa, F.; Nagano, T., *J. Am. Chem. Soc.* **2005,** *127* (35), 12162-12163.

5. Jiao, L.; Pang, W.; Zhou, J.; Wei, Y.; Mu, X.; Bai, G.; Hao, E., *J. Org. Chem.* **2011,** *76* (24), 9988-9996.

6. Lakshmi, V.; Ravikanth, M., *J. Org. Chem.* **2011,** *76* (20), 8466-8471.

7. Leen, V.; Miscoria, D.; Yin, S.; Filarowski, A.; Molisho Ngongo, J.; Van der Auweraer, M.; Boens, N.; Dehaen, W., *J. Org. Chem.* **2011,** *76* (20), 8168-8176.

8. Duran-Sampedro, G.; Agarrabeitia, A. R.; Garcia-Moreno, I.; Costela, A.; Bañuelos, J.; Arbeloa, T.; López Arbeloa, I.; Chiara, J. L.; Ortiz, M. J., *Eur. J. Org. Chem.* **2012,** *2012* (32), 6335-6350.

9. Leen, V.; Yuan, P.; Wang, L.; Boens, N.; Dehaen, W., *Org. Lett.* **2012,** *14* (24), 6150-6153.

10. Lu, H.; Mack, J.; Yang, Y.; Shen, Z., *Chem. Soc. Rev.* **2014,** *43* (13), 4778-4823.

11. Wang, H.; Vicente, M. G. H.; Fronczek, F. R.; Smith, K. M., *Chem. Eur. J.* **2014,** *20* (17), 5064-5074.

12. Zhao, N.; Vicente, M. G. H.; Fronczek, F. R.; Smith, K. M., *Chem. Eur. J.* **2015,** *21*, 6181-6192.

13. Wang, H.; Fronczek, F. R.; Vicente, M. G. H.; Smith, K. M., *J. Org. Chem.* **2014,** *79* (21), 10342-10352.

14. Fischer, H.; Orth, H., *Justus Liebigs Annalen der Chemie* **1933,** *502* (1), 237-264.

15. Ballantine, J. A.; Jackson, A. H.; Kenner, G. W.; McGillivray, G., *Tetrahedron* **1966,** *22*, *Supplement 7* (0), 241-259.

16. Plater, M. J.; Aiken, S.; Bourhill, G., *Tetrahedron* **2002,** *58* (12), 2405-2413.

17. de Almeida, L. S.; Esteves, P. M.; de Mattos, M. C. S., *Tetrahedron Lett.* **2009,** *50* (25), 3001-3004.

18. Madhu, S.; Rao, M. R.; Shaikh, M. S.; Ravikanth, M., *Inorg. Chem.* **2011,** *50* (10), 4392-4400.

19. Misra, R.; Dhokale, B.; Jadhav, T.; Mobin, S. M., *New J. Chem.* **2014,** *38* (8), 3579-3585.

20. Lennox, A. J. J.; Lloyd-Jones, G. C., *Chem. Soc. Rev.* **2014,** *43* (1), 412-443.

21. Ishiyama, T.; Ishida, K.; Miyaura, N., *Tetrahedron* **2001,** *57* (49), 9813-9816.

22. Espinet, P.; Echavarren, A. M., *Angew. Chem. Int. Ed.* **2004,** *43* (36), 4704-4734.

23. Olmsted, J., *The Journal of Physical Chemistry* **1979,** *83* (20), 2581-2584.

24. Boens, N.; Wang, L.; Leen, V.; Yuan, P.; Verbelen, B.; Dehaen, W.; Van der Auweraer, M.; De Borggraeve, W. D.; Van Meervelt, L.; Jacobs, J.; Beljonne, D.; Tonnelé, C.; Lazzaroni, R.; Ruedas-Rama, M. J.; Orte, A.; Crovetto, L.; Talavera, E. M.; Alvarez-Pez, J. M., *J. Phys. Chem. A* **2014,** *118* (9), 1576-1594.

25. Chen, Y.; Zhao, J.; Guo, H.; Xie, L., *J. Org. Chem.* **2012,** *77* (5), 2192-2206.

26. Chen, Y.; Zhao, J.; Xie, L.; Guo, H.; Li, Q., *RSC Adv.* **2012,** *2* (9), 3942-3953.

27. Brizet, B.; Desbois, N.; Bonnot, A.; Langlois, A.; Dubois, A.; Barbe, J.-M.; Gros, C. P.; Goze, C.; Denat, F.; Harvey, P. D., *Inorg. Chem.* **2014,** *53* (7), 3392-3403.

28. Xu, H.-J.; Bonnot, A.; Karsenti, P.-L.; Langlois, A.; Abdelhameed, M.; Barbe, J.-M.; Gros, C. P.; Harvey, P. D., *Dalton Trans.* **2014,** *43* (22), 8219-8229.

29. Rohand, T.; Qin, W.; Boens, N.; Dehaen, W., *Eur. J. Org. Chem.* **2006,** *2006* (20), 4658-4663.

30. Didier, P.; Ulrich, G.; Mely, Y.; Ziessel, R., *Org. Biomol. Chem.* **2009,** *7* (18), 3639-3642.

CHAPTER 4: SYNTHESIS AND REGIOSELECTIVE FUNCTIONALIZATION OF PERHALOGENATED BODIPYS

4.1 Introduction

As discussed in the Chapters 1-3, halogenated BODIPYs are important synthetic targets for various applications. In the last two decades, with development of synthetic chemistry, the different halogen groups can be selectively introduced to all the different positions on the BODIPY platforms for further functionalizations.[1] To the best of our knowledge, BODIPYs **1**[2-3] and **2**[4] with six chloro or bromo groups at all the pyrrolic positions and two fluoro atoms at the boron position have the most (8) halogen groups at the BODIPY cores. Such polyhalogenated BODIPYs were prepared by direct bromination of 8-phenyl BODPY, or by NCS or NBS halogenation at the precursor pyrrole or dipyrromethane stages, followed by (condensation), oxidation and boron complexation. In addition, the hexahalo-BODIPYs allowed for the regioselective substitution reactions at 1,3,5,7-positions and Suzuki cross-coupling reactions at the 1,2,3,5,6,7-positions. Thus, to enrich BODIPY chemistry, a series of global halogenated BODIPYs **3b-5b** with nine halogen groups were prepared by using Br_2 as the halogenation reagents for the first time. Investigation of reactivity via Stillecross-coupling and boron substitution reactions were conducted to show the regioselectivity under these reactions.

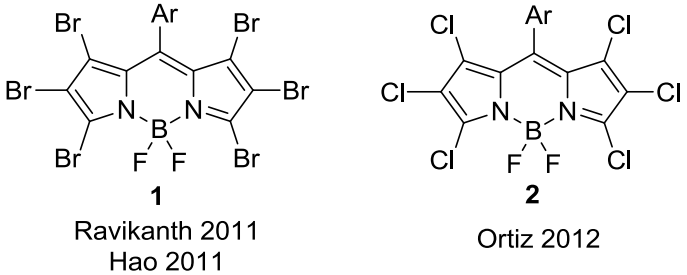

Figure 4-1: Structures of Hexahalogenated BODIPYs.

* Reproduced from Ref. Zhao, N.; Xuan, S.; Byrd, B.; Fronczek, F. R.; Smith, K. M.; Vicente, M. G. H., Synthesis and regioselective functionalization of perhalogenated BODIPYs. *Org. Biomol. Chem.* **2016,** *14*, 6184-6188 with permission from the Royal Society of Chemistry.

4.2 Synthesis of Perhalogenated BODIPYs

As discussed in Chapter 3, the starting BODIPYs **3-5a** were prepared via chlorination using TCCA/AcOH of 8-chloro BODIPY[5-7] in 73-83% yields.[8] Due to the slight electron withdrawing effect of the 8-chloro group at the 8-position and bearing the most positive charge at the 1,7-positions, further chlorination could not occur at the 1,7-positions using different types of chlorination conditions, including TCCA in H_2SO_4. Thus, Br_2/CH_2Cl_2,[2] known a strong halogenation reagent, was selected for the global halogenation, as shown in Scheme 4-1. Treatment of **3a-5a** with 200 equivalents of Br_2 in CH_2Cl_2 at room temperature overnight afforded hepta-halogenated BODIPYs **3b-5b** as the only products, in 78-84% isolated yields. ^{1}H NMR spectra of halogenation reagent, was selected for the global halogenation, as shown in Schemes 4-1, 4-2, and

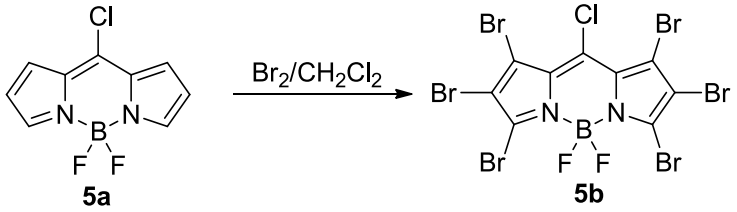

Scheme 4-1: Bromination of BODIPY **3a**.

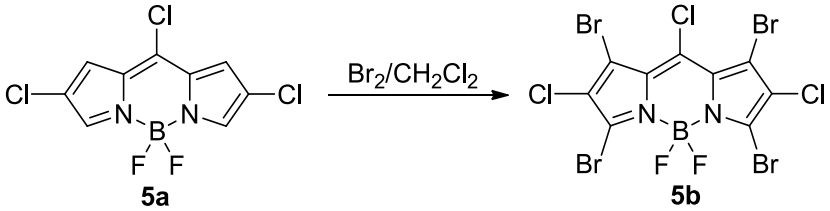

Scheme 4-2: Bromination of BODIPY **4a**.

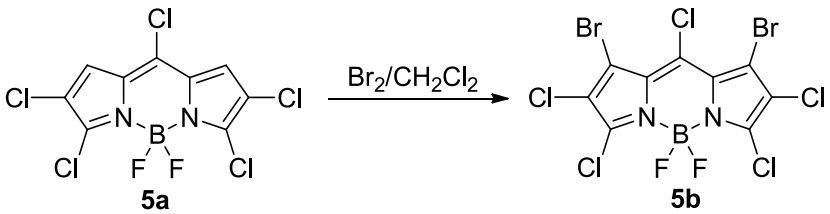

Scheme 4-3: Bromination of BODIPY **5a**.

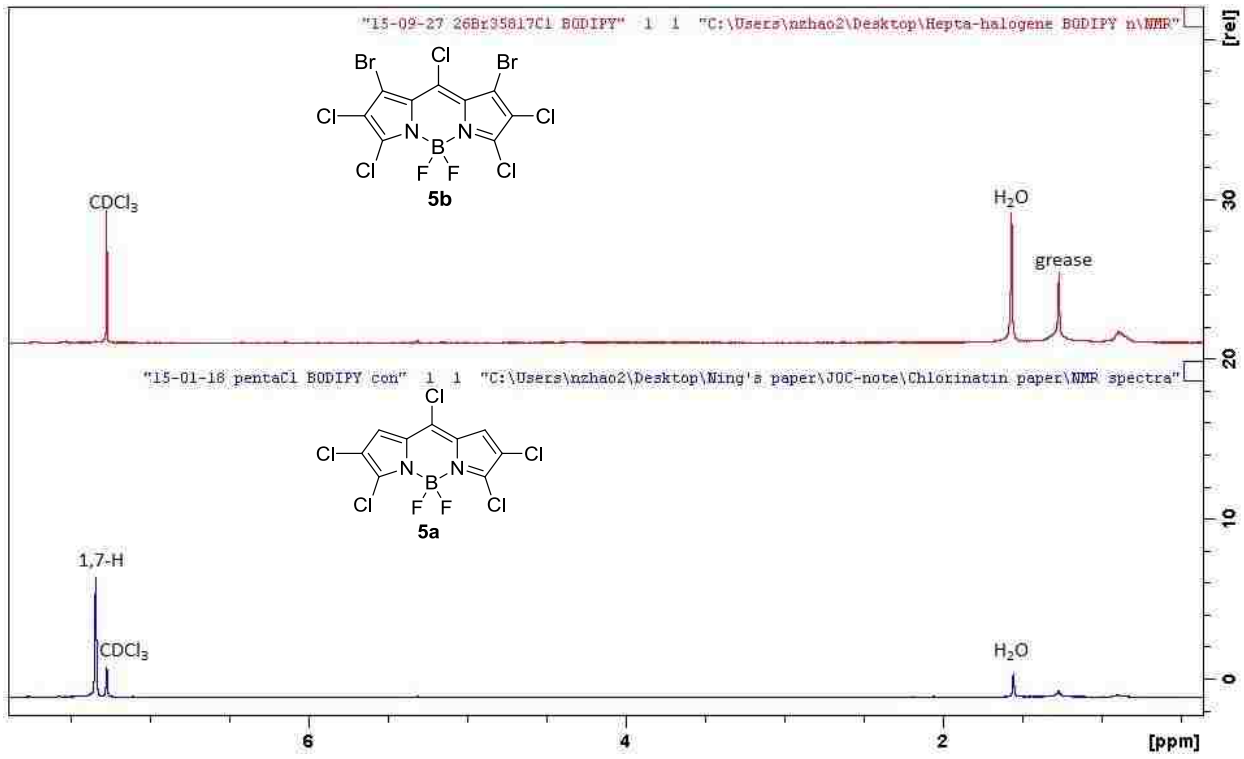

Figure 4-2: ^{1}H NMR (400 MHz) spectra of BODIPY **5a** and **5b** in $CDCl_3$ at room temperature.

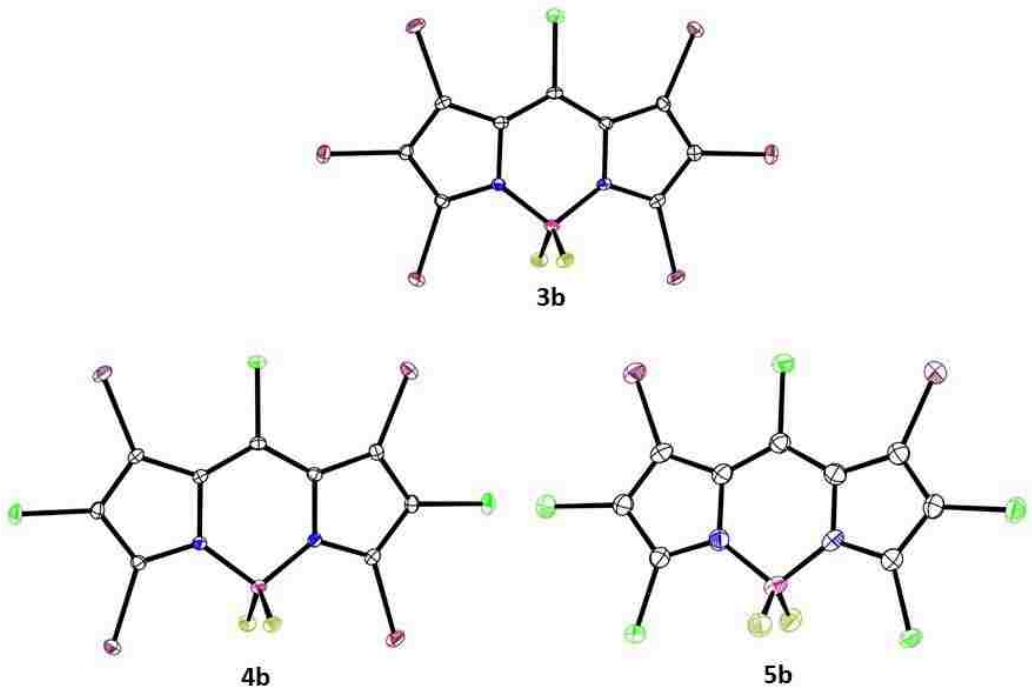

Figure 4-3: X-ray structures of BODIPY **3b**-**5b**.

4-3. Treatment of **3a-5a** with 200 equivalents of Br_2 in CH_2Cl_2 at room temperature and stirring overnight afforded hepta-halogenated BODIPYs **3b-5b** as the only products, in 78-84% isolated yields. The ^1H NMR spectra of **3b-5b** showed the complete disappearance of signals of all the pyrrolic hydrogens. For example, in the case of **5a**, the signals of the 1,7-hydrogens at $\delta = 7.34$ ppm were disappeared in the spectra of **5b**, as shown in Figure 4-2. Also, HRMS (ESI-TOF) spectra clearly showed the predicted isotopes of the halo groups of BODIPYs **3b-5b**.

Suitable crystals of **3b-5b** were obtained by slow evaporation of $CHCl_3$. The results were shown in Figure 4-3, which further confirms the formation of BODIPYs **3b-5b**. In all three BODIPYs, the dipyrrole unit with 11 atoms is nearly planar. There are mean deviation 0.016 Å in **3b**, 0.035 Å in **4b** and 0.035 Å in **5b**. The boron atoms lie slightly out of this core planes by 0.171 Å, 0.195 Å and 0.175 Å for **3b**, **4b**, and **5b**, respectively. The C-Cl bonds in **3b-5b** are in the range 1.695(4) – 1.712(4) Å with a mean value of 1.703 Å, while C-Br distances are in the range 1.842(2) - 1.862(3) Å with a mean value of 1.853 Å.

4.3 Functionalizationa of Perhalogenated BODIPYs 5b.

Based on our previous results, chlorinated BODIPYs show high reactivity under substitution and Pd(0)-catalyzed Stille and/or Suzuki cross-coupling reactions.[8-11] The regio-selectivity of the chloro groups at different positions of the BODIPYs was investigated and showed to be in decreasing order: m-(8)-Cl > α-(3,5)-Cl > β-(2,6)-Cl,[8-11] which allowed for the step-wise functionalization of BODIPYs at the 8-position, 3,5-positions, followed by the 2,6-positions. Due to the high selectivity observed for chlorinated BODIPYs, BODIPY **5b** with the most chloro groups among the three perhalogenated BODIPYs, was chosen for investigation of the reactivity and regioselectivity of the different halogen groups.

Since base is not required, the high yielding[9, 12-13] Stille cross-coupling[14] reactions are

very attractive among the Pd(0)-catalyzed cross-coupling reactions for BODIPY functionalization. By treating BODIPY **5b** with 1 equivalent of 2-(tributylstannyl)thiophene or with tributylphenylstannane in the presence of $Pd(PPh_3)_4$ (3 mol%) in refluxing toluene, TLC and MS both showed a tri-coupled product as the major product, along with unreacted starting material after several hours. This may be due to similar reactivity of the 1,7-bromo and 8-chloro groups

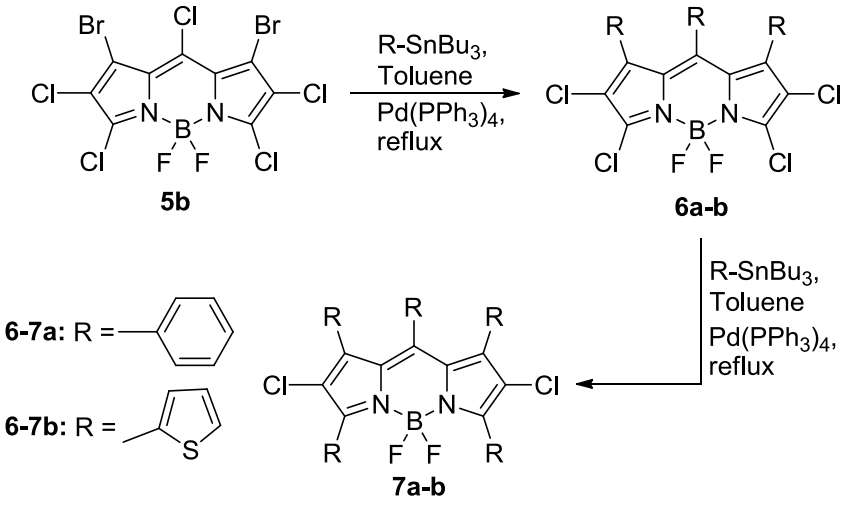

Scheme 4-2: Regioselective cross-coupling reactions of BODIPY **5b**.

under this type of reaction conditions. When 4 equivalents of stannane reagent was used, with refluxing overnight, the coupling reactions regioselectively occurred at 1,7,8-positions and tri-coupled BODIPYs **6a-b** were obtained as the major products, isolated in 57-71% yields, as shown in Scheme 4-2. 1,3,5,7,8-Pentaphenyl (thienyl)-2,6-dichloro-BODIPYs **7a-b** were obtained in 75-92% yield by treating BODIPYs **6a-b** with 10 equivalents of stannane reagent under the same conditions. The compounds were characterized by ^{1}H and ^{13}C NMR, ^{11}B NMR, and HRMS (ESI-TOF).

Suitable crystals of **6a**, **6b**, **7a** and **7b** were obtained by slow evaporation of $CHCl_3$. The results are shown in Figure 4-4, directly confirming the regioselectivity of the Stille cross-coupling reactions on BODIPY **5b**. In the structure of BODIPY **6a** and **6b**, the 12-atom core is nearly planar,

with mean deviation 0.021 Å and 0.049 Å. The three phenyl planes of **6a** and three disordered thiophene rings of **6b** form dihedral angles in the range 63.5-66.6° and 60.3-64.0° with it. BODIPYs **7a** and **7b** have the cores with similar conformation similar to those of **3b**, **4b**, and **5b**. The B atoms of **7a** and **7b** lie 0.183 Å (average of two independent molecules) and 0.106 Å out of the core plane. The phenyl groups of **7a** are disordered in one molecule and ordered in the other, in which they form dihedral angles (52.5-72.1°) with the core. Four of the five thiophene rings of BODIPY **7b** are disordered. A small dihedral angle of 27.4° is formed between the ordered one and the BODIPY core. The disordered thienyl substituents with variable conformations form dihedral angles (52.2-73.2°) with the core.

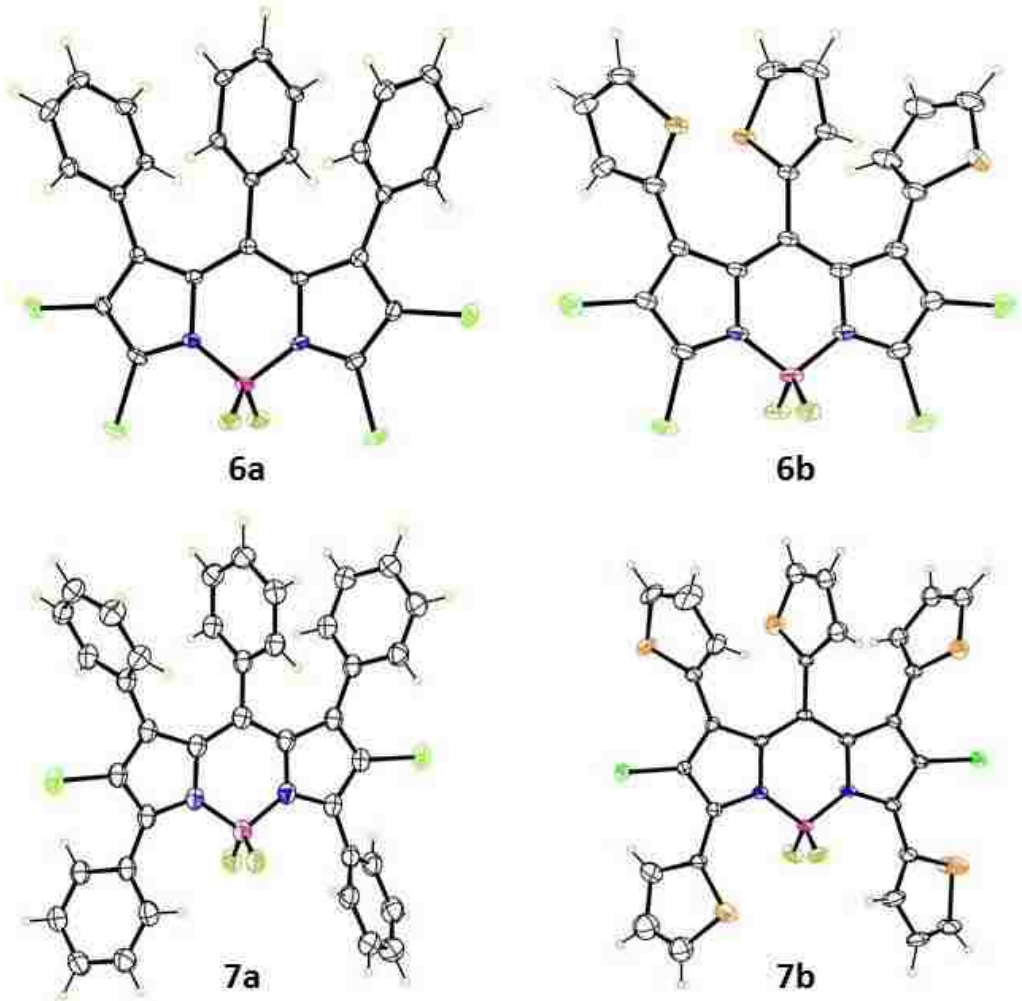

Figure 4-4: X-ray structures of **6a**, **6b**, **7a** and **7b**.

As discussed in the Chapter 3, Pd(PCy_3)G2 can efficiently catalyzed the Stille cross-coupling reactions for 2,6-dichloro BODIPYs.[8] Thus, as shown in Scheme 4-3, by treating BODIPY **7a** with tributylphenyltin (up to 100 equiv) in the presence of Pd(PCy_3)G2, BODIPY **8** was formed as the major product in 30% yield, with trace amount of desired product **9** and a large amount of starting material. The formation of BODIPY **9** was confirmed by HRMS, as shown in Figure 4-5. Low yields of this reaction may be due to the steric interactions with different phenyl groups on BODPY **7a**, as well as the relatively low reactivity of the tributylphenyltin.

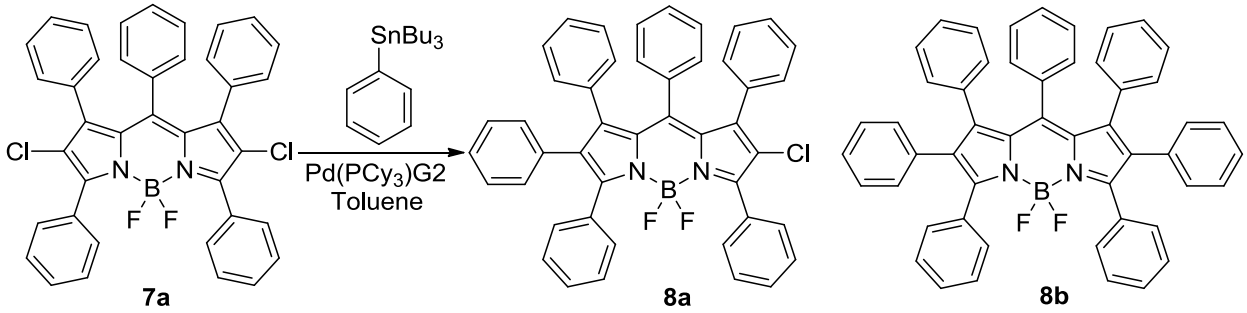

Scheme 4-3: Stille cross-cross coupling reactions of **7a**.

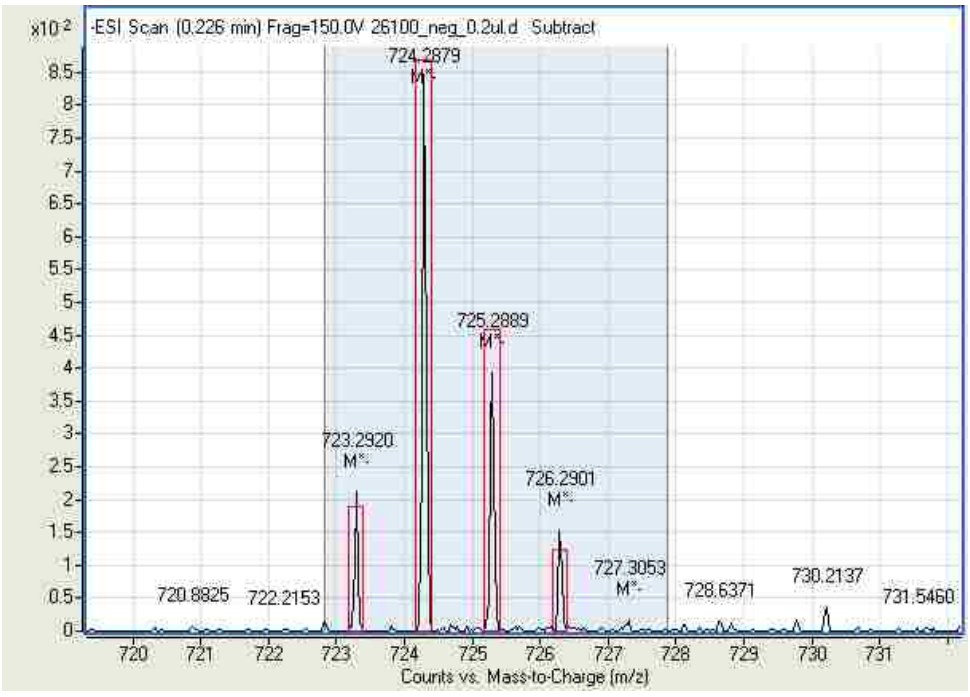

Figure 4-5: HRMS (ESI-TOF) spectra of BODIPY **9**.

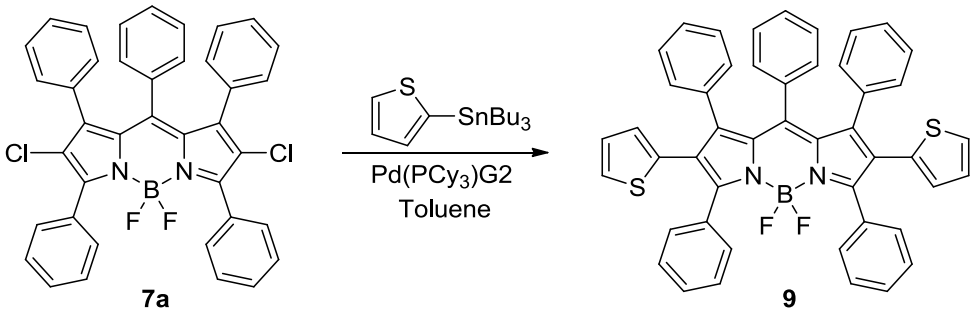

Scheme 4-4: Stille cross-cross coupling reaction of **7a** with (tributylstannyl)thiophene

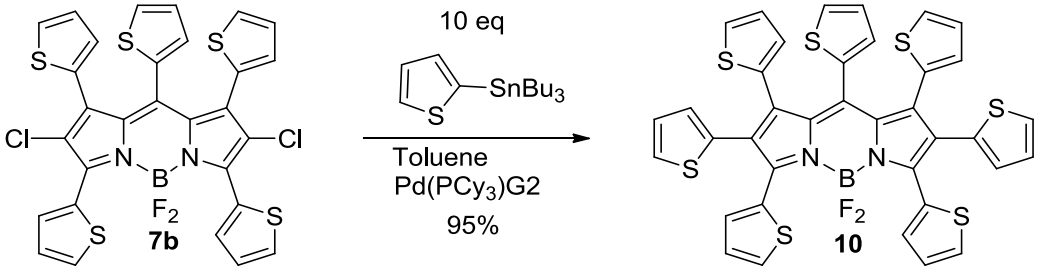

Scheme 4-5: Stille cross-cross coupling reaction of **7b** with (tributylstannyl)thiophene

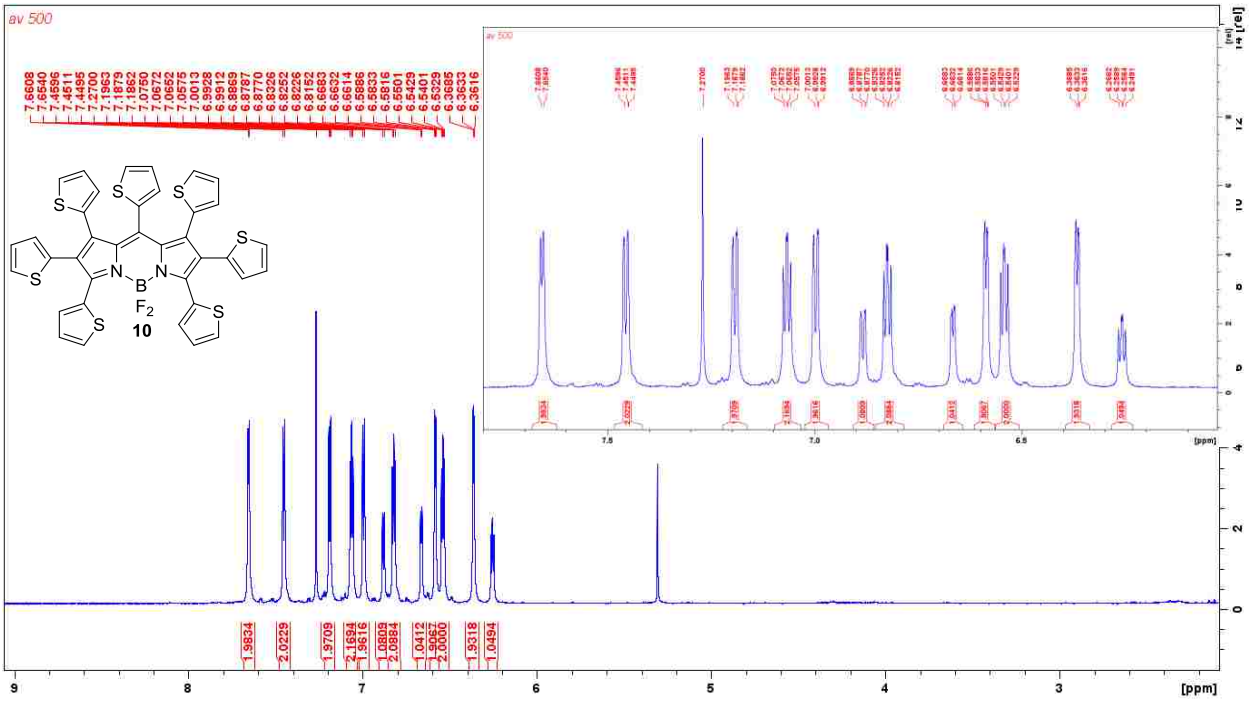

Figure 4-6: ^{1}H NMR (400 MHZ) spectra of BODIPY **10** in $CDCl_3$ at room temperature.

More reactive and less bulky (tributylstannyl)thiophene was chosen for the Stille corss-coupling

reactions of BODIPY **7a**, as shown in Scheme 4-4. The global coupling reaction was accomplished by using Pd(PCy3)G2 as the catalyst, in the presence of 10 equivalents of 2-(tributylstannyl)thiophene to provide 2,6-dithienyl 1,3,5,7,8-pentaphenyl BODIPY **9** in good yield (76%). Similarly, under the same conditions, 1,2,3,5,6,7,8-heptathienyl BODIPY **10** was synthesized in an excellent yield (95%), as shown in Scheme 4-5. These hepta-functionalized BODIPY **9** and **10** were characterized by ^{1}H NMR, ^{13}C NMR, ^{11}B NMR, and HRMS (ESI-TOF). For example, the ^{1}H NMR spectra of BODIPY **10** was shown in Figure 4-6. All 12 groups of characteristic doublet-of-doublets from seven thienyl groups on the BODIPY **10** were clearly separated and shown in this spectra. Also, all the integration of those signals are matching well with the structures. For example, the ^{1}H NMR spectra of BODIPY **10** is shown in Figure 4-6. All 12 groups of characteristic doublet-doublet from seven thienyl groups on the BODIPY **10** are clearly seen in this spectra. Also, all the integration of those signals match well with the structures.

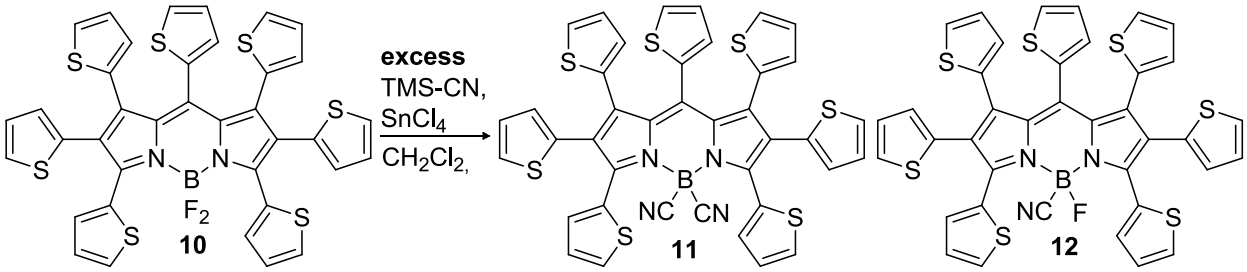

Scheme 4-6: Boron substitution reaction of BODIPY **10** by using $SnCl_4$.

Additionally, the investigation of the functionalization at the boron position was conducted to achieve nona-functionalization. Based on a published procedure,[15-17] BODIPY **10** were reacted with excess amount of trimethylsilyl cyanide catalyzed by tin (IV) chloride ($SnCl_4$) in CH_2Cl_2, as shown in Scheme 4-6. This reaction yielded the mono substituted product **12** after 30 minuites instead of the desired di-CN substituted product **11**. The momo-substitution product was confirmed by the doublet at $\delta \approx$ -5.5 ppm in the ^{11}B NMR, as shown Figure 4-7. In order to obtain the BODIPY

11, a large excess of TMS-CN and $SnCl_4$ were used, along with extend reaction times, but BODIPY **12** was the only product obtained in high yield (> 90%). This reaction under reflux for 2 hours provided a small amount of diCN BODIPY **11** (yield: <5%), although the major product was still BODIPY **12**. Thus, I believed the diCN-functionalization at the boron position of BODIPY **11** was possible to achieve. A stronger Lewis acid (BF_3•OEt_2) with excess TMS-CN in CH_2Cl_2 were used for this boron substitution reaction to provided 4,4'-diCN BODIPY **11** in 93% isolated yield. Similarly, 4,4'-diCN BODIPY **13** was obtained from BODIPY **9** in 92% yield under the same conditions, as shown in Scheme 4-8. A singlet (δ ≈ -16 ppm) in ^{11}B NMR of **13** confirmed the successful di-CN substitution at the boron position, as shown in Appendix C.

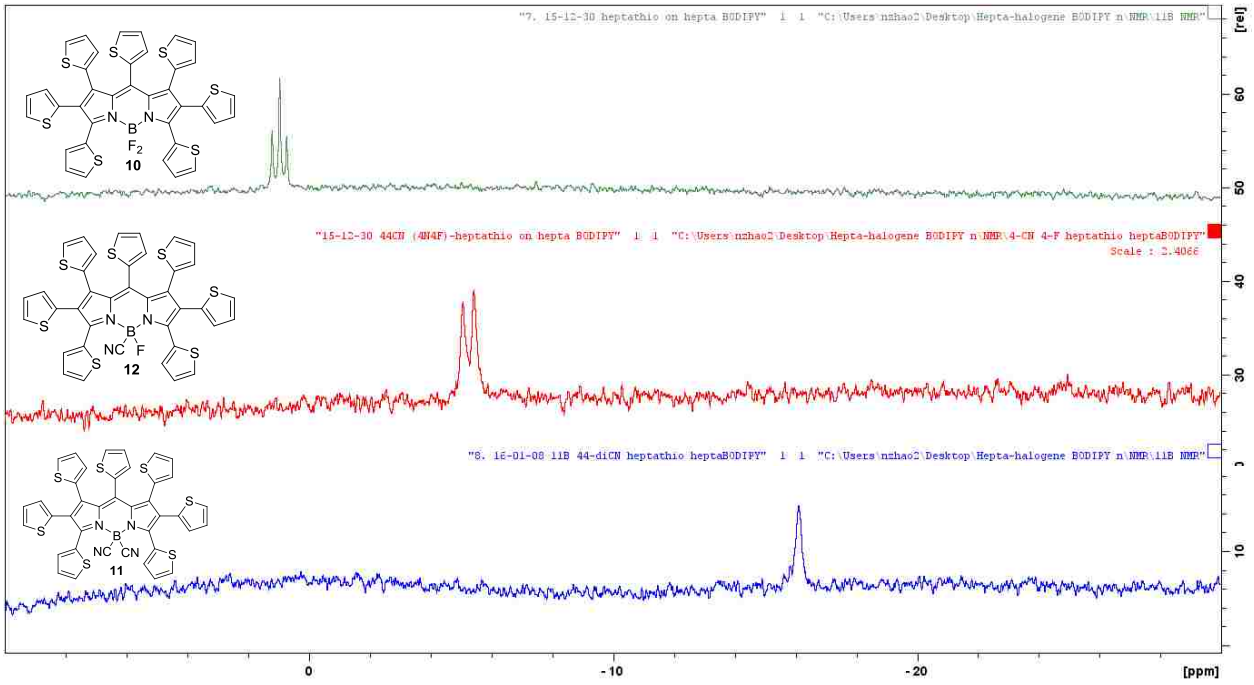

Figure 4-7: ^{11}B NMR (128 MHz) spectra of BODIPYs **10-12** in $CDCl_3$ at room temperature.

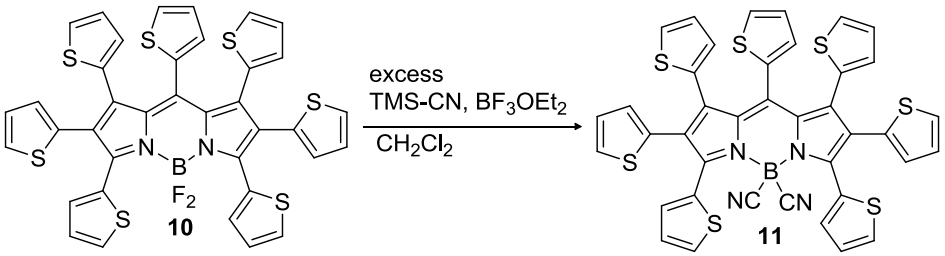

Scheme 4-7: Boron substitution reaction of BODIPY **10** by using BF3•OEt2

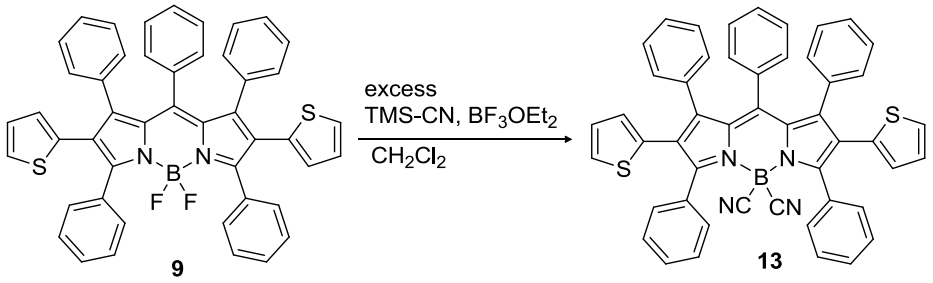

Scheme 4-8: Boron substitution reaction of BODIPY **9** using BF3•OEt2/TMSCN

4.4 Photophysical properties

Table 1: Spectroscopic properties of BODIPYs in CH_2Cl_2 at room temperature.

BODIPY	Absorption λ_{abs} (nm)	Log ε ($M^{-1}cm^{-1}$)	Emission λ_{em} (nm)	Φ_f[a]	Stokes shift (nm)
3b	556	5.02	572	0.17	16
4b	553	5.01	568	0.14	15
5b	546	4.87	560	0.18	14
6a	549	4.77	563	0.57	14
7a	564	4.85	596	0.39	32
9	581	4.66	666	0.08	85
13	585	4.48	676	0.06	91
6b	572	4.72	580	<0.003	8
7b	633	4.56	681	0.02	48
10	643	4.74	713	0.007	70
11	639	4.48	739	0.005	100

[a]Rhodamine B (0.4 in methanol)[18] for **3-5b** and **6a**; cresyl violet (0.55 in methanol)[19] was used as standard for **6b**, **7a**, **9**, and **13**; methylene blue (0.03 in methanol)[19] for **7b** and **10-11**.

The spectroscopic properties of BODIPYs **3b-5b**, **6a**, **6b**, **7a**, **7b**, **9-11** and **13** in CH_2Cl_2 namely their maximum absorption (λ_{abs}) and fluorescence wavelengths (λ_{em}), Stokes shifts, molar extinction coefficients (log ε) and fluorescence quantum yields (Φ_f), are summarized in Table 1. Figures 4-8, 4-9, and 4-10 show the normalized absorption and fluorescence spectra of all the new BODIPYs. Such BODIPYs show characteristic strong and narrow absorption bands (log ε = 4.48-5.02) and emission bands. From BODIPY **3b** to **5b**, the decreasing numbers of bromo groups gave a slightly blue shift in both the absorption and emission due to the less electron-donating chloro

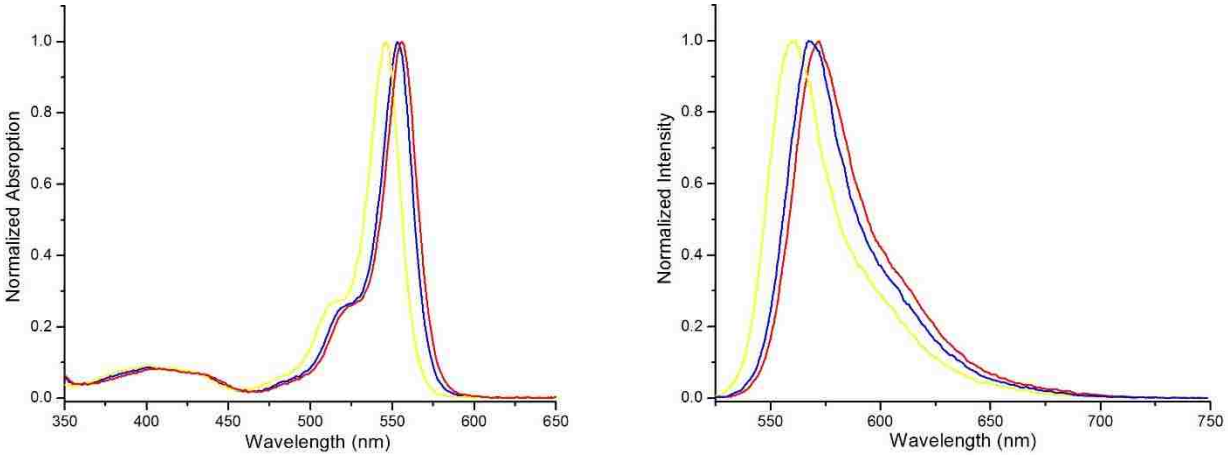

Figure 4-8: Normalized absorption (**a**) and fluorescence (**b**) spectra of BODIPYs **3b** (red), **4b** (blue), and **5b** (yellow) in CH_2Cl_2 at room temperature.

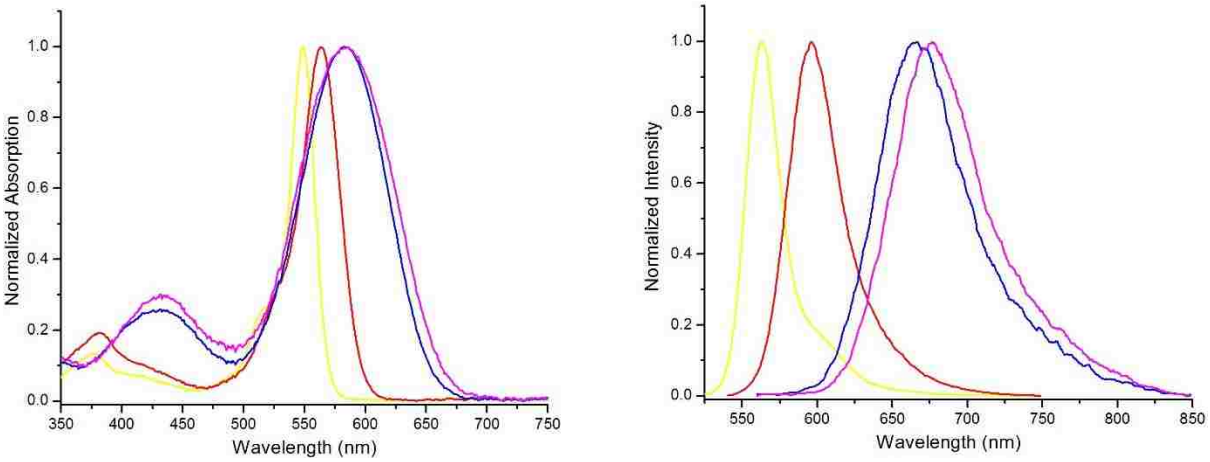

Figure 4-9: Normalized absorption (**a**) and fluorescence (**b**) spectra of BODIPYs **6a** (yellow), **7a** (red), **9** (blue), and **13** (purple) in CH_2Cl_2 at room temperature.

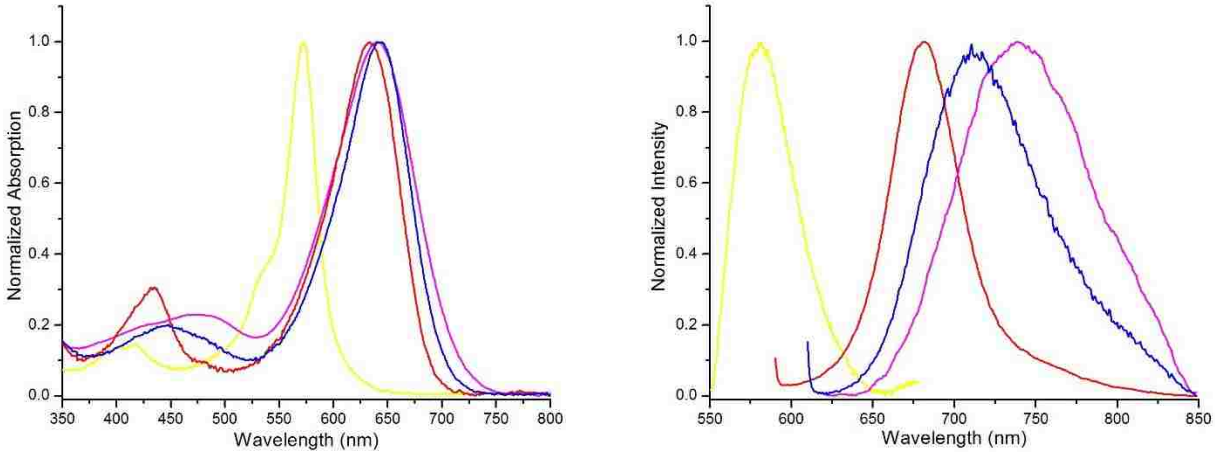

Figure 4-10: Normalized absorption (**a**) and fluorescence (**b**) spectra of BODIPYs **6b** (yellow), **7b** (red), **10** (blue), and **11** (purple) in CH_2Cl_2 at room temperature.

groups. Due to the big dihedral angles (60-67°), the introduction of phenyl and thienyl groups at the 1,7,8 -positions causes the moderate red-shifts (2-23 nm) in both absorption and emission bands of BODIPY **5b**. On the other hand, as reported,[9-10, 20-22] BODIPYs **7a** and **7b** with aryl-functionalization at the 3,5-positions or the 2,6-positions provided the largest red-shifts, which may be due to the decreased HOMO-LUMO gap. For example, there is a red shift of 101 nm in the emission of **7b**, compared with **6b**.

The Stokes shifts varied significantly (8-100 nm) depending on the different functional groups (Cl, Br, phenyl, CN and thienyl) on the BODIPYs. As reported,[9-10, 20-22] compared with phenyl groups, the thienyl groups on the BODIPY core lead to large Stokes shifts (up to 85 nm for BODIPY **9**), maybe due to increased geometry relaxation.[23-24] However, the thienyl groups also greatly decrease the fluorescent quantum yields (< 0.1) due to the free rotation of thienyl groups causing increasing nonradiative process. Further introduction of two cyanide groups at the boron position of BODIPYs **11** and **13** caused increased Stokes shift (91 and 100 nm) and slightly decreased quantum yields.

4.5 Conclusions

The global halogenated BODIPYs **3-5b** were synthesized in good yields, via bromination of chlorinated BODIPY **3a-5a**. The regioselective nona-functionalization of BODIPY **5b** was investigated via Pd(0)-catalyzed Stille cross-coupling and boron substitution reactions. The regioselectivity of the reactions was confirmed by X-ray crystallography and by ^{1}H and ^{13}C NMR spectroscopy and mass spectrometry, and showed the following order of increasing reactivity: 8-Cl ≈ 1,7-Br > 3,5-Cl > 2,6-Cl > 4,4'-F. The thienyl-coupled BODIPYs showed the largest Stokes shifts, as well as the largest red-shifted absorptions and emissions. The nona-functionalized

BODIPY **11** and **13** had the largest Stokes shifts (91-100 nm). However, such BODIPYs displayed the lowest quantum yields (< 0.1).

4.6 Experimental

4.6.1 Synthesis

General: All reagents and solvents were purchased from Sigma-Aldrich, Fisher Scientifics or Alfa Aesar as reagent grades and used without further purification. Argon was used to protect the air-sensitive reactions. Analytical TLC (polyester backed, 60Å, 0.2 mm, precoated, Sorbent Technologies) was used to monitor the reactions. Column chromatography was performed on silica gel (60Å, 230-400 mesh, Sorbent Technologies). All ^{1}H NMR, ^{13}C NMR and ^{11}B NMR spectra were obtained using Bruker AV-400 nanobay or AV-500 spectrometers (400 MHz or 500 MHz for ^{1}H NMR and 100 or 125MHz for ^{13}C NMR) and AV-400 III (128 MHz for ^{11}B NMR) in $CDCl_3$ with trimethylsilane as an internal standard, at room temperature. Chemical shifts (δ) are given in parts per million (ppm) with $CDCl_3$ (7.27 ppm for ^{1}H NMR, 77.0 ppm for ^{13}C NMR) and CD_2Cl_2 (5.32 ppm for 1H NMR, 53.4 ppm for 13C NMR). All high-resolution mass spectra (ESI-TOF) were obtained using a 6210 ESI-TOF mass spectrometer (Agilent Technologies). All UV-Visible spectra were recorded on a Varian Cary 50 (solutions) spectrophotometer at room temperature. Fluorescence spectra were studied on a PTI QuantaMaster4/2006SE spectrofluorimeter corrected emission spectrum. A 10 mm path length quartz cuvette and spectroscopic grade solvents were used for the measurements. For the determination of quantum yields, dilute solutions with different absorbance between 0.02-0.08 at the particular excitation wavelength were used. Molar absorption coefficients (ε) was determined from the plots of integrated absorbance vs concentrations. Rhodamine B in methanol (0.4),[18] crystal violet perchlorate in methanol (0.55 in methanol),[19] and methylene blue (0.03 in methanol)[19] were used as external standards for all the BODIPY

derivatives. The following equation was used for the calculations of the relative fluorescence quantum yields (Φ_f):[25]

$\Phi_s = \Phi_{st} \times (Grad_x/Grand_{st}) \times (n_x^2/n_{st}^2)$

where Φ and n are the fluorescence quantum yields and refractive indexes, respectively; Grad represents gradient of integrated fluorescence intensity vs absorbance at the particular wavelength, subscripts s and x refer to the standards and the tested samples.

BODIPY 3-5a were synthesized according to a published procedure.[8]

General procedure for BODIPY 3-5b:

BODIPY **3-5a** (0.1 mmol) was dissolved in 2 ml DCM. Br_2 (1.02ml, 20 mmol) was added into the flask. The mixture was stirred at room temperature overnight. TLC was used to monitor the reaction. The mixture was poured into saturated $Na_2S_2O_3$ (aq) (100 ml) and extracted by CH_2Cl_2 (20 ml* 3). The organic layers were combined and washed with brine then water. The solvent were removed under reduced pressure. The residue was purified by using column chromatography (CH_2Cl_2/Hexanes 1:1 as eluents) to provide the pure compounds.

BODIPY 3b: Yield: 58 mg, 83%; ^{1}H NMR (400 MHz, $CDCl_3$): no peaks; ^{13}C NMR (125 MHz, $CDCl_3$): 138.1, 134.6, 129.9, 122.5, 118.4; ^{11}B NMR (128 MHz, $CDCl_3$) δ -0.17 (t, $J_{(B,F)}$ = 26.9 Hz); HRMS (ESI-TOF) m/z 692.4972 $[M]^-$; calculated for $C_9BBr_6ClF_2N_2$: 692.4948.

BODIPY 4b: Yield: 47.6 mg, 78%; ^{1}H NMR (400 MHz, $CDCl_3$): no peaks; ^{13}C NMR (125 MHz, $CDCl_3$) δ 138.6, 132.3, 128.9, 128.7, 119.2; ^{11}B NMR (128 MHz, $CDCl_3$) δ -0.19 (t, $J_{(B,F)}$ = 27.1 Hz); HRMS (ESI-TOF) m/z 604.5946 $[M]^-$; calculated for $C_9BBr_4Cl_3F_2N_2$: 604.5958.

BODIPY 5b: Yield: 43.8 mg, 84%; ^{1}H NMR (400 MHz, $CDCl_3$): no peaks; ^{13}C NMR (125 MHz, $CDCl_3$) δ 142.5, 138.8, 126.8, 125.4, 119.6; ^{11}B NMR (128 MHz, $CDCl_3$) δ -0.31 (t, $J_{(B,F)}$ = 26.4 Hz); HRMS (ESI-TOF) m/z 516.6980 $[M]^-$; calculated for $C_9BBr_2Cl_5F_2N_2$: 516.6968 .

General procedure for BODIPY 6a-b

BODIPY **5b** (15.7 mg, 0.03 mmol) and $Pd(PPh_3)_4$ (3 mol%) were added into a 25 ml round-bottomed flask. The flask was evacuated and refilled with nitrogen for three times. Toluene (5 ml) and organostananne reagents (0.14 mmol, 4 equiv) were purged into the flask, and the mixture was heated to 90-100 ^oC and stirred for 6 hours. The reaction was stopped when **6a-b** was showed as major products according to TLC. The solvents were removed under reduced pressure. Then, the crude product was purified by using column chromatography (Ethyl acetate/Hexanes 1: 10 as eluents) to provide the desired products.

BODIPY 6a: Yield: 8.9 mg, 57%; ^1H NMR (500 MHz, $CDCl_3$) δ 6.94-6.97 (m, 2H), 6.87–6.90 (m, 4H), 6.63–6.68 (m, 7H), 6.42–6.45 (m, 2H); ^{13}C NMR (125 MHz, $CDCl_3$) δ 146.3, 143.7, 142.3, 131.2, 131.0, 129.5, 129.3, 129.2, 128.9, 127.5, 127.4, 126.8, 121.9; ^{11}B NMR (128 MHz, $CDCl_3$) δ 0.13 (t, $J_{(B,F)}$ = 27.7 Hz); HRMS (ESI-TOF) m/z 555.0100 $[M]^-$; calculated for $C_{27}H_{15}BCl_4F_2N_2$: 555.0092.

BODIPY 6b: Yield: 12.3 mg, 71%; ^1H NMR (400 MHz, $CDCl_3$) δ 7.17-7.18 (dd, $J_{(H,H)}$ = 5.1, 1.2 Hz, 2H), 6.93-6.94 (dd, $J_{(H,H)}$ = 5.0, 1.3 Hz, 1H), 6.67-6.70 (m, 3H), 6.45-6.46 (dd, $J_{(H,H)}$ = 3.6, 1.2 Hz, 2H), 6.30-6.32 (dd, $J_{(H,H)}$ = 5.0, 3.6 Hz, 1H); ^{13}C NMR (125 MHz, $CDCl_3$) δ 143.0, 138.3, 136.8, 134.0, 131.5, 130.6, 130.4, 130.3, 129.4, 127.9, 126.8, 126.6, 123.4; ^{11}B NMR (128 MHz, $CDCl_3$) δ -0.02 (t, $J_{(B,F)}$ = 27.5 Hz); HRMS (ESI-TOF) m/z 572.8774 $[M]^-$; calculated for $C_{21}H_9BCl_4F_2N_2S_3$: 572.8779.

General procedure for BODIPY 7a-b

BODIPY **6a-b** (0.02 mmol) and $Pd(PPh_3)_4$ (3 mol%) were added into a 25 ml round-bottomed flask. The flask was evacuated and refilled with nitrogen for three times. Toluene (5 ml) and organostananne reagents (0.2 mmol, 10 equiv) were purged into the flask, and the mixture was

reflux overnight. The reaction was stopped when **6a-b** was showed as major products according to TLC. The solvents were removed under reduced pressure. Then, the crude product was purified by using column chromatography (Ethyl acetate/Hexanes 1: 4 as eluents) to provide the desired products.

BODIPY 7a: Yield: 9.6 mg, 75%; ^{1}H NMR (400 MHz, $CDCl_3$) δ 7.70-7.72 (m, 4H), 7.44-7.48 (m, 6H), 6.88-6.95 (m, 6H), 6.79-6.81 (m, 2H), 6.73-6.76 (m, 4H), 6.62-6.64 (m, 1H), 6.45-6.48 (m, 2H); ^{13}C NMR (125 MHz, $CDCl_3$) δ 153.6, 147.2, 143.1, 132.5, 131.2, 130.7, 130.2, 130.1, 129.8, 129.7, 129.6, 129.0, 127.9, 127.3, 126.9, 126.7, 123.4; ^{11}B NMR (128 MHz, $CDCl_3$) δ 0.62 (t, $J_{(B,F)}$ = 30.0 Hz); HRMS (ESI-TOF) m/z 639.1475 $[M]^-$; calculated for $C_{39}H_{25}BCl_2F_2N_2$: 639.1498.

BODIPY 7b: Yield: 12.4 mg, 92%; ^{1}H NMR (500 MHz, $CDCl_3$) δ 7.90-7.91 (dd, $J_{(H,H)}$ = 3.8, 1.2 Hz, 2H), 7.64-7.65 (dd, $J_{(H,H)}$ = 5.1, 1.2 Hz, 2H), 7.20-7.22 (dd, $J_{(H,H)}$ = 5.0, 3.8 Hz, 2H), 7.16-7.17 (dd, J = 5.1, 1.2 Hz, 2H), 6.91-6.92 (dd, $J_{(H,H)}$ = 5.0, 1.2 Hz, 1H), 6.66 – 6.68 (m (overlap), 3H), 6.46-6.47 (dd, $J_{(H,H)}$ = 3.6, 1.2 Hz, 2H), 6.28-6.30 (dd, $J_{(H,H)}$ = 5.0, 3.5 Hz, 1H); ^{13}C NMR (125 MHz, $CDCl_3$) δ 146.8, 137.0, 136.0, 133.67(t, overlap), 133.62, 132.6, 132.5, 131.5, 130.9, 129.5, 129.25, 129.21, 127.5, 127.1, 126.6, 126.3, 125.8; ^{11}B NMR (128 MHz, $CDCl_3$) δ 0.76 (t, $J_{(B,F)}$ =30.7 Hz); HRMS (ESI-TOF) m/z 668.9313 $[M]^-$; calculated for $C_{29}H_{15}BCl_2F_2N_2S_5$: 668.9319.

General procedure for BODIPY 9-10

BODIPY **7a-b** (0.02 mmol) and $Pd(PCy_3)G2$ (3 mol%) were added into a 25 ml round-bottomed flask. The flask was evacuated and refilled with nitrogen for three times. Toluene (5 ml) and 2-(tributylstannyl)-thiophene (74.6 mg, 0.2 mmol) were purged into the flask, and the mixture was reflux overnight. The reaction was stopped when **9-10** was showed as major products according to TLC. The solvents were removed under reduced pressure. Then, the crude product was purified

by using column chromatography (Ethyl acetate/Hexanes 1: 2 as eluents) to provide the desired products.

BODIPY 9: Yield: 11.2 mg, 76%; ^{1}H NMR (400 MHz, $CDCl_3$) δ 7.49-7.51 (m, 4H), 7.30-7.39 (m, 6H), 6.93-6.94 (dd, $J_{(H,H)}$ = 5.1, 1.2 Hz, 2H), 6.77-6.88 (m, 8H), 6.65-6.67 (m, 4H), 6.58-6.62 (m (overlap), 3H), 6.42-6.45 (m, 2H), 6.12-6.13 (dd, $J_{(H,H)}$ = 3.6, 1.2 Hz, 2H). ^{13}C NMR (125 MHz, $CDCl_3$) δ 156.1, 147.4, 143.9, 134.22, 134.19, 132.2, 131.5, 131.3, 130.6, 130.4, 130.1, 129.1, 128.6, 128.0, 127.8, 127.7, 127.2, 126.5, 126.3, 126.1, 125.7; ^{11}B NMR (128 MHz, $CDCl_3$) δ 0.85 (t, J = 30.3 Hz); HRMS (ESI-TOF) m/z 735.2011 $[M]^-$; calculated for $C_{47}H_{31}BF_2N_2S_2$: 735.2032.

BODIPY 10: Yield: 14.6 mg, 95%; ^{1}H NMR (500 MHz,$CDCl_3$) δ 7.65-7.66 (m, 2H), 7.45-7.46 (dd, $J_{(H,H)}$ = 5.1, 1.2 Hz, 2H), 7.19-7.20 (dd, $J_{(H,H)}$ = 5.1, 1.2 Hz, 2H), 7.06-7.08 (dd, $J_{(H,H)}$ = 5.0, 3.7 Hz, 2H), 6.99-7.00 (dd, $J_{(H,H)}$ = 5.1, 1.2 Hz, 2H), 6.88-6.89 (dd, $J_{(H,H)}$ = 5.0, 1.3 Hz, 1H), 6.82-6.83 (dd, $J_{(H,H)}$ = 5.1, 3.6 Hz, 2H), 6.66-6.67 (dd, $J_{(H,H)}$ = 3.6, 1.3 Hz, 1H), 6.58-6.59 (dd, $J_{(H,H)}$ = 3.6, 1.2 Hz, 1H), 6.53-6.55 (dd, $J_{(H,H)}$ = 5.1, 3.5 Hz, 1H), 6.36-6.37 (dd, $J_{(H,H)}$ = 3.5, 1.2 Hz, 2H), 6.25-6.27 (dd, $J_{(H,H)}$ = 5.1, 3.6 Hz, 1H); ^{13}C NMR (125 MHz, $CDCl_3$) δ 149.4, 137.7, 137.4, 134.3, 134.1, 133.41, 133.37, 133.0(t), 132.1, 131.2, 130.53, 130.50, 130.2, 129.4, 129.2, 129.0, 127.1, 126.5, 126.3, 126.2; ^{11}B NMR (128 MHz, $CDCl_3$) δ 0.96 (t, $J_{(B,F)}$ =30.7 Hz); HRMS (ESI-TOF) m/z 764.9862 $[M]^-$; calculated for $C_{37}H_{21}BF_2N_2S_7$: 764.9853.

General procedure for BODIPY 11 and 13

BODIPY **9-10** (0.01 mmol) was dissolved in dry CH_2Cl_2 (2 ml). $BF_3{\cdot}OEt_2$ (12.3 μl, 0.1 mmol) and trimethylsilyl cyanide (26.8 μl, 0.2 mmol) were added into the flask. The mixture was stirred at room temperature for 1h. The reaction was quenched with H_2O (2ml), and extract byCH_2Cl_2 (20 ml* 3). The organic layers were combined and washed with brine then water. The solvent were

removed under reduced pressure. The residue was purified by using column chromatography (CH_2Cl_2/Hexanes 2:1 as eluents) to provide the pure compounds.

BODIPY 13: Yield: 6.9 mg, 92%; ^{1}H NMR (400 MHz, $CDCl_3$) δ 7.60-7.63 (m, 4H), 7.41-7.46 (m, 6H), 6.93-6.95 (dd, $J_{(H,H)}$ = 5.1, 1.2 Hz, 2H), 6.88-6.92 (m, 2H), 6.81-6.85 (m, 6H), 6.68-6.70 (m, 4H), 6.62-6.66 (m, 1H), 6.56-6.59 (dd, $J_{(H,H)}$ = 5.1, 3.7 Hz, 2H), 6.46-6.50 (m, 2H), 6.14-6.16 (dd, $J_{(H,H)}$ = 3.7, 1.2 Hz, 2H). ^{13}C NMR (125 MHz, $CDCl_3$) δ 157.1, 148.4, 144.7, 133.5, 133.1, 131.1, 130.9, 130.7, 130.4, 130.1, 129.7, 129.3, 129.0, 128.37, 128.0, 127.5, 126.8, 126.7, 126.1; ^{11}B NMR (128 MHz, $CDCl_3$) δ -16.30 (s); HRMS (ESI-TOF) m/z 749.2126 $[M]^-$; calculated for $C_{49}H_{31}BN_2S_2$: 749.2125.

BODIPY 11: Yield: 7.3 mg, 93%; ^{1}H NMR (400 MHz,$CDCl_3$) δ 7.80-7.81 (dd, $J_{(H,H)}$ = 3.7, 1.2 Hz, 2H), 7.57-7.59 (dd, $J_{(H,H)}$ = 5.1, 1.2 Hz, 2H), 7.17-7.20 (dd, $J_{(H,H)}$ = 5.0, 3.7 Hz, 2H), 7.15-7.17 (dd, $J_{(H,H)}$ = 5.1, 1.2 Hz, 2H), 7.06-7.08 (dd, $J_{(H,H)}$ = 5.0, 1.2 Hz, 2H), 6.94-6.96 (dd, $J_{(H,H)}$ = 5.0, 1.3 Hz, 1H), 6.77-6.79 (dd, $J_{(H,H)}$ = 5.1, 3.6 Hz, 2H), 6.71-6.72 (dd, $J_{(H,H)}$ = 3.6, 1.3 Hz, 1H), 6.59-6.61 (dd, $J_{(H,H)}$ = 5.1, 3.5 Hz, 2H), 6.54-6.56 (dd, $J_{(H,H)}$ = 3.7, 1.2 Hz, 2H), 6.43-6.44 (dd, $J_{(H,H)}$ = 3.6, 1.2 Hz, 2H), 6.30-6.32 (dd, $J_{(H,H)}$ = 5.0, 3.6 Hz, 1H); ^{13}C NMR (125 MHz, $CDCl_3$) δ 150.5, 139.7, 137.7, 133.85, 133.77, 133.4, 132.8, 132.24, 132.22, 131.2, 130.8, 129.8, 129.6, 129.4, 129.2, 127.6, 127.4, 127.3, 126.6, 126.5, 126.4; ^{11}B NMR (128 MHz, $CDCl_3$) δ -16.12 (s); HRMS (ESI-TOF) m/z 778.9926 $[M]^-$; calculated for $C_{39}H_{21}BN_4S_7$: 778.9946.

4.6.2 Crystal data

Crystal structures of **3b**, **4b**, **5b**, **6a**, **6b**, **7a** and **7b** were determined from data collected at T=90K using MoKα radiation (CuKα for **7a**) on Bruker Apex-II or Nonius KappaCCD diffractometers. **3b** has 13% Br substituted in the Cl site at the meso position. **6b** has all three thiophenes disordered and **7b** has 4 of the 5 thiophenes disordered. **7a** has two independent

molecules, one of which has all phenyl groups ordered while the other has 4 of the 5 disordered. *Crystal data*: **3b**, $C_9BBr_{6.13}Cl_{0.87}F_2N_2$, monoclinic, a = 8.4388(3), b = 8.4196(2), c = 21.5892(6) Å, β = 99.574(2)°, space group $P2_1/n$, Z = 4, 29024 reflections measured, θ_{max} = 36.4°, 7099 unique (R_{int} = 0.036), which were used in all calculations, final R = 0.028 (5672 I>2σ(I) data), w$R(F^2)$ 0.057 (all data), CCDC 1453168; **4b**, $C_9BBr_4Cl_3F_2N_2$, monoclinic, a = 8.3531(5), b = 8.5259(5), c = 20.7030(15) Å, β = 99.009(5)°, space group $P2_1/n$, Z = 4, 39613 reflections measured, θ_{max} = 40.0°, 9029 unique (R_{int} = 0.036), final R = 0.030 (7111 I>2σ(I) data), w$R(F^2)$ 0.055 (all data) , CCDC 1453169; **5b**, $C_9BBr_2Cl_5F_2N_2$, triclinic, a = 8.775(2), b = 9.170(3), c = 9.710(3) Å, α = 98.378(17), β = 106.86(2), γ = 105.71(2)°, space group P-1, Z = 2, 6598 reflections measured, θ_{max} = 28.3°, 3450 unique (R_{int} = 0.025), final R = 0.035 (2962 I>2σ(I) data), w$R(F^2)$ 0.086 (all data), CCDC 1453170; **6a**, $C_{27}H_{15}BCl_4F_2N_2$, monoclinic, a = 12.0397(3), b = 9.5581(2), c = 21.4720(5) Å, β = 105.7660(10)°, space group $P2_1/n$, Z = 4, 22356 reflections measured, θ_{max} = 28.7°, 6116 unique (R_{int} = 0.043), final R = 0.039 (4471 I>2σ(I) data), w$R(F^2)$ 0.086 (all data) CCDC 1453171; **6b**, $C_{21}H_9BCl_4F_2N_2S_3$, triclinic, a = 10.0519(9), b = 10.7177(9), c = 11.8528(10) Å, α = 102.040(4), β = 91.199(4), γ = 91.199(4)°, space group P-1, Z = 2, 36429 reflections measured, θ_{max} = 33.2°, 8575 unique (R_{int} = 0.029), final R = 0.042 (7372 I>2σ(I) data), w$R(F^2)$ 0.132 (all data), CCDC 1453172; **7a**, $C_{39}H_{25}BCl_2F_2N_2$, monoclinic, a = 26.1253(10), b = 12.6428(5), c = 18.6230(7) Å, β = 91.840(2)°, space group $P2_1/c$, Z = 8, 34476 reflections measured, θ_{max} = 61.0°, 9079 unique (R_{int} = 0.039), final R = 0.044 (7087 I>2σ(I) data), w$R(F^2)$ 0.117 (all data), CCDC 1453173; **7b**, $C_{29}H_{15}BCl_2F_2N_2S_5$, monoclinic, a = 9.9110(2), b = 24.3651(5), c = 12.2192(3) Å, β = 110.9070(10)°, space group $P2_1/c$, Z = 4, 41084 reflections measured, θ_{max} = 28.4°, 6904 unique (R_{int} = 0.038), final R = 0.114 (5832 I>2σ(I) data), w$R(F^2)$ 0.296 (all data), CCDC 1453174.

4.7 References

1. Lakshmi, V.; Rajeswara Rao, M.; Ravikanth, M., *Org. Biomol. Chem.* **2015,** *13* (9), 2501-2517.

2. Jiao, L.; Pang, W.; Zhou, J.; Wei, Y.; Mu, X.; Bai, G.; Hao, E., *J. Org. Chem.* **2011,** *76* (24), 9988-9996.

3. Lakshmi, V.; Ravikanth, M., *J. Org. Chem.* **2011,** *76* (20), 8466-8471.

4. Duran-Sampedro, G.; Agarrabeitia, A. R.; Garcia-Moreno, I.; Costela, A.; Bañuelos, J.; Arbeloa, T.; López Arbeloa, I.; Chiara, J. L.; Ortiz, M. J., *Eur. J. Org. Chem.* **2012,** *2012* (32), 6335-6350.

5. Fischer, H.; Orth, H., *Justus Liebigs Annalen der Chemie* **1933,** *502* (1), 237-264.

6. Ballantine, J. A.; Jackson, A. H.; Kenner, G. W.; McGillivray, G., *Tetrahedron* **1966,** *22, Supplement 7* (0), 241-259.

7. Plater, M. J.; Aiken, S.; Bourhill, G., *Tetrahedron* **2002,** *58* (12), 2405-2413.

8. Zhao, N.; Xuan, S.; Fronczek, F. R.; Smith, K. M.; Vicente, M. G. H., *J. Org. Chem.* **2015,** *80* (16), 8377-8383.

9. Wang, H.; Fronczek, F. R.; Vicente, M. G. H.; Smith, K. M., *J. Org. Chem.* **2014,** *79* (21), 10342-10352.

10. Zhao, N.; Vicente, M. G. H.; Fronczek, F. R.; Smith, K. M., *Chem. Eur. J.* **2015,** *21*, 6181-6192.

11. Xuan, S.; Zhao, N.; Zhou, Z.; Fronczek, F. R.; Vicente, M. G. H., *J. Med. Chem.* **2016,** *59* (5), 2109-2117.

12. Leen, V.; Yuan, P.; Wang, L.; Boens, N.; Dehaen, W., *Org. Lett.* **2012,** *14* (24), 6150-6153.

13. Wang, H.; Vicente, M. G. H.; Fronczek, F. R.; Smith, K. M., *Chem. Eur. J.* **2014,** *20* (17), 5064-5074.

14. Espinet, P.; Echavarren, A. M., *Angew. Chem. Int. Ed.* **2004,** *43* (36), 4704-4734.

15. Li, L.; Nguyen, B.; Burgess, K., *Bioorg. Med. Chem. Lett.* **2008,** *18* (10), 3112-3116.

16. Nguyen, A. L.; Bobadova-Parvanova, P.; Hopfinger, M.; Fronczek, F. R.; Smith, K. M.; Vicente, M. G. H., *Inorg. Chem.* **2015,** *54* (7), 3228-3236.

17. Nguyen, A. L.; Fronczek, F. R.; Smith, K. M.; Vicente, M. G. H., *Tetrahedron Lett.* **2015,** *56* (46), 6348-6351.

18. Casey, K. G.; Quitevis, E. L., *The Journal of Physical Chemistry* **1988,** *92* (23), 6590-6594.

19. Olmsted, J., *The Journal of Physical Chemistry* **1979,** *83* (20), 2581-2584.

20. Chen, Y.; Zhao, J.; Guo, H.; Xie, L., *J. Org. Chem.* **2012,** *77* (5), 2192-2206.

21. Chen, Y.; Zhao, J.; Xie, L.; Guo, H.; Li, Q., *RSC Adv.* **2012,** *2* (9), 3942-3953.

22. Rihn, S.; Retailleau, P.; Bugsaliewicz, N.; Nicola, A. D.; Ziessel, R., *Tetrahedron Lett.* **2009,** *50* (50), 7008-7013.

23. Brizet, B.; Desbois, N.; Bonnot, A.; Langlois, A.; Dubois, A.; Barbe, J.-M.; Gros, C. P.; Goze, C.; Denat, F.; Harvey, P. D., *Inorg. Chem.* **2014,** *53* (7), 3392-3403.

24. Xu, H.-J.; Bonnot, A.; Karsenti, P.-L.; Langlois, A.; Abdelhameed, M.; Barbe, J.-M.; Gros, C. P.; Harvey, P. D., *Dalton Trans.* **2014,** *43* (22), 8219-8229.

25. Gorka, A. P.; Nani, R. R.; Zhu, J.; Mackem, S.; Schnermann, M. J., *J. Am. Chem. Soc.* **2014,** *136* (40), 14153-14159.

CHAPTER 5: SYNTHESIS AND ELECTROPOLYMERIZATION OF A SERIES OF 2,2'-(*ORTHO*-CARBORANYL) BISTHIOPHENES

5.1 Introduction

Since conducting polymers were first reported by MacDiarmid, Heeger, and Shirakawa in 1977,[1-2] an intensive research about various types of conducting materials, including polythiophene (PTh), polypyrrole (PPy), and polyaniline (PANI), has been dedicated to this special area.[3] During those studies, several challenges are remained, including poor environmental thermal and oxidative stabilities, and short lifetime during the process of charge-discharge. Such challenges have hindered the commerciality of conducting polymers[4]

Carboranes[5] that contains carbon and boron atoms, which belongs to a class of boron clusters. There are several types of The neutral isomeric carboranes *ortho-*, *meta-*, and *para-* $C_2B_{10}H_{12}$ **1-3**, and the negatively charged *nido*-$C_2B_9H_{12}^-$ **4**, and the *closo*-$CB_{11}H_{12}^-$ **5** carboranes, as shown in Figure 1. This special clusters have several different unique physical and chemical properties, such as high thermostability, electro-deficiency, and hydrophobicity, which have led to their broad applications in various disciplines, including in catalysis, molecular recognition, cancer

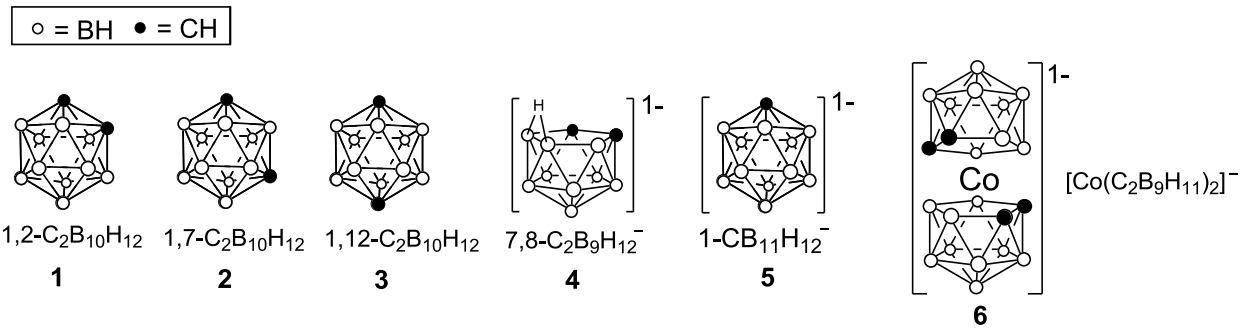

Figure 5-1: Neutral, anionic *nido* and *closo*- carboranes.

* Reproduced from Zhao, N.; Fabre, B.; Bobadova-Parvanova, P.; Fronczek, F. R.; Vicente, M. G. H. Synthesis and electropolymerization of a series of 2,2'-(*ortho*-carboranyl) bisthiophenes. Submitted.

therapy treatments, and in electronics.[5-7] These distinctive clusters are readily and easily synthesized and functionalized. For example, the carbon atoms in these clusters are usually treated as convenient sites for introducing other organic molecules. In recent years, the synthesis of carborane-containing polymers[8-9] has attracted intense attention, as well as their investigation for applications as conducting,[10] pre-ceramic,[11] luminescent,[12-13] and thermally robust[14-15] materials.

Multiple methodologies for incorporating carboranes into polymers can be found in the literature: (1) $[Co(C_2B_9H_{11})_2]^-$ **6** can be used as doping agent in the process of monomer electropolymerization[16-19]; (2) anion $[Co(C_2B_9H_{11})_2]^-$ **6** also can be introduced at the 2-position[20] or N-position[21] in pyrrole monomers, (e.g. **7**) which can be electropolymerized to the self-doped polymers; (3) neutral carboranes (*o-*, *m-*, *p-*) can be introduced to 2-,[22-23] 3-, or 4- positions[24-27] of pyrroles or thiophenes for electropolymerizations under suitable conditions; (4) thiophene or pyrrole monomers can be copolymerized with carborane containing monomers by electrochemical[21, 28] or chemical[29-30] methods for the carborane-incorporation into the main chain.

Carborane-containing monomers and conducting polymers usually possess several improved properties. For example, carborane-containing monomers with enhanced oxidation potentials can more easily overcome the "polythiophene paradox",[31] and the generated polymers have remarkable thermal and chemical stability. However, several challenges in this area remain. Among them, significant decreased conductivity, and blue-shifted π - π^* transition band from the

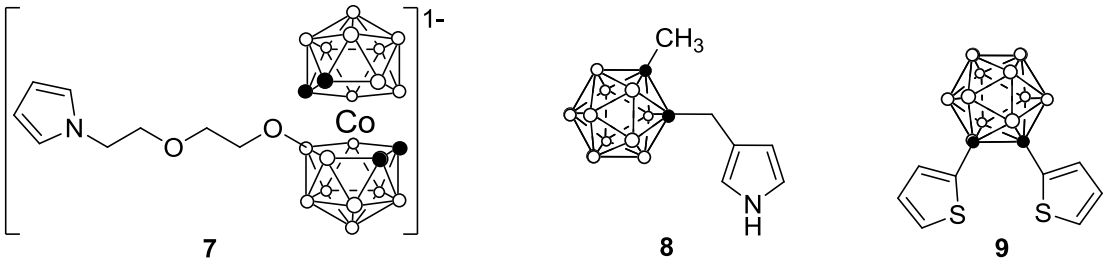

7 **8** **9**

Figure 5-2: Structures of compounds **7-9**.

UV-vis spectraare often observed. For example, the conductivity of poly(**8**) (10^{-2} S cm^{-1})[25] and poly(**9**) (20 S cm^{-1})[22] was much lower than that of unsubstituted polypyrrole (200 S cm^{-1}) and polythiophene (100 S cm^{-1}), respectively.[32] The steric hindrance and less conjugated backbones caused by the electron-withdrawing carborane groups may be a possible reason for this observed phenomenon. Besides, some monomers containing carborane groups located very close to the aromatic rings failed to electropolymerized.[23-24, 26-27]

On the other hand, polymeric materials with specific properties (e.g. photovoltaic properties and controlled length of the main chain) could be prepared by polymerization of well-designed and synthesized structurally-modified π-conjugated oligomers.[33-34] As we know, during electropolymerization of thiophene monomers, oligomers with higher oxidation potential are usually generated.[31] Such oligomers always caused in the generated materials significantly deteriorated chemical and mechanical properties. However, short-chain oligomers (such as tetra-thiophenes) can overcome the "polythiophene paradox" and be polymerized to more defined polymeric materials, but may show decreased conductivity.[35-37] In the last two decades, a range of thiophene oligomers[34] and pyrrole oligomers[38-40] have been synthesized and reported. The versatility of oligomer over monomer allow for a better control of the number and ratio of different components in the final products.[34]

Previous work in our group showed the high conductivity and lifetime, with high thermal stability and enhanced oxidation resistance, of poly(*ortho*-carboranylbisthiophene) **9**.[22] Thus, in this Chapter, a new series of derivatives of *ortho*-carboranyl-bisthiophene contianing thienyl, vinyl, and pyrrole groups at the 5- or 5,5'-positions was synthesized and investigated. Due to decreased steric hindrance and electronic effect induced by the carborane clusters, such modifications were expected to lead to more conjugated main chains and more aerated polymer

structures. On the other hand, pyrrolic groups in the oligomers and polymers are reported to stabilize the radical cations formed during electropolymerization, which led to a π-π intermolecular dimerizations.[41-42] This type of phenomena may bring supramolecular π-dimers with enhanced conductivity.[42-44] Thus, we anticipate compound **12a** with electron-rich *N*-methylpyrrolic groups at the 5,5'-positions will be easier to polymerize to form a more conductive material.

5.2 Synthesis and Characterization of *ortho*-carboranyl-bisthiophenes

2,2'-Carboranyldithiophene **9** was synthesized by using a slightly modified procedure from that reported, in 30% overall yield,[22-23] as shown in Scheme 5-1. Commercially available 2-iodothiophene reacted with 2-[(trimethylsilyl)ethynyl]-thiophene in the presence of 1,8-diazabicycloundec-7-ene (DBU) and bis(triphenylphosphine)-palladium(II) dichloride and copper(I) iodide to yield 2,2'-ethylenedithiophene in 87% yield.[45] Reaction between 2,2'-ethylenedithiophene and decaborane in the presense of diethyl sulfide and toluene provdie the desired precursor 2,2'-carboranyldithiophene **9** in moderate yield (35%),[22-23] as shown in Scheme 5-2.

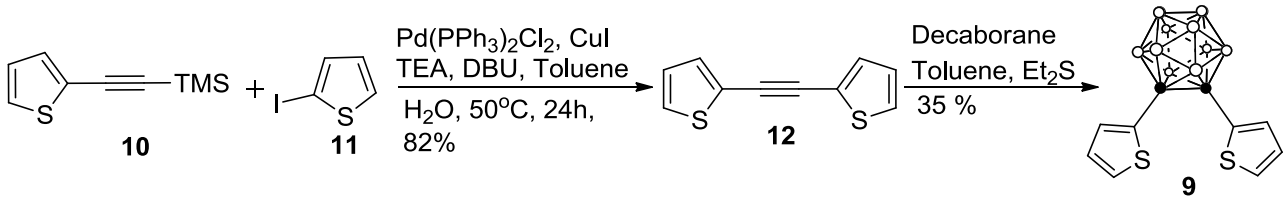

Scheme 5-1: Synthesis of carboranyl-bisthiophenes **9**.

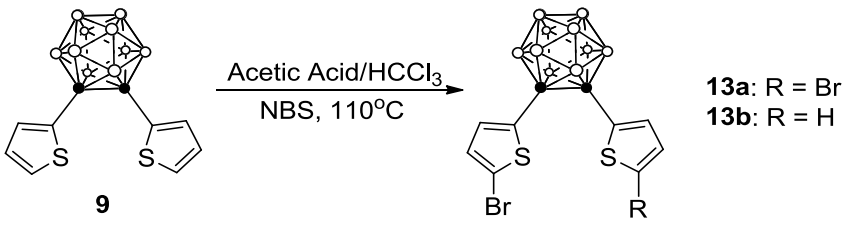

Scheme 5-2: Synthesis of brominated carboranyl-bisthiophenes **13a-b**.

Due to the strong electron-withdrawing effect of the carborane group, the α-positions of 2,2'-carboranyldithiophene **9** are significantly deactivated toward bromination. Therefore, high temperature and polar solvents are necesasry for the reaction to occur. Bromination of 2,2'-carboranyldithiophene **9** using 6 equivalents of NBS in chloroform ($CHCl_3$) and acetic acid (AcOH) (1:1), at 130 ^oC overnight, produced the dibromo product **13a** in 76% yield, as shown in Scheme 5-1.[46] However, no bromination reaction occured at lower temperature, or using DMF, CCl_4, THF or only $CHCl_3$ as the solvent. Also, the mixtures of multiple brominated products were obtained by using pure acetic acid as the only solvent at 110 ^oC.[46] However, using lower temperatures, or different amounts of NBS, or different ratios of $CHCl_3$/AcOH (e.g. 2 :1)

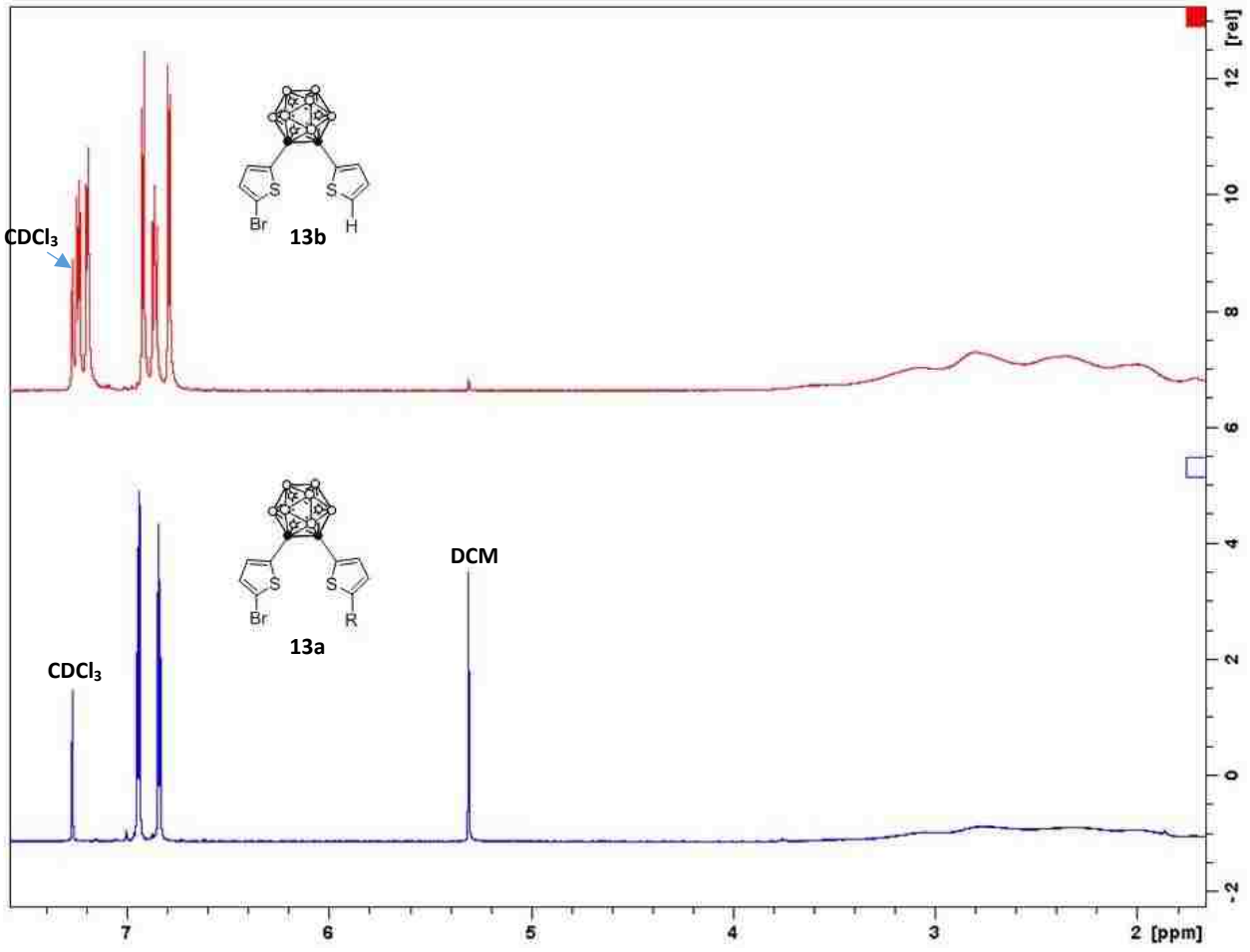

Figure 5-3: ^1H NMR (400 MHz) of **10a** and **10b** in $CDCl_3$ at room temperature.

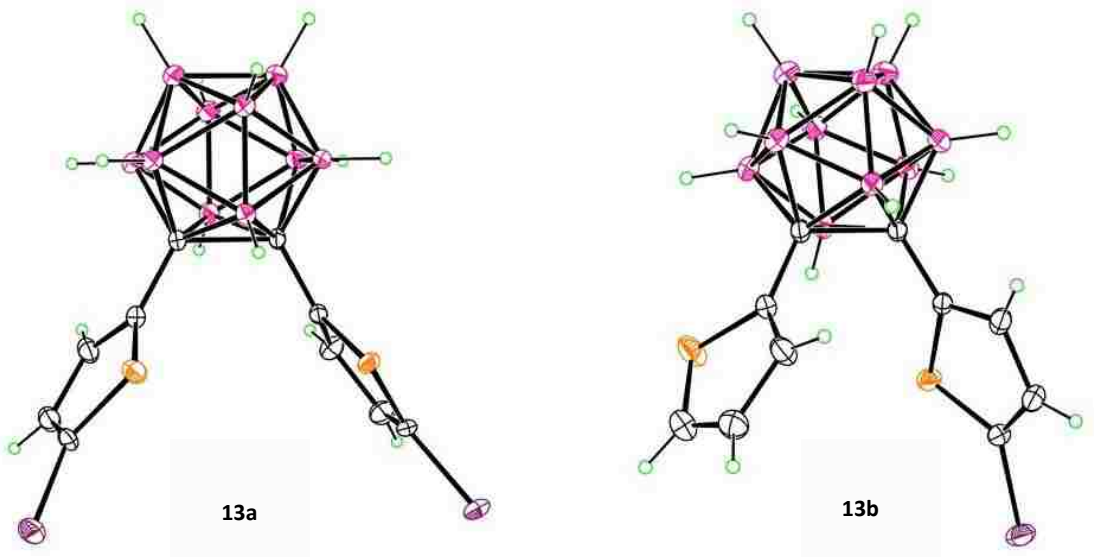

Figure 5-4: X-ray structures of **10a** and **10b**.

decreased the yield of dibromo product **13a**, but increased the yield of the mono-brominated product **13b** side-product. For example, **13b** was obtained as the major product in 50% yield, along with 15% of **13a**, under the similar conditions, with 3 equivalents of NBS at 110 ^{o}C. As shown in Figure 5-3, the ^{1}H NMR provided direct evidence of sucessful bromination of **9**. Compound **13a** with a symmetric system showed two groups of characristic doublet-of-doublets at the thiophene at δ = 6.84 and 6.89 ppm, while **13b** with an unsymmetric structure displayed five sets of doublet-doublet at δ = 6.79, 6.86, 6.92, 7.20, 7.25 ppm, repectively.

Suitable crystals of **13a** and **13b** were obtained by slow evaporation in hexanes. The results are displayed in Figure 5-4. Compound **13a** contains four independent molecules, two of which have the S atoms from thiophenes relatively *syn* (approximate Cs symmetry). In these two molecules, there are 63.8 and 72.3º dihedral angles formed by the thiophene planes. Each of the other two independent molecules have one disordered thiophene into both *anti* and *syn* conformations,but the dominant conformer is *anti* (approximate symmetry C_2). In the disordered molecules, there are 63.5 and 66.2º of the dihedral angles that forming by the thiophene planes.

The distances of carborance C-C bonds are in the range of 1.732(4)-1.734(4) Å. On the other hand, compound **13b** has only one independent molecule lying on a crystallographic two-fold axis. Thus a dihedral angle of 54.2º for the thiophenes are anti formed, and showed a exact C_2 symmetry. The distances of carborance C-C bond is 1.7338(13), which is longer than an alkyne triple bond distance (1.2130(10) Å).

The reactivity of newly generated dibromo-carboranylbisthiophene **13b** was firstly investigated by Sonogashira cross-coupling reactions, as shown in Scheme 5-3. The Sonogashira

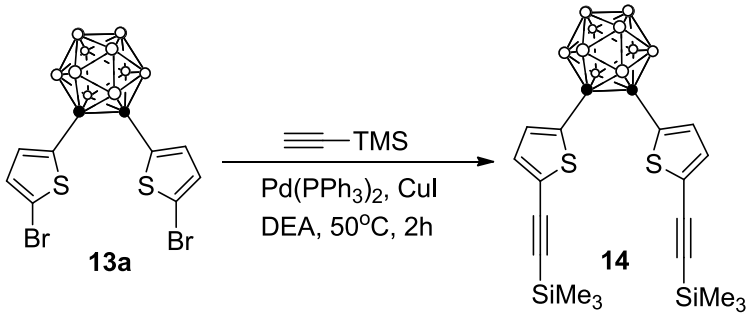

Scheme 5-3: Sonogashira cross-coupling reaction of **13a**.

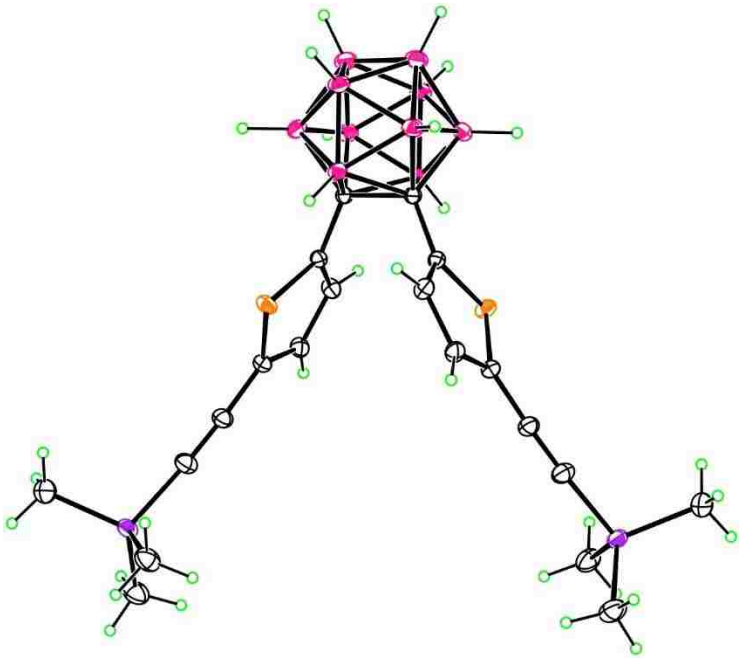

Figure 5-5: X-ray structures of **14**.

type reaction between **13a** and ethynyltrimethylsilane (5 equiv.) in the presence of bis(triphenylphosphine)palladium(II) dichloride ($Pd(PPh_3)_2Cl_2$) and copper(I) iodide (CuI) as the catalysts, produced the corresponding di-ethynyl product **14**, in 80% yield. A suitable crystal of **14** for X-ray analysis was obtained by slow evaporation in hexanes. The result is displayed in Figure 5-5. Compound **14** lies on a crystallographic two-fold axis. The *anti* thiophenes form a dihedral angle of 54.2°. The distance of the C-C bond in the carborane is 1.7338(13) Å.

On the other hand, the reactivity of newly generated dibromo carboranylthiophene **13a** and **14b** were investigated by Stille cross-coupling reactions, as shown in Scheme 5-3. The Stille type reactions of **13a** with 3 equivalents of 1-methyl-2-(tributylstannyl)pyrrole, 2-(tributylstannyl)thiophene or tributyl(vinyl)tin in the presence of tetrakis(triphenylphosphine)palladium (0) as the catalyst, and in refluxing toluene for 2-4 hours yielded di(thienyl-N-methylpyrrole)-*o*-carborane **15a,** di(bisthienyl)-*o*-carborane **15b** and di(2'-vinylthienyl)-o-carborane **16a**, respectively, in good to excellent yields (68%-95%). Besides, the same type of reaction between **13b** and tributyl(vinyl)tin produced the corresponding mono-vinyl

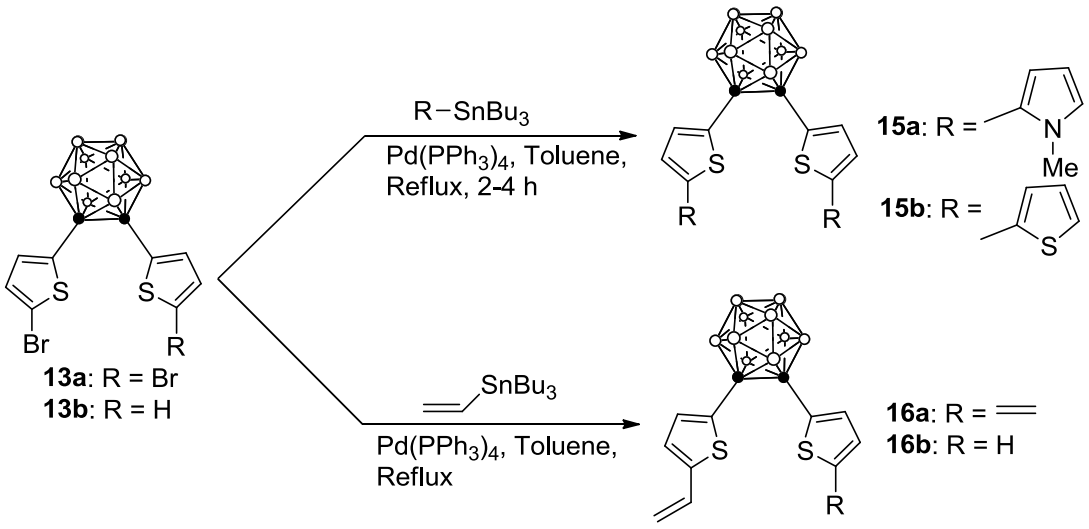

Scheme 5-4: Stille cross-coupling reactions of **13a**.

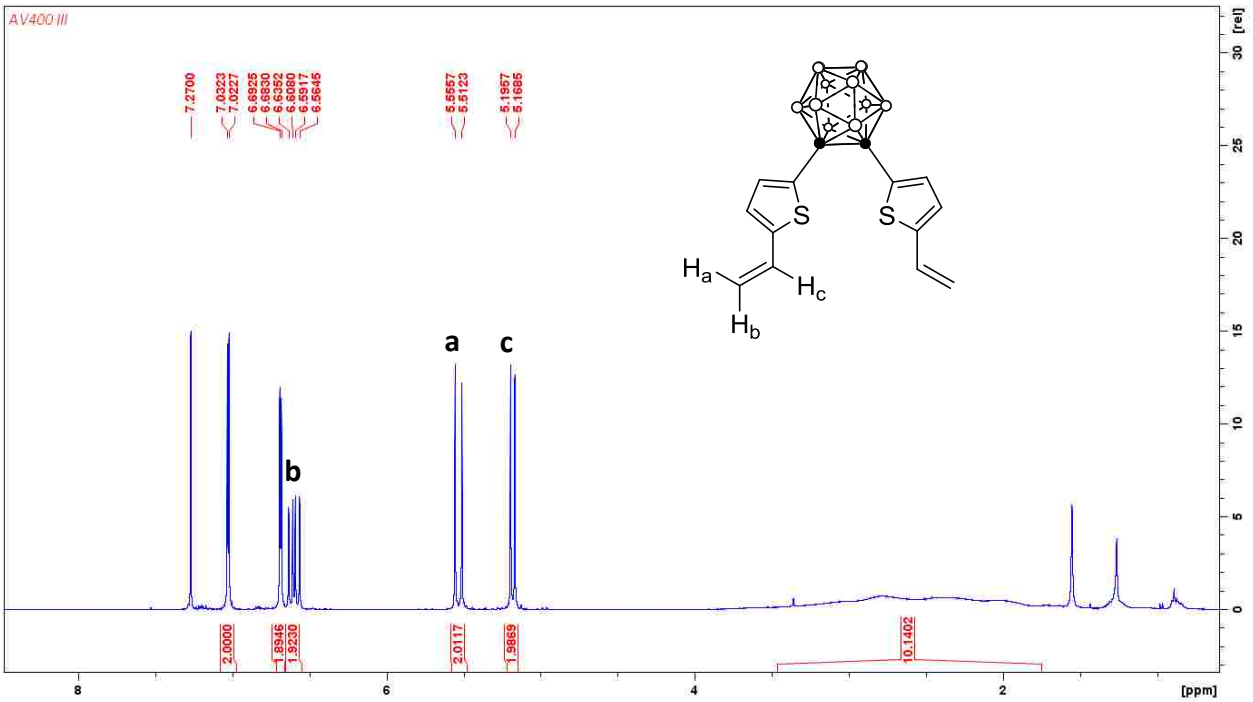

Figure 5-6: ^{1}H NMR (400 MHz) of **16a** in $CDCl_3$ at room temperature.

product **16b** in 75% yiled. These new carboranylthiophenes were characterized by ^{1}H NMR, ^{13}C NMR and mass spectrometry. For example, the ^{1}H NMR of compound **16a** displayed the characteristic doublet-of-doublets of the thiophene rings, as well as the broad peaks belonging to the carborane groups. The signals of the vinyl groups also were also assigned in the spectra, as seen in Figure 5-6 with the doublet-of-doublet of H_a splitting by H_b and H_c at the 5,5'-divinyl groups.

Suitable crystals of **15a-b** and **16a-b** for X-ray analysis were obtained by slow evaporation in hexanes. The results are displayed in Figure 5-7. Compounds **15a** and **15b** both have approximate C_2 symmetry, with the thiophene planes forming dihedral angles of 52.6 and 61.6°. The thiophene and N-methylpyrrole rings of **15a** have their S and N atoms *anti*, with N-C-C-S torsion angles of 164.04(11) and 151.81(12)°. The distance of C-C bond of the carborane is 1.753(2) Å. Both the terminal thiophenes of **15b** are disordered, presenting both *syn* and *anti* bisthiophenes. The distance of C-C at the carborane is 1.730(11) Å. Compound **16a** has approximate C_2 symmetry, which forms a dihedral angle of 63.3° with the thiophene

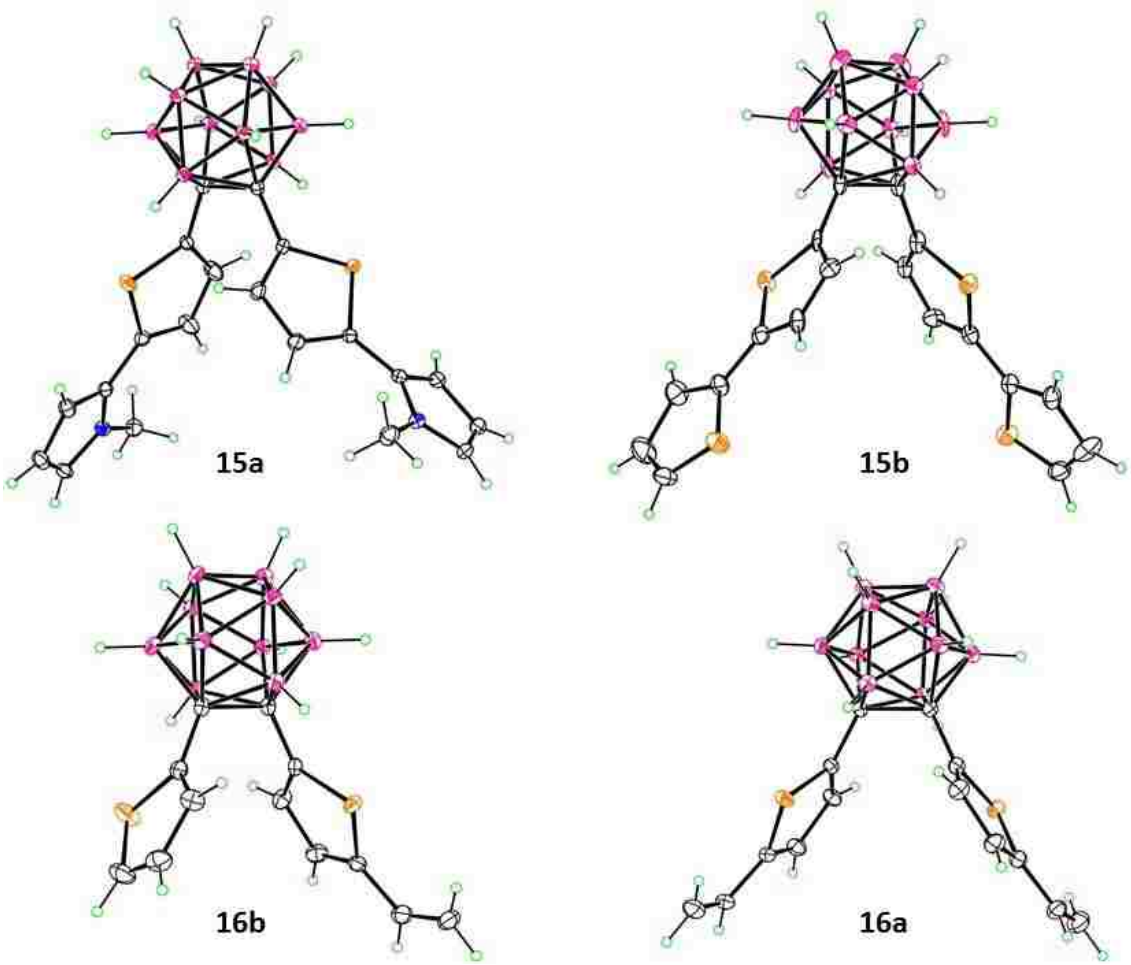

Figure 5-7: X-ray structures of **15a-b** and **16a-b**.

planes, and the vinyl groups are *syn* to the S atoms of thiophene. The distance of C-C bond of the carborane is 1.7364(14) Å. The thiophene rings of **16b** are *anti* and form a dihedral angle of 58.6º, the vinyl group is *syn* to the S atom of the thiophene, and the distance of C-C at the carborane is 1.740(2) Å.

5.3 Electrochemistry of the Monomers and Their Corresponding Polymer Films

The electrochemical experiments of **15a**, **15b**, **16a**, and **16b** were performed by Dr. Bruno Fabre (Universite de Rennes, France). The cyclic voltammetry (CV) characterization of the *o*-carboranes derivatives **15a-b** and **16a-b** at 5 mM in anhydrous dichloromethane (CH_2Cl_2) and Bu_4NPF_6 (2×10^{-1} M) (except for **15a** examined in acetonitrile and Bu_4NPF_6 (0.1 M)) displayed two irreversible oxidation peaks when cycled between 0.0 and 2.2 V vs Ag/Ag^+ 10^{-2} M (Figure 5-

8a and Table 1). As we know, there are no oxidization of unsubstituted carboranes under these electrolytic conditions, these can be assigned to the process of the oxidation of the aromatic rings into radical cation species. Furthermore, the decresing order of the anodic potentials of these systems were found as **16a** ≈ **16b** > **15b** > **15a**, in perfect agreement with the trend that reported for the electrochemical oxidation of the corresponding aromatic rings without the substitution of carborane, namely2-vinylthiophene[47] > bithiophene[48] > 2-(2-thienyl)-1*H*-pyrrole.[49-50] For compound **15a**, the oxidation processes at 0.74 V can be assigned to the oxidation of the pyrrole rings, while the oxidation processes at 1.30 V can be assigned to the oxidation of the thiophene rings, respectively.

We next investigated the electrochemical behavior of these systems under the scanning at the negative potentials. As shown in Figure 5-8, two quasi-reversible closely spaced systems around -1.40 V were shown during the reduction process, which can be evidently verified on the backward scans of the corresponding time semi-derivative curves, as shown in Figure 5-8b. Such

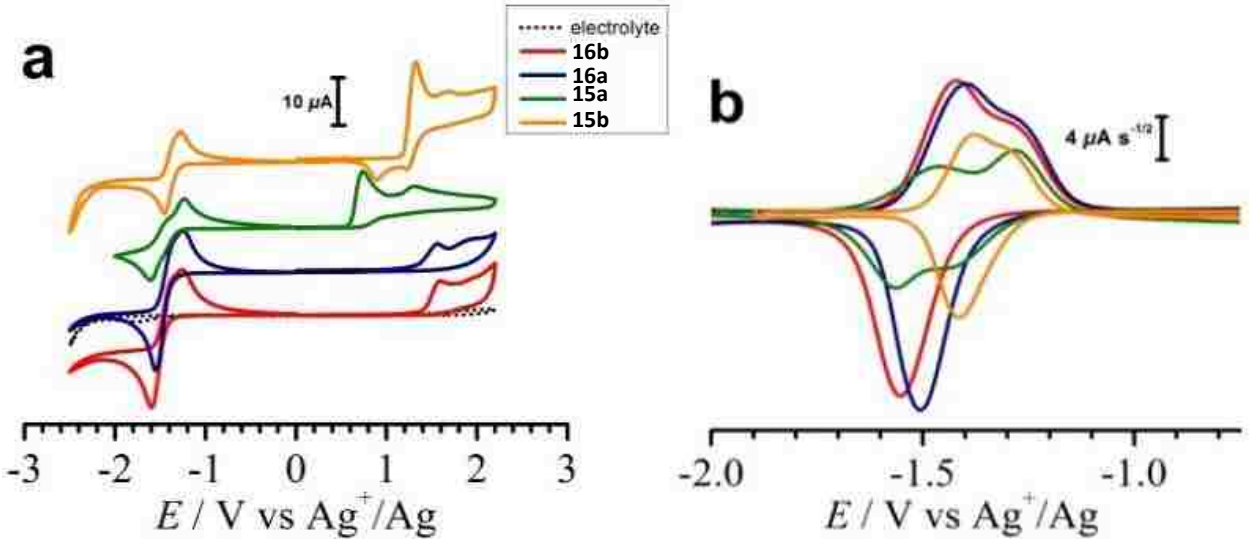

Figure 5-8: (**a**) Cyclic voltammograms at 0.1 V s^{-1} of different *o*-carborane derivatives (5 mM) in CH_2Cl_2 + Bu_4NPF_6 (0.2 M) (for **15b**, **16a** and **16b**) or CH_3CN + Bu_4NPF_6 (0.1 M) (for **15a**). (**b**) Corresponding time semi-derivative voltammograms for the cathodic region.

Table 1. Cyclic voltammetry data of the *o*-carboranyl derivatives (5 mM) in CH_3CN or CH_2Cl_2 medium. Potential scan rate: 0.1 V s^{-1}. All potentials are reported vs. 10^{-2} M Ag^+/Ag.

	Monomer		**Polymer**	
	E_{ox}/ V[a]	E_{red} / V[b]	E_{ox} / V[c]	E_{red} / V[d]
15a[e]	0.74; 1.30	-1.42	0.40; 0.75	-1.50
15b[f]	1.32; 1.68	-1.39	0.95; 1.30	-1.36
16a[f]	1.56; 1.93	-1.40	—[g]	—[g]
16b[f]	1.58; 1.96	-1.43	—[g]	—[g]

[a] Irreversible anodic peak potentials corresponding to the monomer oxidation. [b] Formal potential corresponding to the quasi-reversible reduction step. [c] Formal potential corresponding to the reversible *p*-doping/undoping of the electrogenerated polymer (average of anodic and cathodic peak potentials).[d] Formal potential corresponding to the reduction of the carborane (average of anodic and cathodic peak potentials. [g] No conducting polymer film was electrogenerated; electrode passivation was observed.). [f] in CH_2Cl_2 + Bu_4NPF_6 (0.2 M)

phenomena is due to the reduction of the carborane to form the radical anion and dianion backward scans of the corresponding time semi-derivative curves, as shown in Figure 5-8b. Such phenomena is due to the reduction of the carborane to form the radical anion and dianion species, as reported.[51-52] These studies discussed above suggest that the electronic charge of these *o*-carboranes derivatives is located within the carborane cage.[52] In addition, due to similar geometry of these molecules with *o*-carborane, same potential for the four molecules was observed during the cathodic process.

Among all these carboranyl compounds, only **15a** and **15b** led to the formation of a conducting polymer deposit on the electrode surface during the electrochemical oxidation. Such films could be successfully electrogenerated either potentiostatically or potentiodynamically with no obvious effect of the electropolymerization method on their respective electrochemical responses. Figure 5-9 shows the results of representative cyclic voltammograms corresponding to the potentiodynamical electropolymerization of compounds **15a** and **15b**. As shown in the Figure, the growth of a conducting deposit onto the electrode surface could be verified by the progressive increase of both anodic and cathodic currents with the number of scans. On the other hand,

electropolymerization of compounds **16a** and **16b** did not yield a desired conducting polymer deposit on the electrode, whatever the tested experimental conditions, including different oxidation potentials, monomer concentrations, electrochemical technique and solvents. A poorly electroactive film was electrogenerated instead, which led to the progressive passivation of the electrode surface. This phenomenon may be due to vinyl groups at the 5,5'-positions of the thiophene rings that might inhibit the electropolymerization process.

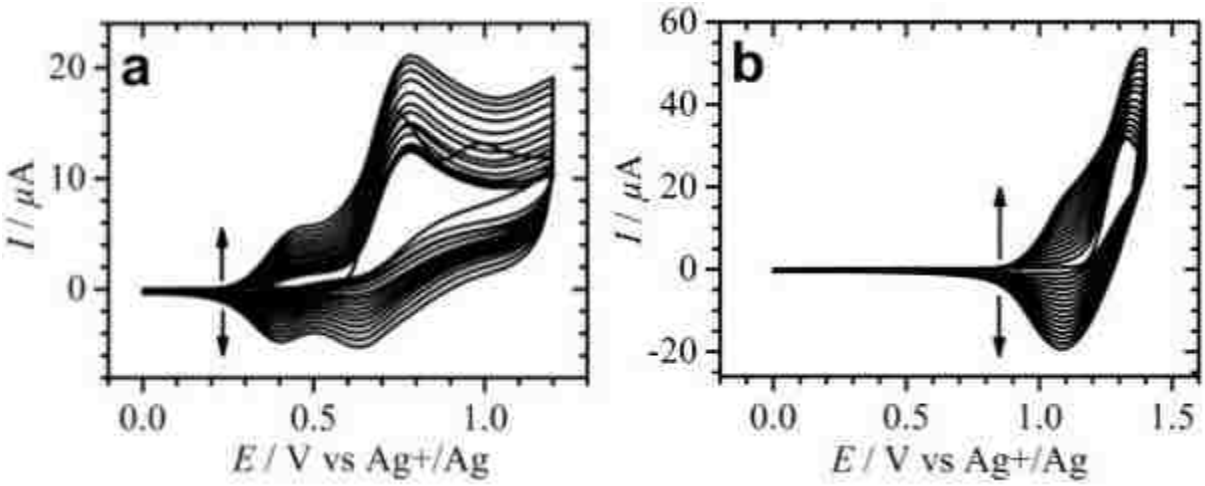

Figure 5-9: Successive cyclic voltammograms of **15a** (**a**) and **15b** (**b**) at 5 mM in CH_3CN + 0.1 M Bu_4NPF_6 (**a**) or CH_2Cl_2 + Bu_4NPF_6 (0.2M) (**b**) Potential scan rate: 0.1 V s^{-1}.

The newly generated polymer films, poly(**15a**) and poly(**15b**), were tested in a monomer-free electrolytic medium, as shown in Figure 5-10. As shown in the Table 1, p-doping/undoping of the expected conjugated segments for poly(**15a**) and poly(**15b**) corresponds to two broad reversible redox processes, which were namely 2, 2'-bi-1*H*-pyrrole, 1, 1'-dimethyl-1,6-di-2-thienyl, and quaterthienyl units, respectively. The linear correlation between the anodic peak current intensities corresponding to these two systems of **15a** and **15b** (I_{pa}^1 and I_{pa}^2) and the potential scan rate *v* was observed, as reported for surface-immobilized electroactive species.[53] In addition, the estimation of the relatively low doping level δ[54] of poly(**15a**) and poly(**15b**) was obtained as 0.10-0.15 and 0.15-0.20 positive charge per monomer unit, compared with

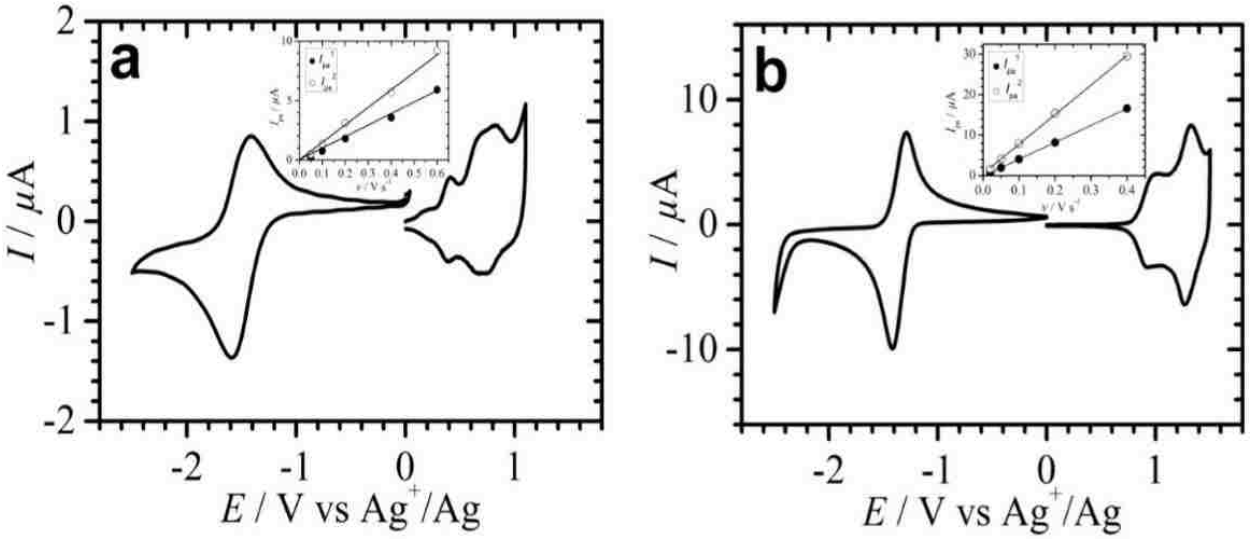

Figure 5-10: Electrochemical responses of the electrogenerated poly(**15a**) (**a**) and poly(**15b**) (**b**) films at 0.1 V s^{-1} with the corresponding I_{pa} - v plots for the two anodic processes (insets). Electrolyte: CH_3CN + Bu_4NPF_6 (0.1 M) (**a**) or CH_2Cl_2 + Bu_4NPF_6 (0.2 M) (**b**). The consumed electropolymerization charges are 20 (**a**) and 64 mC cm^{-2} (**b**).

unsubstituted poly(2-(2-thienyl)-1*H*-pyrrole)[49] and polythiophene.[37] Such results suggested the lower oxidation level of both polymers, which can further verify that incorporated carborane groups of **15a** and **15b** were crucial on the ion transport in these films.

A reversible system at -1.50 and -1.36 V is shown in Figure 5-10 for both poly(**15a**) and poly(**15b**), in the cathodic potential range. Such system corresponds to the reduction of the incorporated carborane groups in the polymer. The linear correlation between the peak currents ascribed to this system and the potential scan rate v was observed during the polymer redox process. However, during the electropolymerization reaction, the redox signature of the carborane groups became less and less evident, as the film thickness increased resulting from the anodic charge. Such attractive effects of the film thickness on the electroactivity of the surface-confined reducible pair have previously been reported by our group with polythiophenes containing in-chain cobaltabisdicarbollide centers.[20] It should be noted that the polymer was in its neutral reduced state (e.g. electronically insulating state) during the cathodic process occurring within a potential range. As a result, the insulating polymer matrix's carborane is expected to be reduced by electron

hopping onto the electrode surface. Electroneutrality of the material is achieved by cation migration through the film. For the thick films, a large amount of carboranes within the film is not electrochemically active due to the electrolyte cations' lack of access to them.

5.4 Computational Studies

In order to better understanding of the properties, both the monomers and the dimers of carboranyl-bisthiophenes **15a-b** and **16a-b** were modeled computationally, by Dr. Peita Bobadova-Parvanova (Rockhurst University, USA).The results from these studies were shown in Figure 5-11, showing the energies and the form of their frontier molecular orbitals (MO). The HOMO and LUMO of 2,2'-carboranyldithiophene **9** are also provided for better comparison with other derivatives. Generally, all compounds displayed similar orbitals: little contribution of carborane cages was observed to both HOMO and LUMO. There is π-bonding character for C-C atoms and mostly non-bonding character for the rest of the atoms in the backbone in the HOMO, while there is bonding character between adjacent thiophene units and carborane groups on the

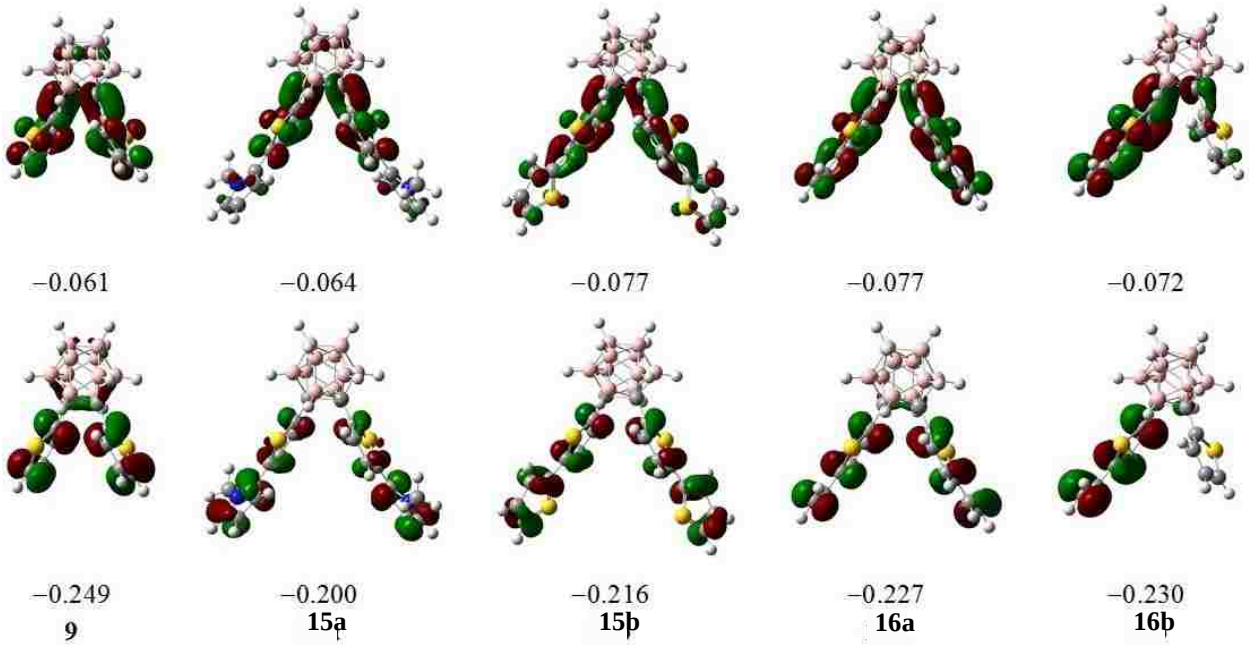

Figure 5-11: Frontier orbitals of carboranyl-bisthiophenes **15a-b**, and **16a-b**. 2,2'-carboranyldithiophene **9** is given for comparison. Energies in a.u.

Table 2: Band gap energies, syn-anti difference energies, and energies of dimerization and intracyclization for carboranyl-bisthiophenes **9**, **15a-b** and **16a-b**.

Compound	Band Gap (eV)	$\Delta E_{\text{syn-anti}}$ (kcal/mol)	ΔE_{dimer}(kcal/mol)	$\Delta E_{\text{intracycl}}$(kcal/mol)
9	5.11			
15a	3.68	0.27	7.81	8.05
15b	3.78	0.39	8.30	7.93
16a	4.11	0.39	1.53	7.61
16b	4.30			

LUMO. Compared to **9**, functional groups at the 5- or 5,5'-positions gave a destabilization effect of HOMO by 0.5 to 1.4 eV, which is showing a decreasing order: pyrrole > thienyl > vinyl. Such trend is in an agreement with that observed in the electrochemical characterization. There is only a small effect in the range of 0.1-0.4 eV on the LUMO. Consequently, the trend of resulting band gaps for all substituted carboranyl-bisthiophenes follows the trend of HOMO destabilization, and smaller band gaps of all the other compounds is shown in Table 2 with the effect being most pronounced for **15a** (≈ 1.4 eV) than compound **9**.

The energy difference between the *anti* and *syn* comformers of **15a-b** and **16a** is also shown in Table 2. The *syn* conformers are more stable with a very small energy difference (< 0.5 kcal/mol), which is consistent with the X-ray analysis. Such finding is also in agreement with the calculations of compound **9** and its *meta*, and *para* analogues, as previously reported.[23]

The energies required for formation of the dimer (namely ΔE_{dimer}) and the energy required for intracyclization (namely $\Delta E_{\text{intracycl}}$) are also listed in the last two columns of Table 2. Compounds **15a** and **15b** have similarrequired energies for dimerization as that of **9**, which are around 8 kcal/mol. Interestingly, it appears the dimerization of **16a** is more easy to achieve, since the dimerization energy is affected by the vinyl substitution with a more pronounced effect. As

reported,[23] intramolecular cyclization in the early stage is another possible mechanism for the polymerization. As shown in Table 2, no significant differences of $\Delta E_{\text{intracycl}}$ among pyrrole, thienyl, vinyl, or unsubstituted carboranyl-bisthophenes are observerd, which are in the range of 7 to 8 kcal/mol. All planar structures of such compounds are obtained as previously reported for **9**.[23]

5.5 Synthesis of a Carborane-containing Tetrasulfido Annulene

The synthesis of porphyrin isomers, such as porphycene and corrphycene, and of extended and contracted porphyrins and corroles, have been active areas of research in the last decades, due to the unique properties of these systems, and their potential applications in various areas as porphyrin biomimetics. Herein, in this Section, the synthesis of first carborane-fused porphyrin analogue was attempted via a Sonogashira palladium-catalyzed cross-coupling reaction as shown in Scheme 5-5. Such carborane-containing macrocycle could add insight into the "aromaticity" of the *ortho*-carborane cluster, since the "C-C" bond of the ortho-carborane would replace the "C=C" bridge in the tetrasulfido annulene, allowing further investigations of the effect of *ortho*-carborane on a conjugated system of an annulene.

The deprotection of **14** was performed using potassium carbonate, rather than TBAF, to minimize deboronation of the *ortho*-carborane cage. Potassium carbonate was added to a solution of compound **14** in methanol/hexanes (1:1) at 0 ^{o}C and the reaction was monitored by ^{1}H-NMR. After 2 h, the cleavage of the TMS groups was completed to give compound **17** in 74% yield, and no *nido*-carborane side product was detected. The Sonogashira coupling reaction of **13a** and **17** under similar conditions gave only trace amount of the carborane-containing tetrasulfido annulene **19**. Due to the potential deboronation reaction during the Sonogashira coupling in the presence of TEA, inorganic bases, including $NaHCO_3$ and K_2CO_3 were used instead. In addition, the coupling

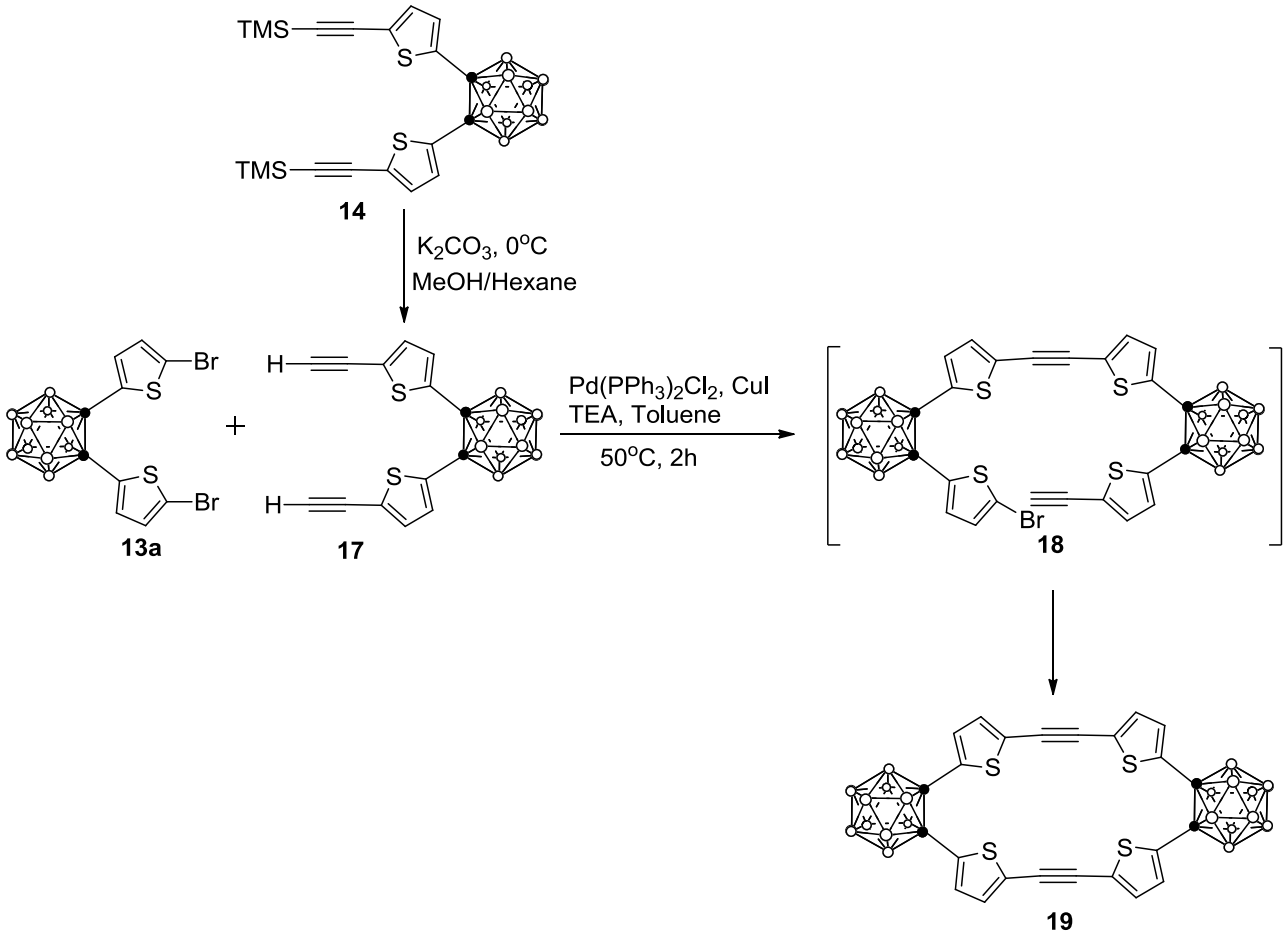

Scheme 5-5: Synthesis of carborane-containing tetrasulfido annulene **19**.

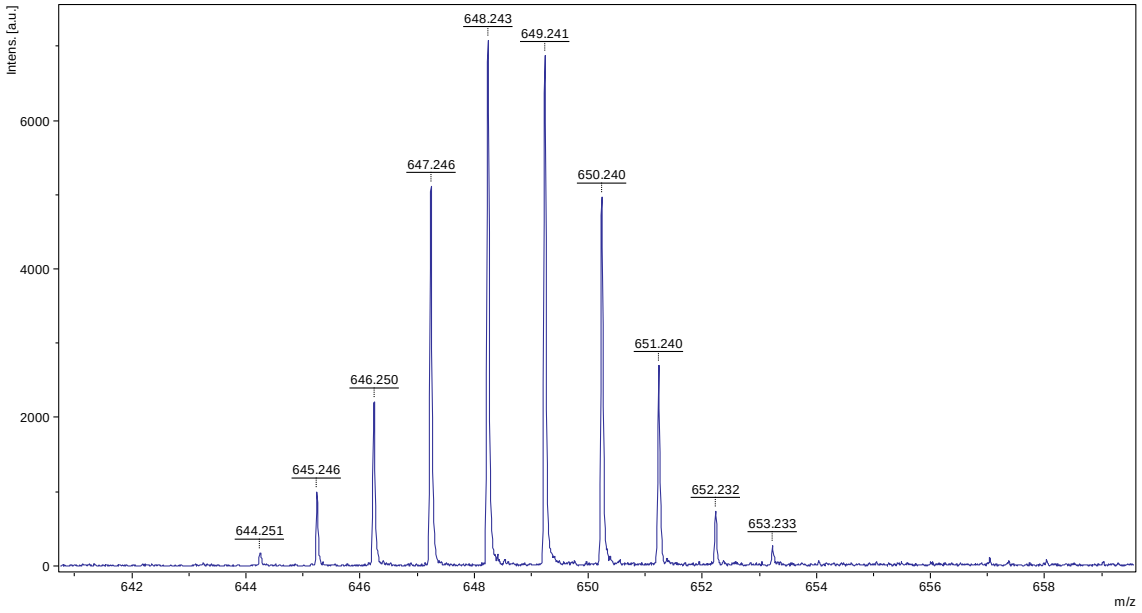

Figure 5-12: MALDI-TOF of compound **19**.

reaction was performed at different temperatures (from room temperature to 80 ^{o}C) and the reaction time was varied (from 2h to overnight), but only trace amounts of annulene **19** were isolated. The MALDI-TOF spectrum of the purified product, shown in Figure 3, shows the base peak at m/z 648.243 corresponding to $[M-B]^{+}$.

The computiation studies of this reaction were conducted by Danile LaMaster in my group. The low yield of annulene **19** is probably a reflection of the spatial constraints of the alkynes. By altering the orientation of the sulfurs, either up or down, five different conformations of annulene **19**, shown in Figure 5-13, are possible. In the optimized annulene structures, the alkynes were bent at both ends by between 8.1° and 11.8°. The rigidity of the sp-hybridized systems also causes a

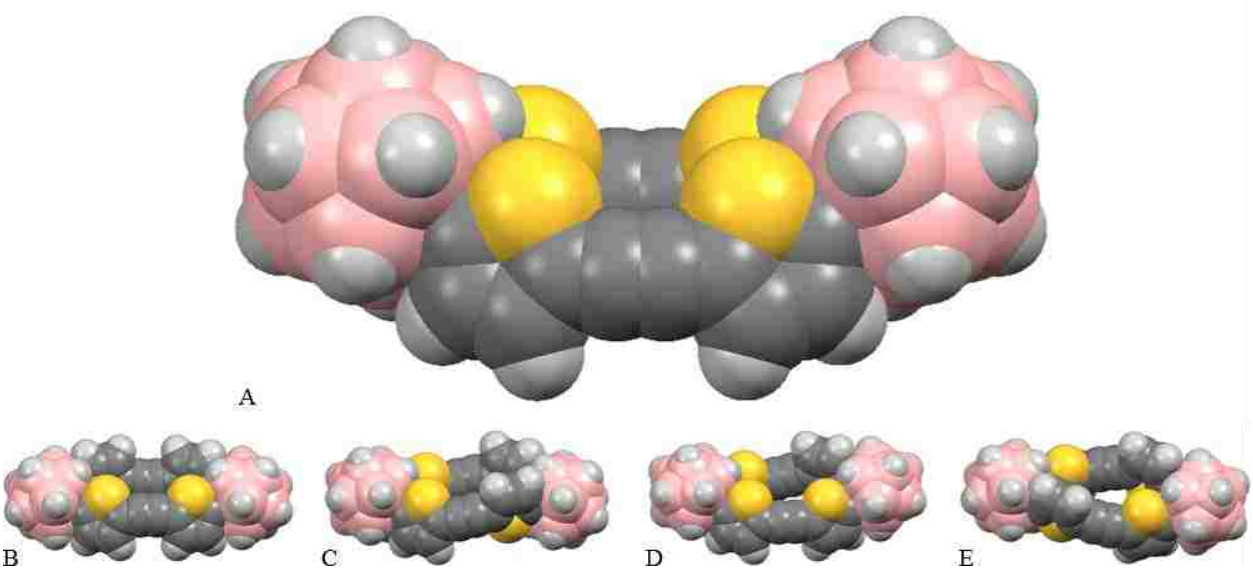

Figure 5-13 : Space-filling models of the the five conformations of compound **19**. Conformation A is the most stable.

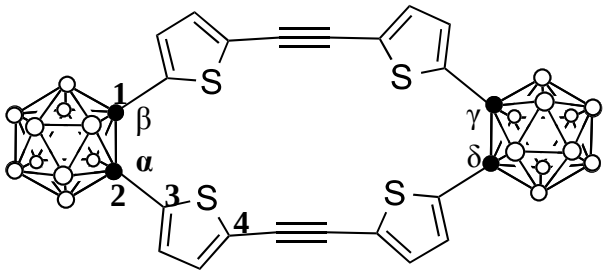

Figure 5-14: Dihedral angle of interest (α) is the angle between the planes defined by carbons 1,2,3 & 2,3,4 in annulene **19**.

Table 3: Absolute Values of Compounds **18**A-E and **19**A-E Internal Dihedral Angles

Angle	Compoound	Conformation				
		A	B	C	D	E
α	18	99.6°	92.0°	99.6°	99.6°	92.8°
	19	71.2°	43.9°	71.7°	58.5°	48.1°
β	18	94.6°	90.2°	94.8°	93.6°	93.3°
	19	70.3°	43.4°	72.1°	73.6°	48.2°
γ	18	94.4°	90.4°	98.9°	94.8°	96.6°
	19	71.0°	44.0°	72.0°	49.8°	48.2°
δ	18	101.9°	90.3°	99.3°	101.9°	92.4°
	19	70.2°	43.2°	71.6°	50.9°	48.1°

distortion in the dihedral (torsion) angles between the alpha carbons of the thiophene rings and the carborane carbons (depicted in Figure 5-14 and the angles are listed in Table 3). This distortion forces the thiophene C_{α}-$C_{carb.}$ bond out of the plane of the ring which causes the p-orbitals of the alpha carbons to rotate out of plane with each other just enough to maintain the σ-bond; however this rotation decreases orbital overlap between the *p*-orbitals of the thiophenes' α- and β- C atoms which decreases the aromatic stabilization of the rings.

To evaluate the destabilization due to ring strain, the formation enthalpies, $\Delta H_f^{\circ}(298K)$, and heats of combustion, $\Delta H_c^{\circ}(298K)$, of the five macrocycles (**19A-E**) and their syn mono-coupled precursors (**18A-E**) were modelled computationally. The calculated $\Delta H_c^{\circ}(298K)$ are based on complete combustion reactions. While use of isodesmic and homodesmic reactions in calculating formation enthalpies will yield more accurate results, they could not be used as experimental data for carboranes is not available due to the variation in the carboranes' combustion products based on other atoms present. The results of the thermodynamics study are summarized in Table 4 below. It was found that the macrocycles have almost as much strain energy as a benzyne

ring. We believe this to be the reason the annulene appears in MS (MALDI) but is not stable enough for purification.

Table 4. Results of the Thermodynamic Evaluation of Strain

Coupling Product	ΔH_f°(298K) (kcal/mol)	ΔH_c°(298K) (kcal/mol)	E_{strain} (kcal/mol)
18A	-7823.7177	-4899.3961	29.2790
19A	-7721.7612	-4928.6750	
18B	-7824.1885	-4898.9252	34.4081
19B	-7717.1029	-4933.3333	
18C	-7824.5855	-4898.5283	30.8280
19C	-7721.0800	-4929.3562	
18D	-7823.2842	-4899.8296	31.2889
19D	-7719.3178	-4931.1184	
18E	-7824.3685	-4898.7453	30.5495
19E	-7721.1414	-4929.2948	
Benzene	-1240.4062	-694.7953	38.0562
Benzyne	-1056.9950	-732.8516	
Note: Benzene & benzyne are included as a standard reference for comparison.			

5.6 Conclusion

A new series of *o*-carborane containing thiophene oligomers were synthesized in good yields from 5,(5')-(di)bromo-2,2'-carboranyldithiophene **13a-b** viapalladium(0)-catalyzed Sonogashira and Stille cross-coupling reactions. Such new compounds were well characterized by ^{1}H and ^{13}C NMR and MS. Seven X-ray structures were obtained to further confirm the regioselectivity of the reactions and the solid state confirmations of the molecules.

The electrochemical characterization of these compounds were performed and showed the decreased anodic potential in the following order: **16a** ≈ **16b** > **15b** > **15a**, which agrees well with the trend observed from DFT calculations. Moreover, poly(**15a**) and poly(**15b**) could be

successfully electro-generated from **15a** and **15b** under suitable conditions. Compared with the parent conducting polymers, the lower doping levels δ determined for both newly generated polymers suggest the notable effect of the incorporated carborane clusters. DFT calculations also showed low energy required for the intramolecular cyclization of **15a** and **15b**, which may lead to more organized structures of the generated polymers. Therefore, both carborane-functionalized poly(**15a**) and poly(**15b**) are promising candidates of conducting materials with enhanced chemical and thermal stabilities.

Finally, the synthesis of first carborane-fused porphyrin analogue **19** was attempted under various conditions, and the MALDI was obtained to confirm the formation. However, such a reaction gave a very low yields, may due to a large steric strain, which was investigated by computational studies.

5.6 Experimental

5.6.1 Synthesis

General: All the reagents and solvents were purchased from VWR, Fisher or Sigma-Aldrich without further purification. All the reactions were monitored by Sorbent TLC using 0.2 mm silica gel or neutral alumina with UV- 254/366 nm. Silica gel (230×400 mesh) and neutral alumina (50-200 μm, Act. I) for column chromatography were purchased from Sorbent. All NMR spectra were collected using a Bruker AV-400 MHz, AV-500 MHz or DPX-400 MHz NMR spectrometers in $CDCl_3$ at room temperature. The chemical shifts (δ) are reported in ppm with $CDCl_3$ (δ = 7.27 ppm for ^{1}H NMR and 77.0 ppm for ^{13}C NMR) as reference. All mass spectra were collected using an Agilent 6210 ESI-TOF MS, Varian Saturn 2000 Ion Trap with CP 3800 GC MS and Applied Biosystems QSTAR for MALDI.

2,2'-*o*-Carboranyl-bisthiophene 9 was synthesized using a slightly modified published procedure.[22]

5,5'-Dibromo-2,2'-Co-arboranyl-bisthiophene 13a: To a 50 mL flask equipped with a magnetic stirrer were added **9** (630 mg, 2.04 mmol) and NBS (2.18 g, 12.24 mmol). The flask was evacuated and refilled with argon 3 times. Chloroform (15 mL) and acetic acid (10 mL) were added into the flask. The mixture was stirred and refluxed overnight under Ar. The reaction was stopped when starting material disappeared, according to TLC. After cooling to room temperature, the mixture was poured into water. Dichloromethane (30 mL × 3) was used to extract the organic components. The organic layers were combined and washed with saturated aqueous $NaHCO_3$ and brine. The organic layer was dried using dry sodium sulfate then the solvents were removed under reduced pressure. The residue was purified by silica gel column chromatography using hexane as the eluent, to give **13a** as a white solid product (722.9 mg, 76% yield). mp 99-100 ^oC. ^1H NMR (400 MHz, $CDCl_3$) δ 6.94-6.95 (d, J = 4.0 Hz, 1H), 6.84-6.85 (d, J = 4.0 Hz, 1H), 1.60-3.50 (br, 10 H); ^{13}C NMR (400 MHz, $CDCl_3$): 135.6, 132.8, 130.3, 116.8, 80.0; MS (GC-MS) m/z $[M]^+$ 466.0, calculated for $C_{10}H_{14}B_{10}Br_2S_2$ 466.0.

5-Bromo-2,2'-o-Carboranyl-bisthiophene 13b: A similar procedure as that described above was used, starting from **9** (257 mg, 0.83 mmol), NBS (443 mg, 2.49 mmol), chloroform (4 mL), and acetic acid (4 mL). The mixture was stirred and refluxed overnight under Ar. After cooling to room temperature, the mixture was poured into water, extracted with dichloromethane (10 mL × 3) and the organic layers washed with saturated aqueous $NaHCO_3$ and brine. The resulting residue was purified by silica gel column chromatography using hexane as the eluent to give **13b** as a white solid (160.8 mg, 50%).

mp 107-108 ºC. ^{1}H NMR (400 MHz, $CDCl_3$) δ 7.23-7.25 (dd, *J* = 5.2, 1.2 Hz, 1H), 7.19-7.20 (dd, *J* = 3.7, 1.2 Hz, 1H), 6.92-6.93 (d, *J* = 4.0 Hz, 1H), 6.85-6.87 (dd, *J* = 5.1, 3.8 Hz, 1H), 6.79-6.80 (d, *J* = 4.0 Hz, 1H), 1.60-3.50 (br,10H); ^{13}C NMR ($CDCl_3$, 400Hz): 135.9, 134.5, 132.7, 132.6, 130.0, 129.7, 127.2, 116.4, 80.8, 80.0; MS (GC-MS) m/z $[M]^+$ 387.3, calculated for $C_{10}H_{15}B_{10}BrS_2$ 387.1.

2,2'-o-Carboranyldi(2-trimethylsilylethynylthiophene) 14: To a 25 mL flask equipped with a magnetic stirrer were added **13a** (92.3 mg, 0.2 mmol), $Pd(PPh_3)_2Cl_2$ (27 mg, 6 mol%) and CuI (14 mg, 10 mol%). The flask was evacuated and refilled with argon 3 times. Dry diethylamine (DEA) (5 mL) and ethynyltrimethylsilane (58.9 mg, 0.6 mmol) were added into the flask. The mixture was stirred at 60 ºC under argon for 2 h. The reaction was stopped when all the starting material disappeared according to TLC. After cooling to room temperature, the solvent was removed under reduced pressure. The catalysts were removed by filtration through a pad of silica gel and washed with dichloromethane. The organic solvents were removed under reduced pressure and the resulting residue was purified by silica gel column chromatography using hexane as the eluent, to give **14** as a white solid (132.6 mg, 80%). mp 140-141 ºC. ^{1}H NMR (400 MHz, $CDCl_3$) δ 7.00 (d, *J* = 3.9 Hz, 1H), 6.92 (d, *J* = 3.9 Hz, 1H), 1.60-3.50 (10H, br), 0.23 (s, 18H); ^{13}C NMR (400 MHz, $CDCl_3$): 134.9, 132.3, 132.1, 127.4, 101.7, 96.0, 80.3, -0.3; MS (GC-MS) m/z $[M]^+$ 500.8, calculated for $C_{20}H_{32}B_{10}Si_2S_2$ 501.2.

General procedure for Stille reactions

Into a 100 ml flask equipped with a magnetic stirrer were added **13a** or **13b** (0.1 mmol) and $Pd(PPh_3)_4$ (12 mg, 10 mol%). The flask was evacuated and refilled with argon 3 times. Toluene (10 ml) and stannane reagent (3 equiv for the synthesis of **15a,b** and **16a**, or 1.5

equiv for synthesis of **16b**) were added into the flask. The mixture was stirred and refluxed for 2-4 h under nitrogen. The reaction was stopped when starting material disappeared according to TLC. The catalysts were removed by filtration through a pad of celite and washed with dichloromethane. The solvents were removed under reduced pressure. The residue was purified by silica gel column chromatography using hexane/dichloromethane as the eluents to give the desired products.

Di(thienyl-N-methylpyrrole)-o-carborane 15a: 44.3 mg**,** 95%; mp 152-154 ^{o}C; ^{1}H NMR (400 MHz, $CDCl_3$) δ 7.14 (d, *J* = 3.9 Hz, 2H), 6.73 (d, *J* = 3.9 Hz, 2H), 6.67 (m, 2H), 6.26 (dd, *J* = 3.7, 1.7 Hz, 2H), 6.11 (dd, *J* = 3.6, 2.8 Hz, 2H), 3.60 (s, 6H), 1.60-3.50 (10H, br); ^{13}C NMR ($CDCl_3$, 100Hz): 139.3, 133.0, 132.7, 125.8, 125.1, 124.0, 110.8, 108.2, 81.6, 35.3; HRMS (ESI-TOF) m/z $[M+H]^+$ 468.2595, calculated for $C_{20}H_{26}N_2S_2B_{10}$ 468.2600.

Di(bisthienyl)-o-carborane 15b: 43.5 mg, 92%; mp 172-174 ^{o}C; ^{1}H NMR (400 MHz, $CDCl_3$) δ 7.22–7.24 (m, 2H), 7.12-7.13 (m, 2H), 7.09-7.10 (d, *J* = 3.9 Hz, 2H), 6.98-7.00 (dd, *J* = 5.0, 3.7 Hz, 2H), 6.88 (d, *J* = 3.9 Hz, 2H), 1.60-3.50 (br, 10H); ^{13}C NMR (126 MHz, $CDCl_3$) δ 141.5, 135.8, 133.2, 132.8, 128.0, 125.7, 124.8, 123.3, 81.4; MALDI-TOF m/z $[M+H]^+$ 473.138 , calculated for $C_{18}H_{20}S_4B_{10}$ 473.143.

5,5'-Divinyl-2,2'-Carboranyldithiophene 16a: 24.5 mg, 68%; mp 144-147 ^{o}C; ^{1}H NMR (400 MHz, $CDCl_3$) δ 7.02-7.03 (d, *J* = 3.9 Hz, 2H), 6.68-6.69 (d, *J* = 3.8 Hz, 2H), 6.56-6.63 (dd, *J* = 17.4, 10.9 Hz, 2H), 5.51-5.56 (d, *J* = 17.4 Hz, 2H), 5.17-5.20 (d, *J* = 10.9 Hz, 2H), 1.60-3.50 (br, 10H); ^{13}C NMR (126 MHz, $CDCl_3$) δ 146.7, 132.9, 132.7, 129.0, 125.4, 115.5, 81.3. MS (GC-MS) m/z $[M]^+$ 360.5, calculated for $C_{14}H_{20}B_{10}S_2$ 360.2.

5-Vinyl-2,2'-Carboranyldithiophene 16b: 25.1 mg, 75%; mp 91-93 ^{o}C; ^{1}H NMR ($CDCl_3$, 400 Hz) δ 7.19–7.22 (m, 2H), 7.01-7.02 (d, *J* = 3.8 Hz, 1H), 6.83-6.85 (dd, *J* = 5.0, 3.9 Hz,

1H), 6.66-6.67 (d, *J* = 3.8 Hz, 1H), 6.55-6.62 (dd, *J* = 17.4, 10.9 Hz, 1H), 5.50-5.54 (d, *J* = 17.4 Hz, 1H), 5.16-5.19 (d, *J* = 10.9 Hz, 1H), 1.60-3.50 (br, 10H); ^{13}C NMR ($CDCl_3$, 100 Hz) δ 146.6, 134.8, 133.0, 132.7, 132.6, 129.5, 129.0, 127.1, 125.3, 115.5, 81.0; MS (GC-MS) m/z $[M]^+$ 334.3, calculated for $C_{12}H_{18}B_{10}S_2$ 334.2.

5.6.2 Crystal data

Diffraction data for **13a**, **13b**, **14**, **15a**, **16a** and **16b** were collected at T=100K on a Brüker Kappa Apex-II DUO diffractometer equipped with MoKα radiation and a Triumph curved monochromator (CuKα radiation from a microfocus source for **15b**). For **15b**, data were from a Nonius KappaCCD diffractometer with MoKα radiation at T=90K. In **13a**, there are four independent molecules, and for two of them, disorder exists in the conformation of one of the bromothiophenes. A similar disorder exists for the nonbrominated thiophene of **13b**, and for the terminal thiophenes in **15b**. In **14**, the molecule lies on a crystallographic twofold axis. CIFs are provided as supplementary material. CCDC deposition numbers are 1012320-1012322 for **13a**, **13b**, **14**, and 1484163-1484166 for **15a**, **15b**, **16a**, and **16b**, respectively.

5.6.3 Electrochemical Characterizations

Tetra-*n*-butylammonium hexafluorophosphate Bu_4NPF_6 was purchased from Fluka (puriss, electrochemical grade). Anhydrous dichloromethane (less than 50 ppm water from Merck) and acetonitrile (anhydrous, >99.8%, from Sigma-Aldrich) were used as received. The electrolytic medium was dried *in situ* over activated, neutral alumina from Aldrich. Alumina was previously activated at 450°C under vacuum for several hours. Linear potential cyclic voltammetry experiments were performed with an Autolab PGSTAT 30 potentiostat from Eco Chemie B.V., equipped with General Purpose Electrochemical

System GPES software. The working electrode was a 1 mm-diameter platinum disk (area: 0.8 mm^2) and the counter electrode was a glassy carbon rod. Potentials were relative to the system 10^{-2} M Ag^+ | Ag in acetonitrile and the ferrocene/ferrocenium couple in CH_2Cl_2 + 0.2 M Bu_4NPF_6 was observed at $E°'$ = 0.19 V vs this reference. All electrochemical measurements were carried out inside a home-made Faraday cage at room temperature (20±2°C) and under a constant flow of argon.

5.6.4 Computer Modeling for Section 5-4

The geometries of all structures were optimized without symmetry constraints using B3LYP/6-31+G(d,p) level calculations. The hybrid Becke's Three Parameter DFT Functional was used.[55-56] The solvent effects were taken into account using the Polarized Continuum Model (PCM).[57-58] All calculations were performed using the Gaussian 09 program package.[59]

5.6.5 Computer Modeling for Section 5-5

The structures investigated were optimized, without symmetry constraints, using the NWChem 6.3 software package,[60] with density functional theory and the B3LYP hybrid functional[55-56] and the 6-31+G** basis set obtained from the EMSL Basis Set Exchange.[61-62] Vibrational frequency analysis calculations both confirmed all structures were at energetic minima and provided the necessary thermodynamic data. The vibrational frequencies were scaled by a factor of 0.964._ENREF_6_63[63] The formation enthalpies, $\Delta_f H°$, at both 0K and 298K, were calculated as follows:

$$\Delta_f H^\circ(M, 298K) = \Delta_f H^\circ(M, 0K) + H^\circ_{corr}(M) - \sum_{atoms} x H^\circ_{corr}(X) \qquad \text{Eq1}$$

$$\Delta_f H^\circ(M, 0K) = \sum_{atoms} x \Delta_f H^\circ(X, 0K) - \sum D_0(M) \qquad \text{Eq2}$$

$$\sum \boldsymbol{D_0(M)} = \sum_{\boldsymbol{atoms}} \boldsymbol{\varepsilon_0(X)} - \boldsymbol{\varepsilon_0(M)} - \boldsymbol{\varepsilon_{zpe}(M)} \qquad \text{Eq3}$$

where H°_{corr} is the thermal correction to the enthalpy, ΣD_0 is the atomization energy, ε_0 is the total electronic energy, and ε_{ZPE} is the zero-point vibrational energy. The atomic formation enthalpies and thermal corrections to the enthalpy used were experimental data.[64] Calculations were performed on the Louisiana State University: High Performance Computing Department's SuperMike-II cluster. It should be noted that the mono-coupled structures used in the calculations are not the same as what would have been obtained experimentally. To simplify the calculations and reduce the computational cost, the remaining bromine atom was replaced with a hydrogen. Effects of the solvent continum were not taken into account nor were effects of the additional two hydrogens on the mono-coupled systems versus the macrocycles since it was consistent through all six systems and the reference system.

5.7 Reference

1. Chiang, C. K.; Fincher, C. R.; Park, Y. W.; Heeger, A. J.; Shirakawa, H.; Louis, E. J.; Gau, S. C.; MacDiarmid, A. G., *Phys. Rev. Lett.* **1977,** *39* (17), 1098-1101.

2. Shirakawa, H.; Louis, E. J.; MacDiarmid, A. G.; Chiang, C. K.; Heeger, A. J., *J. Chem. Soc., Chem. Commun.* **1977,** (16), 578-580.

3. Heinze, J.; Frontana-Uribe, B. A.; Ludwigs, S., *Chem. Rev.* **2010,** *110* (8), 4724-4771.

4. Skotheim, T. A.; Reynolds, J., *Handbook of Conducting Polymers*. CRC Press: Boca Raton, 2007.

5. Grimes, R. N., *Carboranes*. 2nd ed.; Academic Press: Oxford, 2011.

6. Hosmane, S. N., *Boron Science new technologies and applications*. CRC Press: New York, 2012.

7. Vicente, M. G. H.; Sibrian-Vazquez, M., Syntheses of boronated porphyrins and their application in BNCT. In *The Handbook of Porphyrin Science*, Kadish, K. M. S., K. M.; Guilard, R., Ed. World Scientific Publishers: Singapore, 2010; Vol. 4, pp 191-248.

8. Dash, B. P.; Satapathy, R.; Maguire, J. A.; Hosmane, N. S., *New J. Chem.* **2011,** *35* (10), 1955-1972.

9. Doshi, A.; Jäkle, F., 1.27 - Boron-Containing Polymers A2 - Poeppelmeier, Jan ReedijkKenneth. In *Comprehensive Inorganic Chemistry II* 2nd ed.; Reedijk, J.; Poeppelmeier, K., Eds. Elsevier: Amsterdam, 2013; Vol. 1, pp 861-891.

10. N. Zhao, P. Bobadova-Parvanova and M. G. H. Vicente;, in Boron Chemistry in Organometallics, Catalysis, Materials and Medicine, eds. N. S. Hosmane and R. Eagling, World Scientific Publishers, accepted

11. Guron, M. M.; Wei, X.; Welna, D.; Krogman, N.; Kim, M. J.; Allcock, H.; Sneddon, L. G., *Chem. Mater.* **2009,** *21* (8), 1708-1715.

12. Simon, Y. C.; Peterson, J. J.; Mangold, C.; Carter, K. R.; Coughlin, E. B., *Macromolecules* **2009,** *42* (2), 512-516.

13. Mukherjee, S.; Thilagar, P., *Chem. Commun.* **2016,** *52* (6), 1070-1093.

14. Houser, E. J.; Keller, T. M., *Macromolecules* **1998,** *31* (12), 4038-4040.

15. Kolel-Veetil, M. K.; Keller, T. M., *J. Polym. Sci., Part A: Polym. Chem.* **2006,** *44* (1), 147-155.

16. Masalles, C.; Borrós, S.; Viñas, C.; Teixidor, F., *Adv. Mater.* **2000,** *12* (16), 1199-1202.

17. Masalles, C.; Borrós, S.; Viñas, C.; Teixidor, F., *Adv. Mater.* **2002,** *14* (6), 449-452.

18. Masalles, C.; Teixidor, F.; Borrós, S.; Viñas, C., *J. Organomet. Chem.* **2002,** *657* (1–2), 239-246.

19. David, V.; Viñas, C.; Teixidor, F., *Polymer* **2006,** *47* (13), 4694-4702.

20. Fabre, B.; Hao, E.; LeJeune, Z. M.; Amuhaya, E. K.; Barrière, F.; Garno, J. C.; Vicente, M. G. H., *ACS Appl. Mater. Interfaces* **2010,** *2* (3), 691-702.

21. Masalles, C.; Llop, J.; Viñas, C.; Teixidor, F., *Adv. Mater.* **2002,** *14* (11), 826-829.

22. Hao, E.; Fabre, B.; Fronczek, F. R.; Vicente, M. G. H., *Chem. Commun.* **2007,** (42), 4387-4389.

23. Barrière, F.; Fabre, B.; Hao, E.; LeJeune, Z. M.; Hwang, E.; Garno, J. C.; Nesterov, E. E.; Vicente, M. G. H., *Macromolecules* **2009,** *42* (8), 2981-2987.

24. Hao, E.; Fabre, B.; Fronczek, F. R.; Vicente, M. G. H., *Chem. Mater.* **2007,** *19* (25), 6195-6205.

25. Fabre, B.; Chayer, S.; Vicente, M. G. H., *Electrochem. Commun.* **2003,** *5* (5), 431-434.

26. Clark, J. C.; Fabre, B.; Fronczek, F. R.; Vicente, M. G. H., *J. Porphyrins Phthalocyanines* **2005,** *09* (11), 803-810.

27. Fabre, B.; Clark, J. C.; Vicente, M. G. H., *Macromolecules* **2006,** *39* (1), 112-119.

28. Cansu-Ergun, E. G.; Cihaner, A., *J. Electroanal. Chem.* **2013,** *707*, 78-84.

29. Marshall, J.; Fei, Z.; Yau, C. P.; Yaacobi-Gross, N.; Rossbauer, S.; Anthopoulos, T. D.; Watkins, S. E.; Beavis, P.; Heeney, M., *J. Mater. Chem. C* **2014,** *2* (2), 232-239.

30. Marshall, J.; Hooton, J.; Han, Y.; Creamer, A.; Ashraf, R. S.; Porte, Y.; Anthopoulos, T. D.; Stavrinou, P. N.; McLachlan, M. A.; Bronstein, H.; Beavis, P.; Heeney, M., *Polym. Chem.* **2014,** *5* (21), 6190-6199.

31. Krische, B.; Zagorska, M., *Synth. Met.* **1989,** *28* (1), 263-268.

32. Bredas, J. L.; Street, G. B., *Acc. Chem. Res.* **1985,** *18* (10), 309-315.

33. Martin, R. E.; Diederich, F., *Angew. Chem. Int. Ed.* **1999,** *38* (10), 1350-1377.

34. Mishra, A.; Ma, C.-Q.; Bäuerle, P., *Chem. Rev.* **2009,** *109* (3), 1141-1276.

35. Krische, B.; Zagorska, M., *Synth. Met.* **1989,** *33* (3), 257-267.

36. Roncali, J., *Chem. Rev.* **1992,** *92* (4), 711-738.

37. Krische, B.; Zagorska, M.; Hellberg, J., *Synth. Met.* **1993,** *58* (3), 295-307.

38. van Haare, J. A. E. H.; Groenendaal, L.; Havinga, E. E.; Janssen, R. A. J.; Meijer, E. W., *Angew. Chem. Int. Ed.* **1996,** *35* (6), 638-640.

39. Sessler, J. L.; Aguilar, A.; Sanchez-Garcia, D.; Seidel, D.; Köhler, T.; Arp, F.; Lynch, V. M., *Org. Lett.* **2005,** *7* (10), 1887-1890.

40. López-Pérez, A.; Robles-Machín, R.; Adrio, J.; Carretero, J. C., *Angew. Chem. Int. Ed.* **2007,** *46* (48), 9261-9264.

41. Nishinaga, T.; Tateno, M.; Fujii, M.; Fujita, W.; Takase, M.; Iyoda, M., *Org. Lett.* **2010,** *12* (23), 5374-5377.

42. Nishinaga, T.; Kageyama, T.; Koizumi, M.; Ando, K.; Takase, M.; Iyoda, M., *J. Org. Chem.* **2013,** *78* (18), 9205-9213.

43. Miller, L. L.; Mann, K. R., *Acc. Chem. Res.* **1996,** *29* (9), 417-423.

44. Song, C.; Swager, T. M., *Org. Lett.* **2008,** *10* (16), 3575-3578.

45. Mio, M. J.; Kopel, L. C.; Braun, J. B.; Gadzikwa, T. L.; Hull, K. L.; Brisbois, R. G.; Markworth, C. J.; Grieco, P. A., *Org. Lett.* **2002,** *4* (19), 3199-3202.

46. Marsella, M. J.; Piao, G.; Tham, F. S., *Synthesis* **2002,** *2002* (09), 1133-1135.

47. Randazzo, M. E.; Toppare, L.; Fernandez, J. E., *Macromolecules* **1994,** *27* (18), 5102-5106.

48. Roncali, J.; Garnier, F.; Lemaire, M.; Garreau, R., *Synth. Met.* **1986,** *15* (4), 323-331.

49. Pozo-Gonzalo, C.; Salsamendi, M.; Pomposo, J. A.; Grande, H.-J.; Schmidt, E. Y.; Rusakov, Y. Y.; Trofimov, B. A., *Macromolecules* **2008,** *41* (19), 6886-6894.

50. Cristina, P.-G.; Pomposo, J. A.; Alduncin, J. A.; Salsamendi, M.; Mikhaleva, A. b. I.; Krivdin, L. B.; Trofimov, B. A., *Electrochim. Acta* **2007,** *52* (14), 4784-4791.

51. Hosoi, K.; Inagi, S.; Kubo, T.; Fuchigami, T., *Chem. Commun.* **2011,** *47* (30), 8632-8634.

52. Fox, M. A.; Nervi, C.; Crivello, A.; Low, P. J., *Chem. Commun.* **2007,** (23), 2372-2374.

53. Bard, A. J.; Faulkner, L. R., *Electrochemical Methods. Fundamentals and Applications*. Wiley & Sons: New York, 1980.

54. δ is the total number of positive charge per monomer unit and is calculated from the integration of the cyclic voltammetry curve corresponding to the oxidation step of the polymer matrix, assuming an electropolymerization yield of 100%.

55. Lee, C.; Yang, W.; Parr, R. G., *Physical Review B* **1988,** *37* (2), 785-789.

56. Becke, A. D., *The Journal of Chemical Physics* **1993,** *98* (7), 5648-5652.

57. Tomasi, J.; Mennucci, B.; Cammi, R., *Chem. Rev.* **2005,** *105* (8), 2999-3094.

58. Miertuš, S.; Scrocco, E.; Tomasi, J., *Chem. Phys.* **1981,** *55* (1), 117-129.

59. Gaussian 09, M. J. Frisch, G. W. Trucks, H. B. Schlegel, G. E. Scuseria, M. A. Robb, J. R. Cheeseman, G. Scalmani, V. Barone, B. Mennucci, G. A. Petersson, H. Nakatsuji, M. Caricato, X. Li, H. P. Hratchian, A. F. Izmaylov, J. Bloino, G. Zheng, J. L. Sonnenberg, M. Hada, M. Ehara, K. Toyota, R. Fukuda, J. Hasegawa, M. Ishida, T. Nakajima, Y. Honda, O. Kitao, H. Nakai, T. Vreven, J. A. Montgomery, Jr., J. E. Peralta, F. Ogliaro, M. Bearpark, J. J. Heyd, E. Brothers, K. N. Kudin, V. N. Staroverov, R. Kobayashi, J. Normand, K. Raghavachari, A. Rendell, J. C. Burant, S. S. Iyengar, J. Tomasi, M. Cossi, N. Rega, J. M. Millam, M. Klene, J. E. Knox, J. B. Cross, V. Bakken, C. Adamo, J. Jaramillo, R. Gomperts, R. E. Stratmann, O. Yazyev, A. J. Austin, R. Cammi, C. Pomelli, J. W. Ochterski, R. L. Martin, K. Morokuma, V. G. Zakrzewski, G. A. Voth,

P. Salvador, J. J. Dannenberg, S. Dapprich, A. D. Daniels, Ö. Farkas, J. B. Foresman, J. V. Ortiz, J. Cioslowski, and D. J. Fox, Gaussian, Inc., Wallingford CT, 2009.

60. Valiev, M.; Bylaska, E. J.; Govind, N.; Kowalski, K.; Straatsma, T. P.; Van Dam, H. J. J.; Wang, D.; Nieplocha, J.; Apra, E.; Windus, T. L.; de Jong, W. A., *Comput. Phys. Commun.* **2010,** *181* (9), 1477-1489.

61. Feller, D., *J. Comput. Chem.* **1996,** *17* (13), 1571-1586.

62. Schuchardt, K. L.; Didier, B. T.; Elsethagen, T.; Sun, L.; Gurumoorthi, V.; Chase, J.; Li, J.; Windus, T. L., *Journal of Chemical Information and Modeling* **2007,** *47* (3), 1045-1052.

63. NIST Computational Chemistry Comparison and Benchmark Database NIST Standard Reference Database Number 101 Release 16a, August 2013, Editor: Russell D. Johnson III http://cccbdb.nist.gov/

64. Curtiss, L. A.; Raghavachari, K.; Redfern, P. C.; Pople, J. A., *The Journal of Chemical Physics* **1997,** *106* (3), 1063-1079.

APPENDIX A: CHARACTERIZATION DATA FOR COMPOUNDS IN CHAPTER 2

Figure A1: ^{1}H NMR spectra of pyrrole **2b**

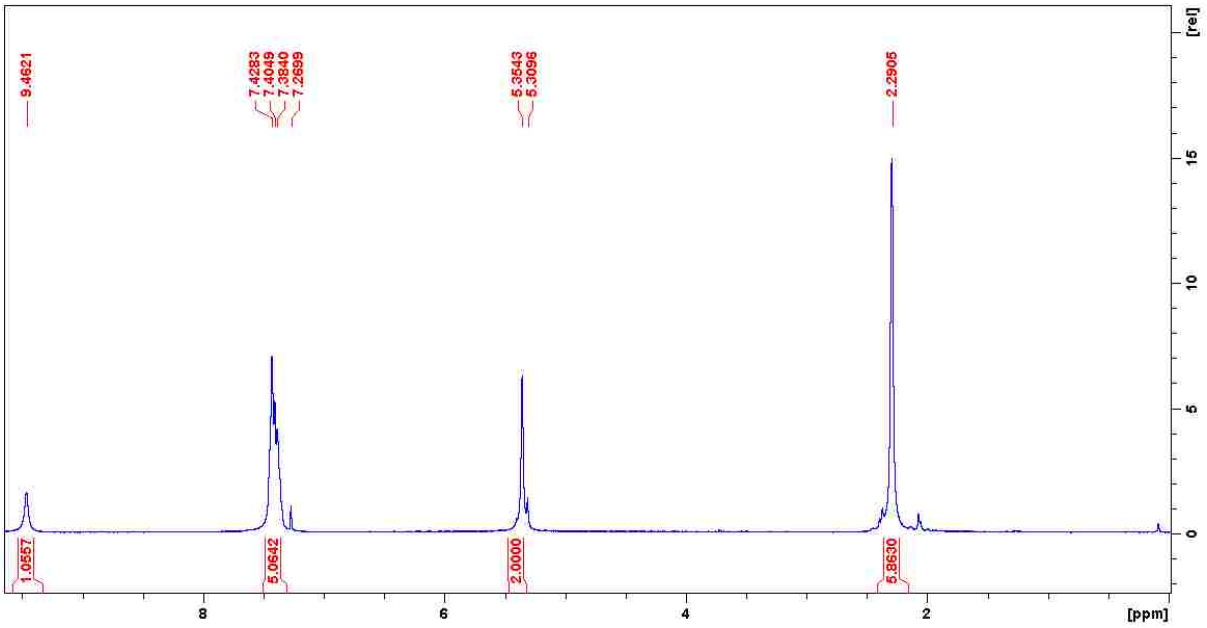

Figure A2: ^{13}C NMR spectra of pyrrole **2b**

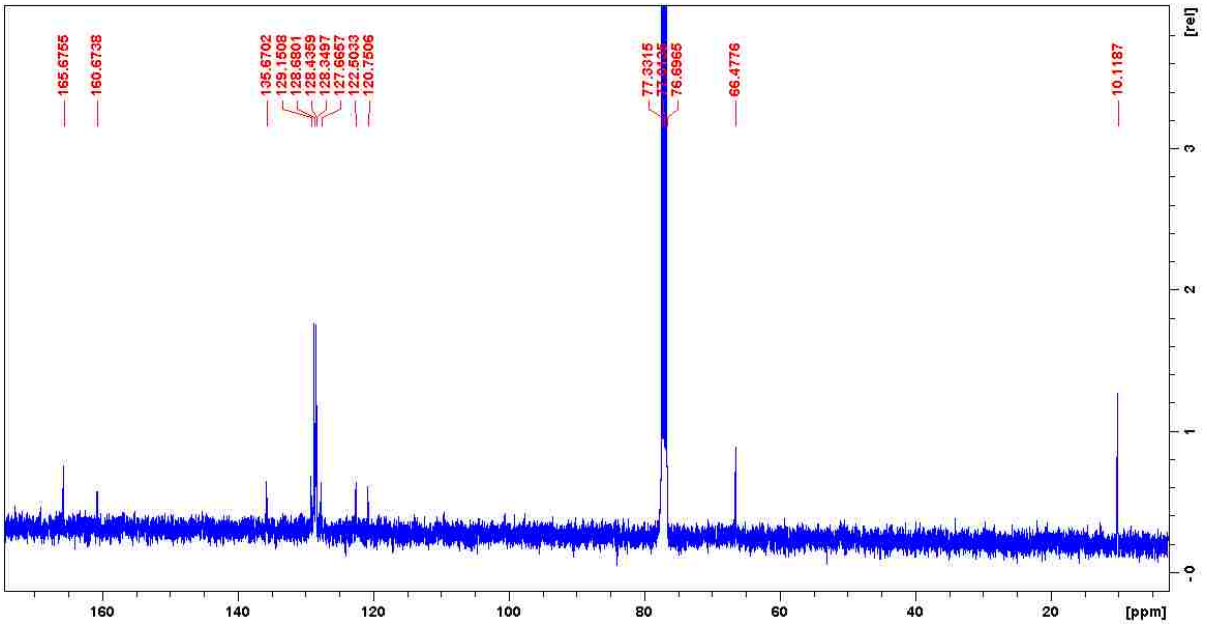

Figure A3: ^{1}H NMR spectra of pyrrole **2c**

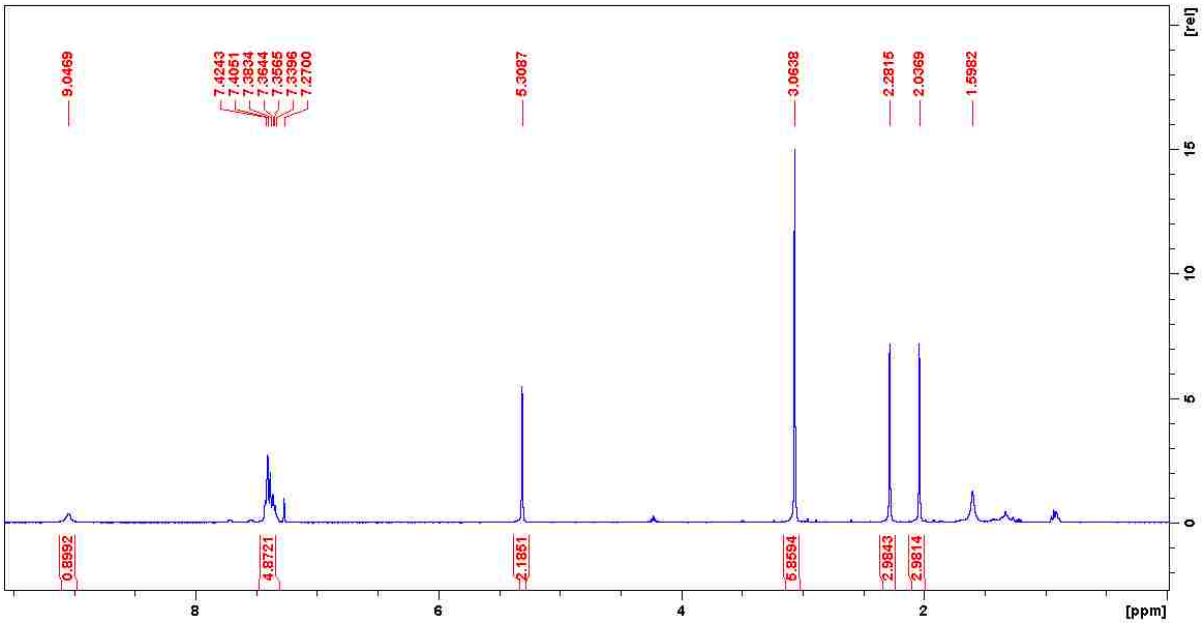

Figure A4: ^{13}C NMR spectra of pyrrole **2c**

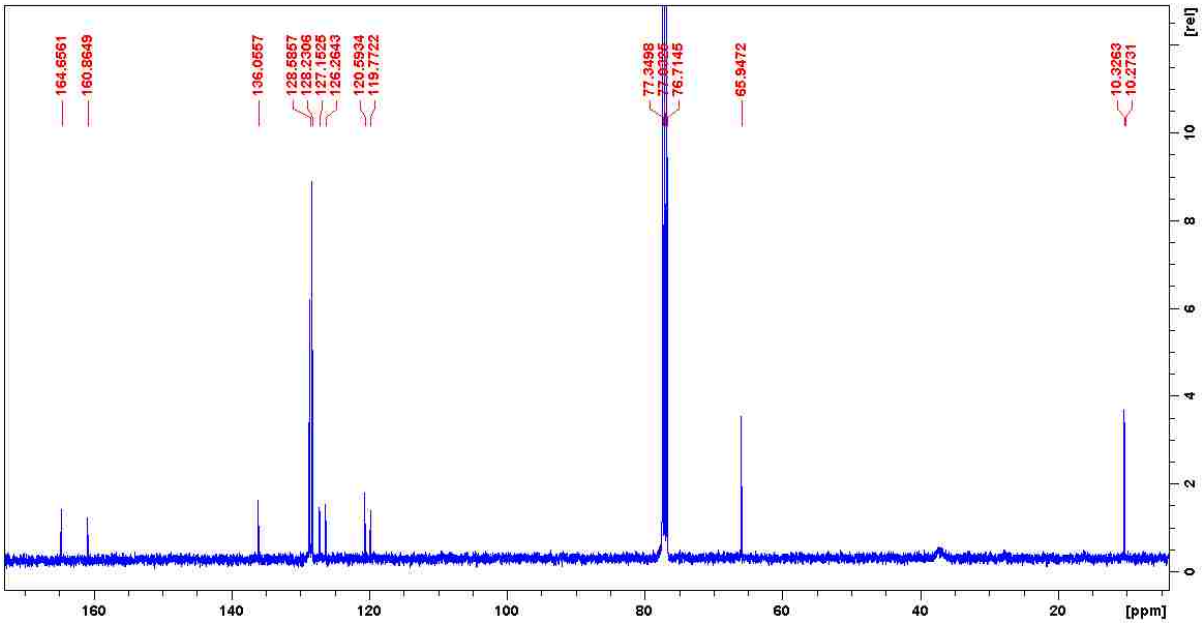

Figure A5: ^{1}H NMR spectra of pyrrole **8**

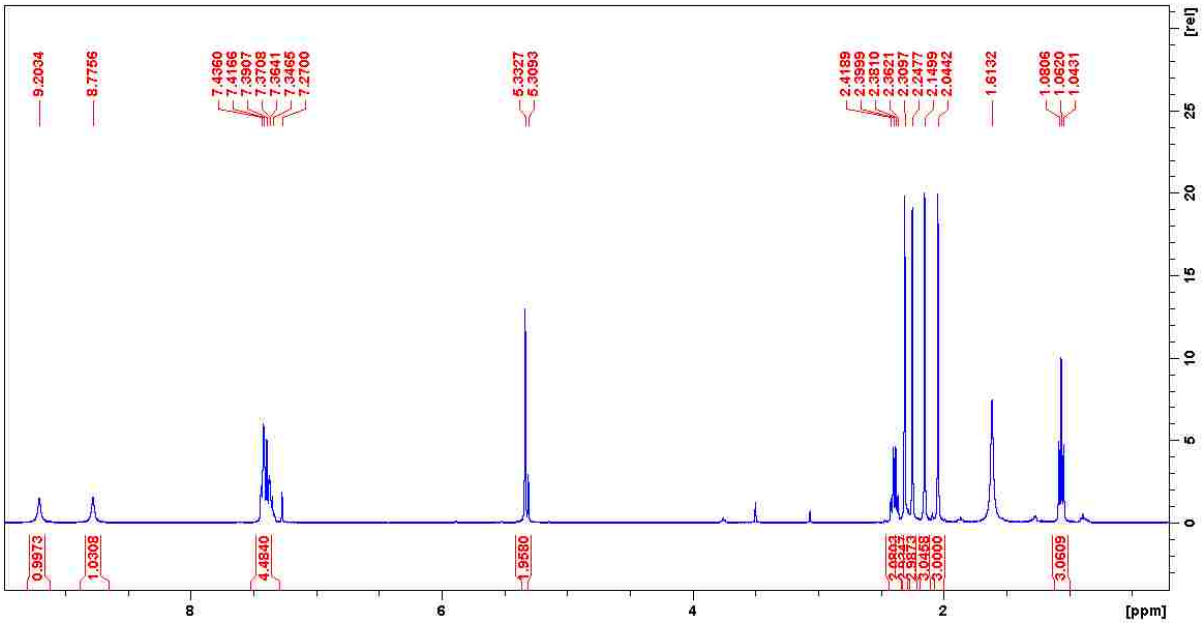

Figure A6: ^{13}C NMR spectra of pyrrole **8**

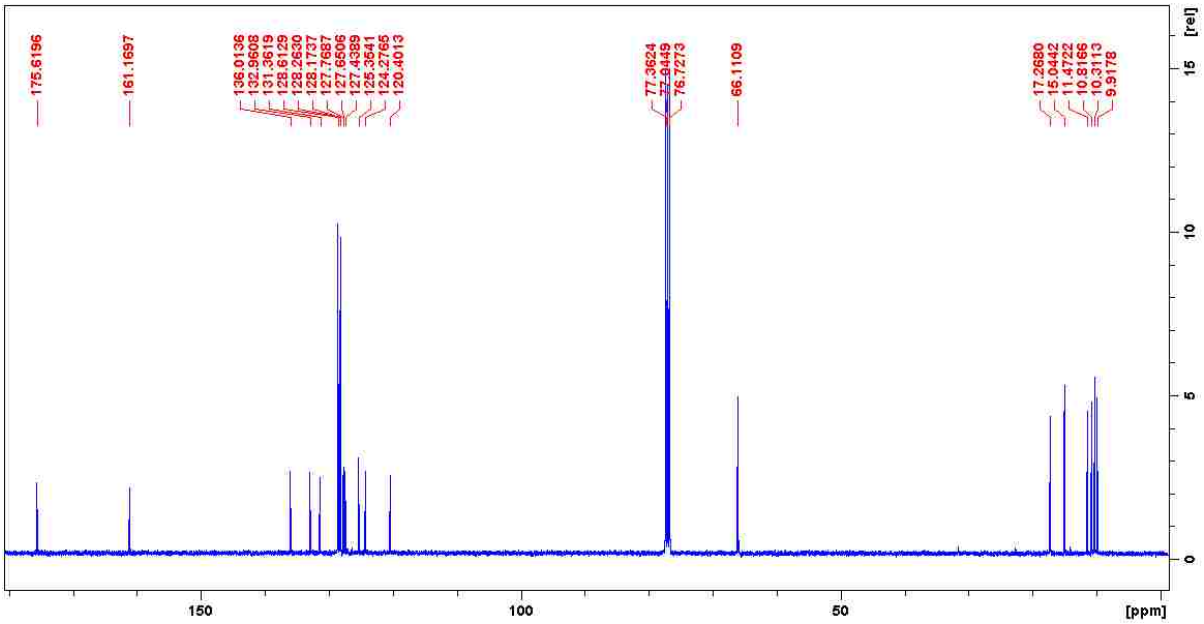

Figure A7: ^{1}H NMR spectra of compound **11**

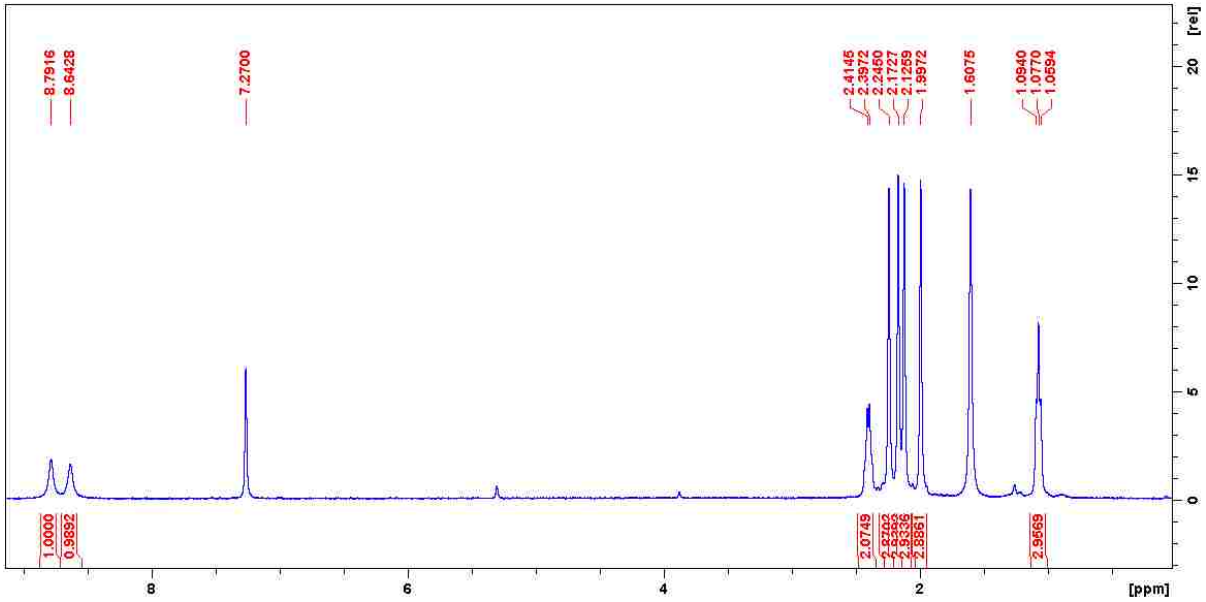

Figure A8: ^{13}C NMR spectra of compound **11**

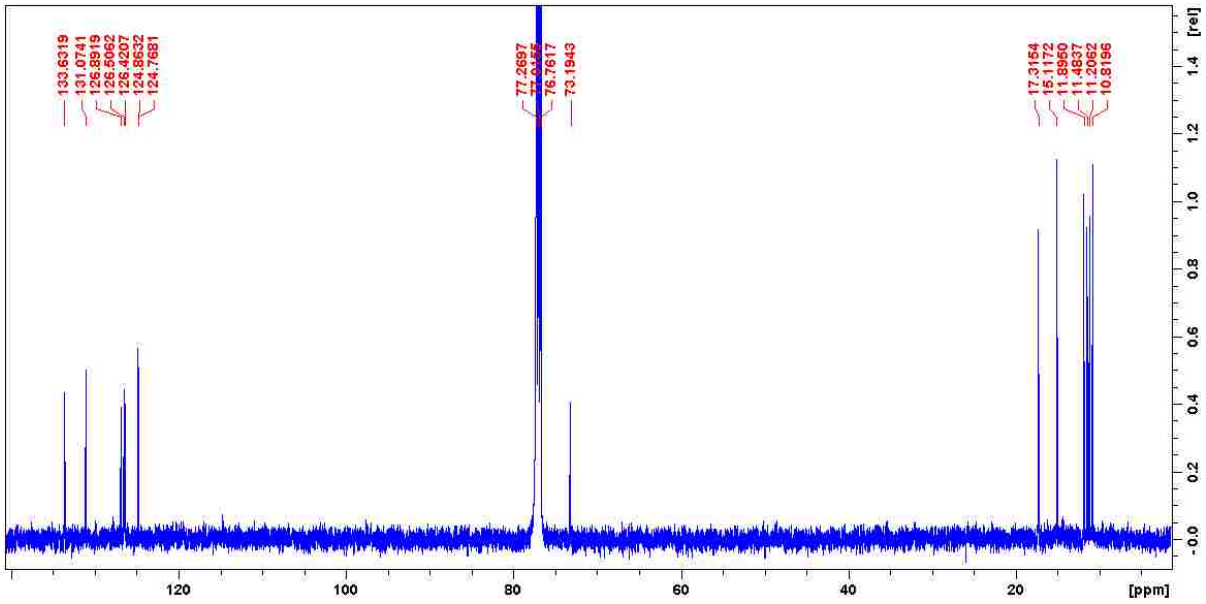

Figure A9: ^{1}H NMR spectra of BODIPY **1a**

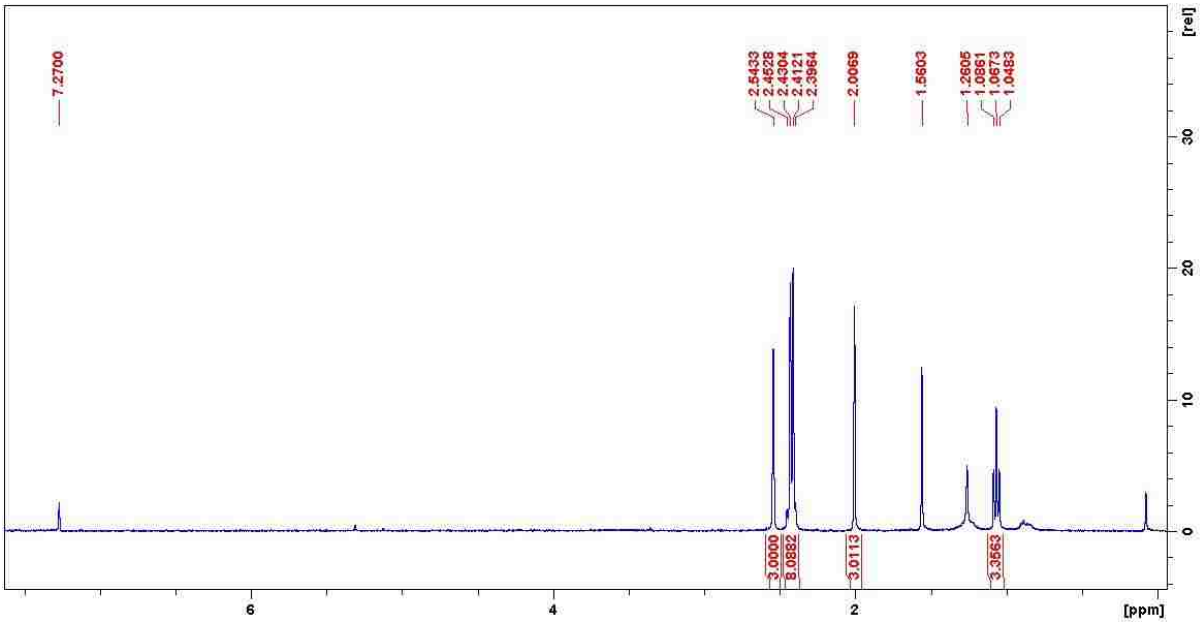

Figure A10: ^{13}C NMR spectra of BODIPY **1a**

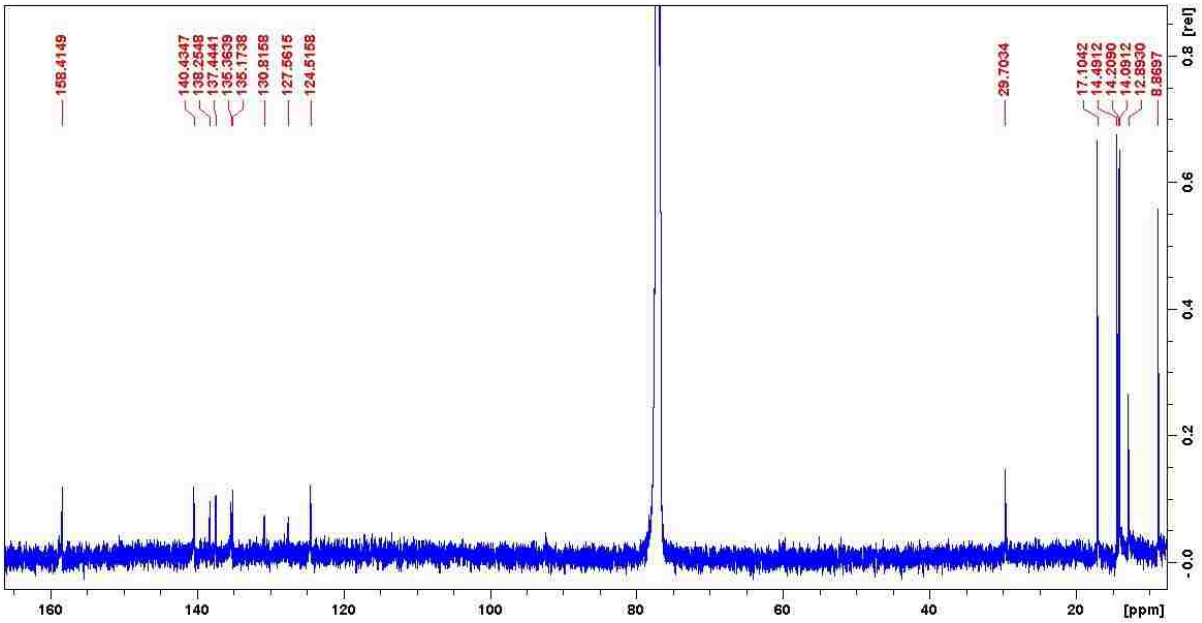

Figure A11:[1]H NMR spectra of BODIPY **1b**

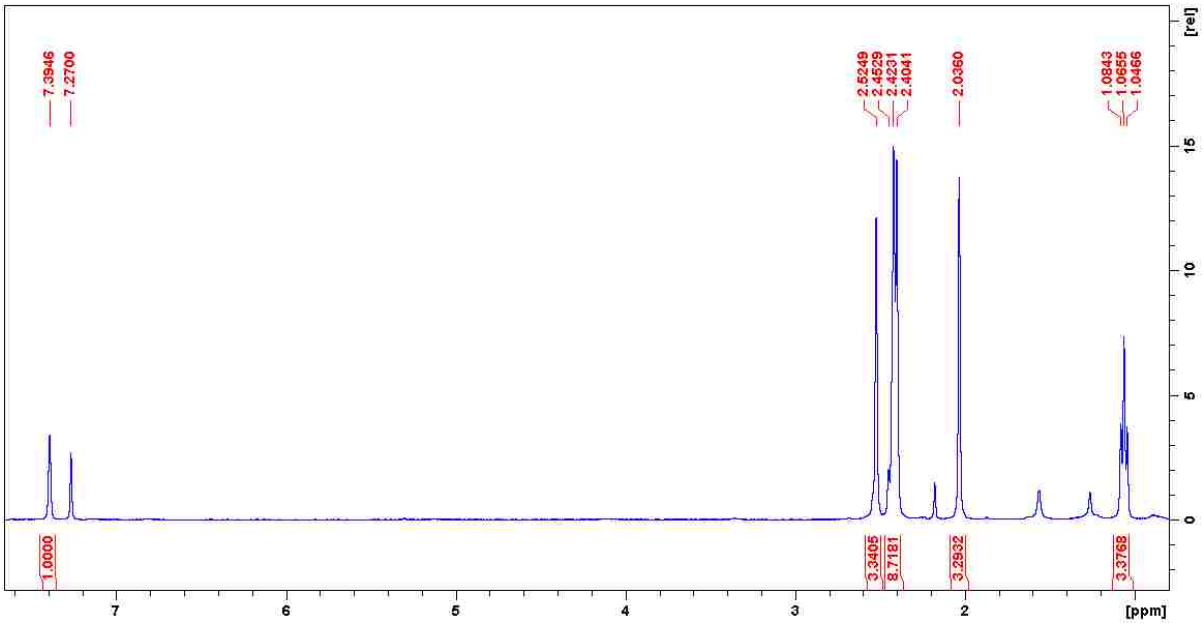

Figure A12: [13]C NMR spectra of BODIPY **1b**

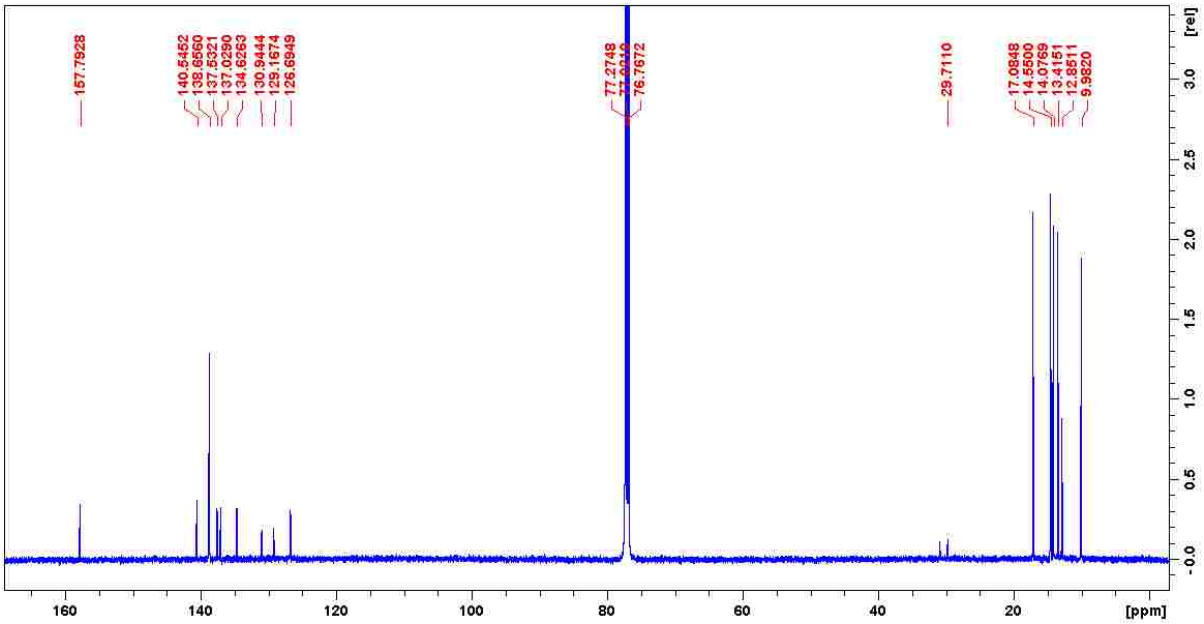

Figure A13: [1]H NMR spectra of BODIPY **12a**

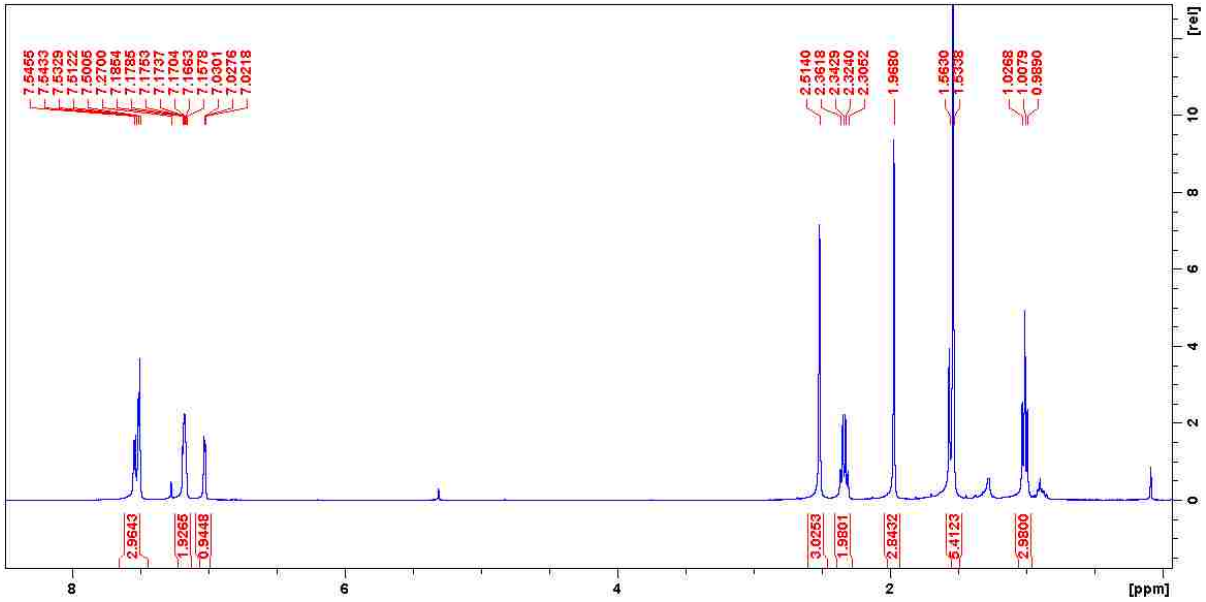

Figure A14: [13]C NMR spectra of BODIPY **12a**

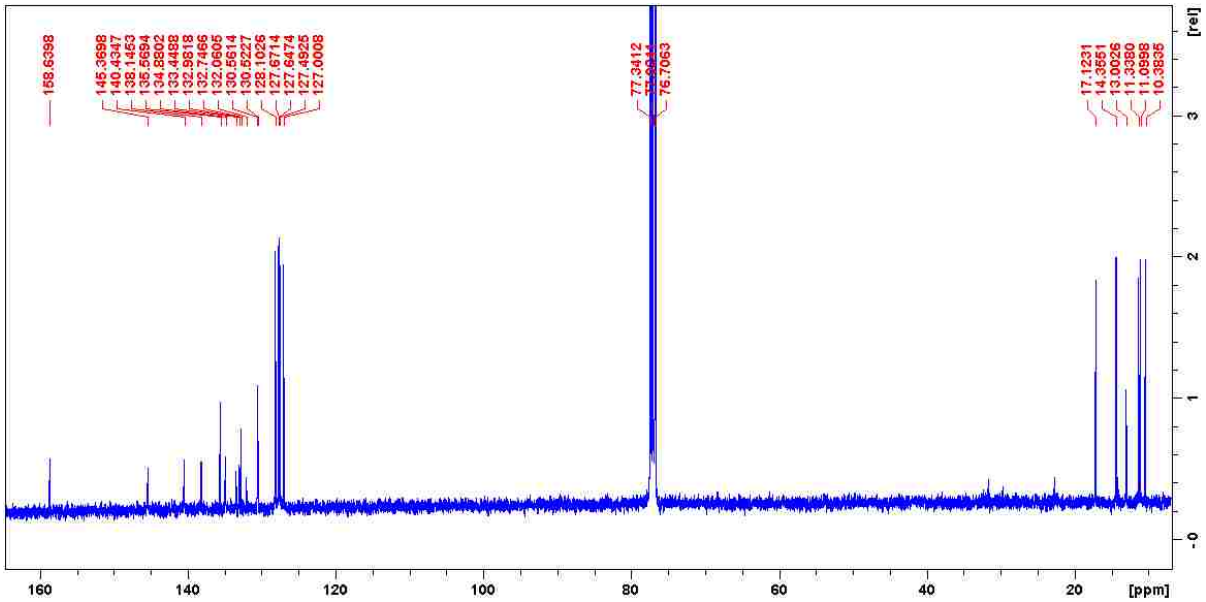

Figure A15: ^{1}H NMR spectra of BODIPY **12b**

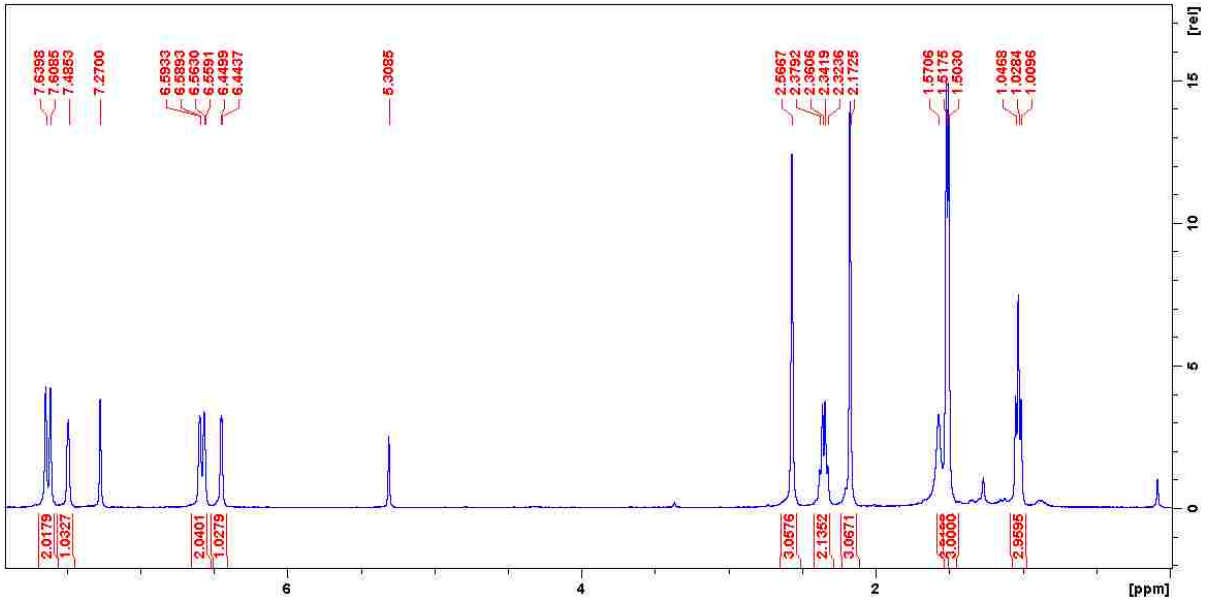

Figure A16: ^{13}C NMR spectra of BODIPY **12b**

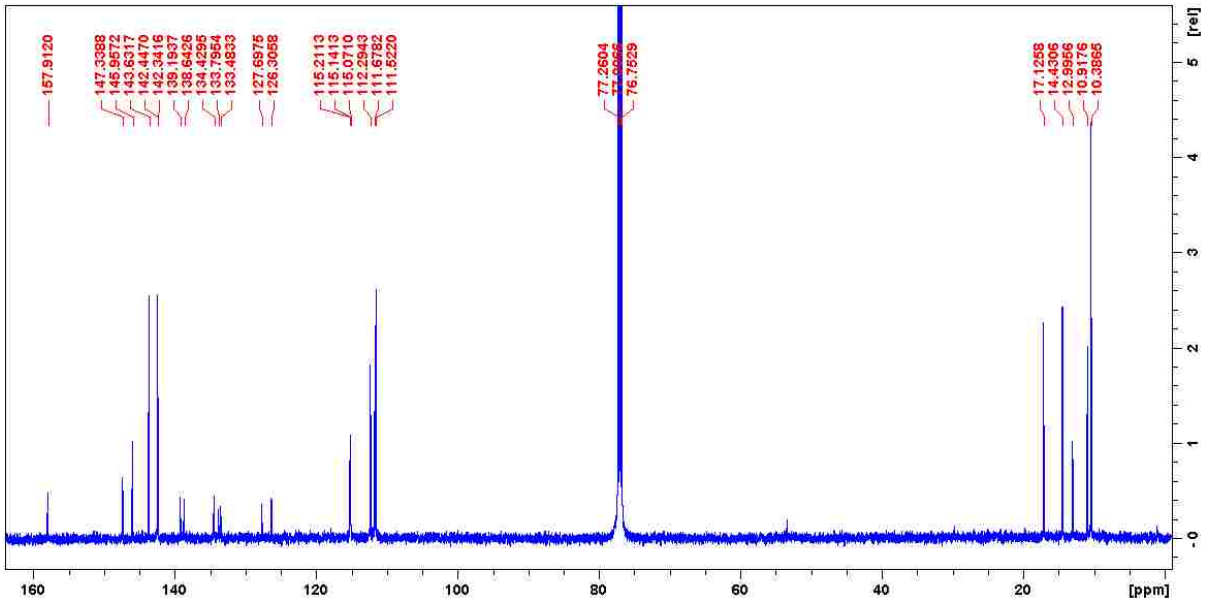

Figure A17: ^{1}H NMR spectra of BODIPY **12c**

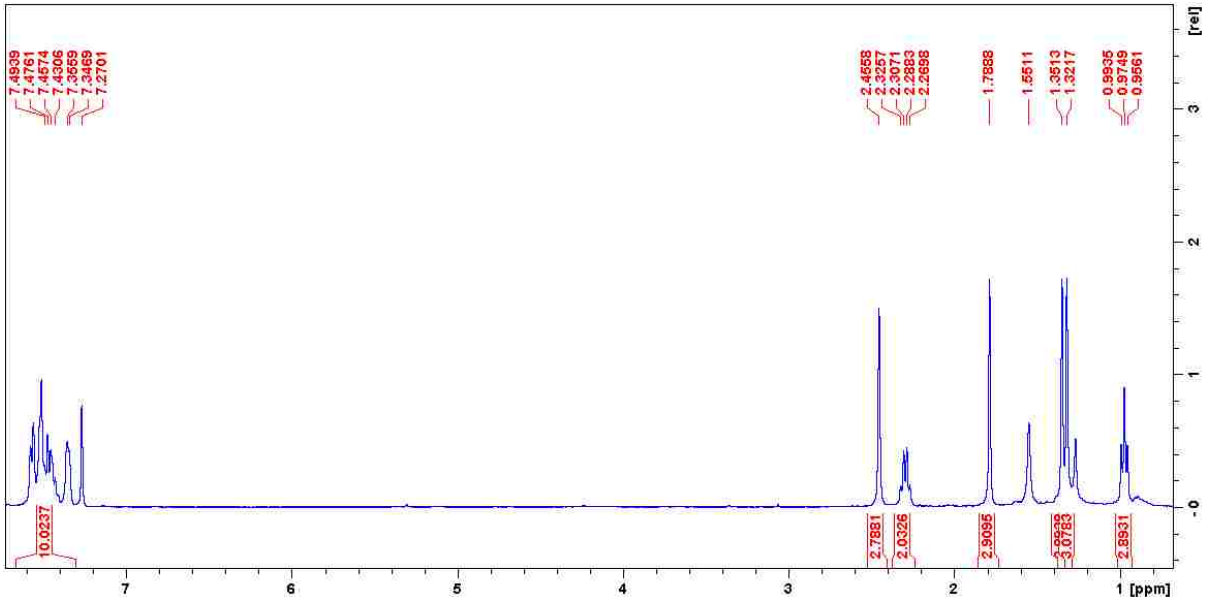

Figure A18: ^{13}C NMR spectra of BODIPY **12c**

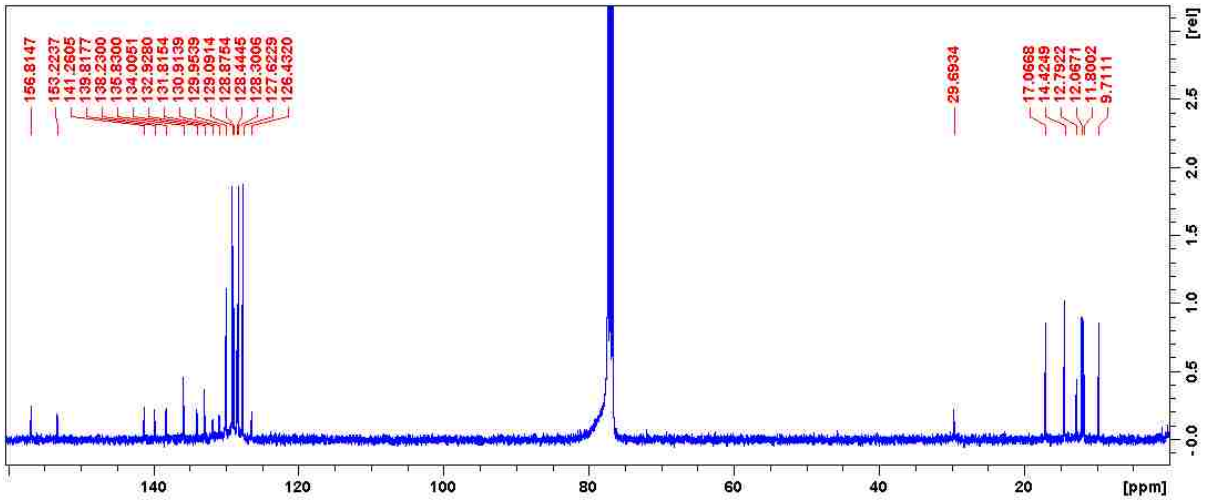

Figure A19: ^{1}H NMR spectra of BODIPY **13a**

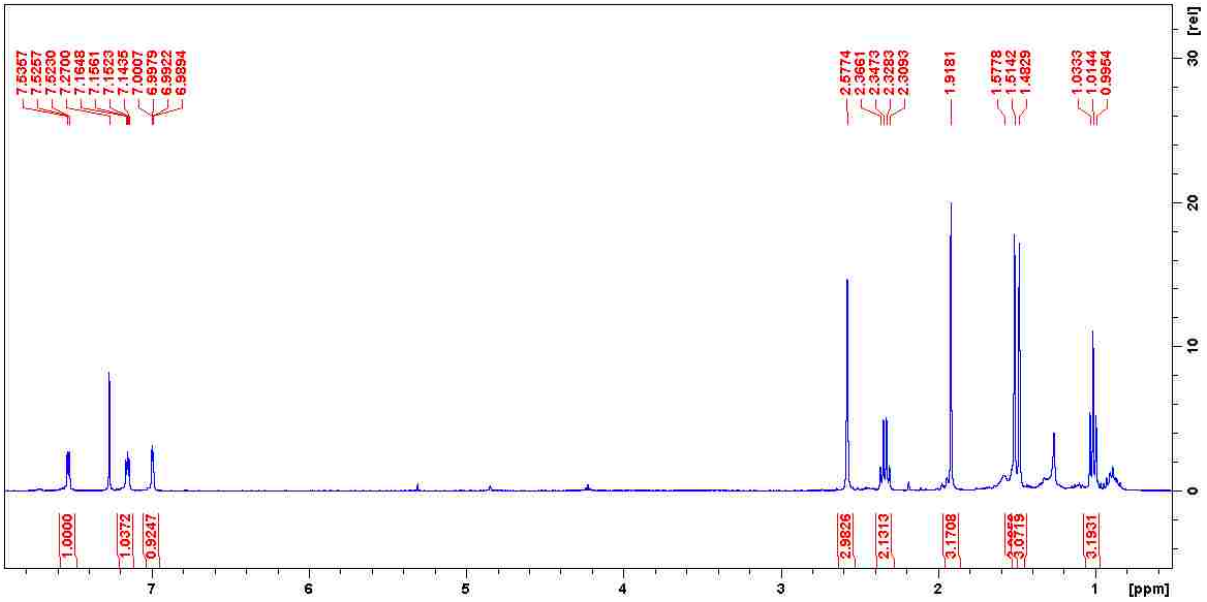

Figure A20: ^{13}C NMR spectra of BODIPY **13a**

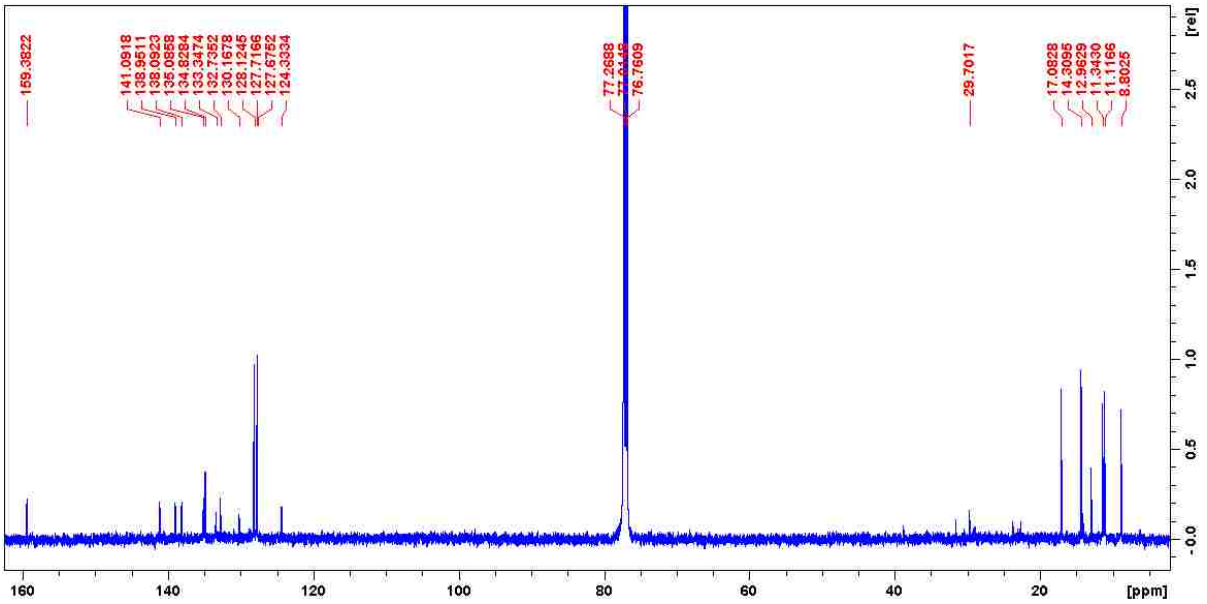

Figure A21: ^{1}H NMR spectra of BODIPY **13b**

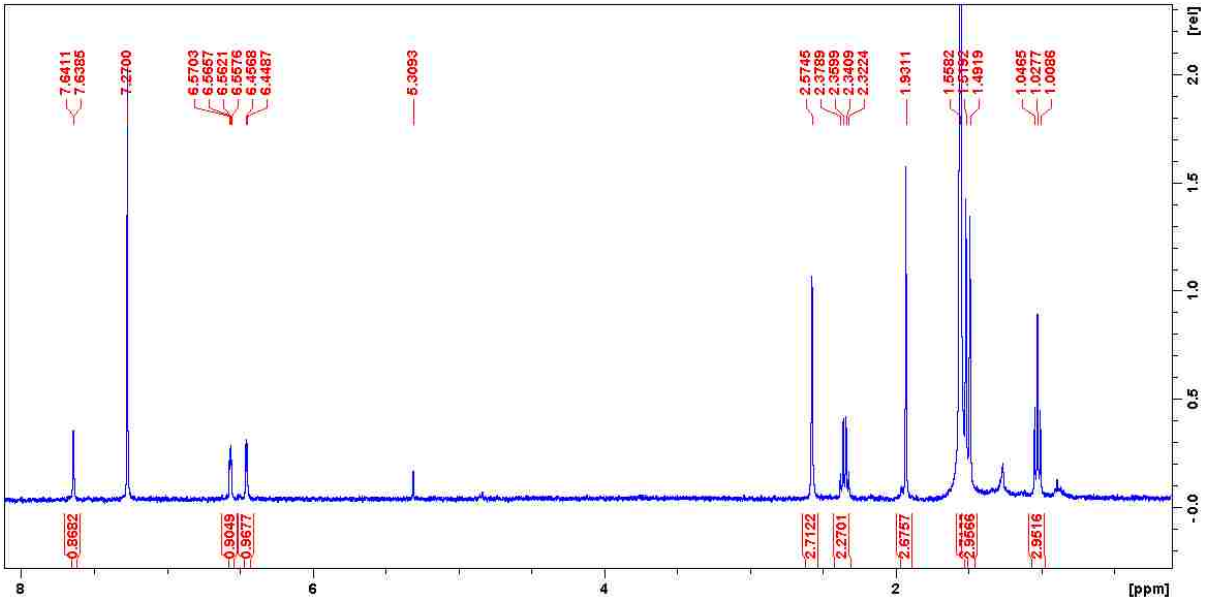

Figure A22: ^{13}C NMR spectra of BODIPY **13b**

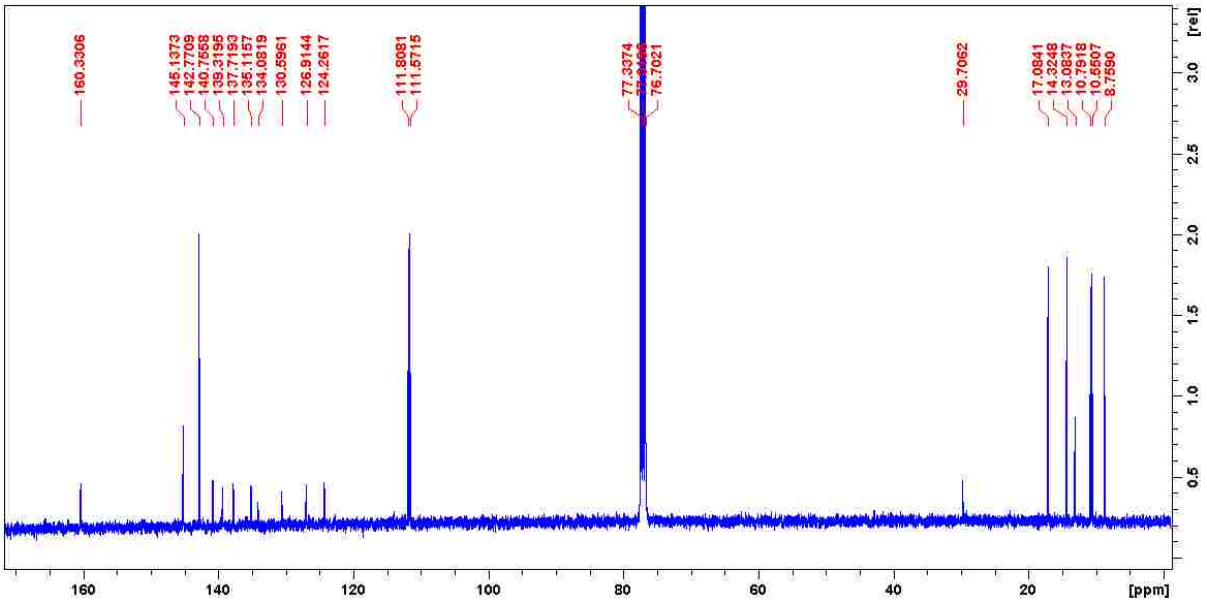

Figure A23: ^{1}H NMR spectra of BODIPY **13c**

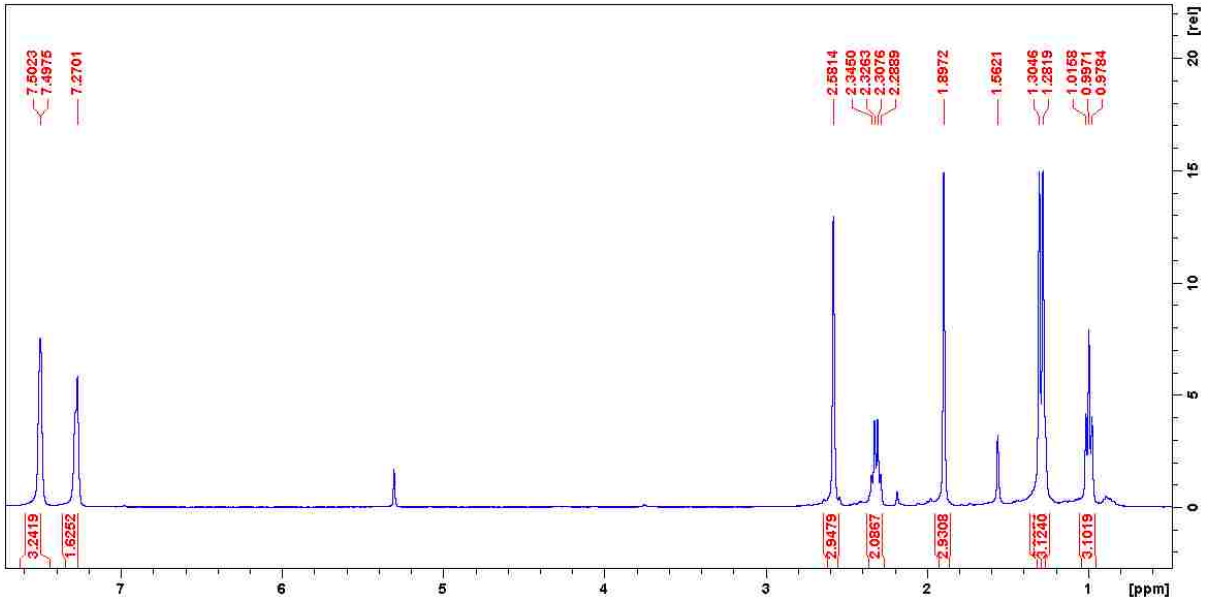

Figure A24: ^{13}C NMR spectra of BODIPY **13c**

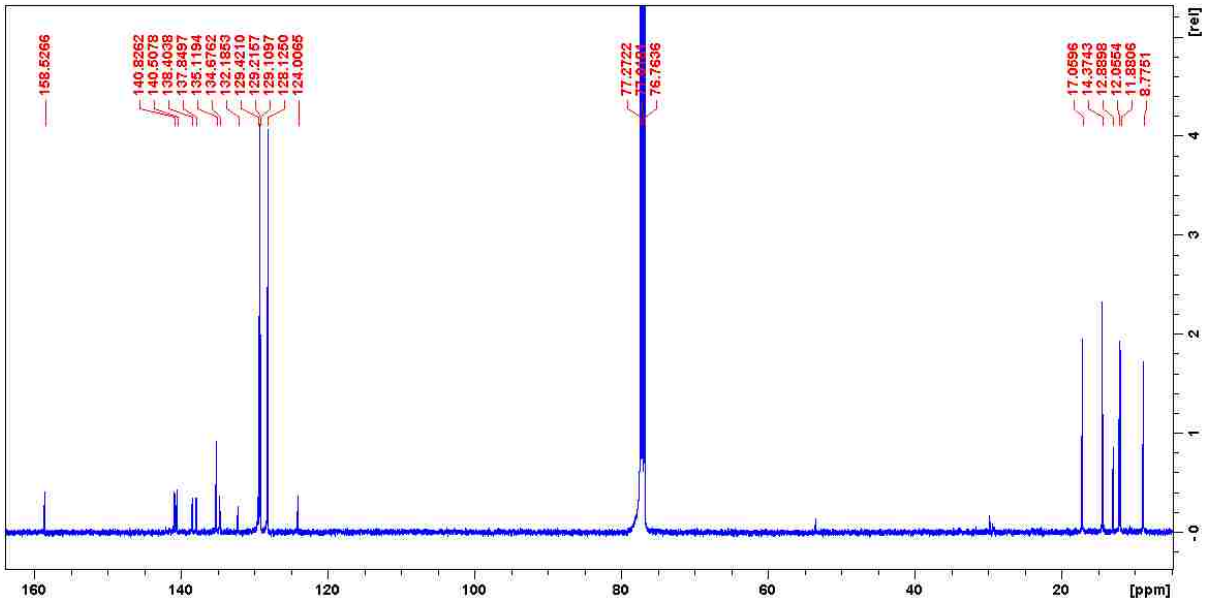

Figure A25: ^{1}H NMR spectra of BODIPY **14**

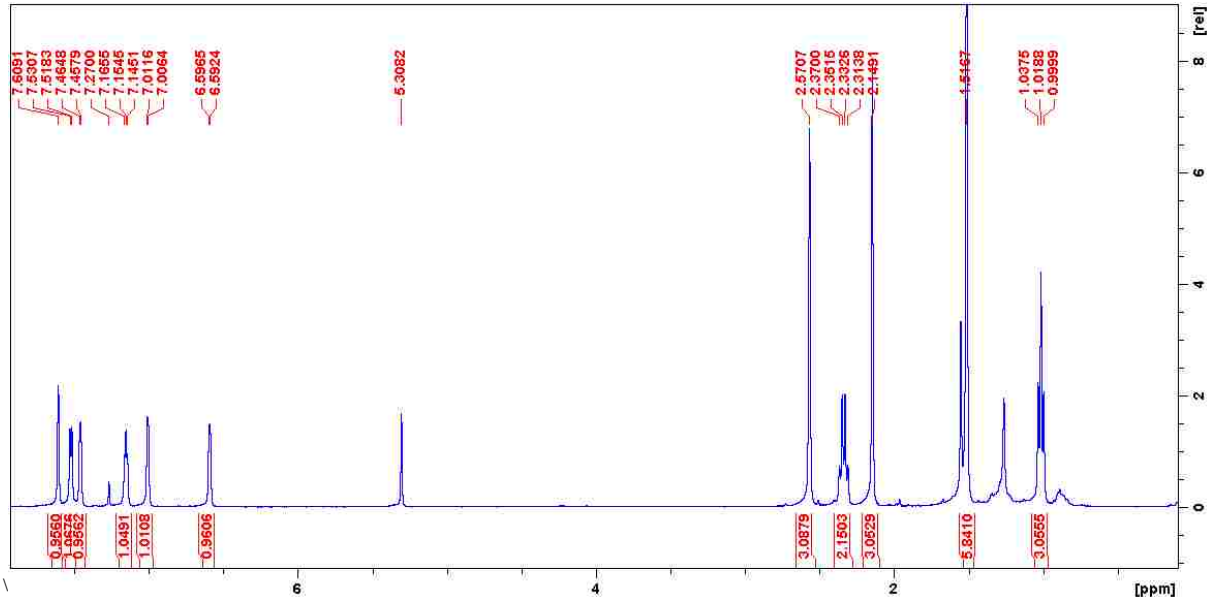

Figure A26: ^{13}C NMR spectra of BODIPY **14**

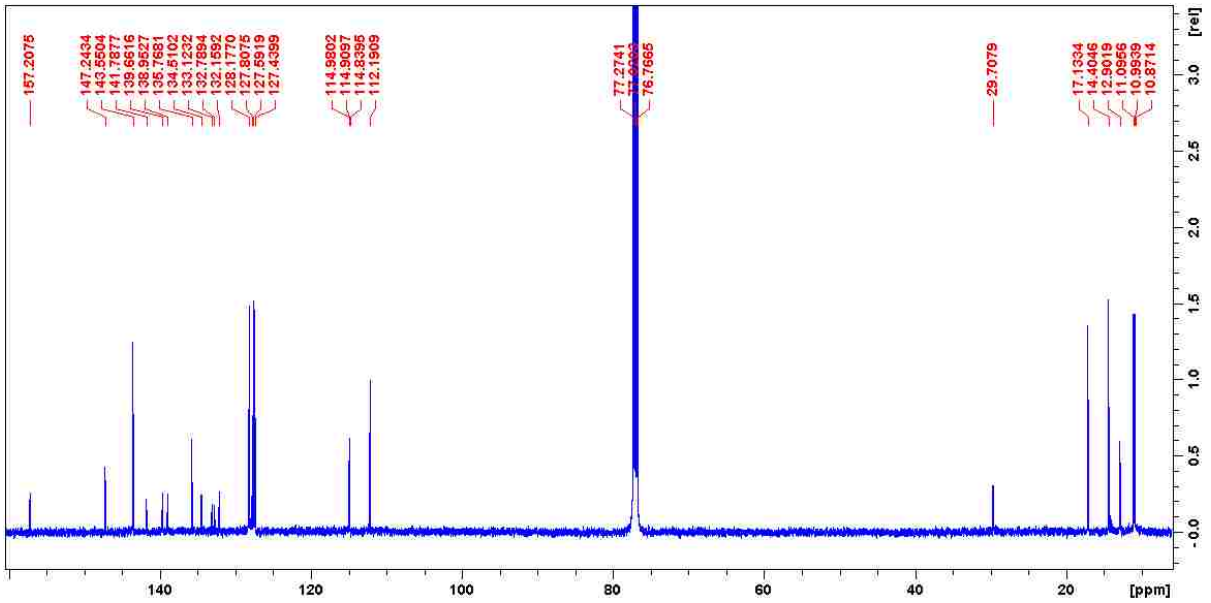

Figure A27: ^{1}H NMR spectra of BODIPY **15**

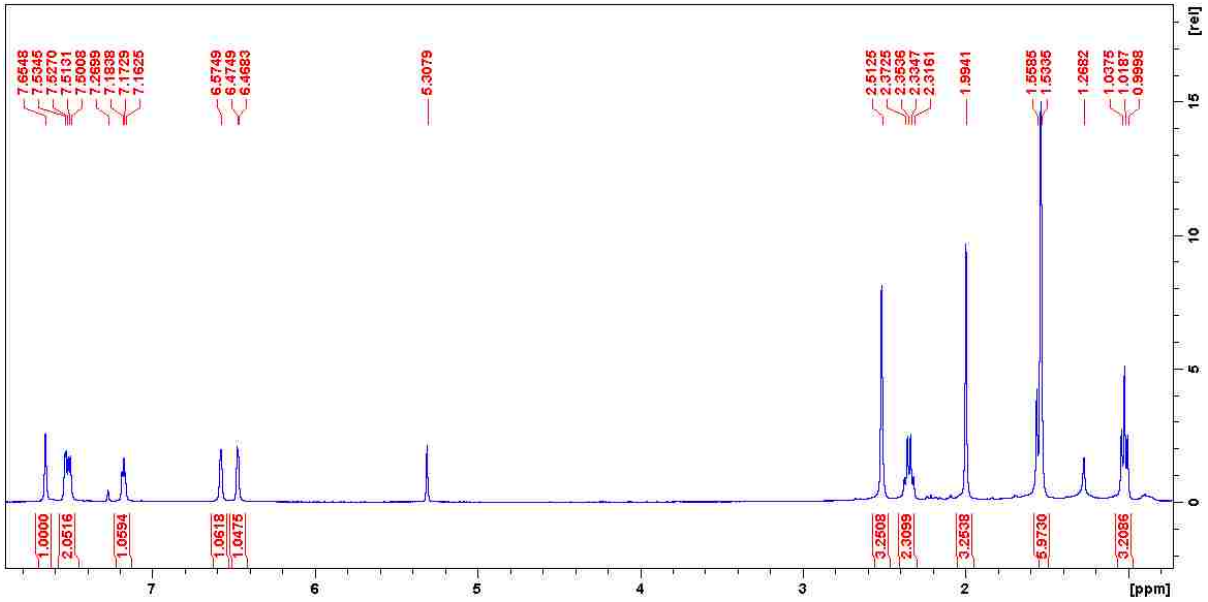

Figure A28: ^{13}C NMR spectra of BODIPY **15**

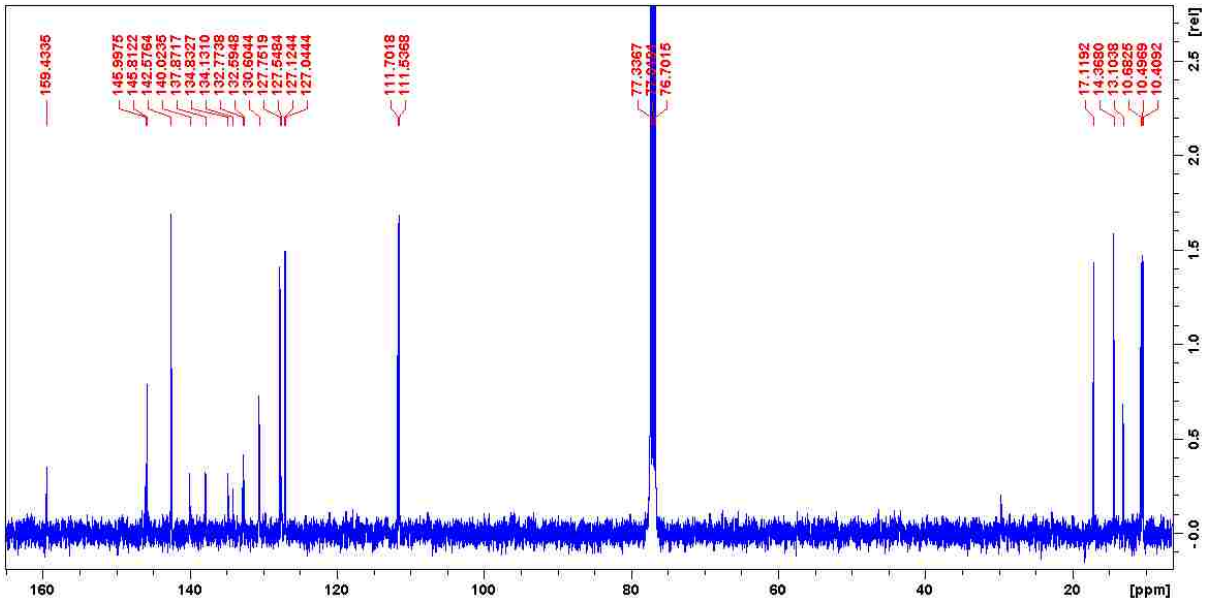

Figure A29: ^{1}H NMR spectra of BODIPY **16**

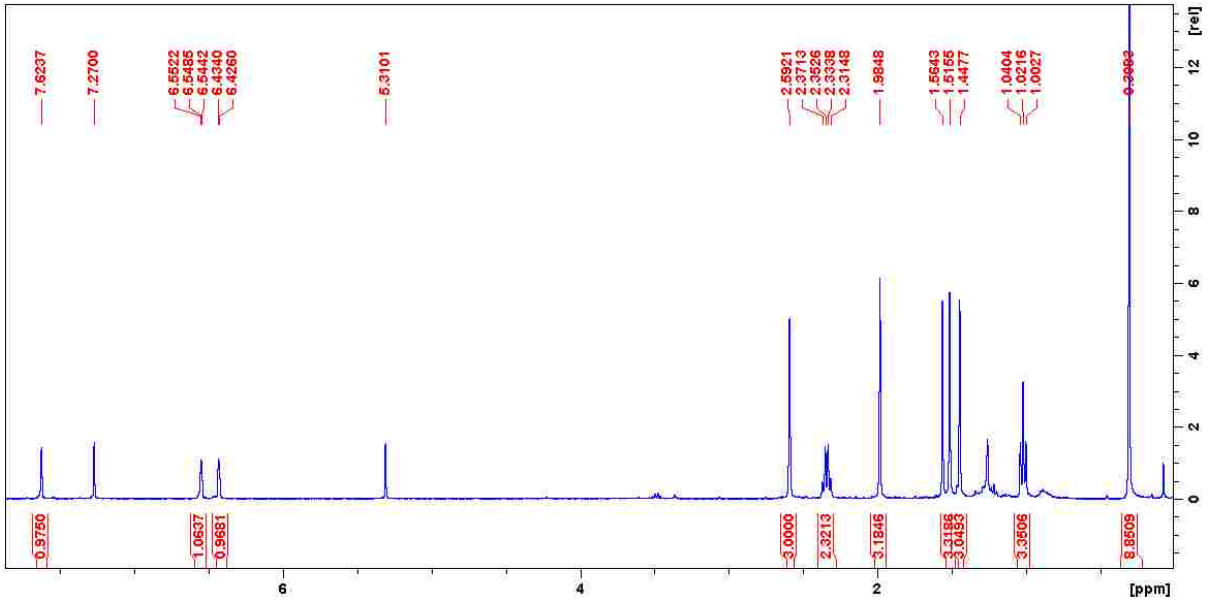

Figure A30: ^{13}C NMR spectra of BODIPY **16**

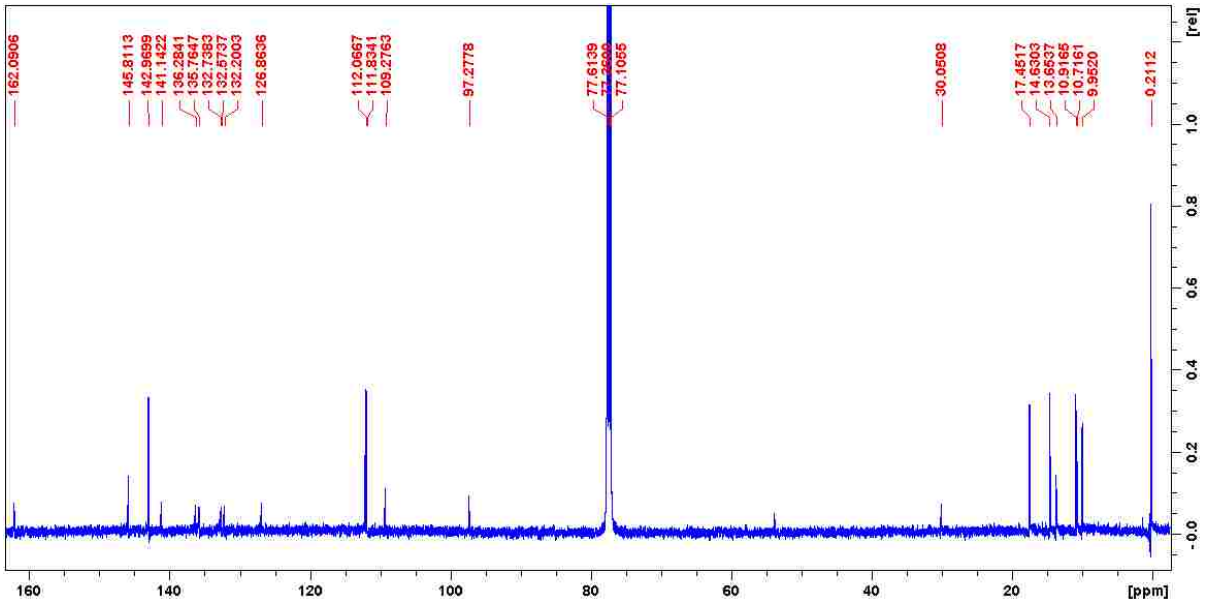

Figure A31: ^{1}H NMR spectra of BODIPY **17**

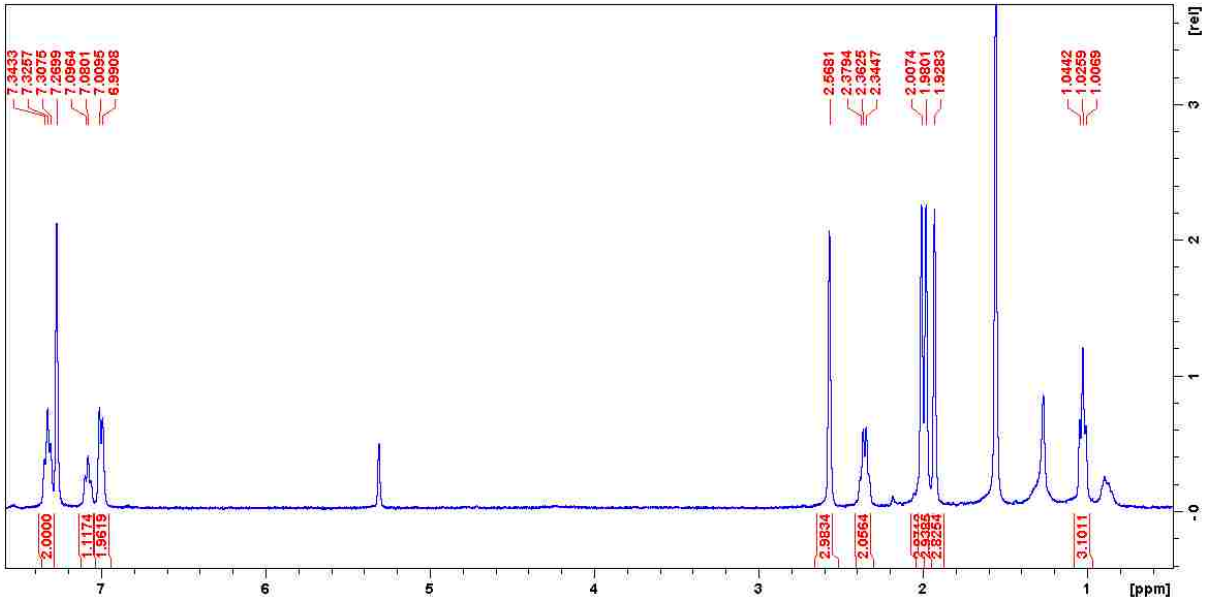

Figure A32: ^{13}C NMR spectra of BODIPY **17**

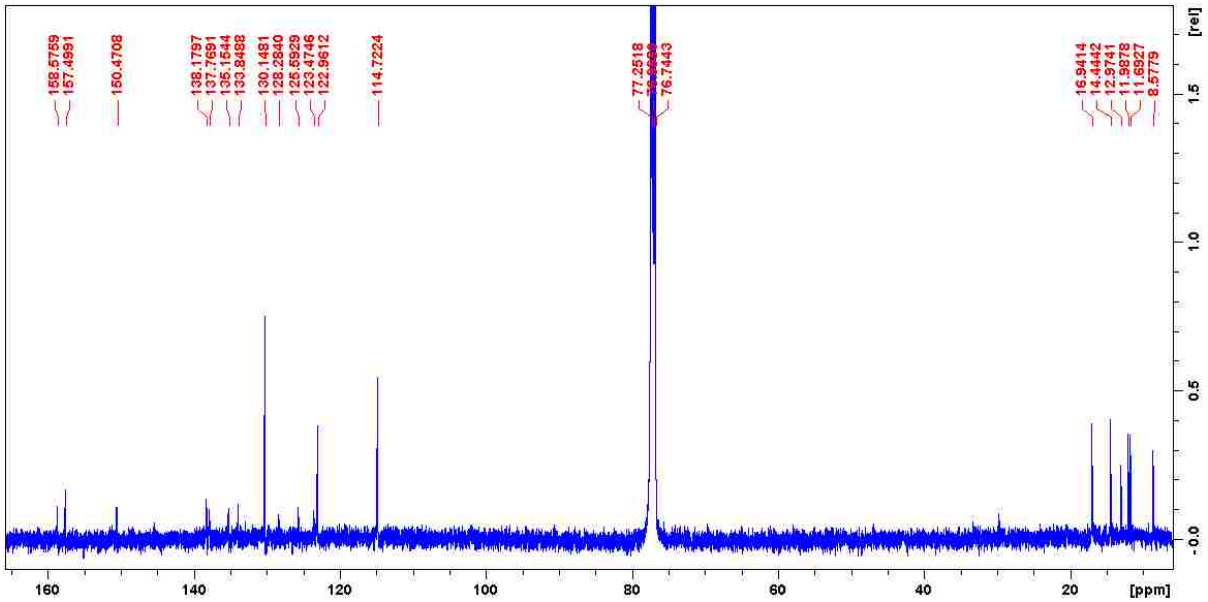

Figure A33: ^{1}H NMR of BODIPY **18**

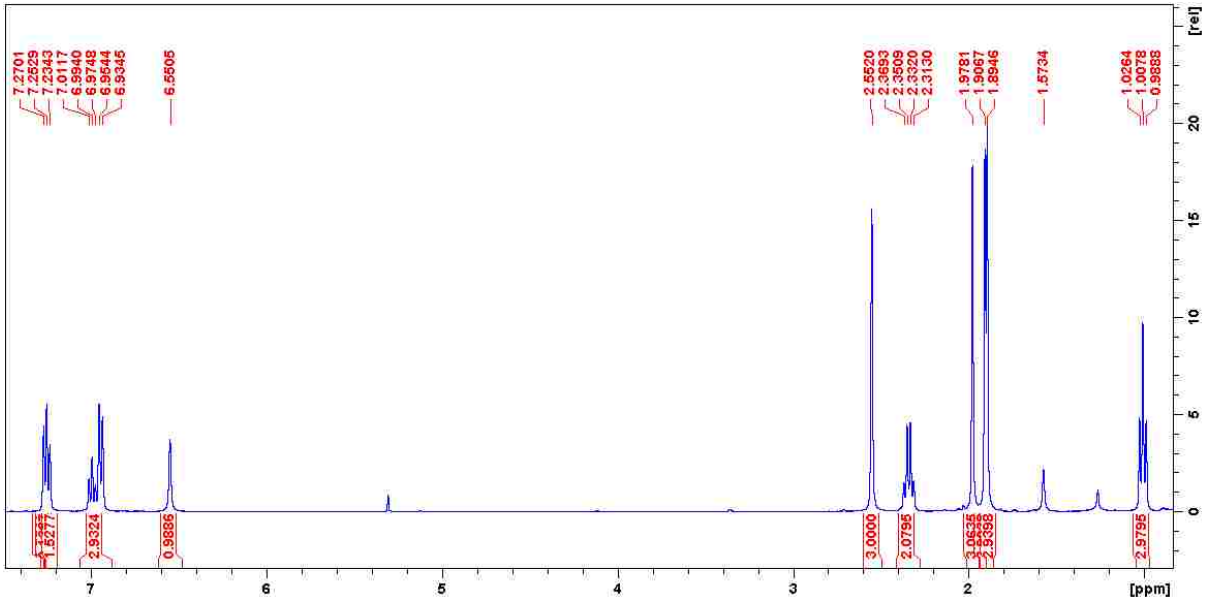

Figure A34: ^{13}C NMR of BODIPY **18**

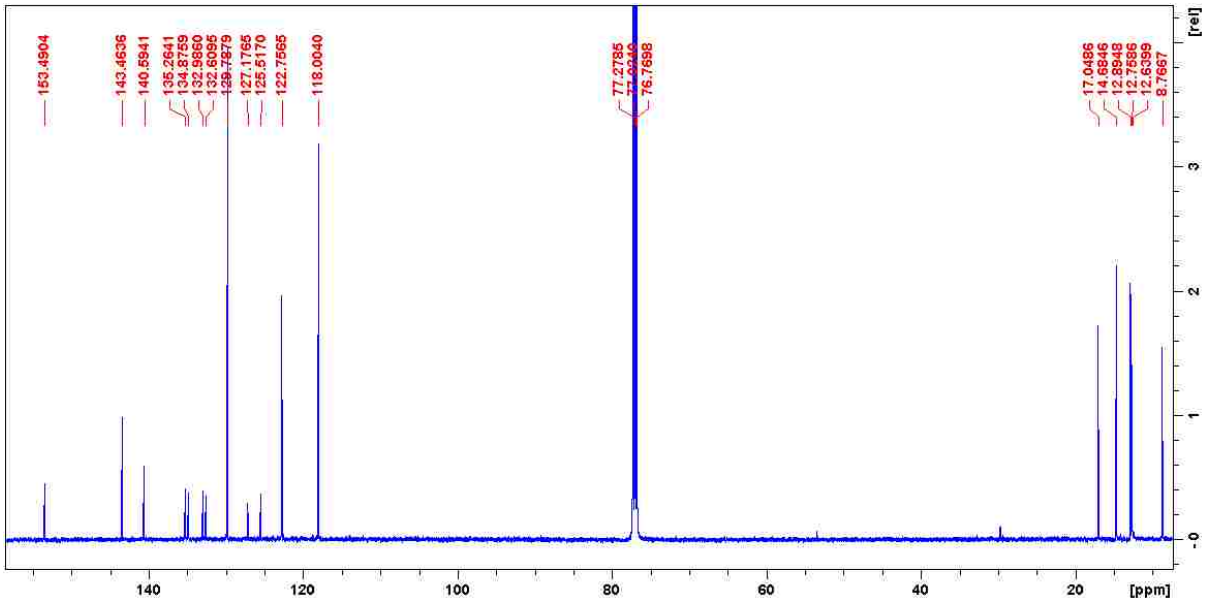

Figure A35: ^{1}H NMR spectra of BODIPY **19**

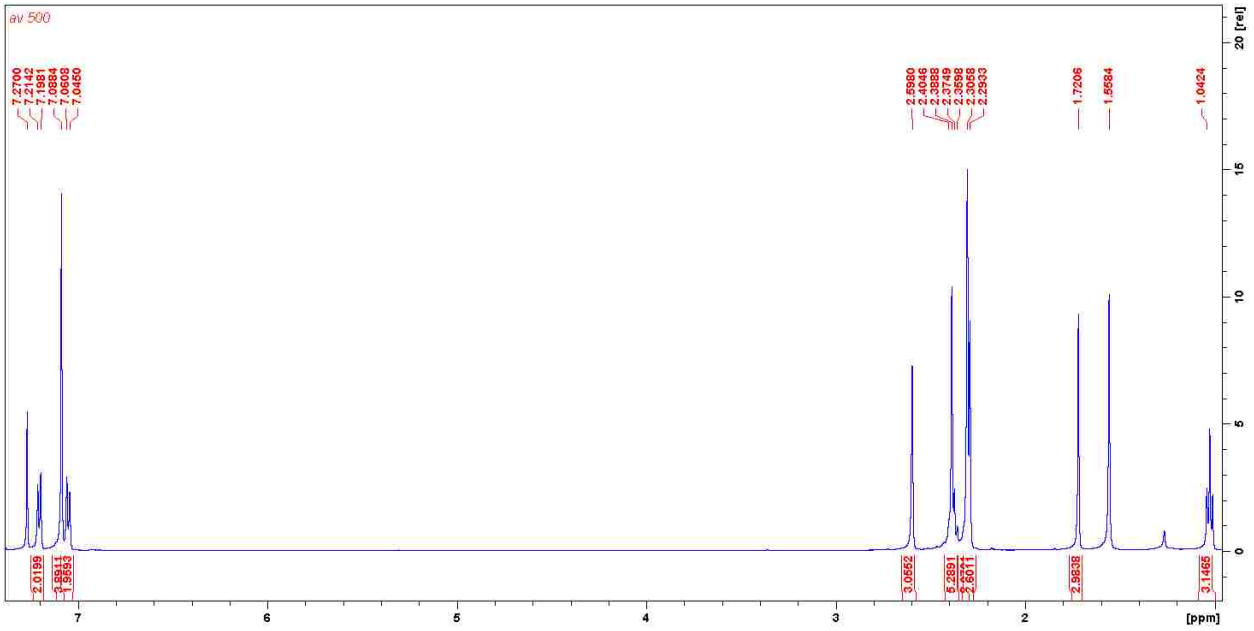

Figure A36: ^{13}C NMR spectra of BODIPY **19**

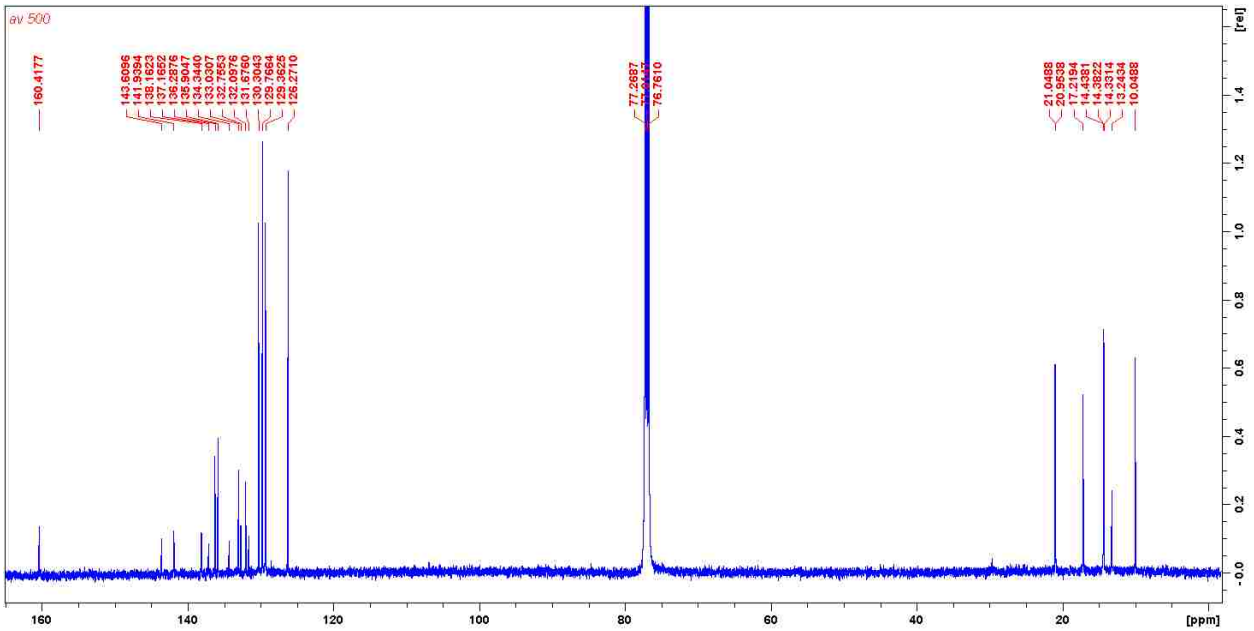

Figure A37: ^{1}H NMR spectra of BODIPY **20**

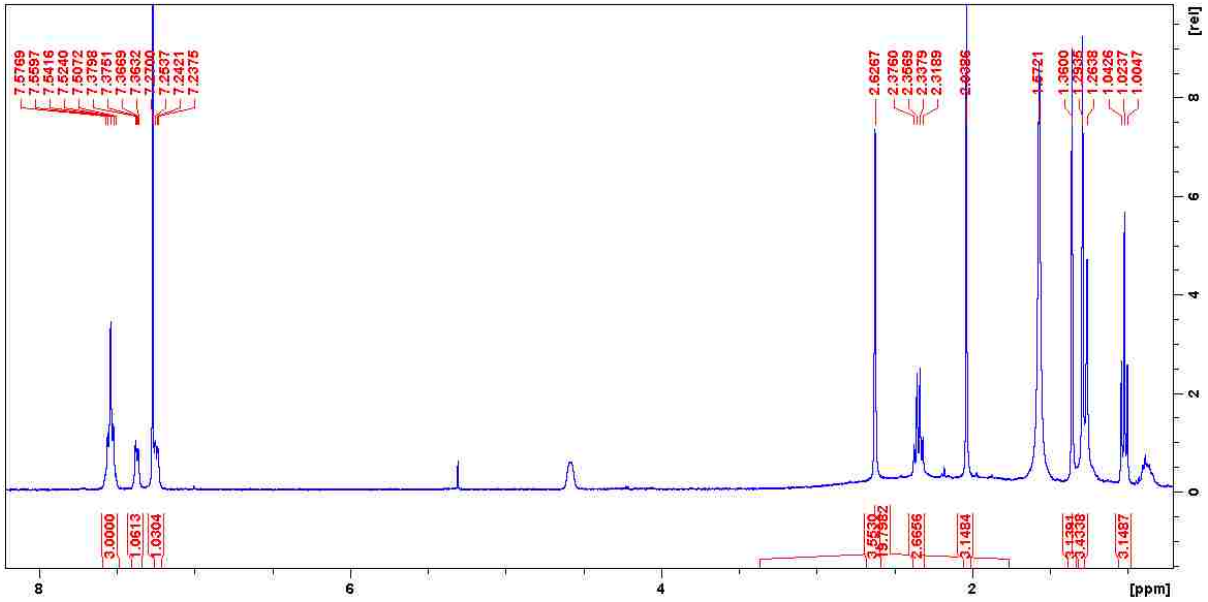

Figure A38: ^{13}C NMR spectra of BODIPY **20**

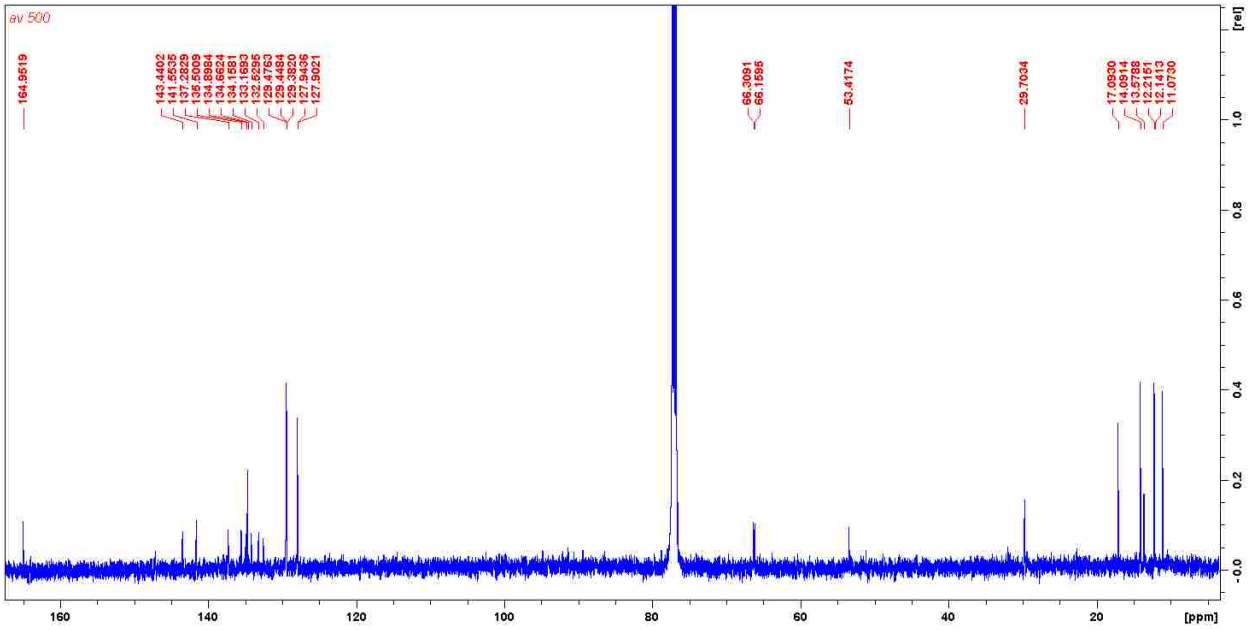

Figure A39: ^{1}H NMR spectra of BODIPY **21**

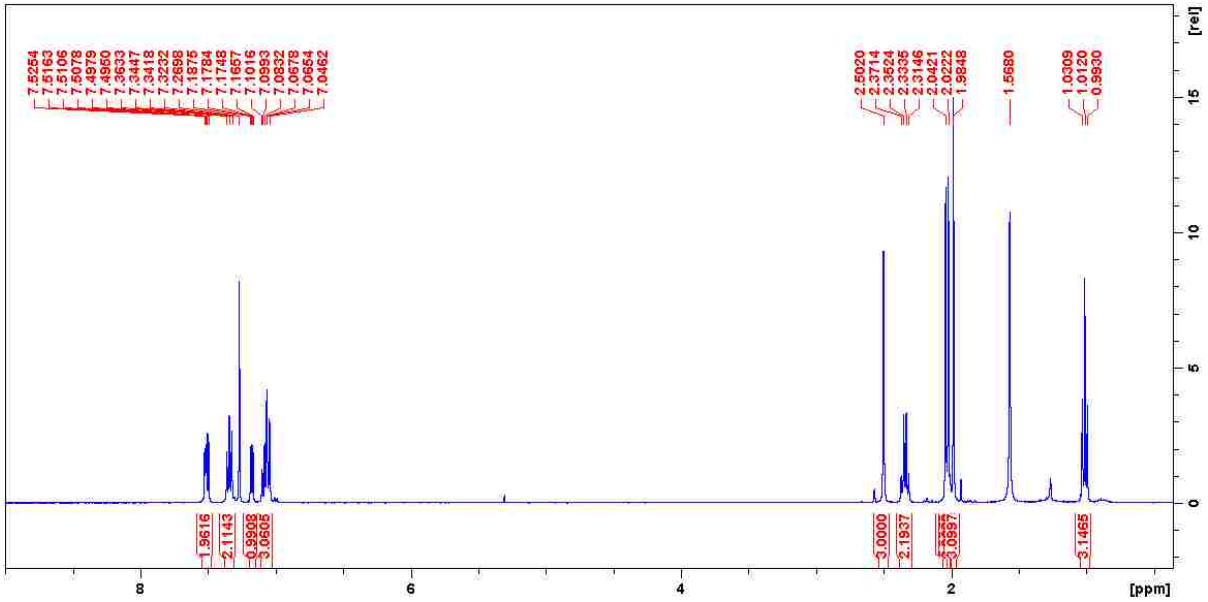

Figure A40: ^{13}C NMR spectra of BODIPY **21**

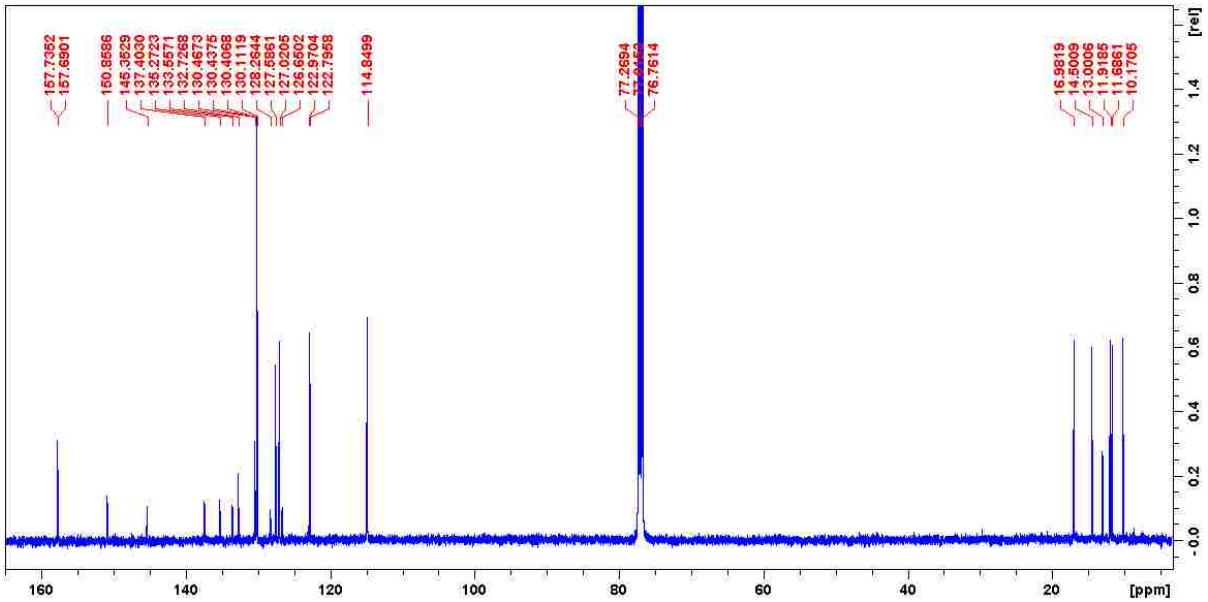

Figure A41: ^{1}H NMR spectra of BODIPY **22**

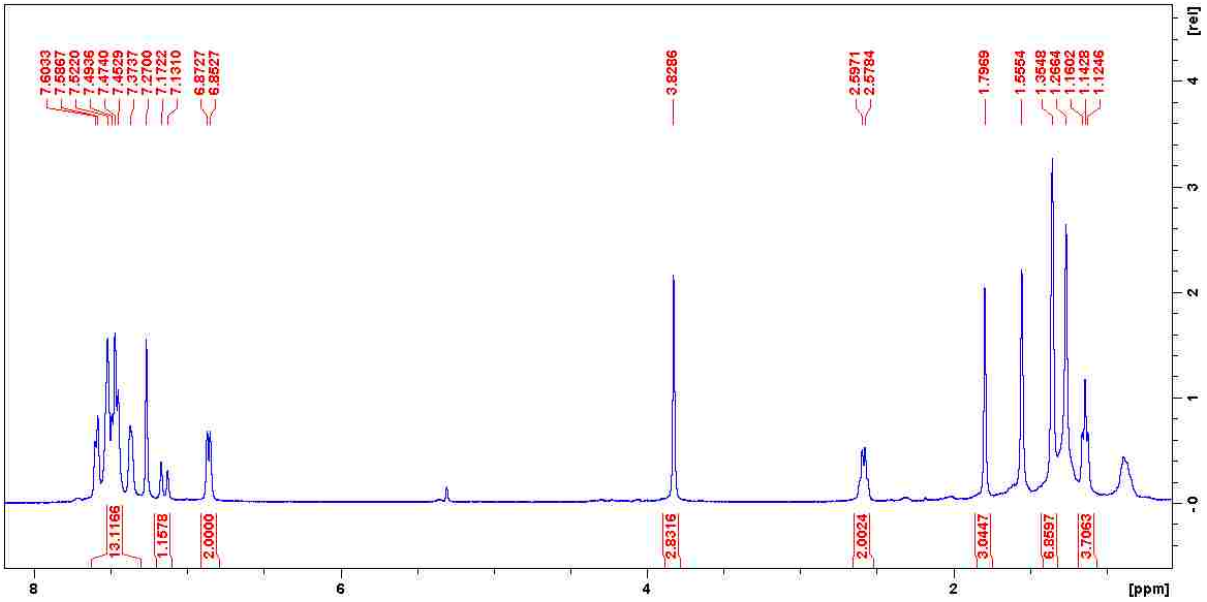

Figure A42: ^{13}C NMR spectra of BODIPY **22**

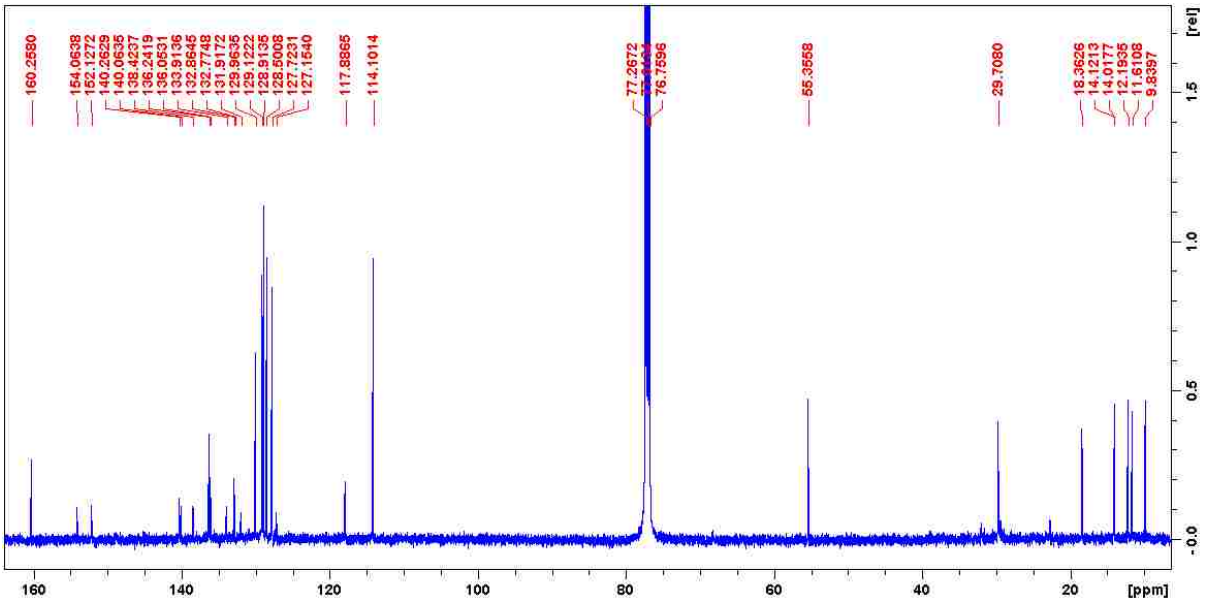

Figure A43: ^{1}H NMR spectra of BODIPY **24**

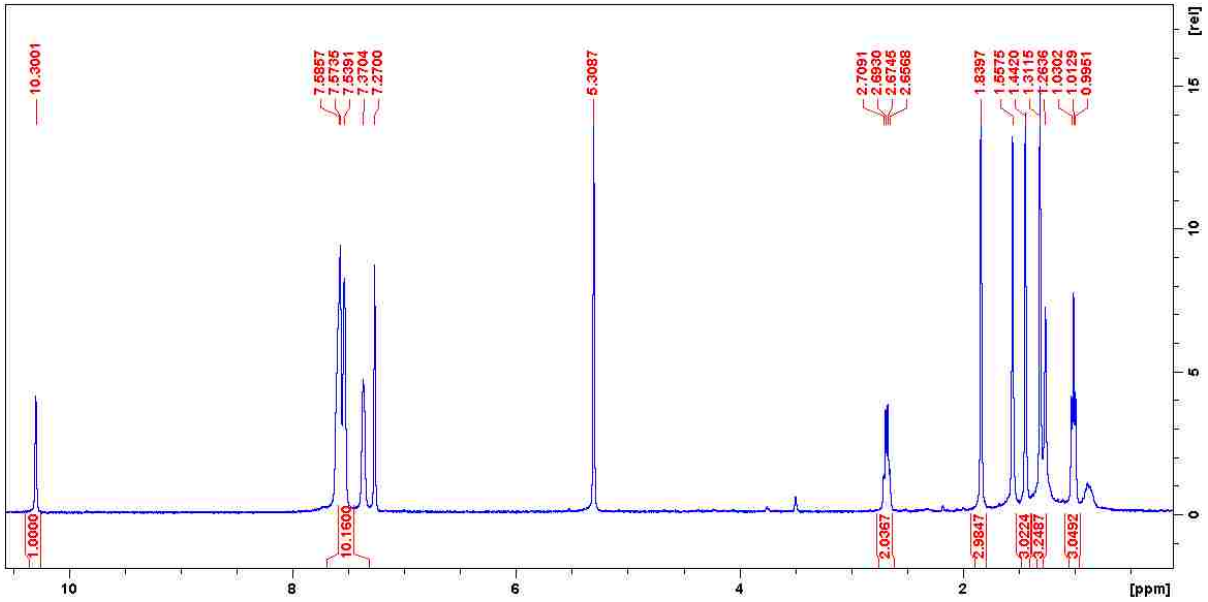

Figure A44: ^{13}C NMR spectra of BODIPY **24**

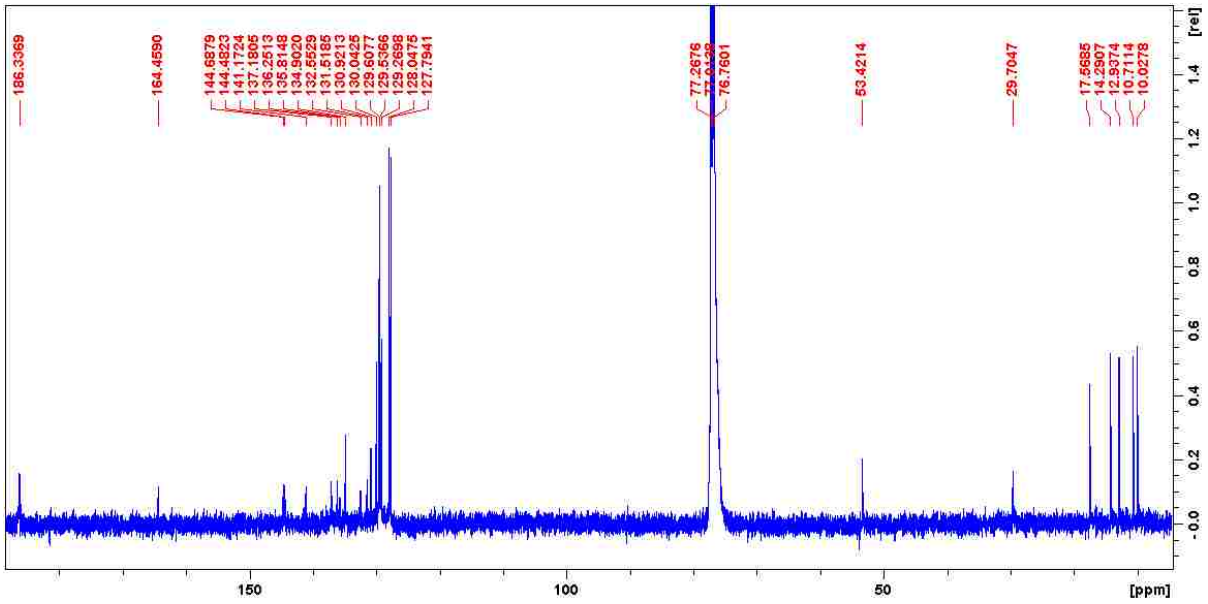

APPENDIX B: CHARACTERIZATION DATA FOR COMPOUNDS IN CHAPTER 3

Figure B1: ^{1}H NMR of BODIPY **14**

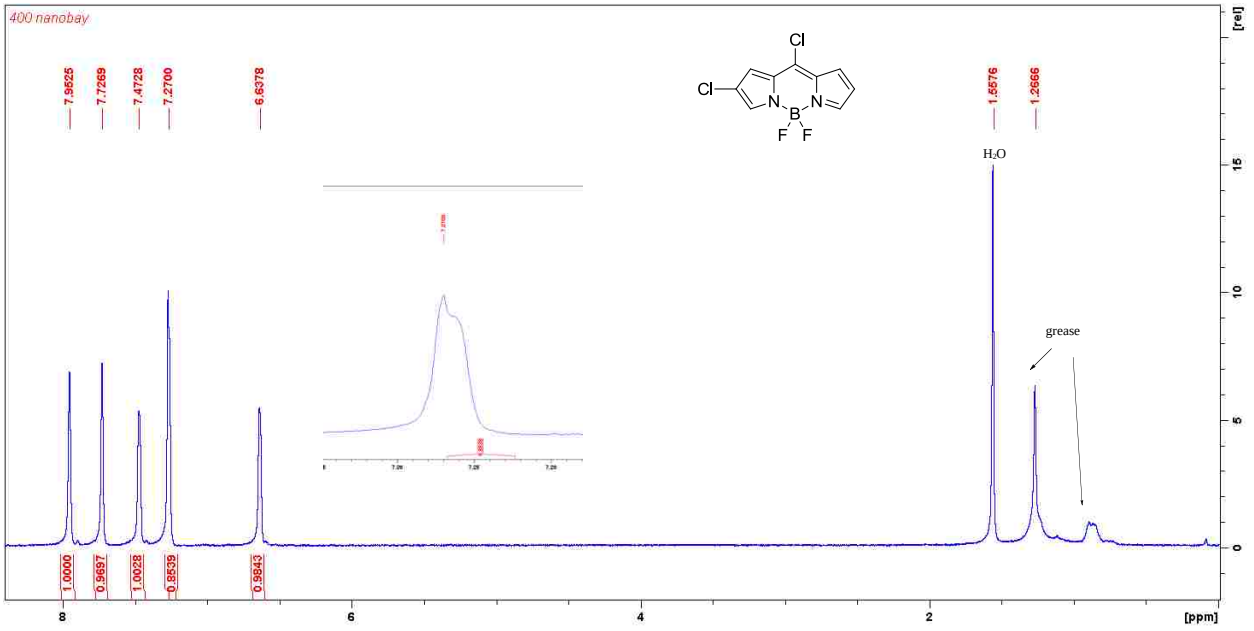

Figure B2: ^{13}C NMR of BODIPY **14**

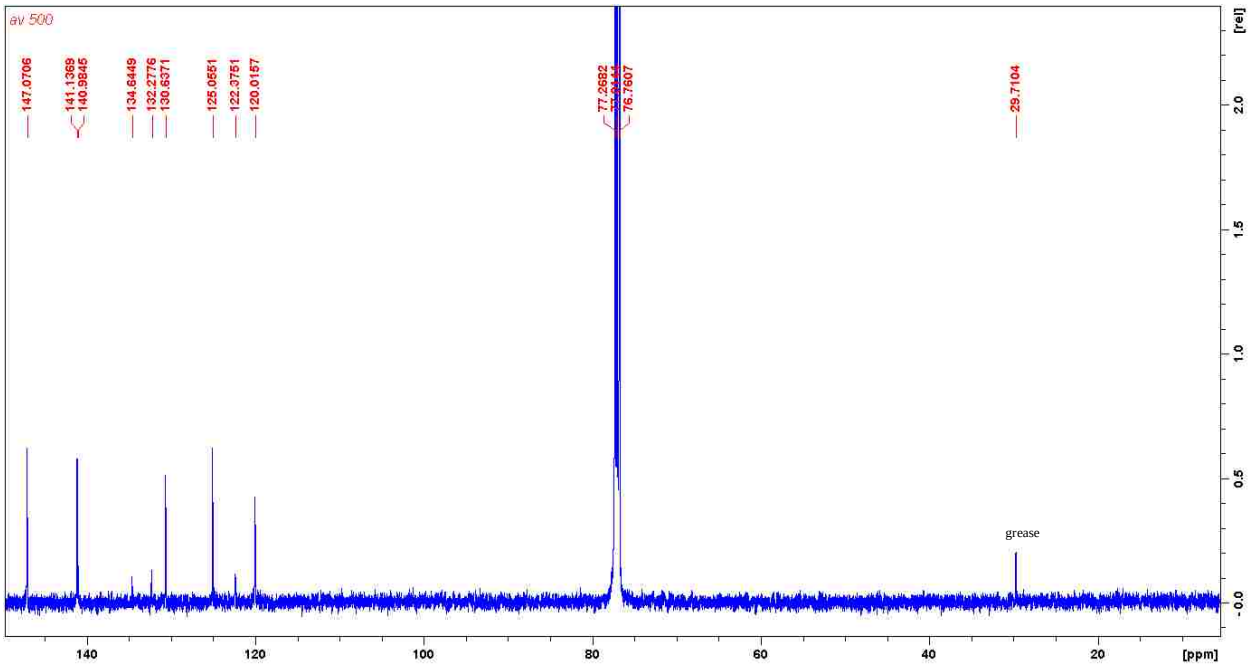

Figure B3: ^{1}H NMR of BODIPY **15**

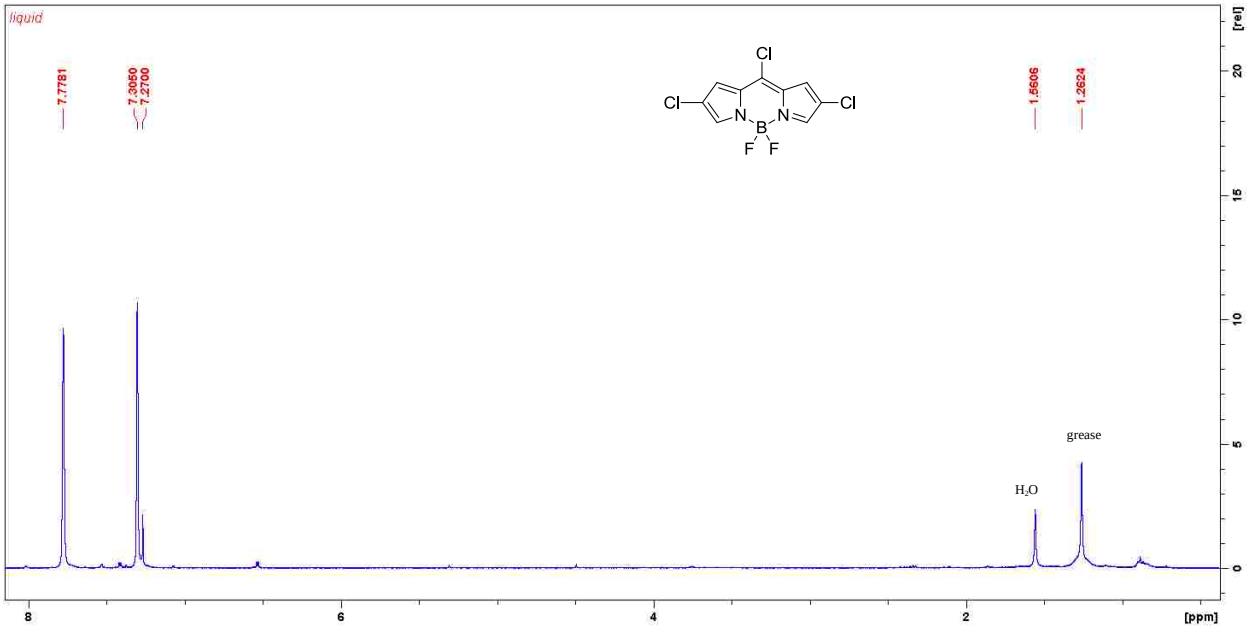

Figure B4: ^{13}C NMR of BODIPY **15**

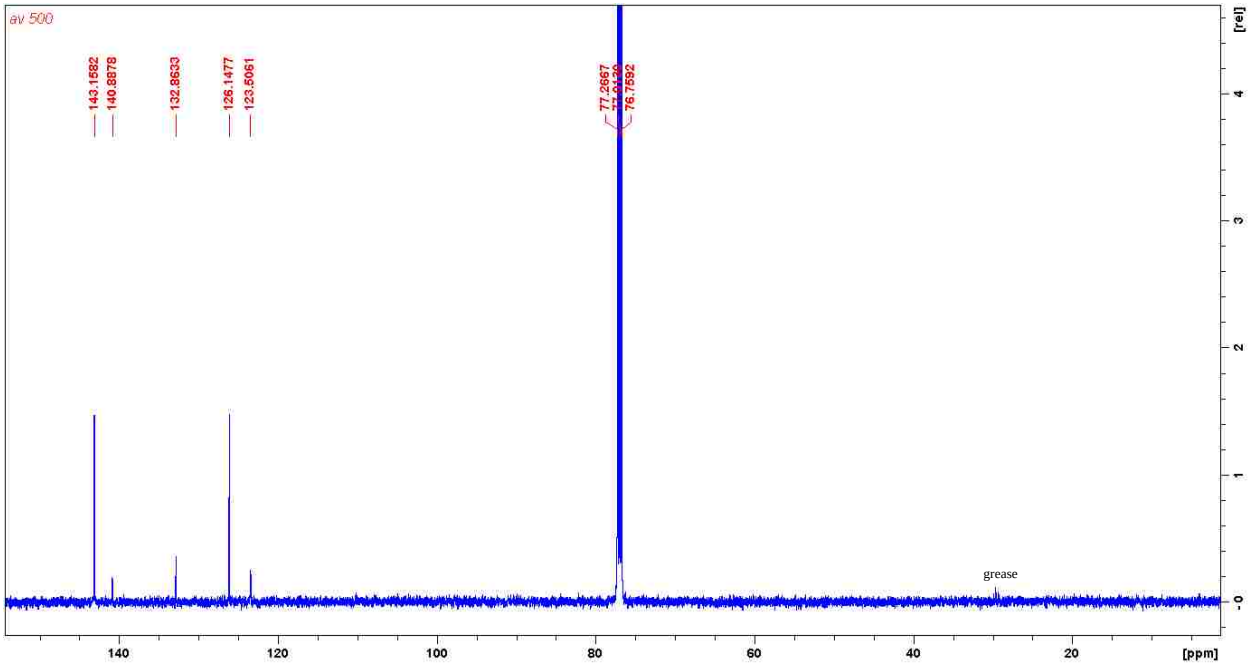

Figure B5: ^{1}H NMR of BODIPY **16**

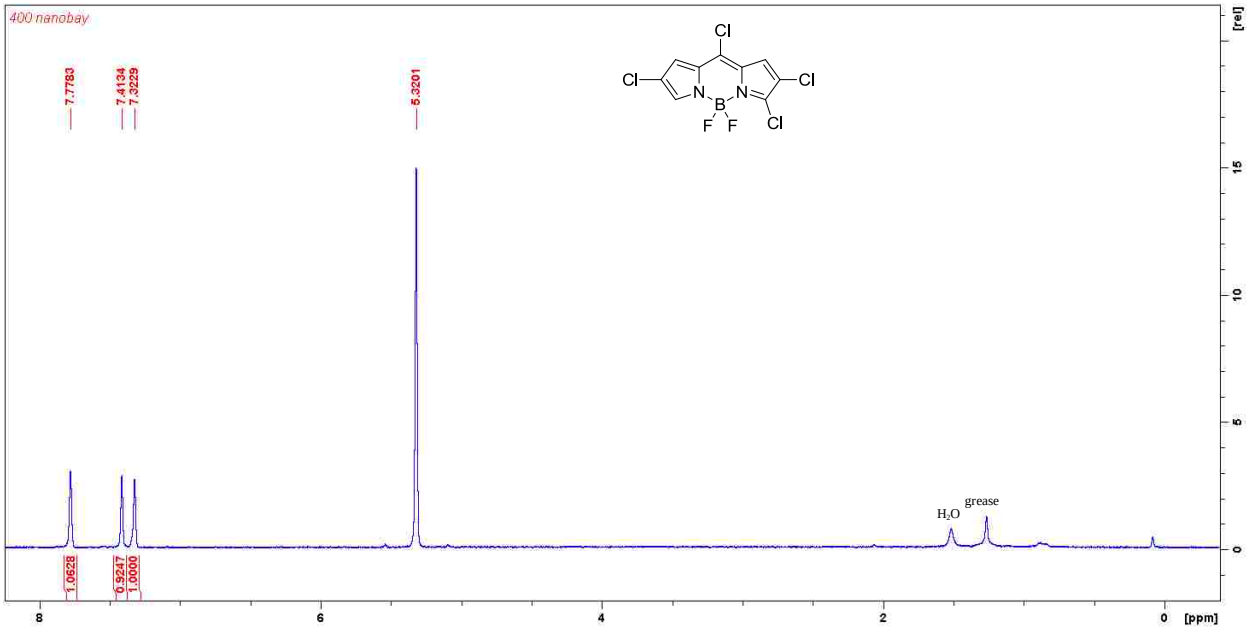

Figure B6: ^{13}C NMR of BODIPY **16**

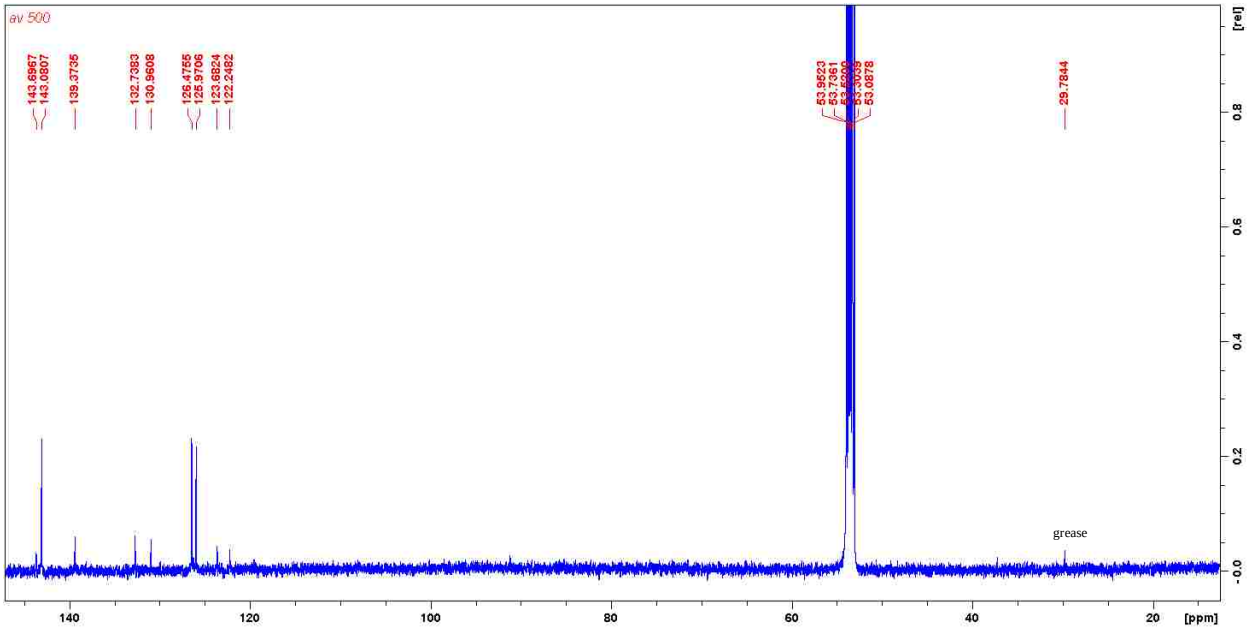

Figure B7: ^{1}H NMR of BODIPY **13**

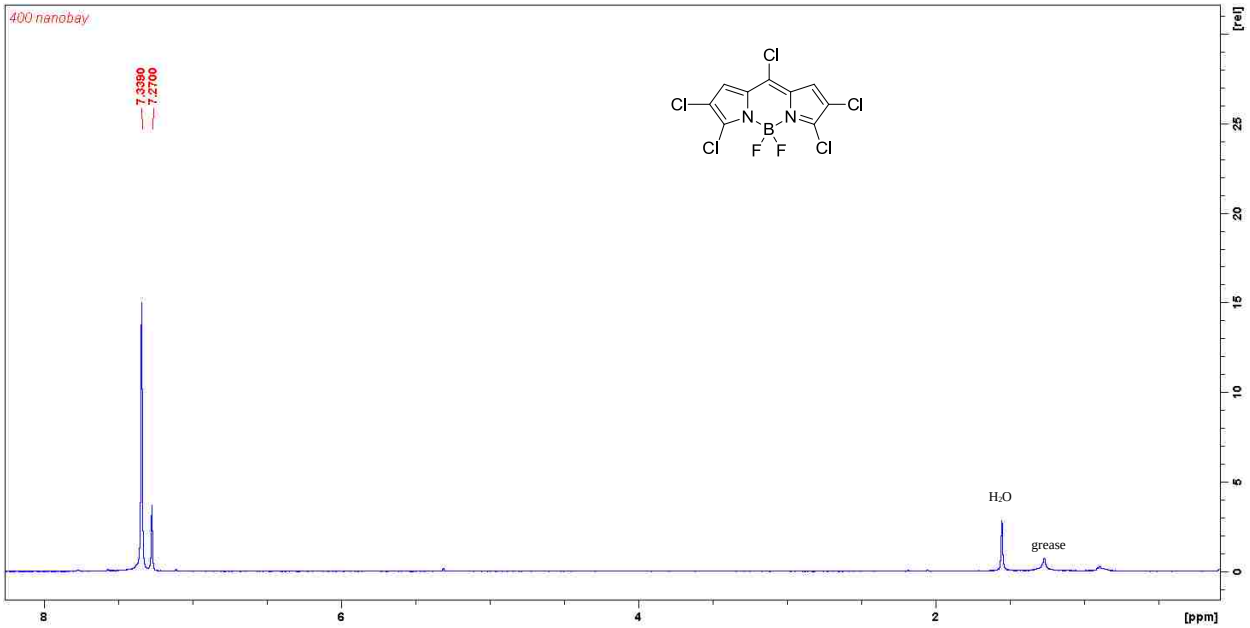

Figure B8: ^{13}C NMR of BODIPY **13**

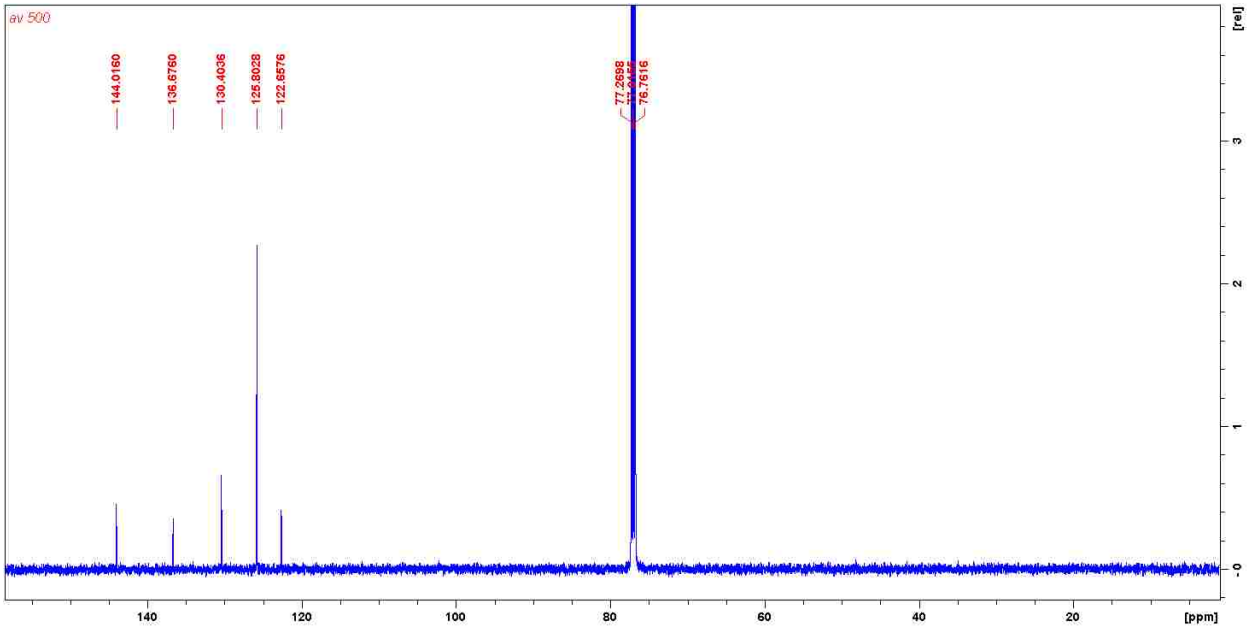

Figure B9: ^{1}H NMR of BODIPY **20**

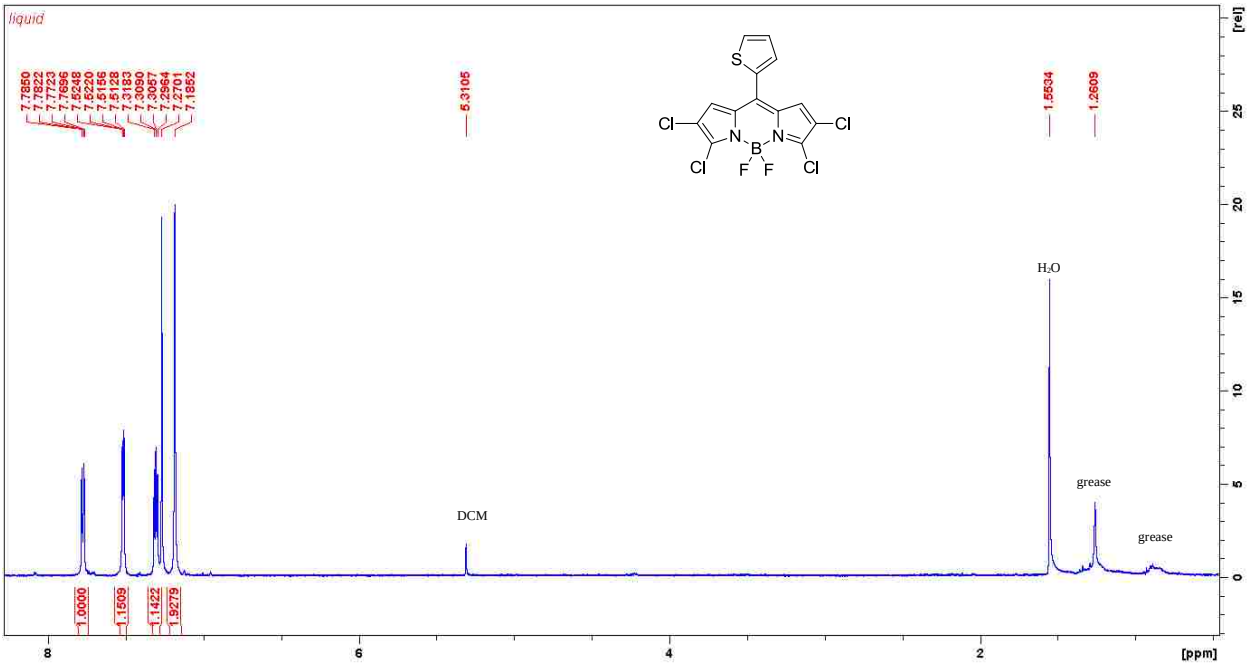

Figure B10: ^{13}C NMR of BODIPY **20**

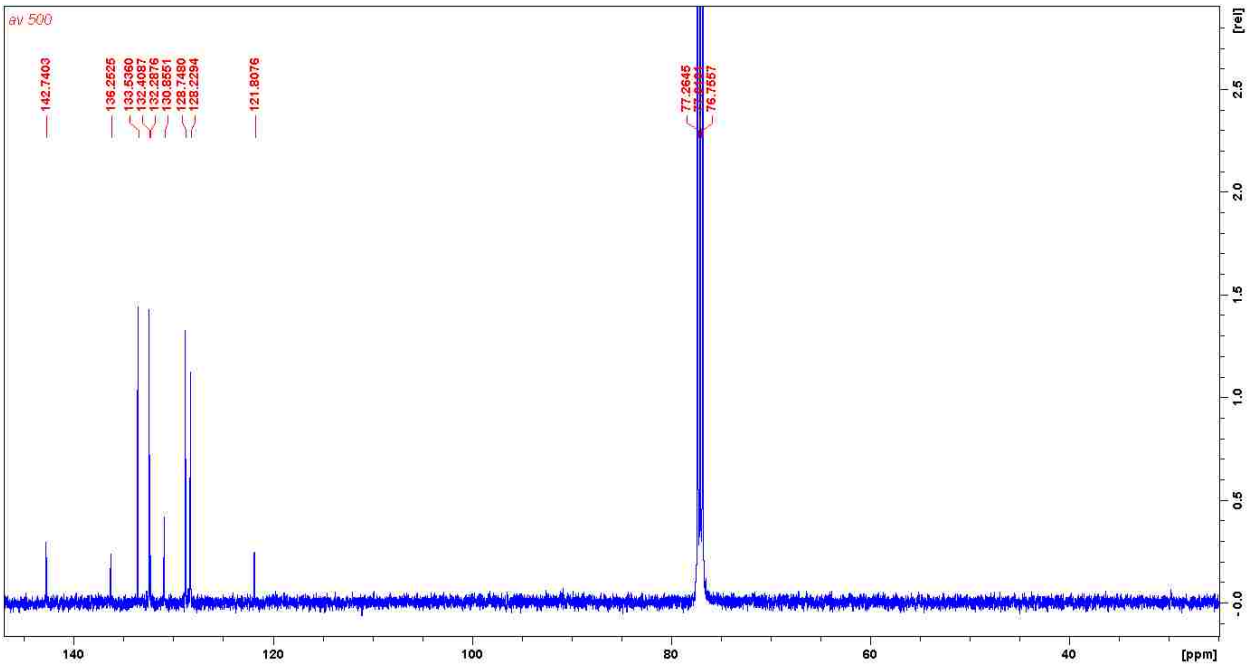

Figure B11: ^{1}H NMR of BODIPY **20**

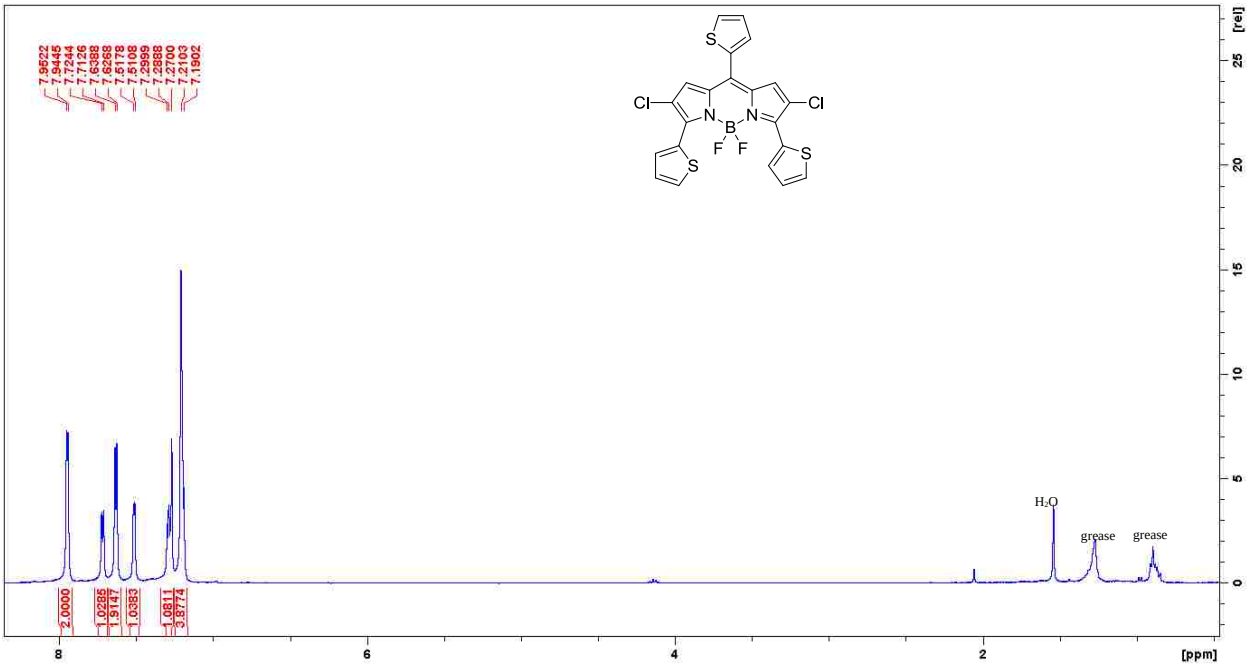

Figure B12: ^{13}C NMR of BODIPY **21**

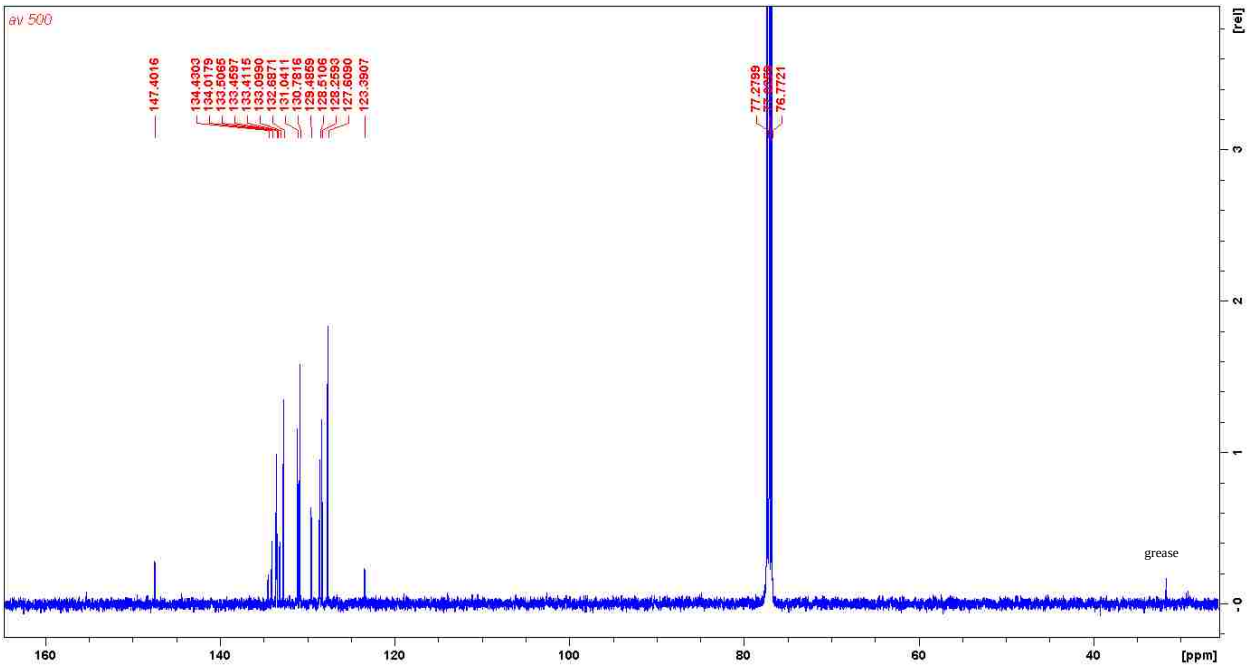

Figure B13: ^{1}H NMR of BODIPY **22**

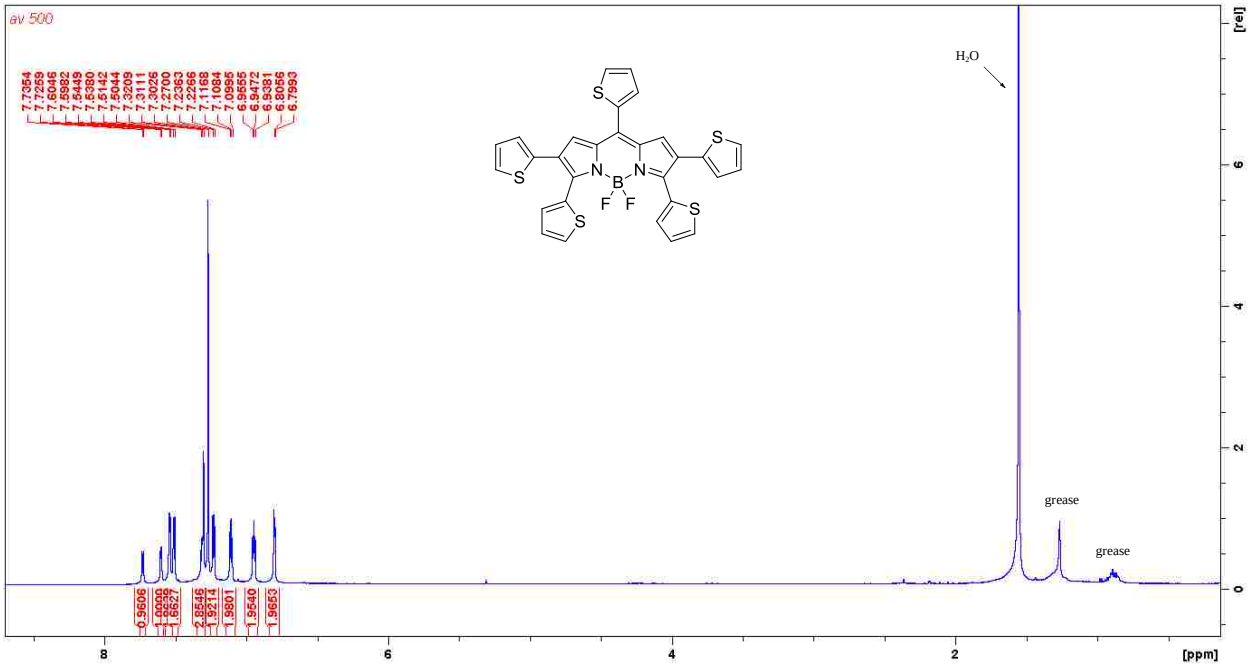

Figure B14: ^{13}C NMR of BODIPY **22**

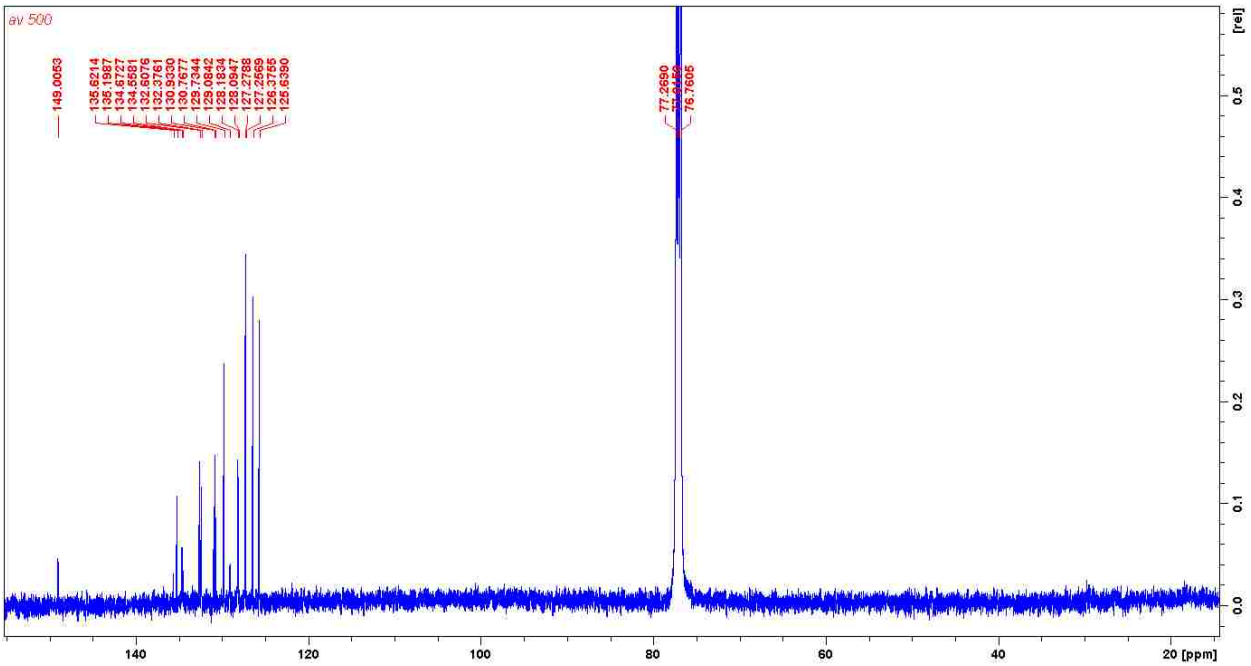

Figure B15: ^{1}H NMR of BODIPY **17**

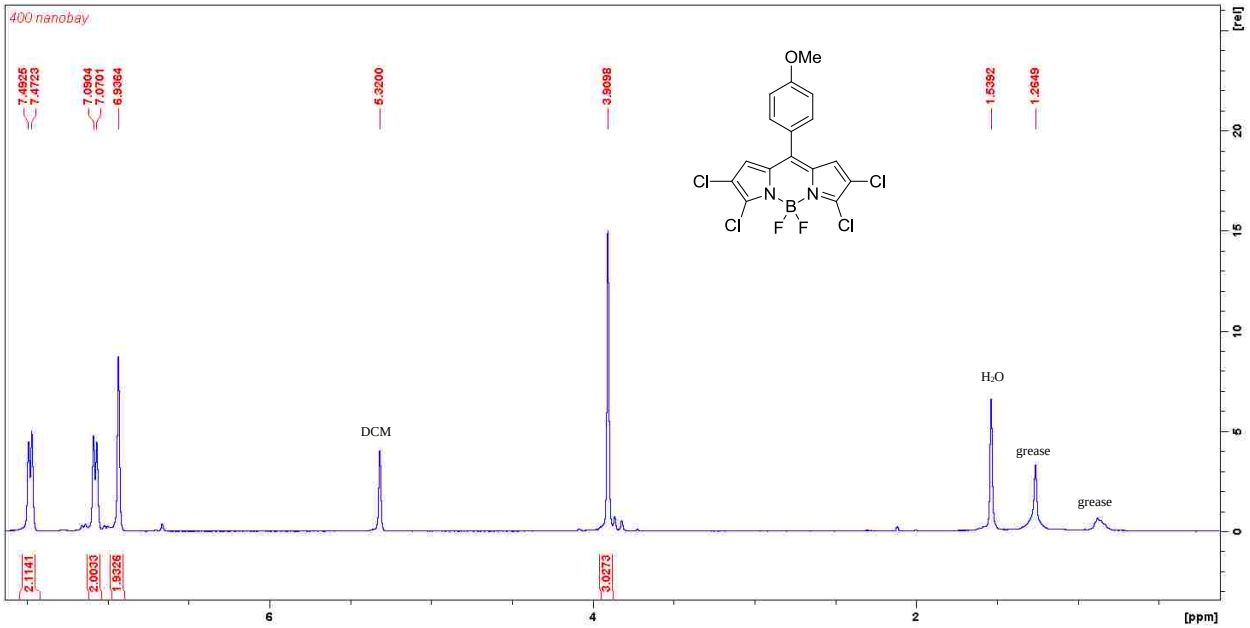

Figure B16: ^{13}C NMR of BODIPY **17**

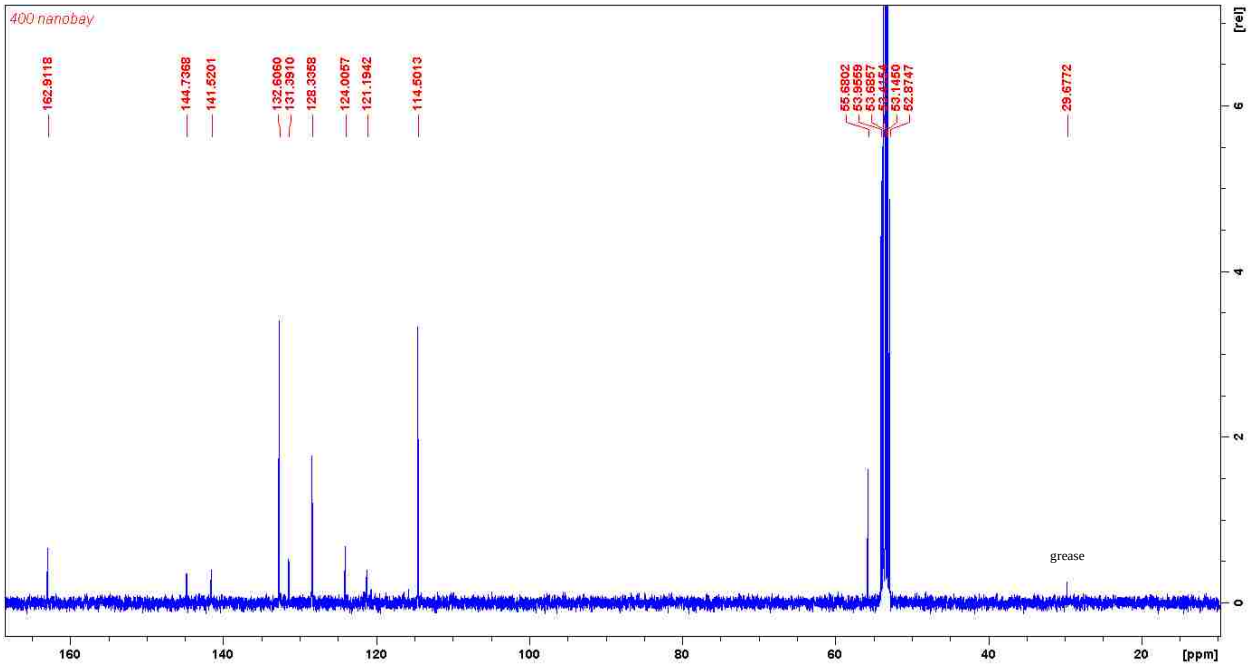

Figure B17: ^{1}H NMR of BODIPY **18**

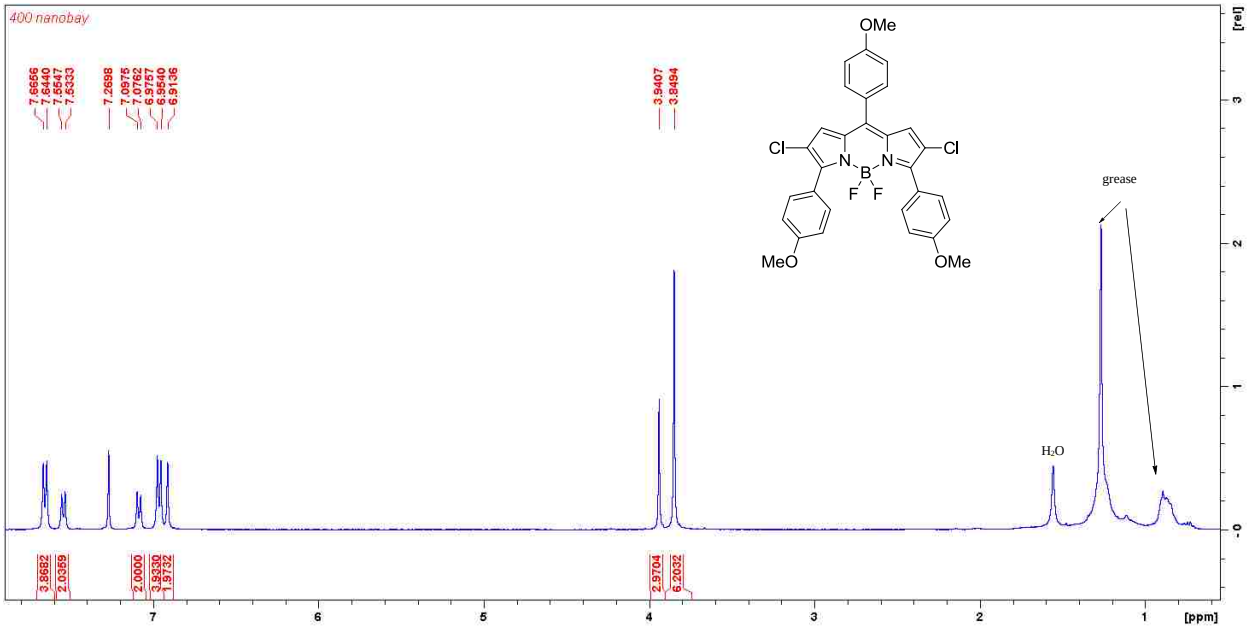

Figure B18: ^{13}C NMR of BODIPY **18**

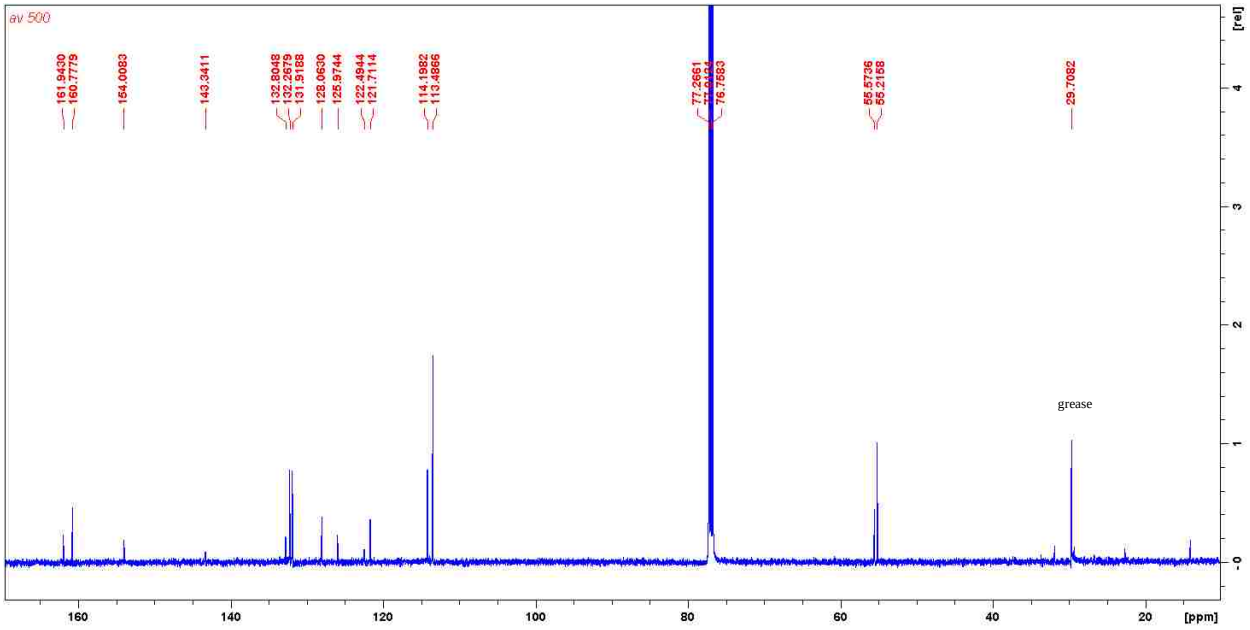

Figure B19: ^{1}H NMR of BODIPY **19**

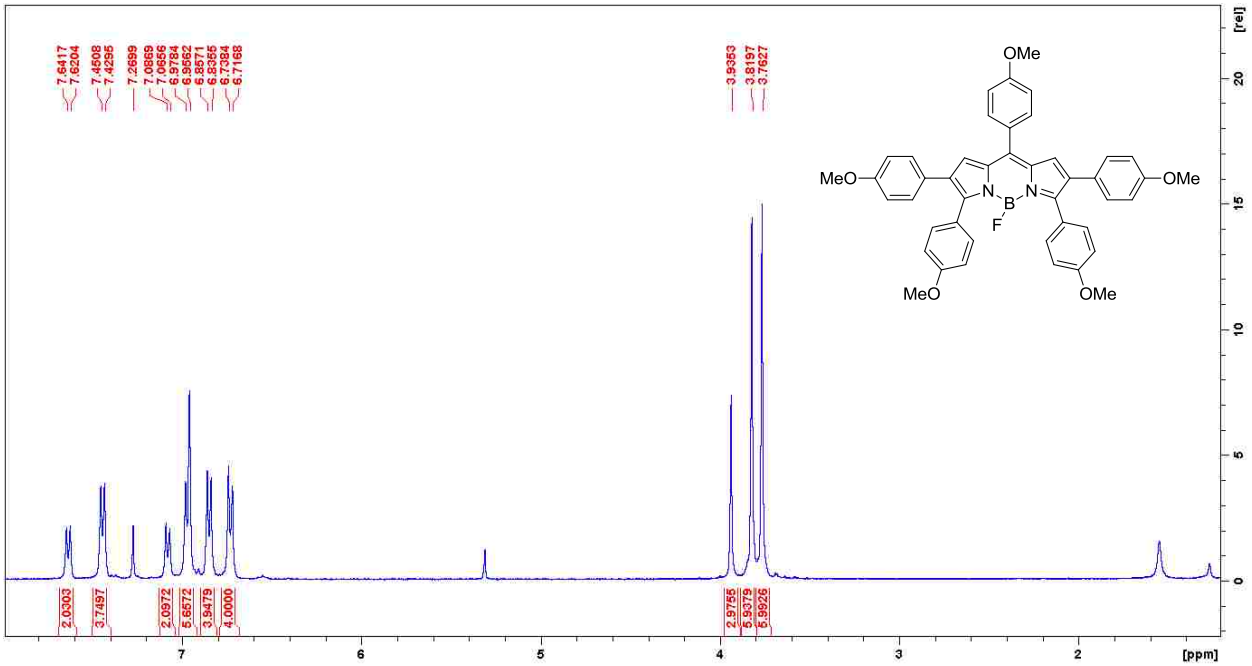

Figure B20: ^{13}C NMR of BODIPY **19**

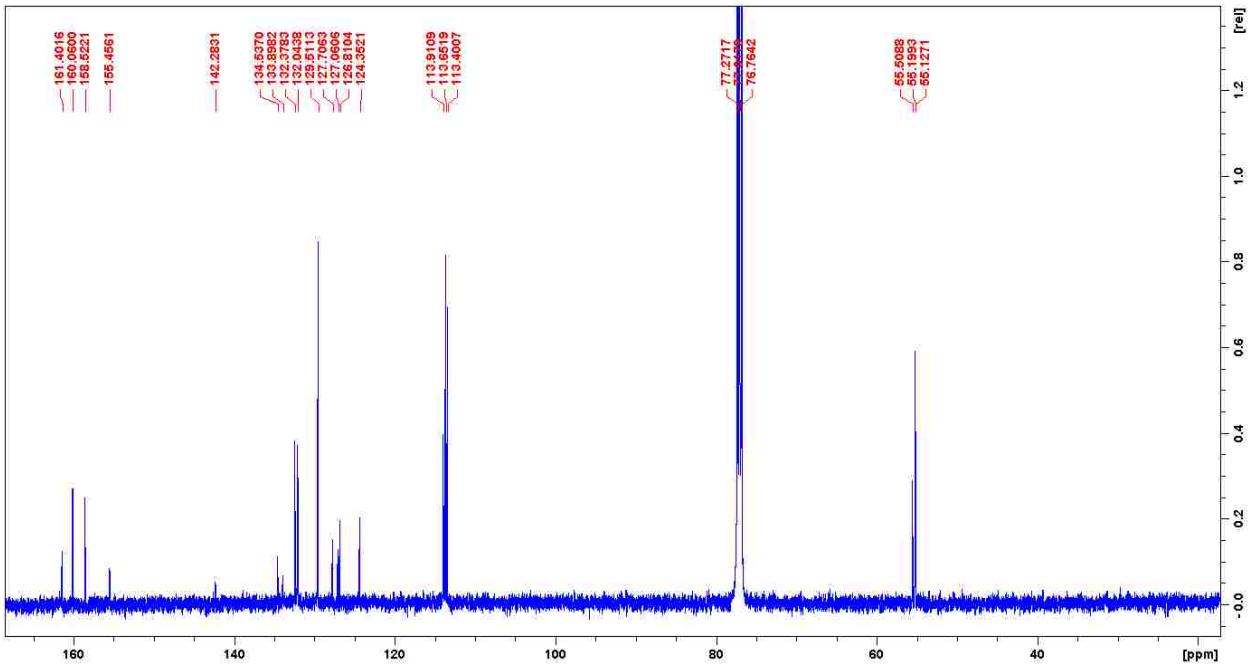

Figure B21: ^{1}H NMR of BODIPY**23**

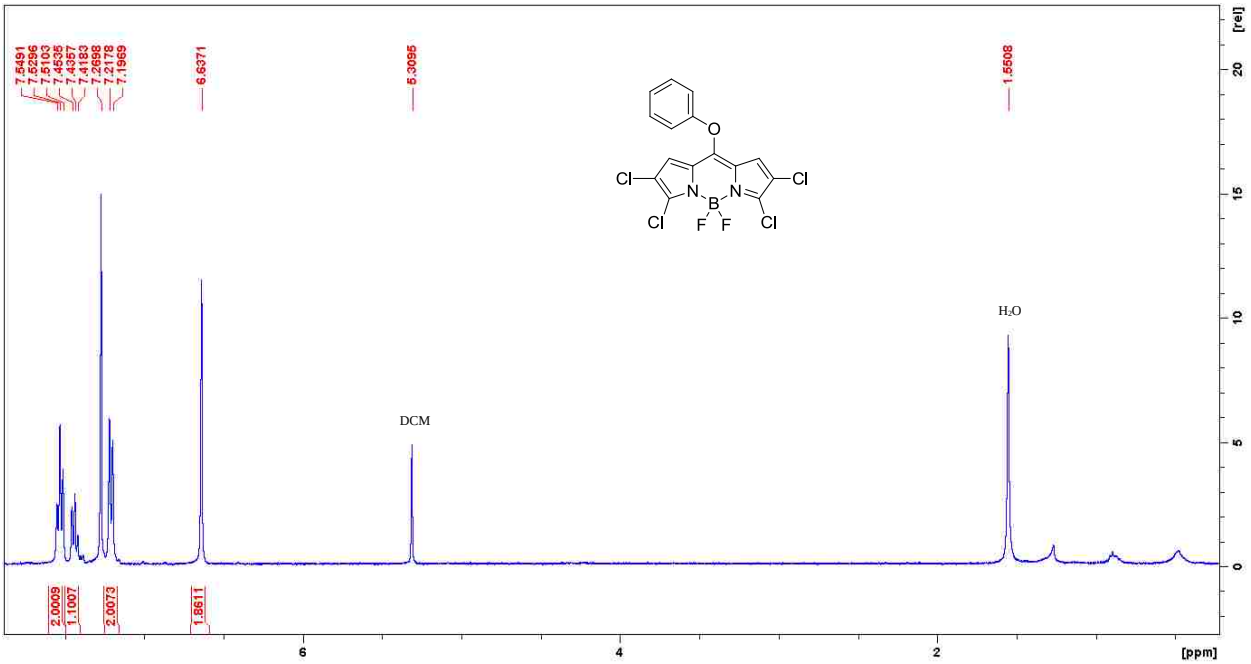

Figure B22: ^{13}C NMR of BODIPY **23**

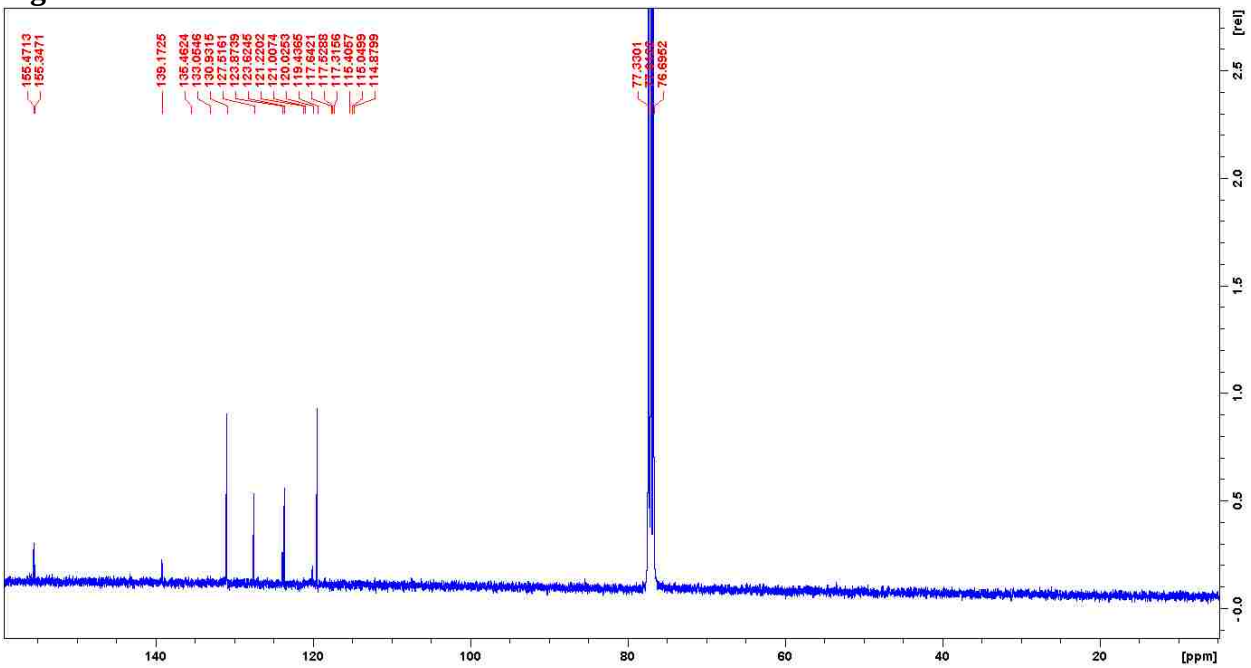

Figure B23: ^{1}H NMR of BODIPY **24**

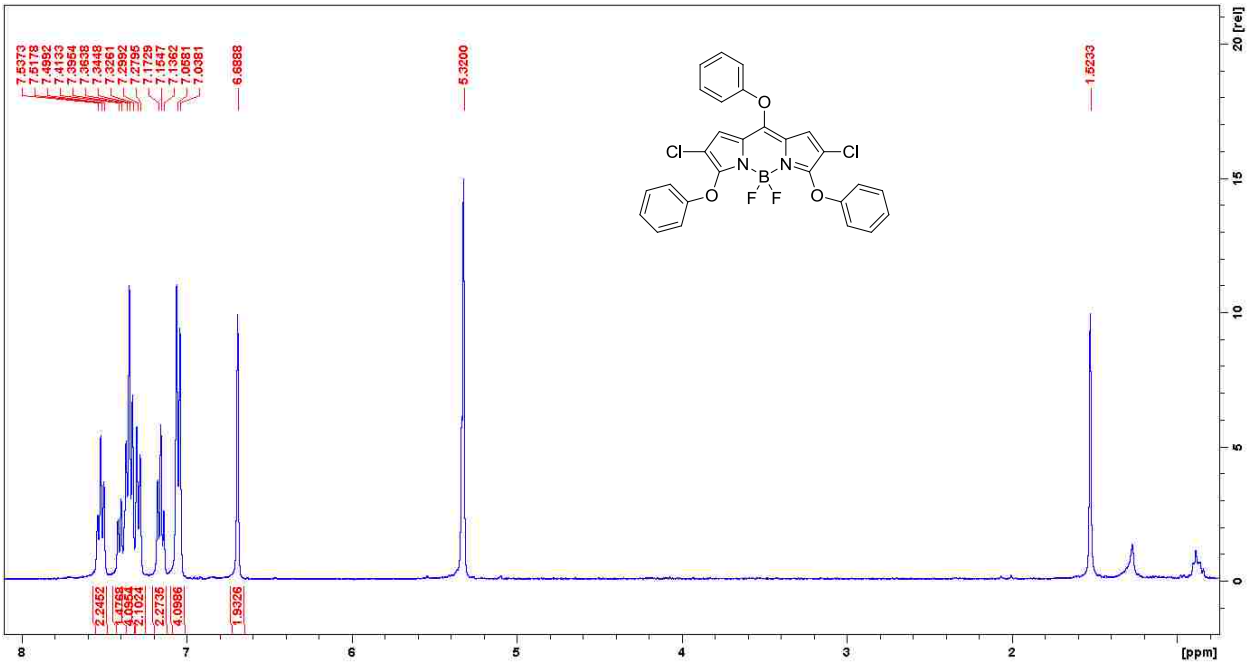

Figure B24: ^{13}C NMR of BODIPY **24**

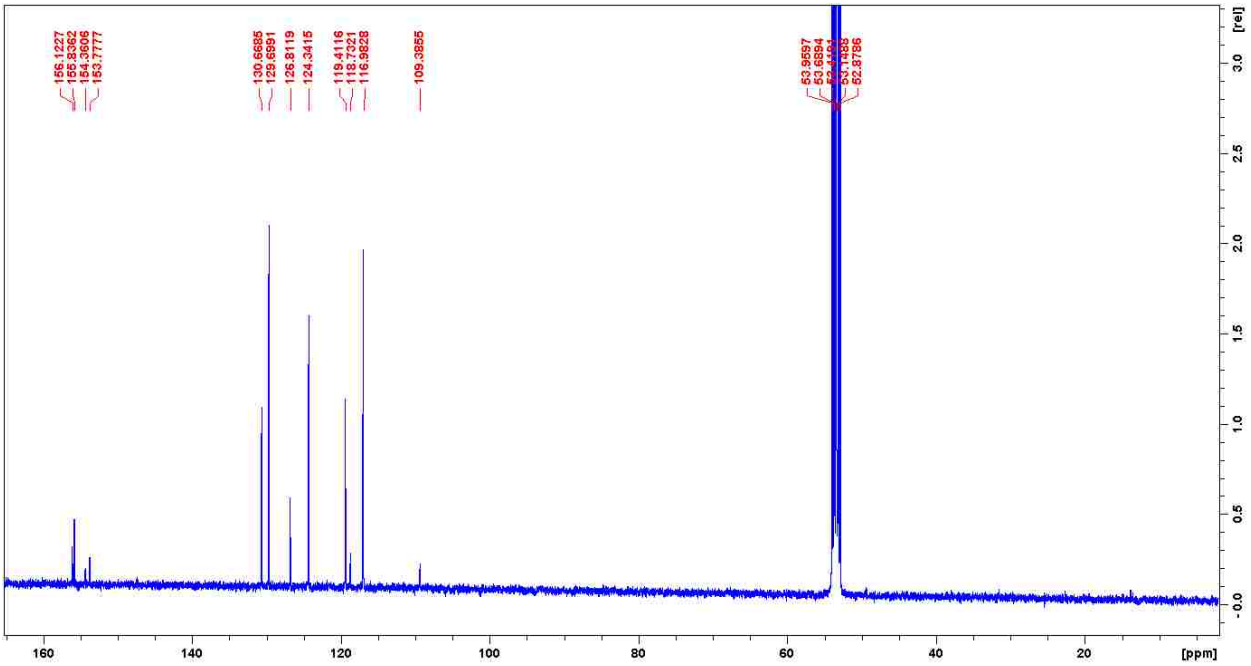

Figure B25: ^{1}H NMR of BODIPY **26**

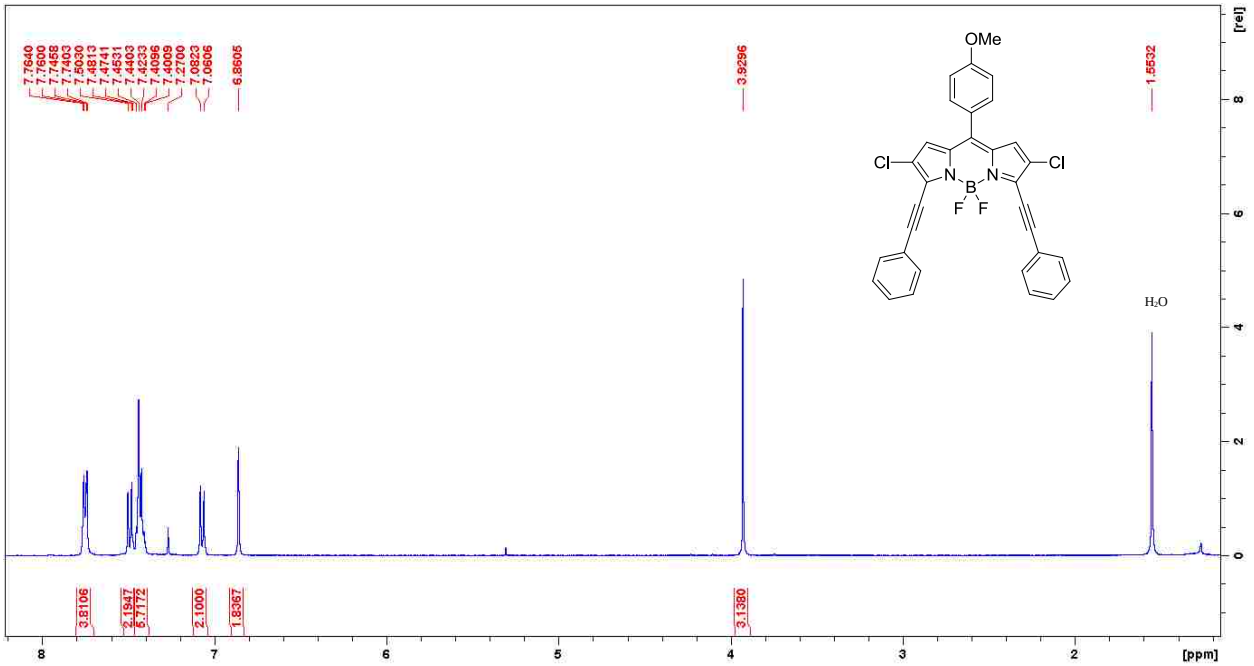

Figure B26: ^{13}C NMR of BODIPY **26**

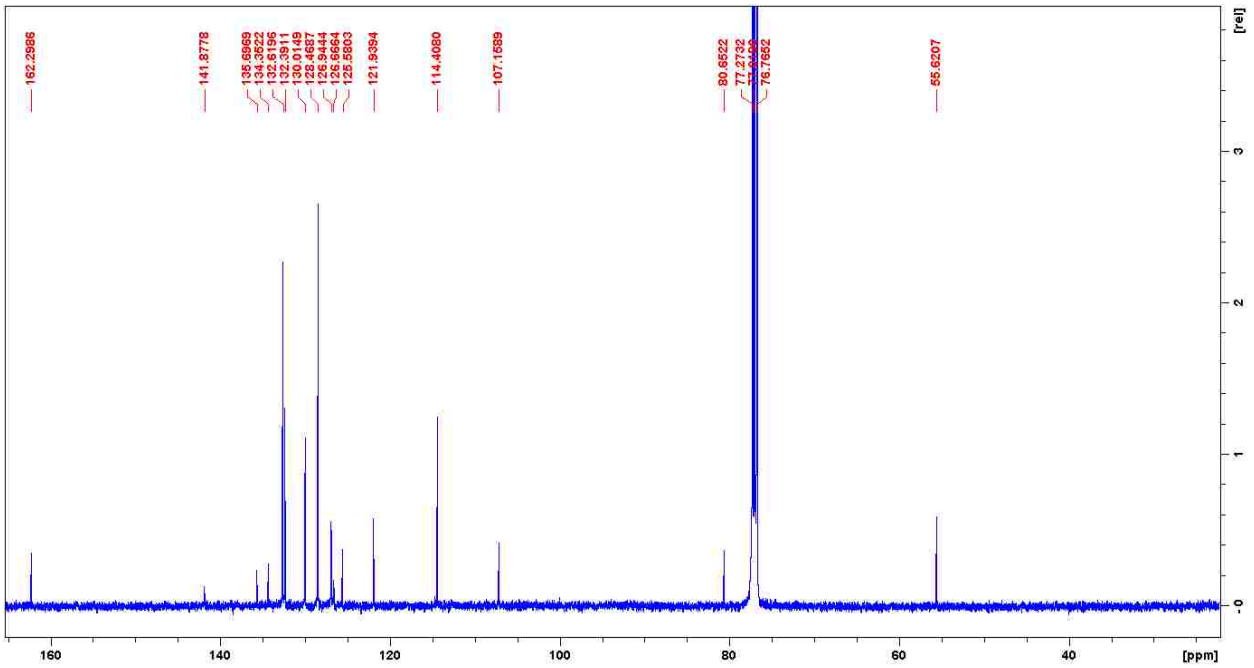

Figure B27: ^{1}H NMR of BODIPY **27**

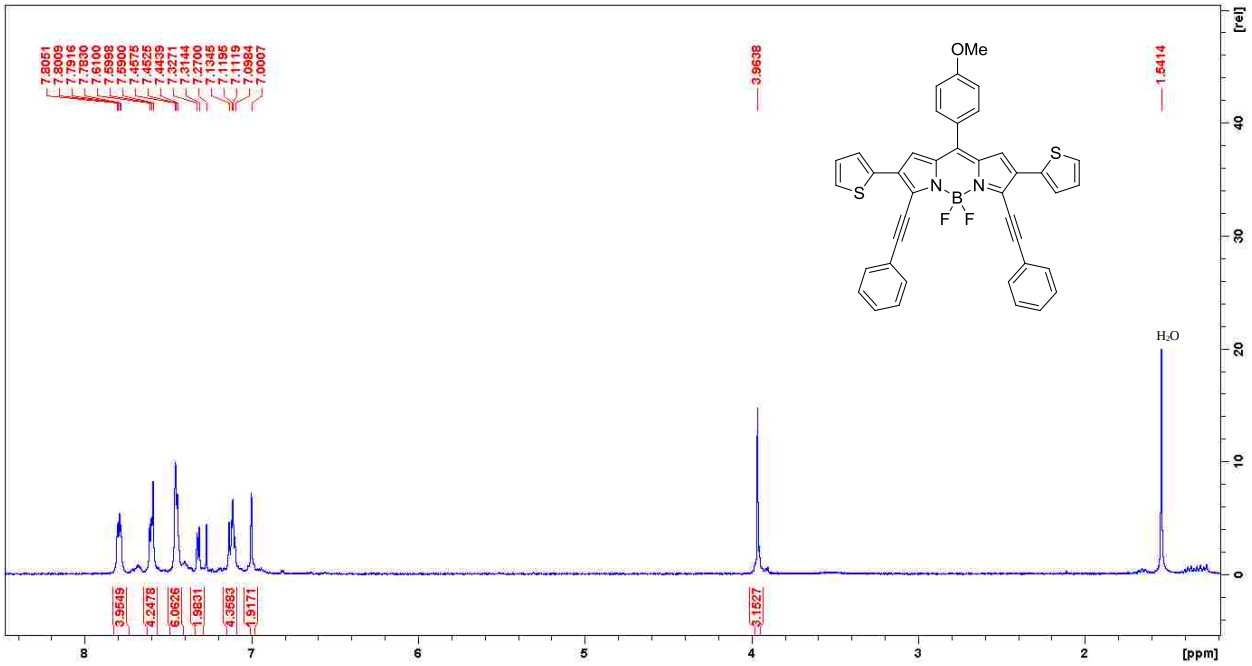

Figure B28: ^{13}C NMR of BODIPY **27**

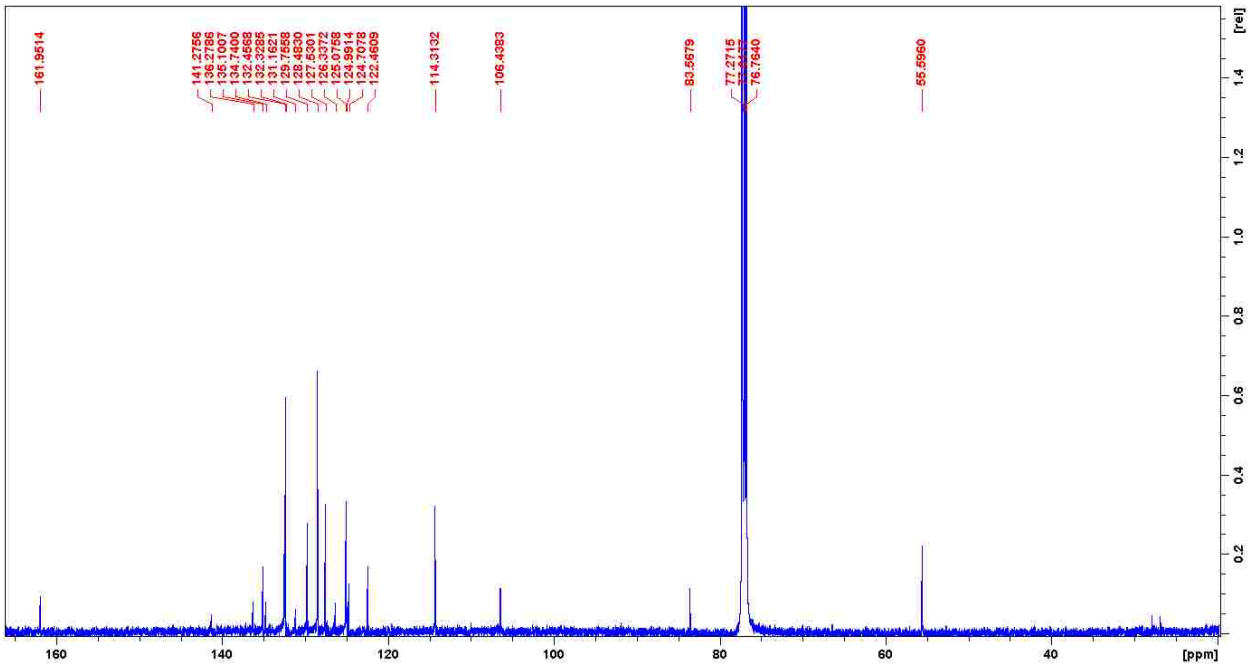

APPENDIX C: CHARACTERIZATION DATA FOR COMPOUNDS IN CHAPTER 3

Figure C1: ^{13}C NMR of BODIPY **3b**

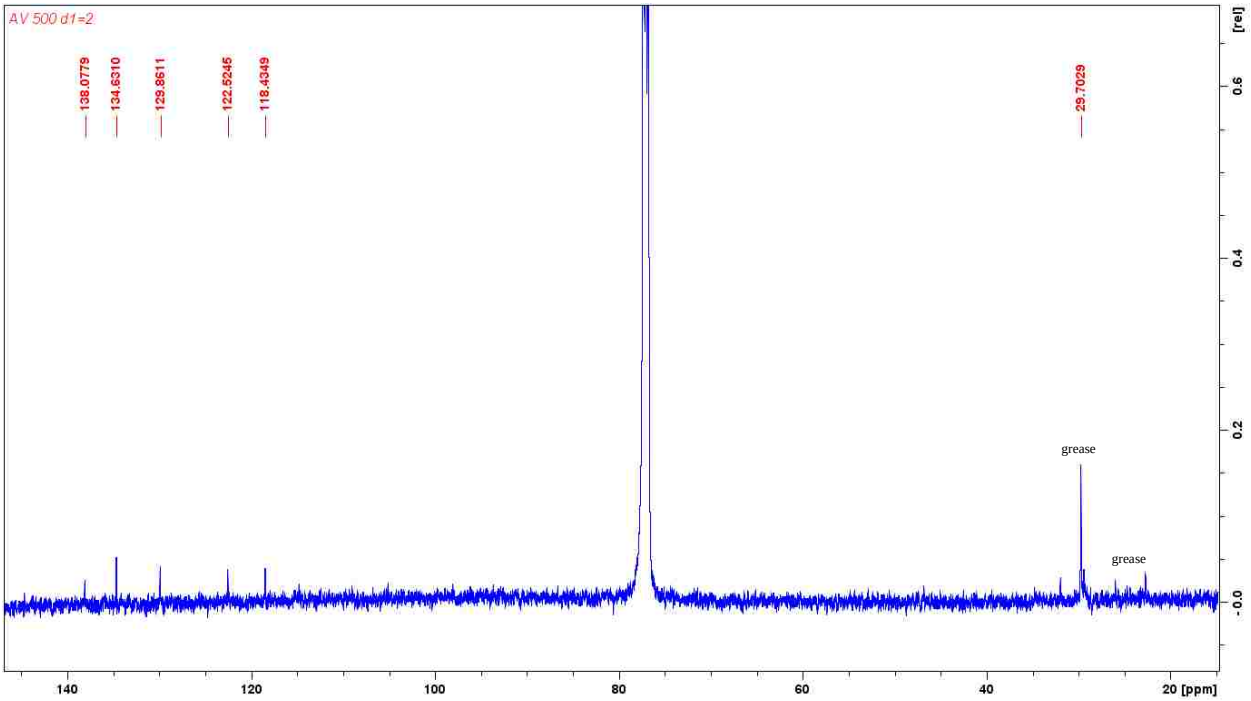

Figure C2: ^{13}C NMR of BODIPY **4b**

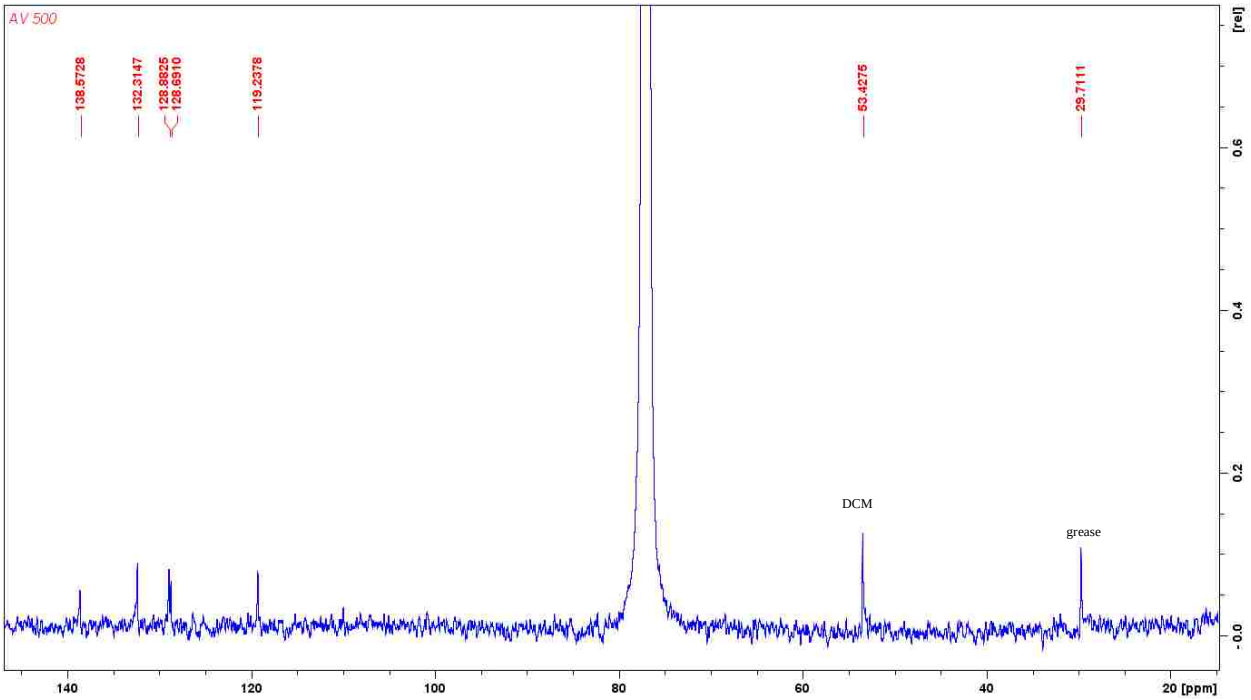

Figure C3: ^{13}C NMR of BODIPY **5b**

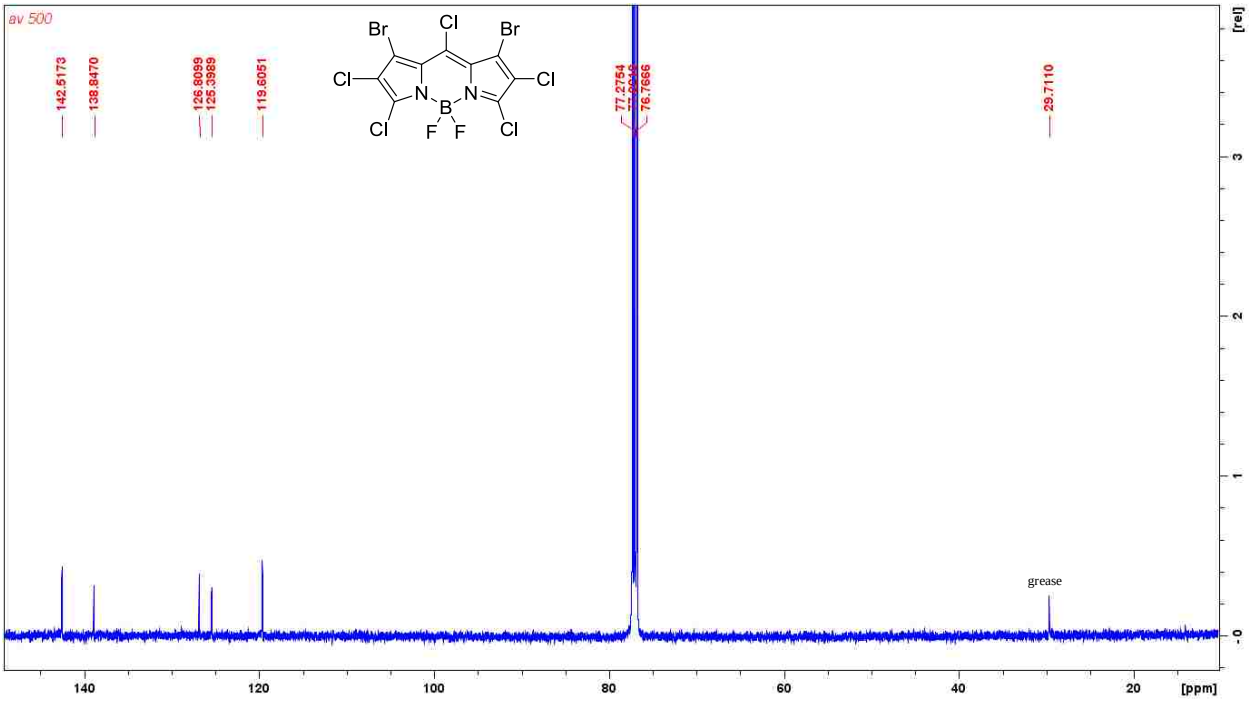

Figure C4: ^{1}H NMR of BODIPY **6a**

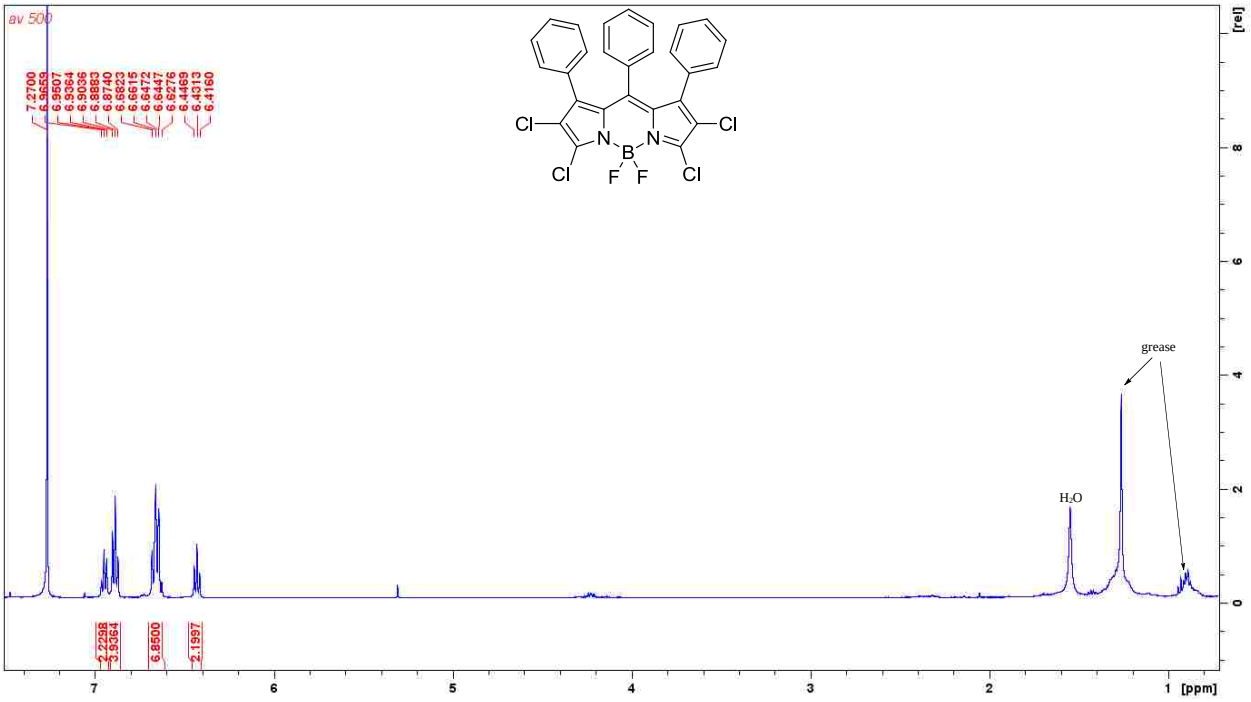

Figure C5: ^{13}C NMR of BODIPY **6a**

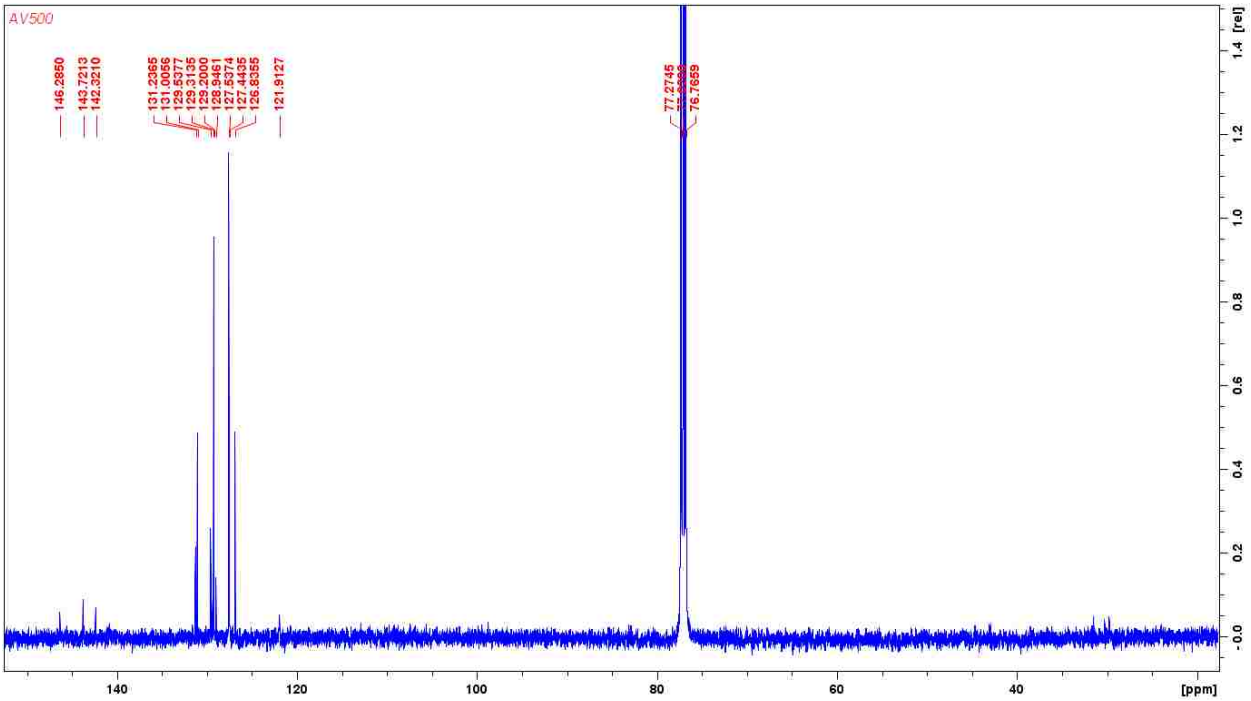

Figure C6: ^{1}H NMR of BODIPY **7a**

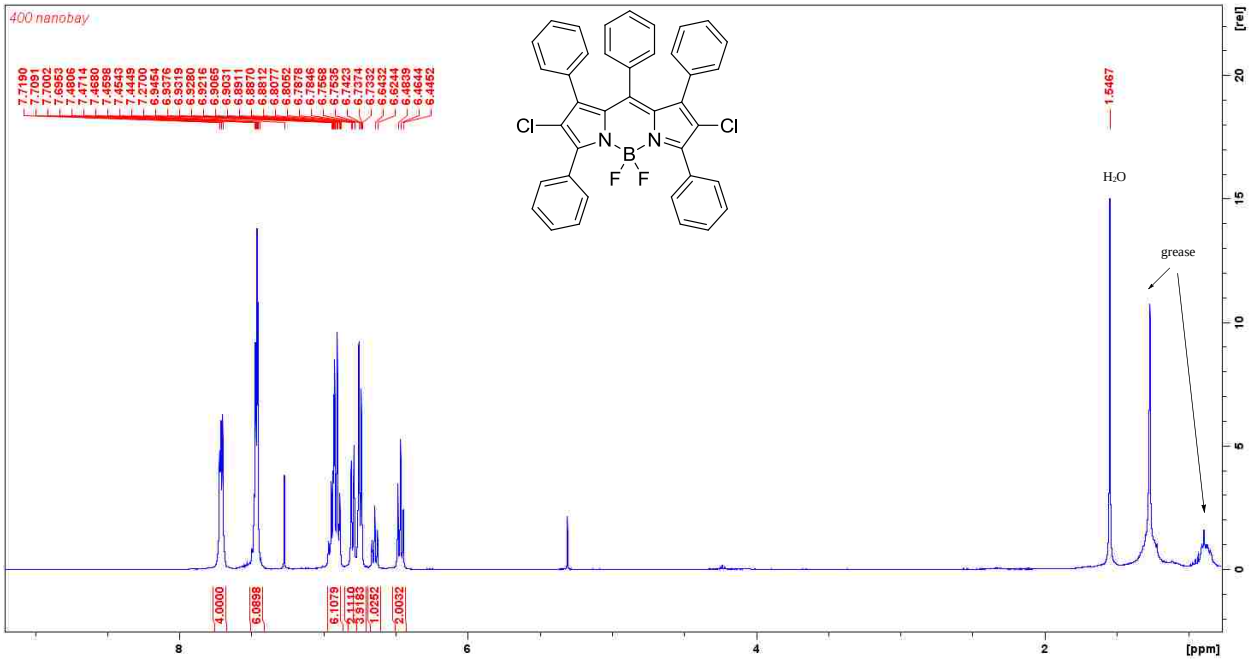

Figure C7: ^{13}C NMR of BODIPY **7a**

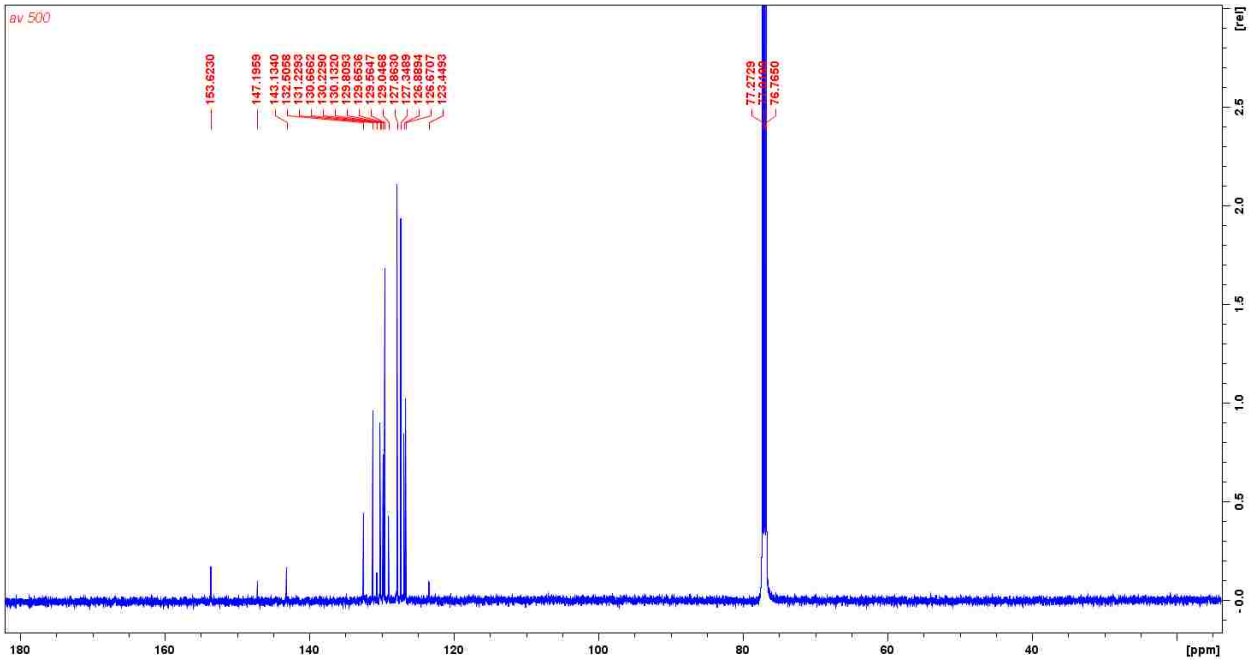

Figure C8: ^{1}H NMR of BODIPY **9**

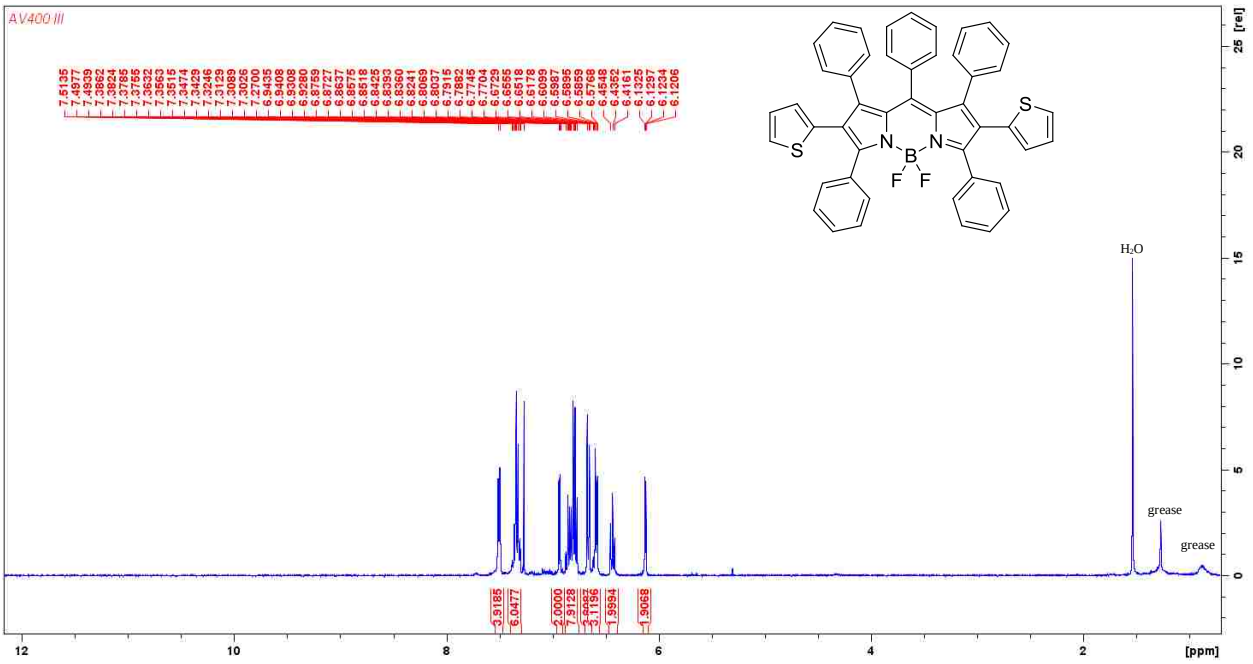

Figure C9: ^{13}C NMR of BODIPY **9**

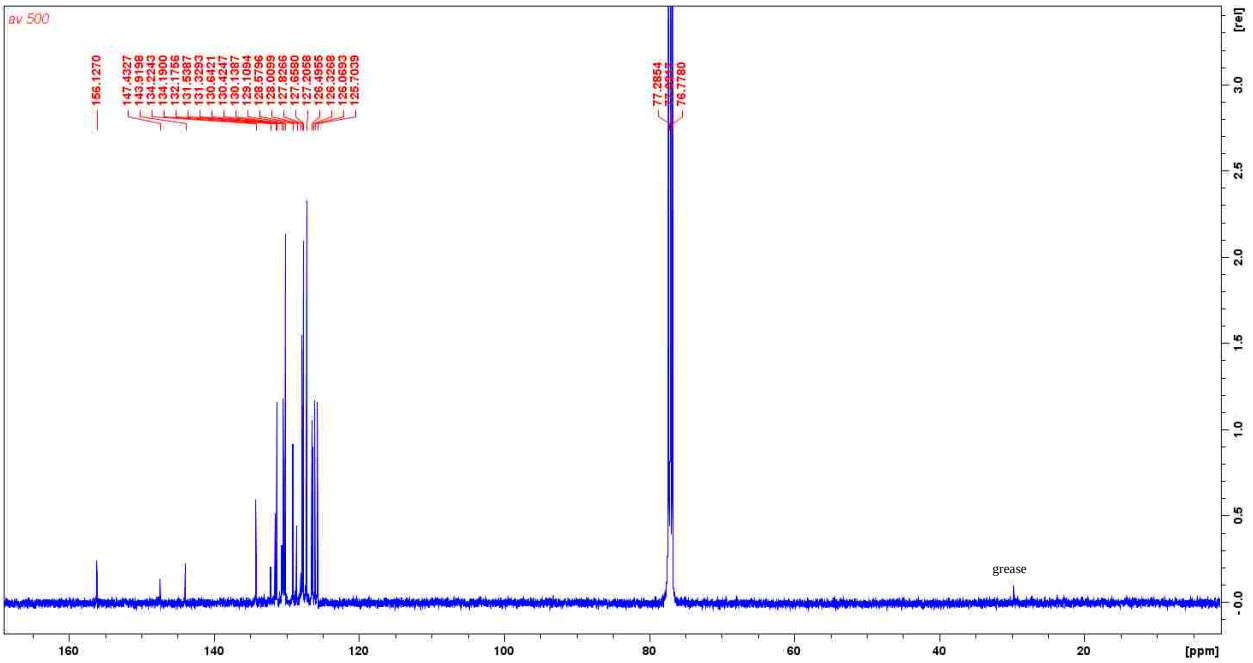

Figure C10: ^{1}H NMR of BODIPY **13**

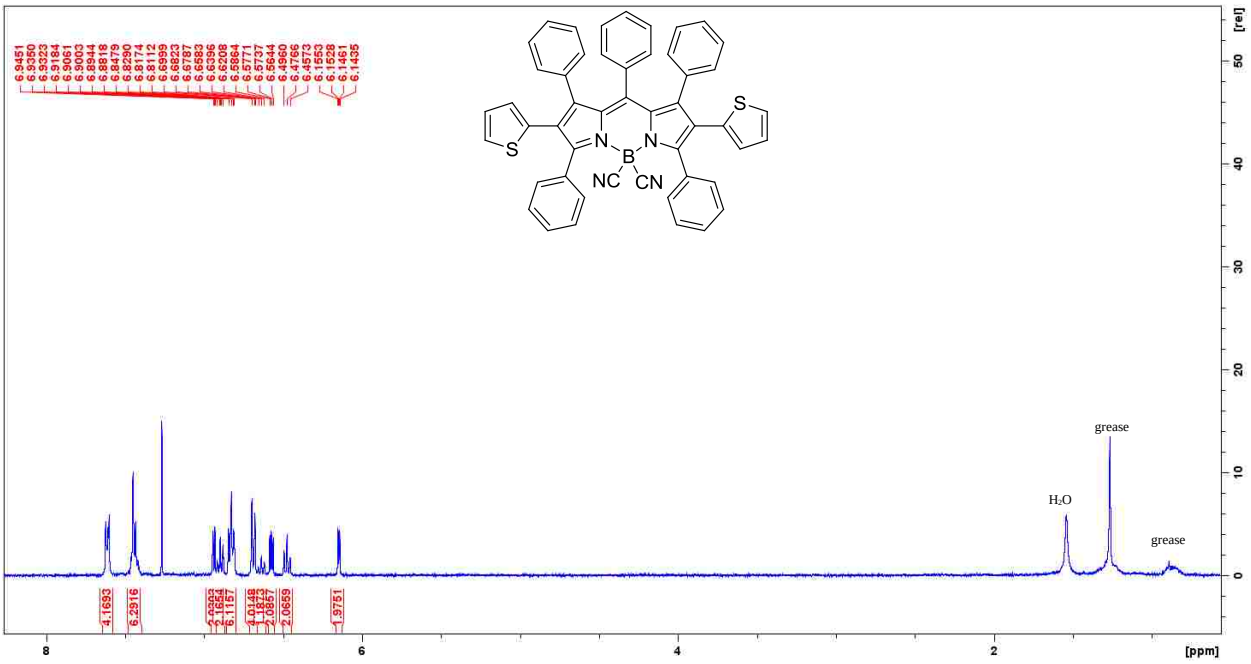

Figure C11: ^{13}C NMR of BODIPY **13**

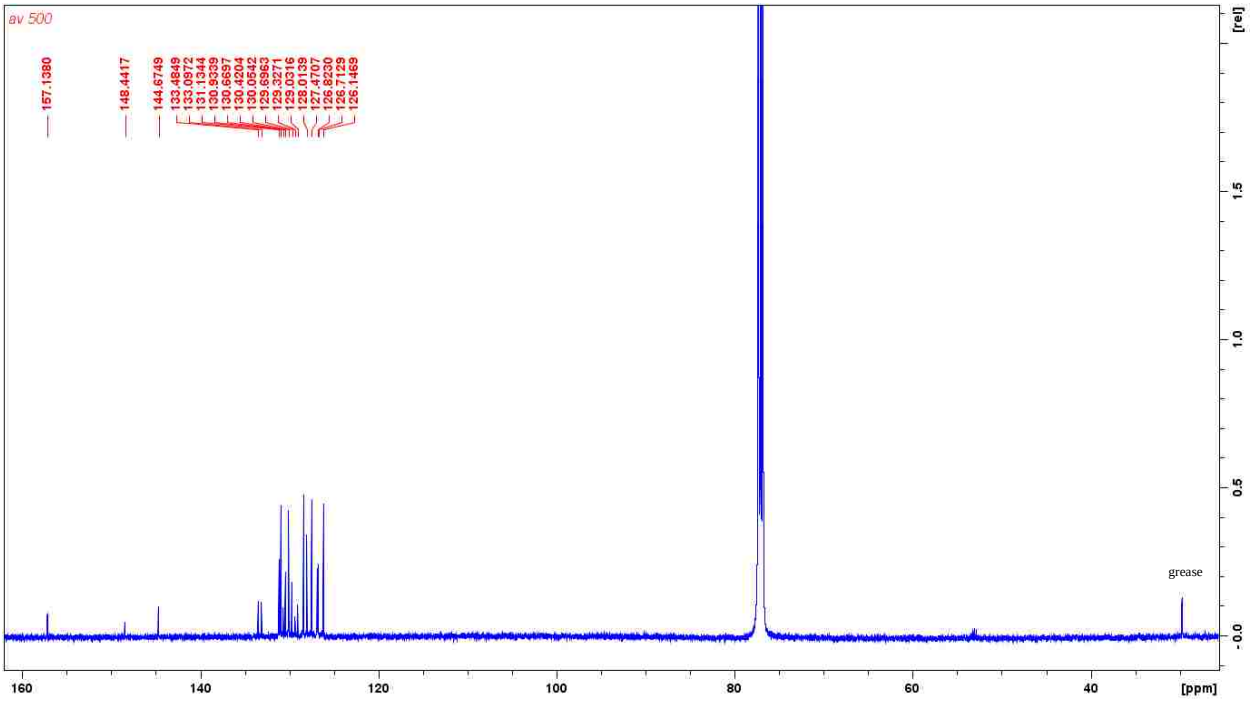

Figure C12: ^{1}H NMR of BODIPY **6b**

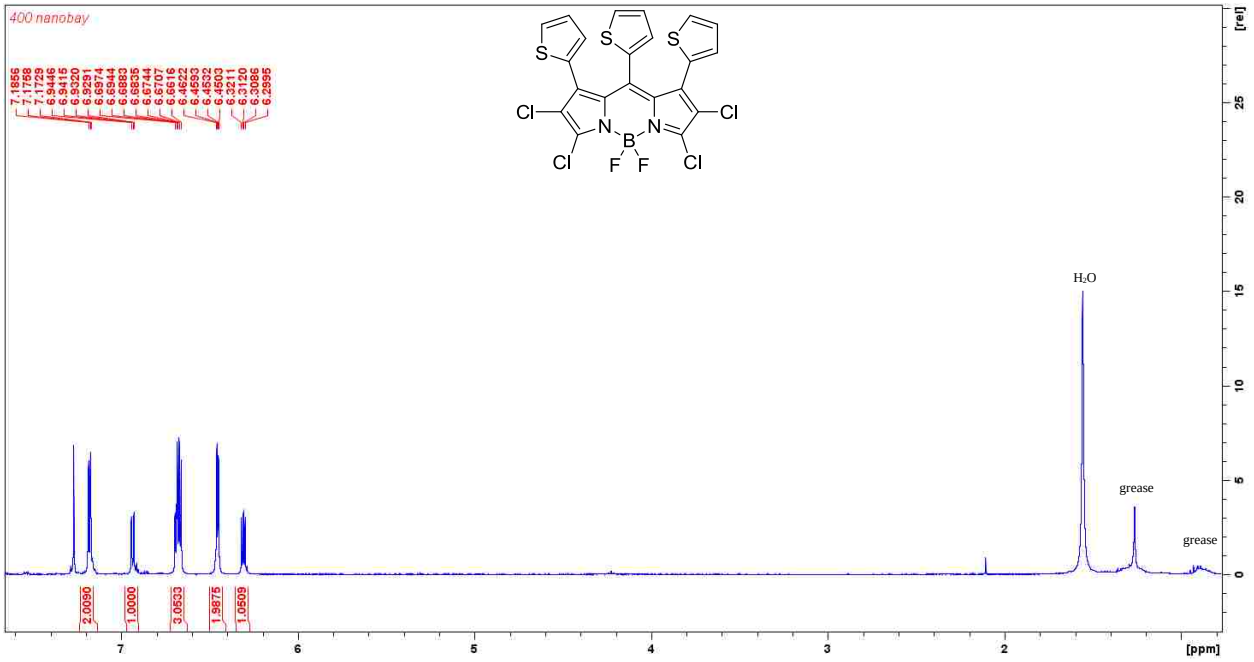

Figure C13: ^{13}C NMR of BODIPY **6b**

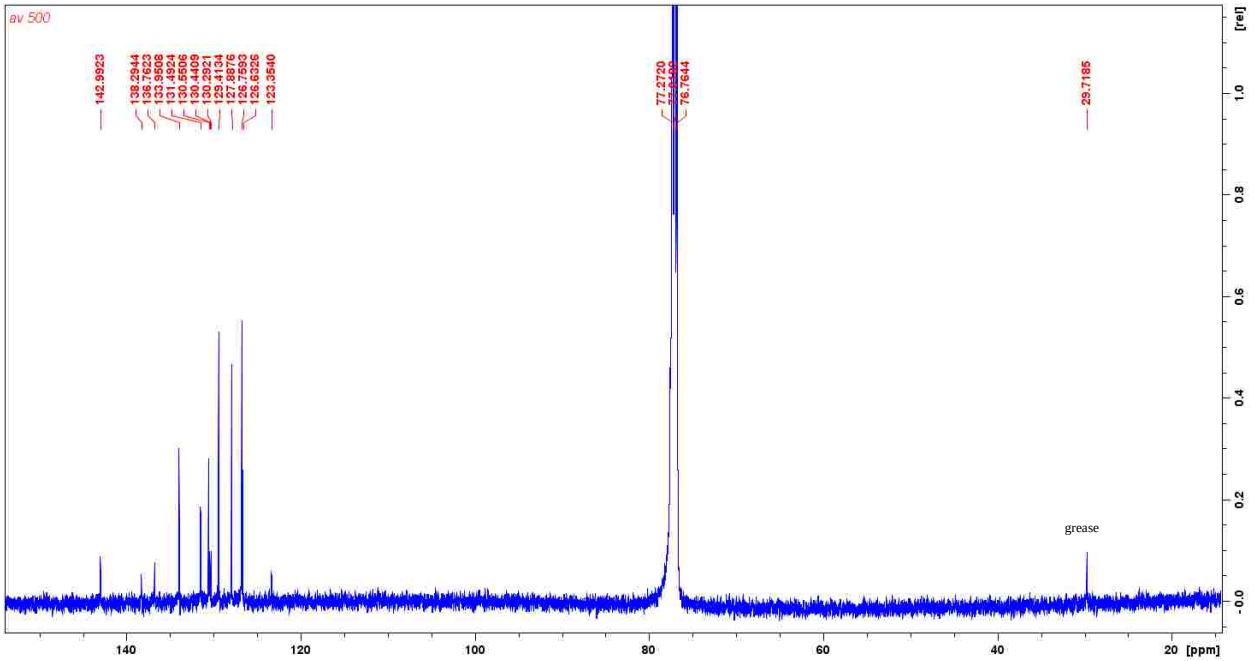

Figure C14: ^{1}H NMR of BODIPY **7b**

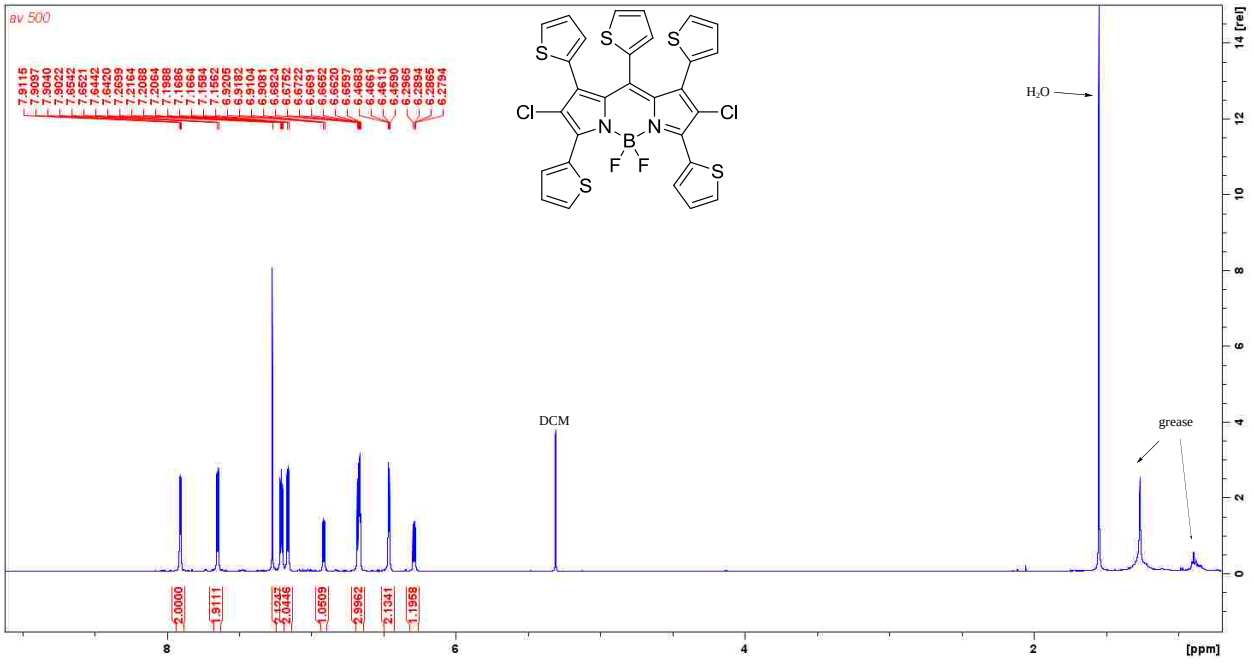

Figure C15: ^{13}C NMR of BODIPY **7b**

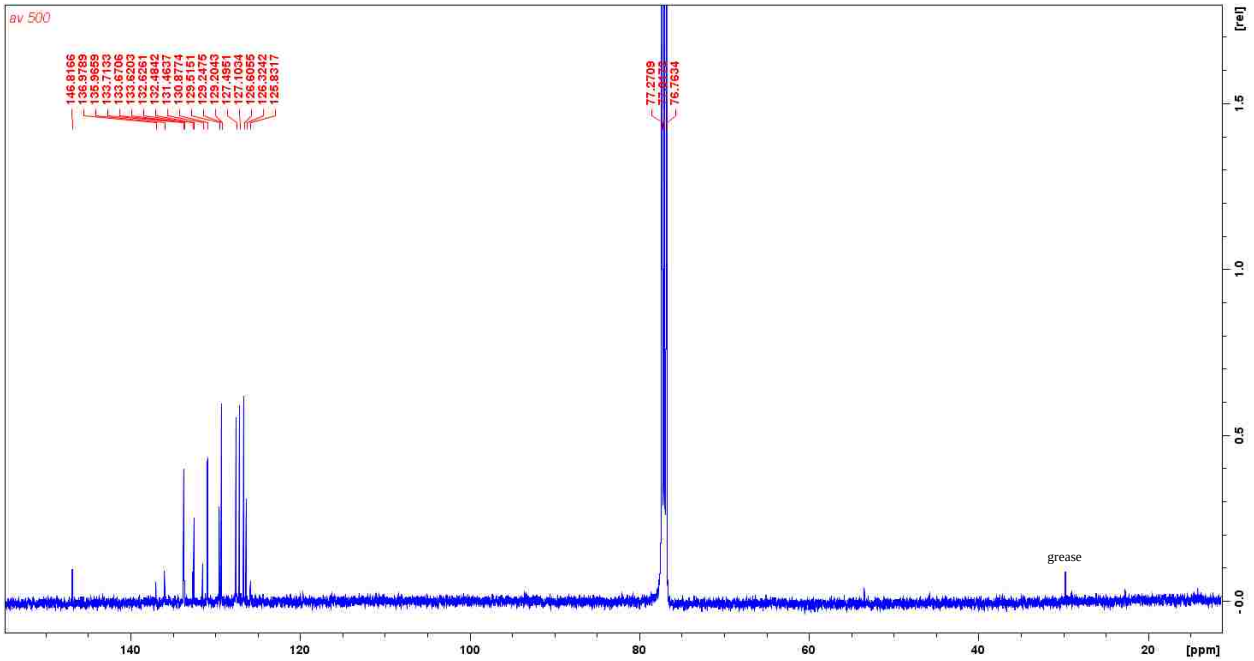

Figure C16: ^{1}H NMR of BODIPY **10**

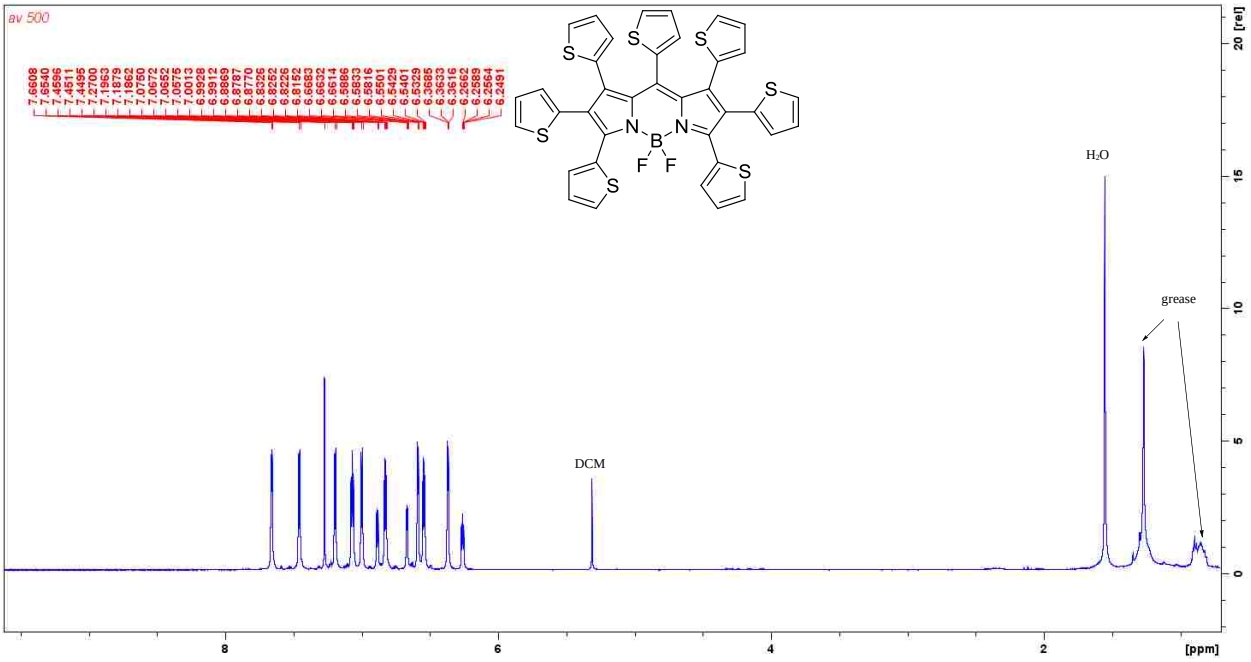

Figure C17: ^{13}C NMR of BODIPY **10**

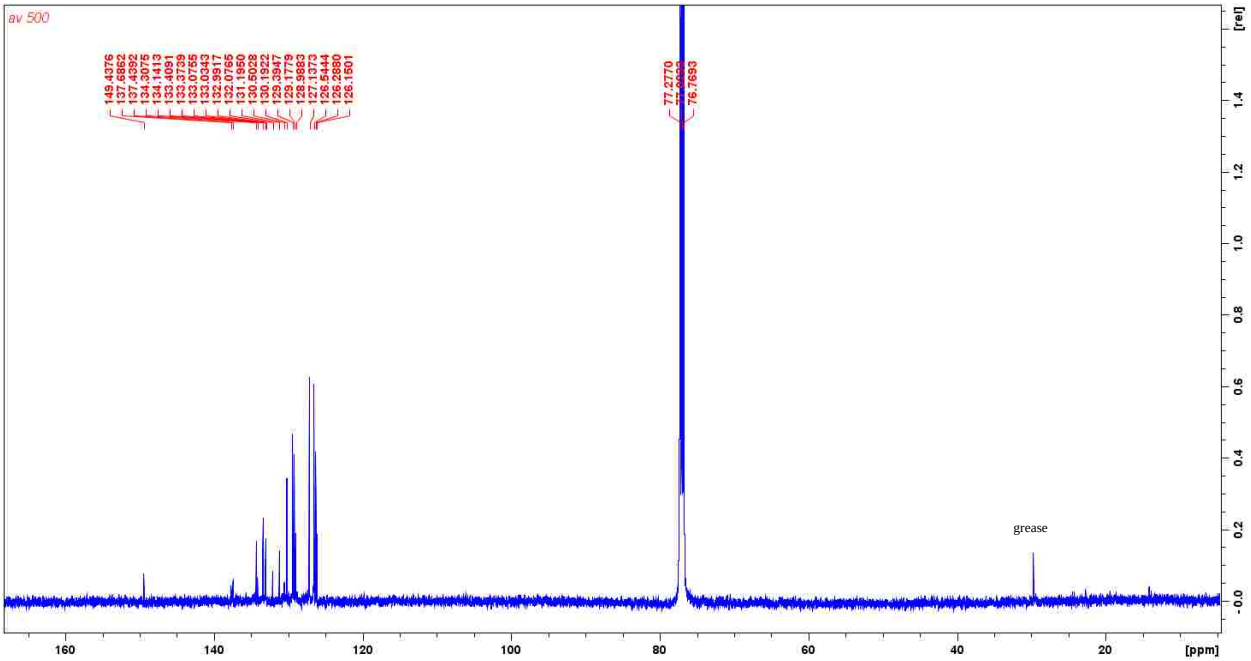

Figure C18: ^{1}H NMR of BODIPY **11**

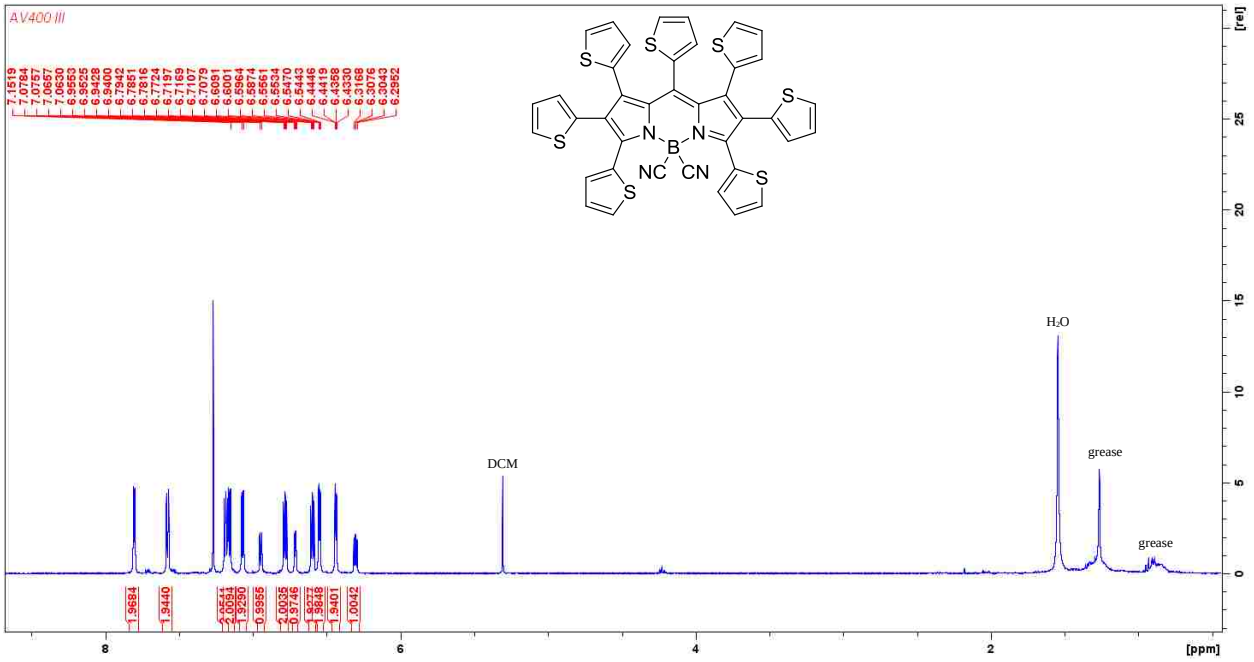

Figure C19: ^{1}H NMR of BODIPY **11**

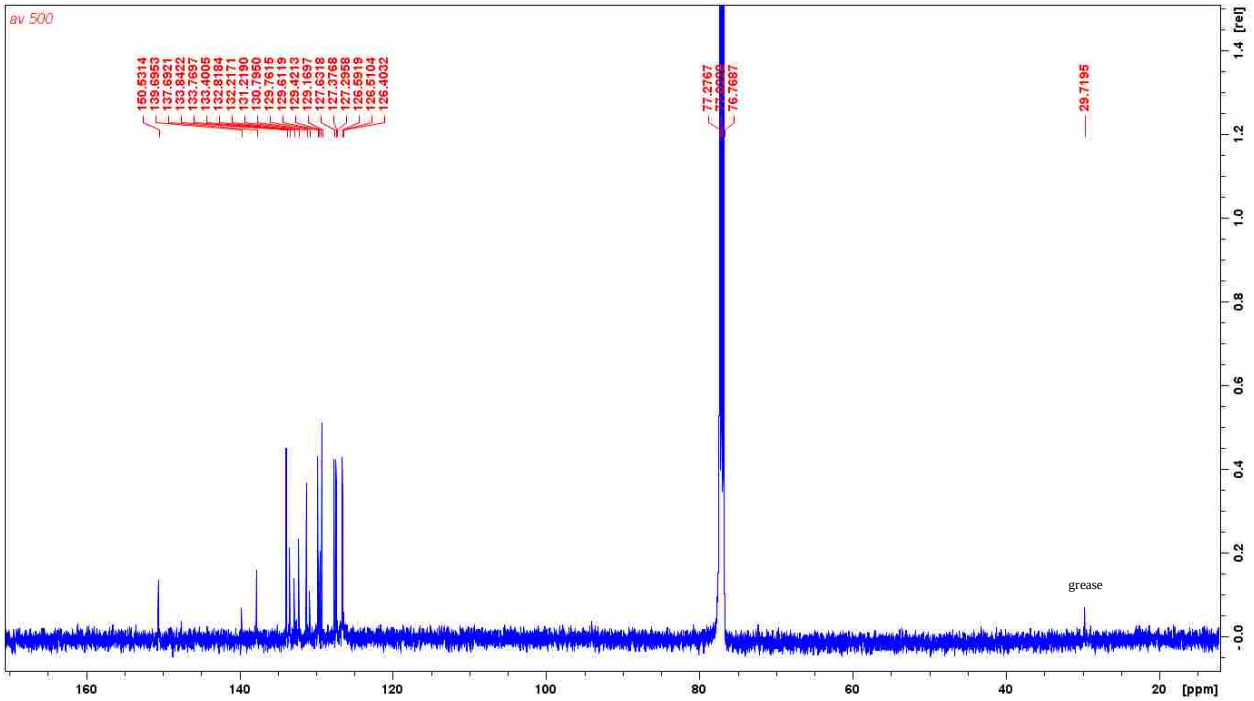

Figure C20: ^{11}B NMR of BODIPY **3b**

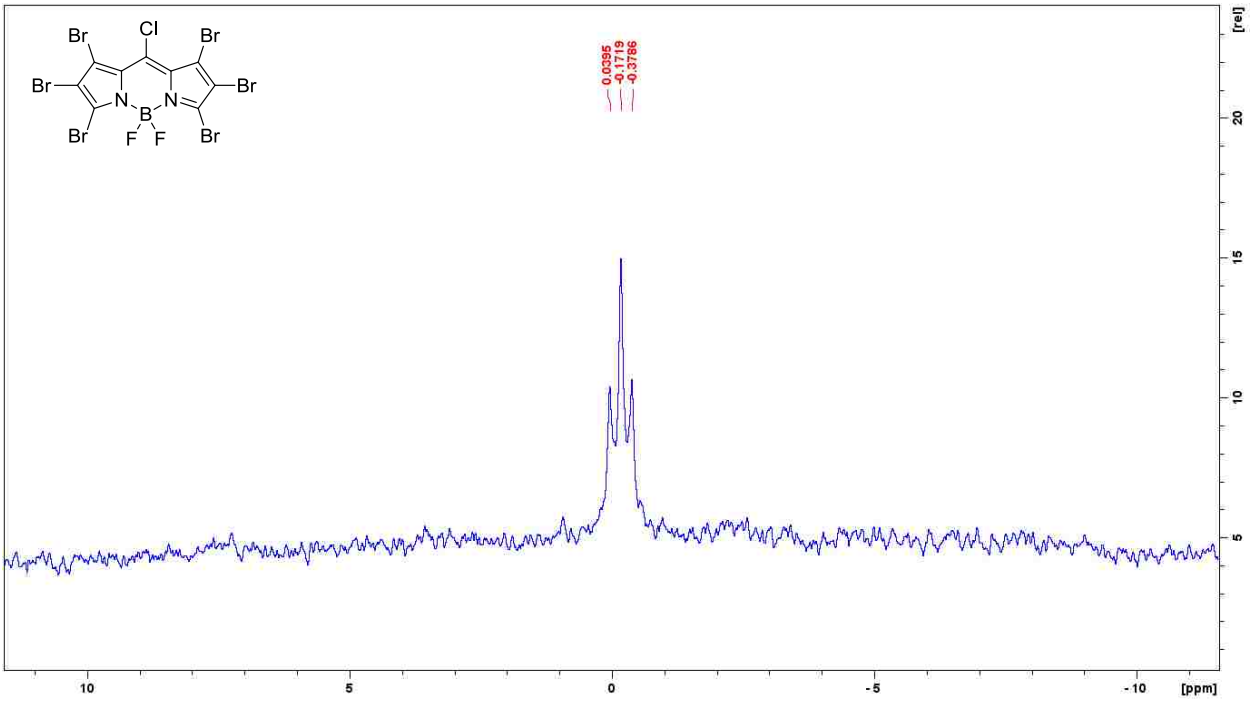

Figure C21: ^{11}B NMR of BODIPY **4b**

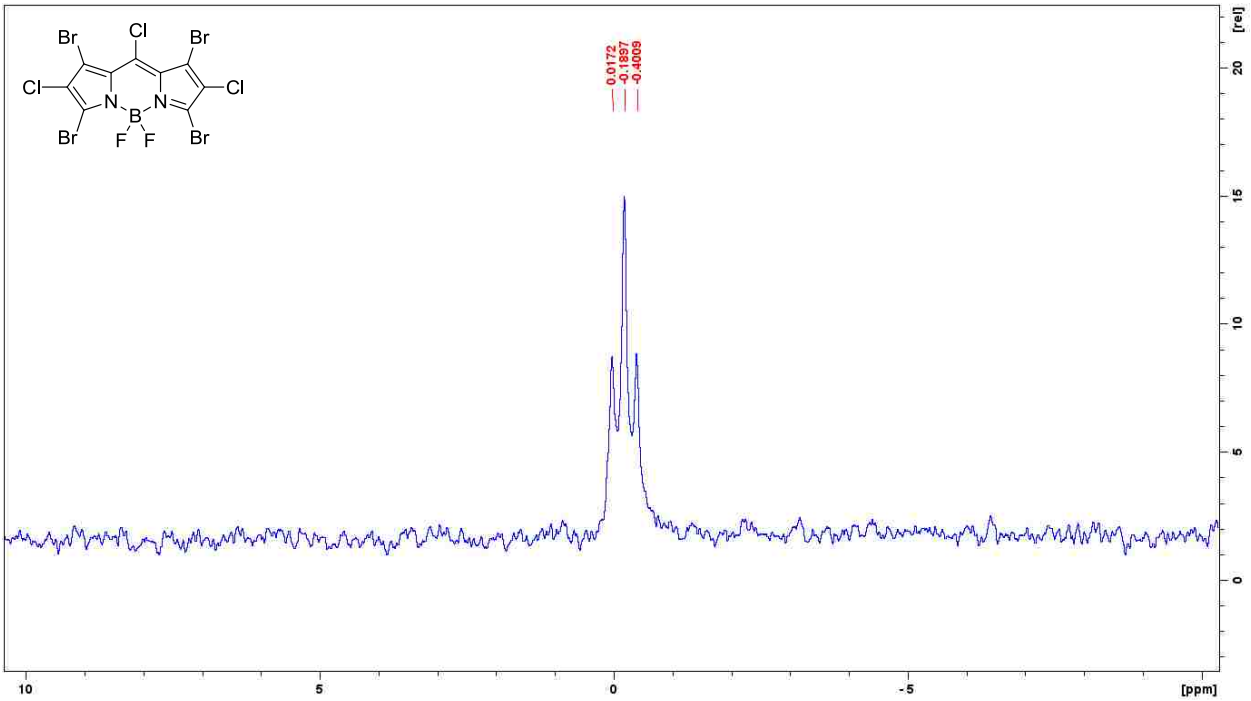

Figure C22: ^{11}B NMR of BODIPY **5b**

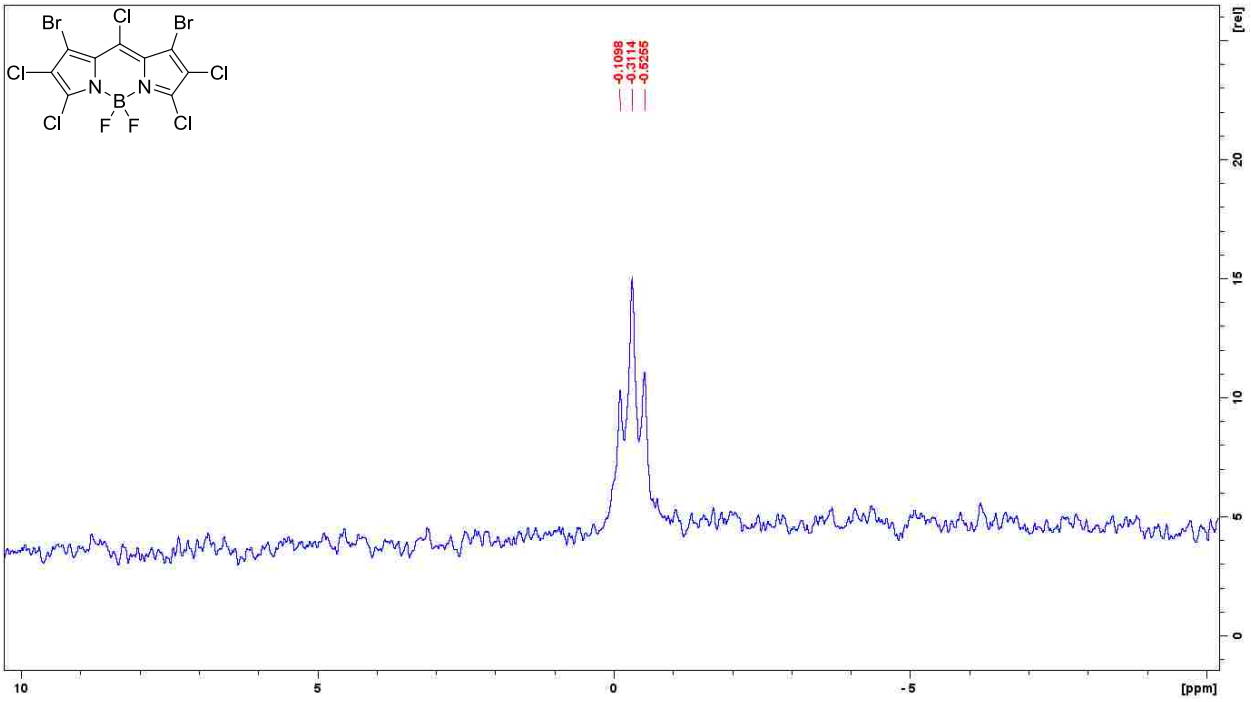

Figure C23: ^{11}B NMR of BODIPY **6a**

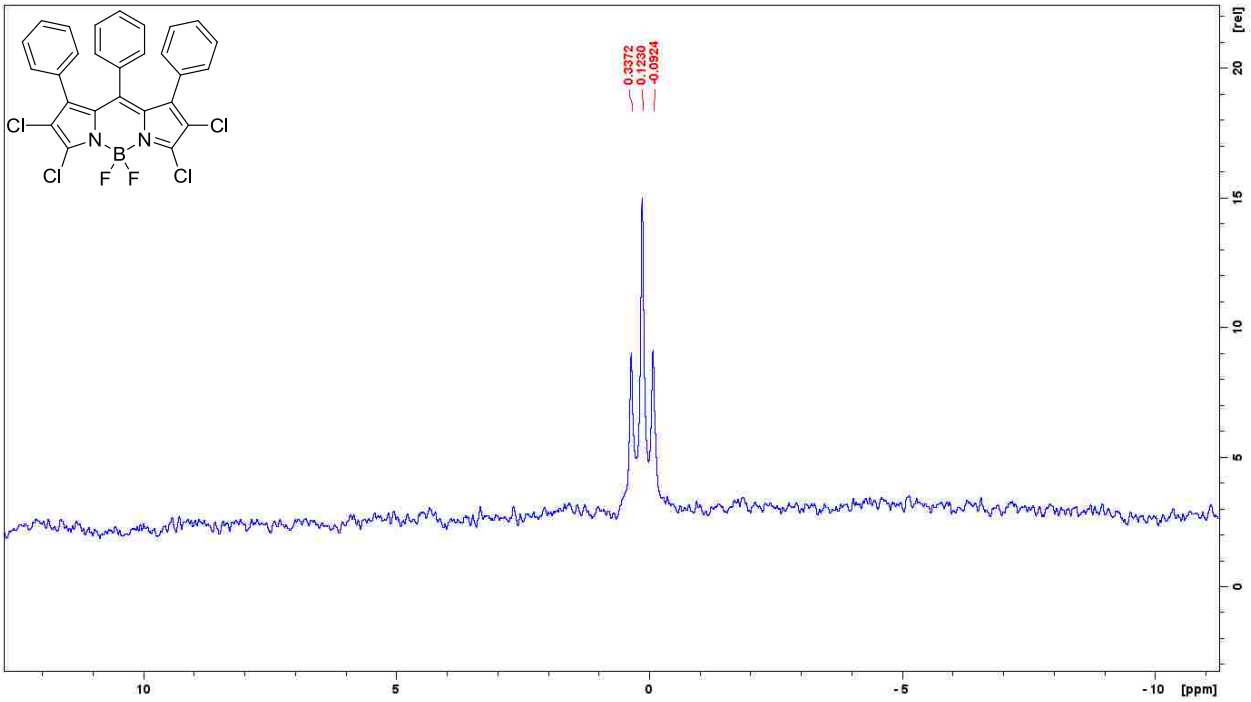

Figure C24: ^{11}B NMR of BODIPY **13**

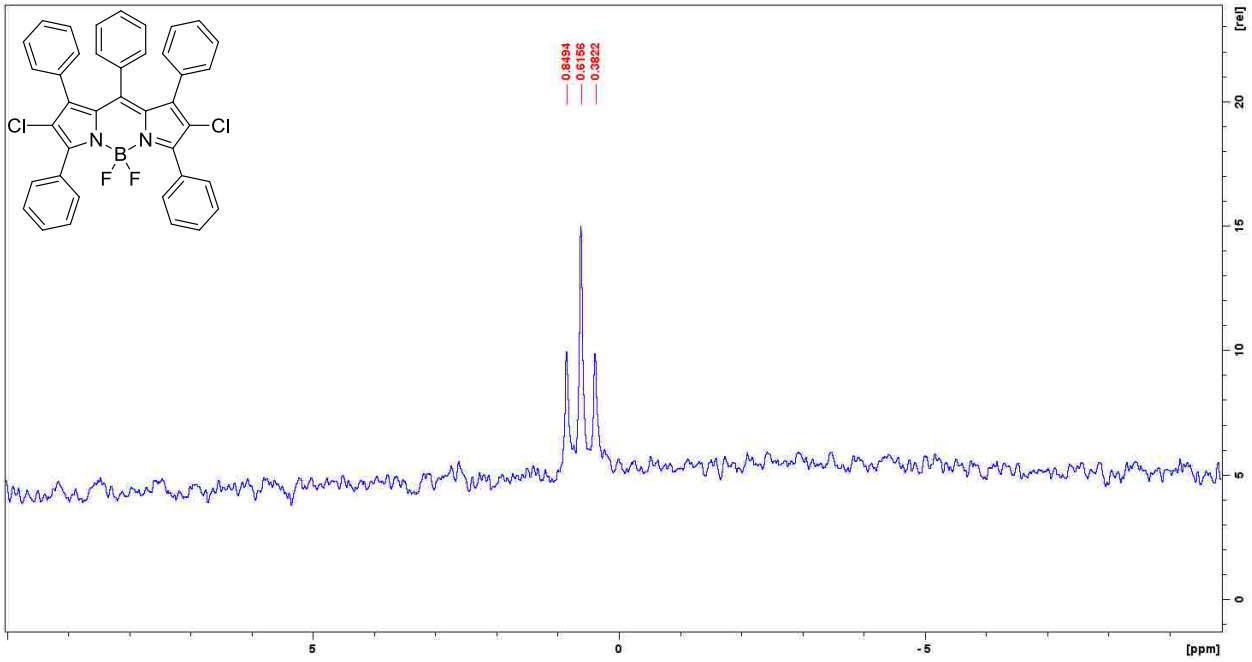

Figure C25: ^{11}B NMR of BODIPY **13**

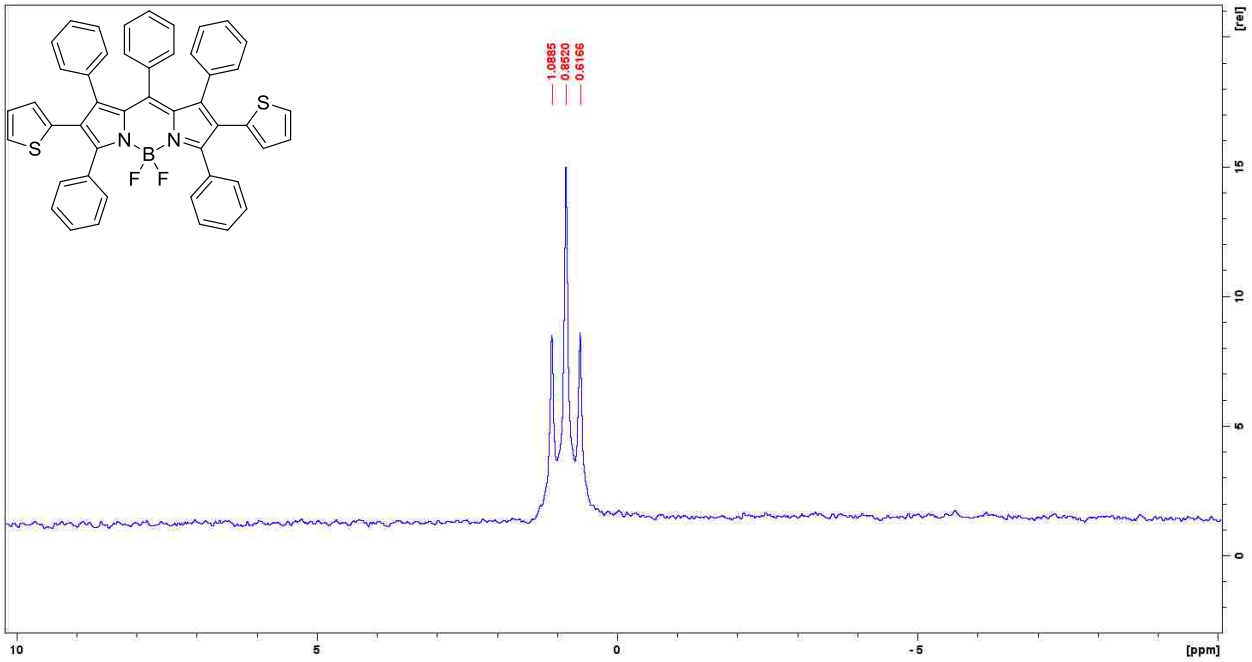

Figure C26: ^{11}B NMR of BODIPY **6a**

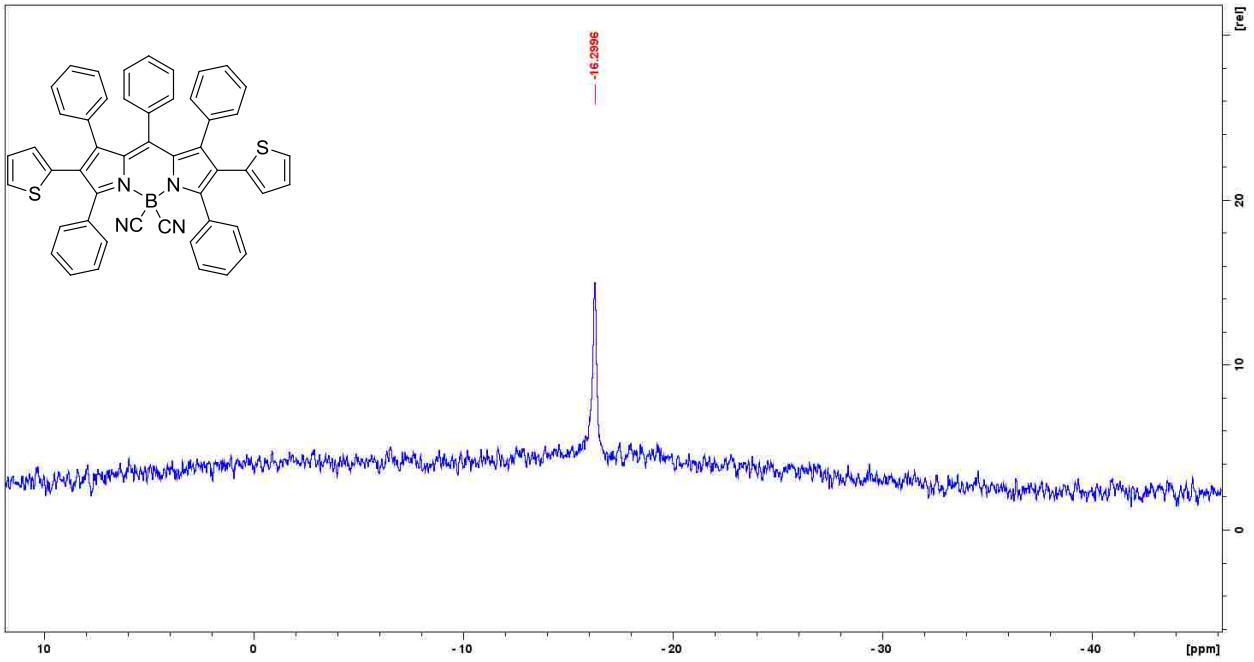

Figure C27: ^{11}B NMR of BODIPY **6b**

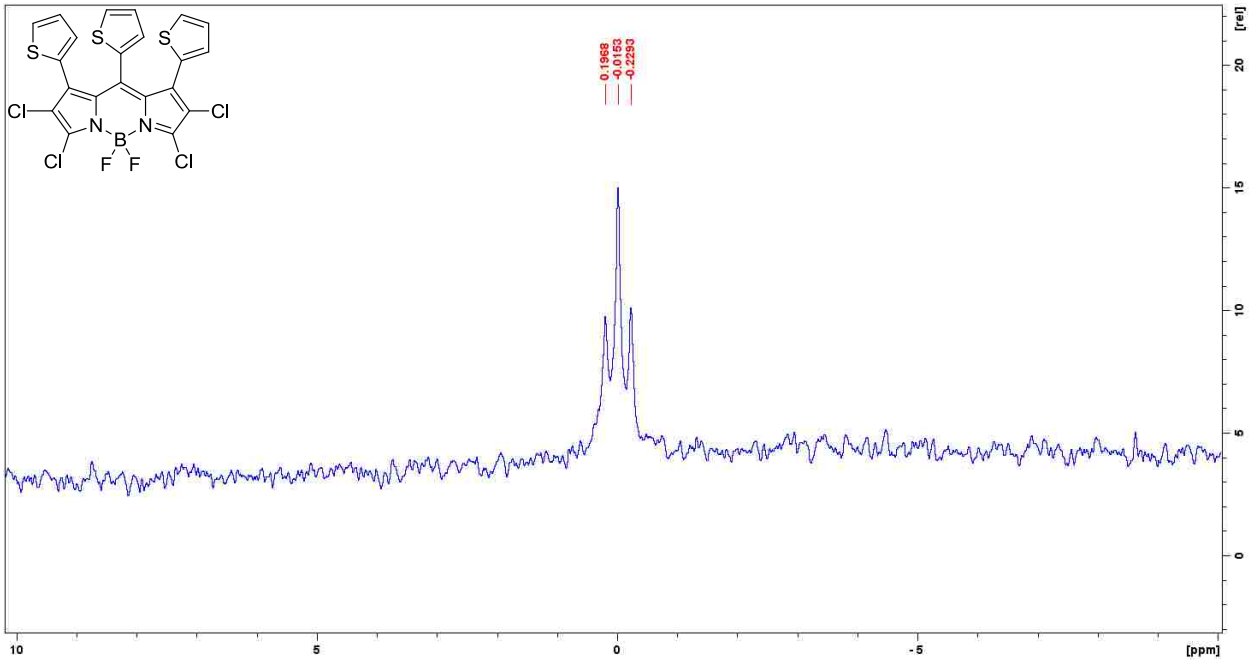

Figure C28: ^{11}B NMR of BODIPY **7b**

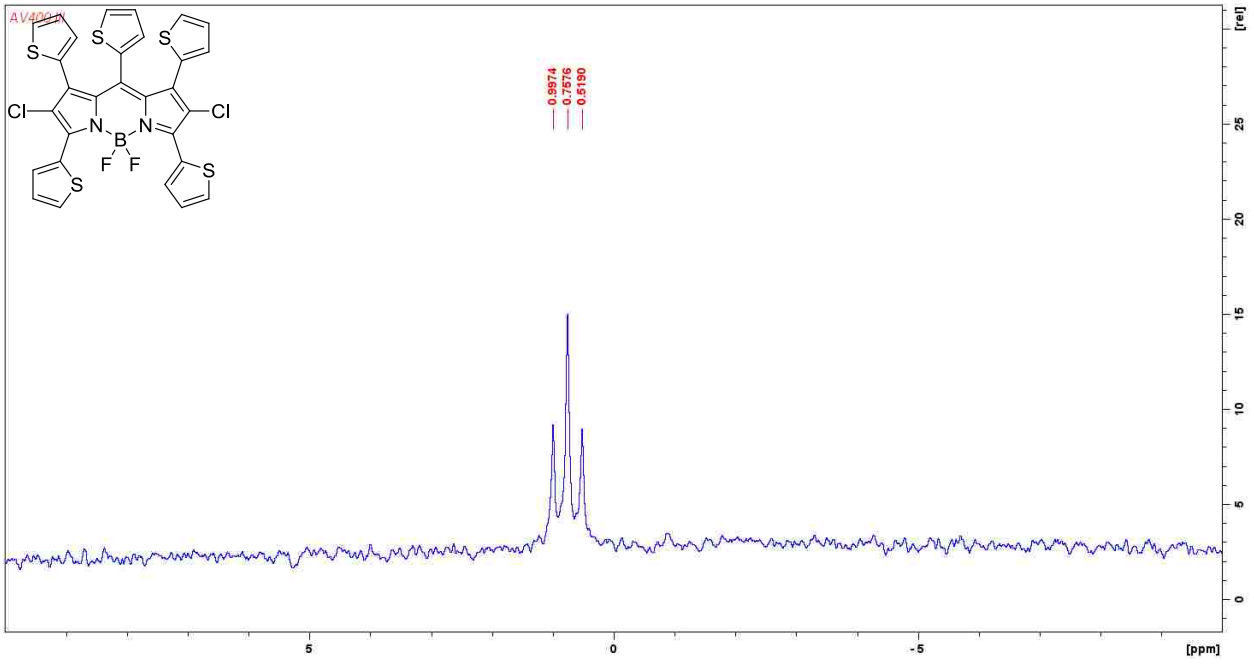

Figure C29: ^{11}B NMR of BODIPY **7b**

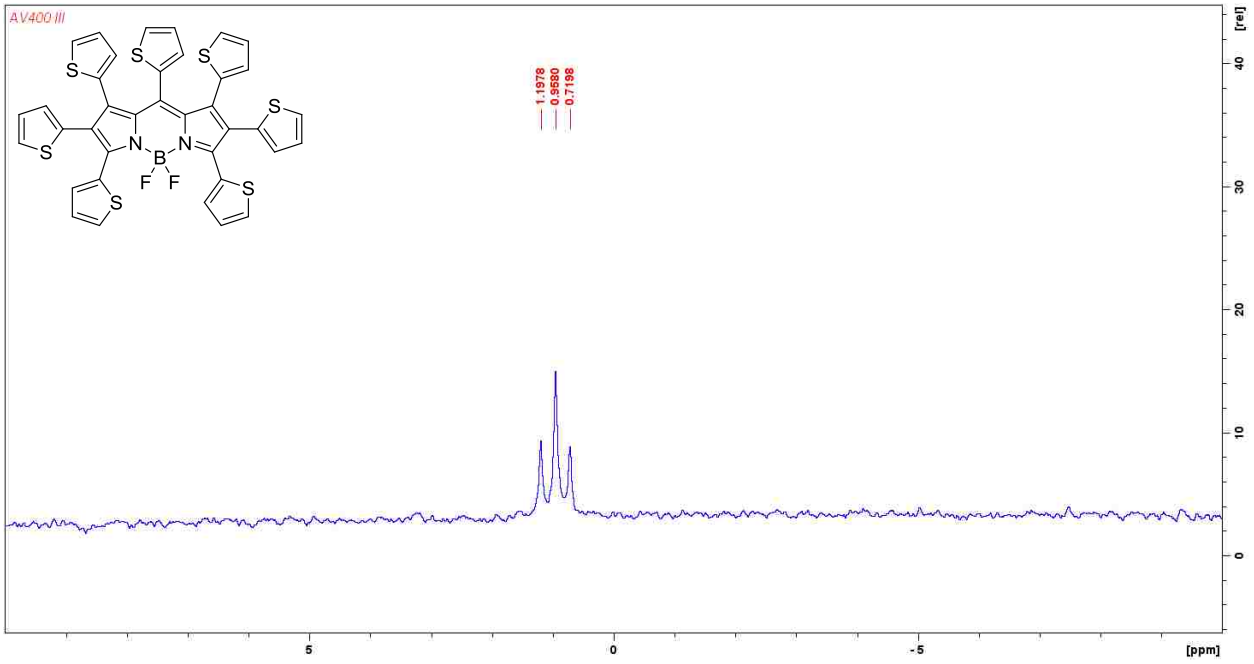

Figure C30: ^{11}B NMR of BODIPY **11**

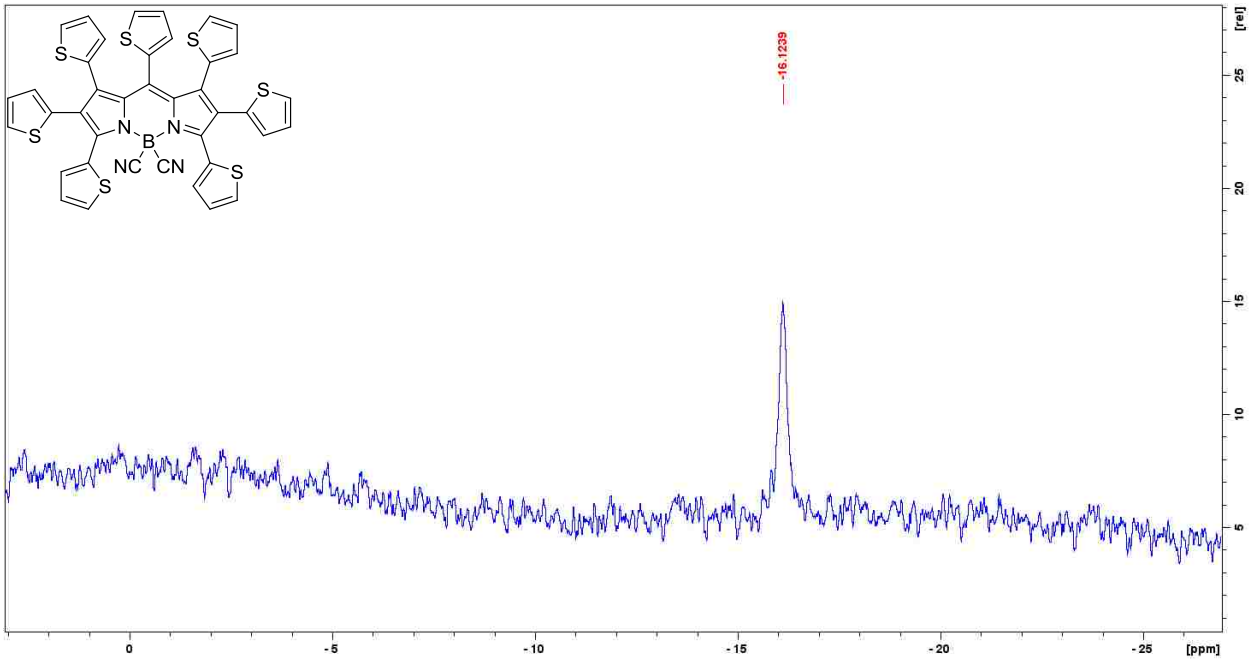

APPENDIX D: CHARACTERIZATION DATA FOR COMPOUNDS IN CHAPTER 4

Figure D1: ^{1}H NMR of compound **10a**

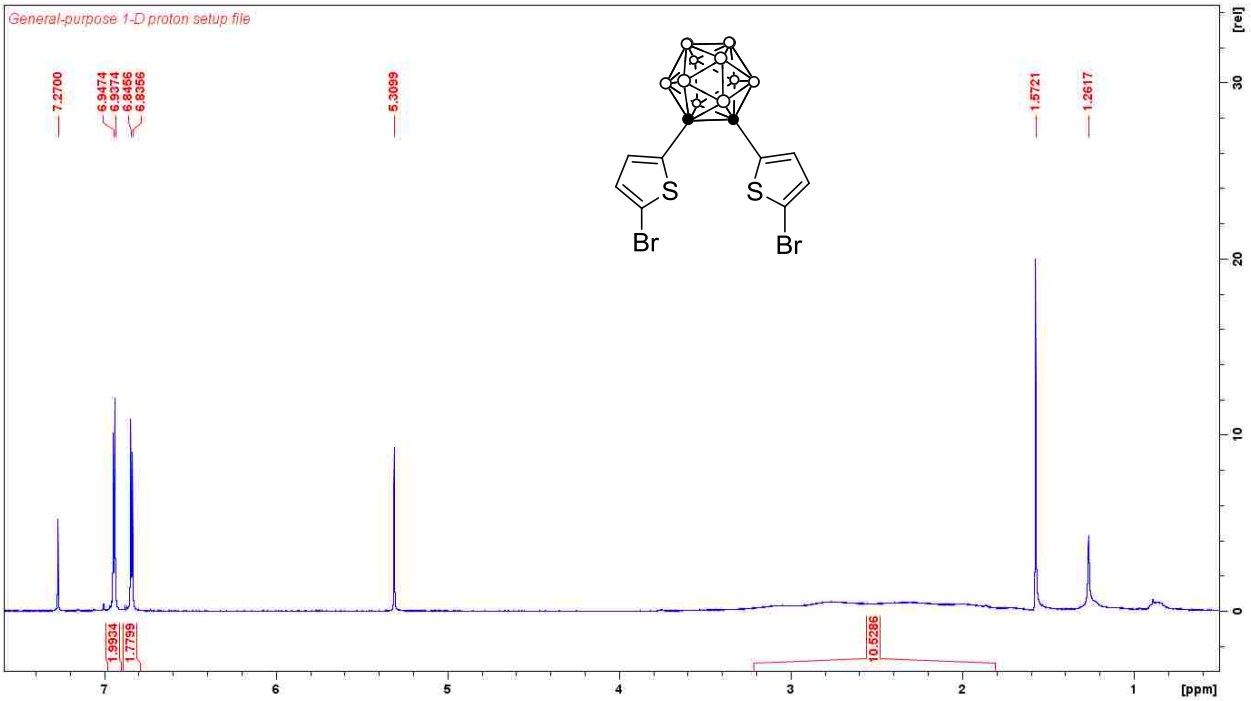

Figure D2: ^{13}C NMR of compound **10a**

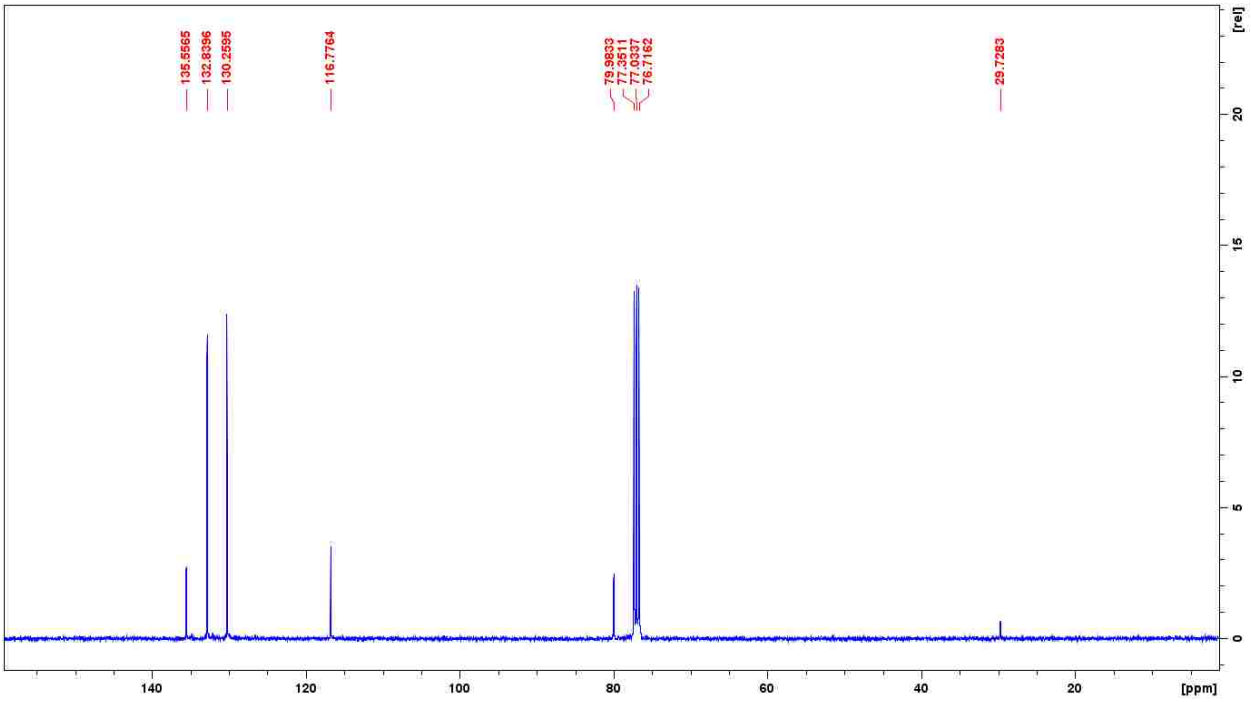

Figure D3: ^{1}H NMR of compound **10b**

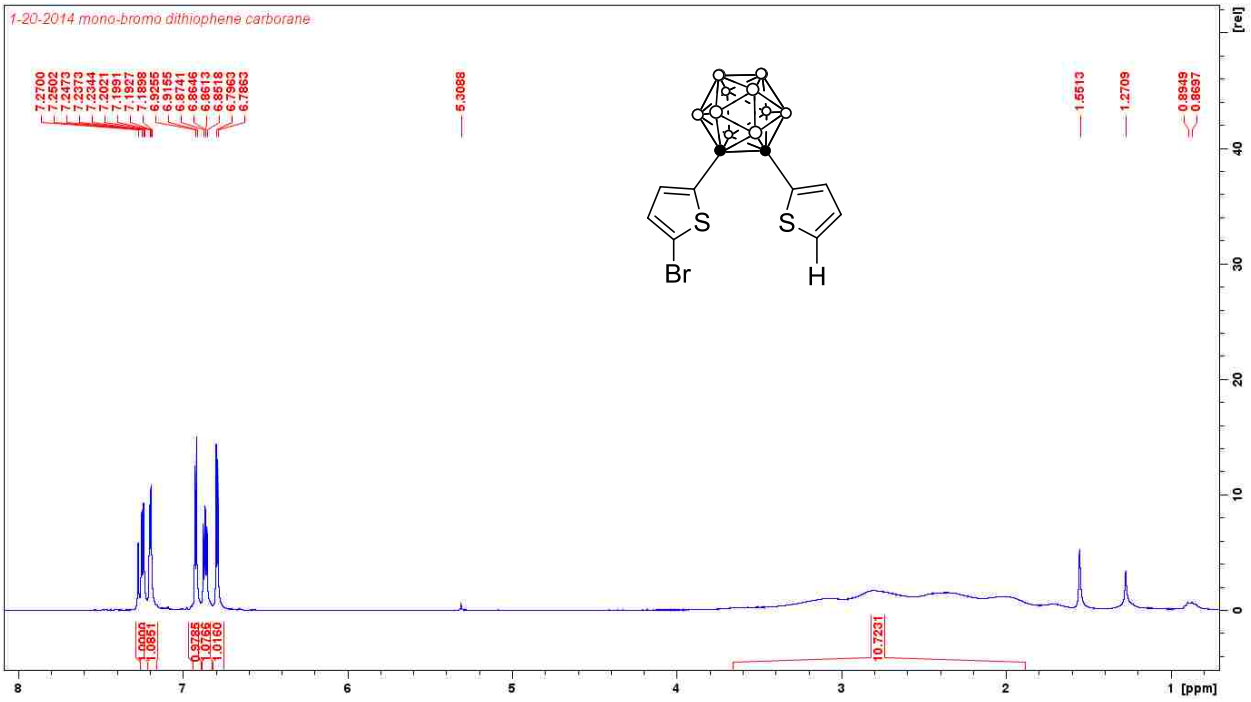

Figure D4: ^{13}C NMR of compound **10b**

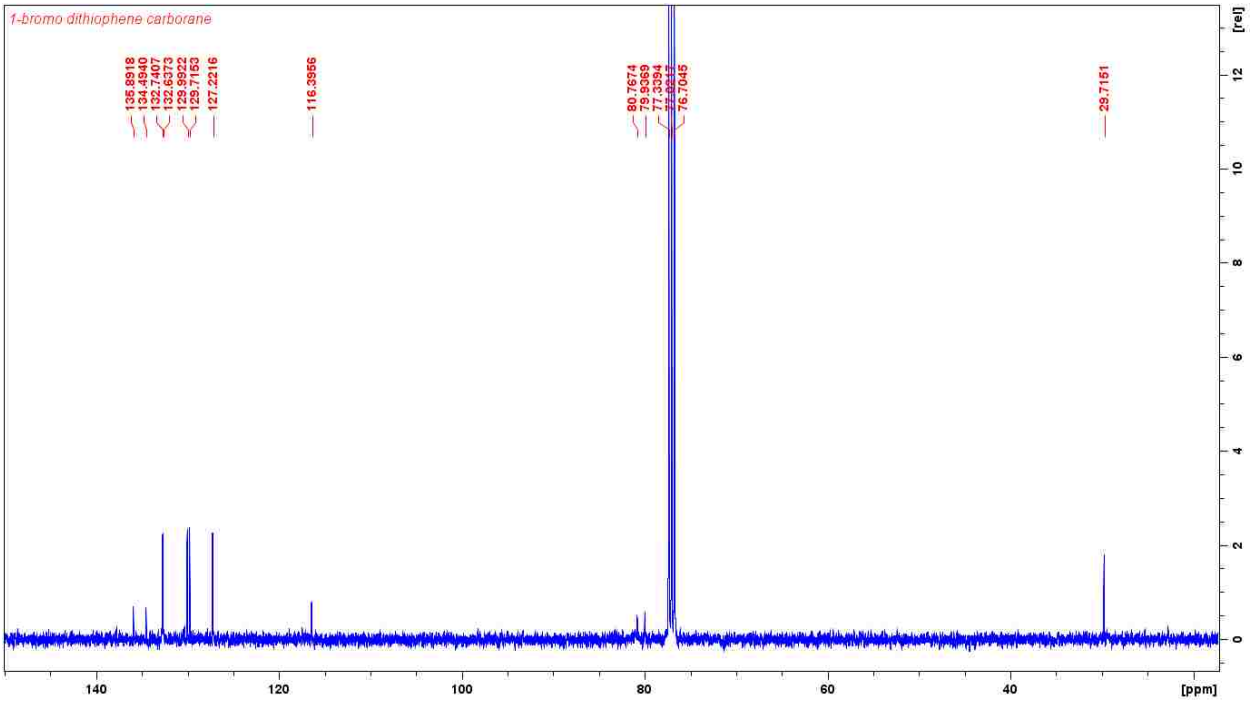

Figure D5: ^{1}H NMR of compound **11**

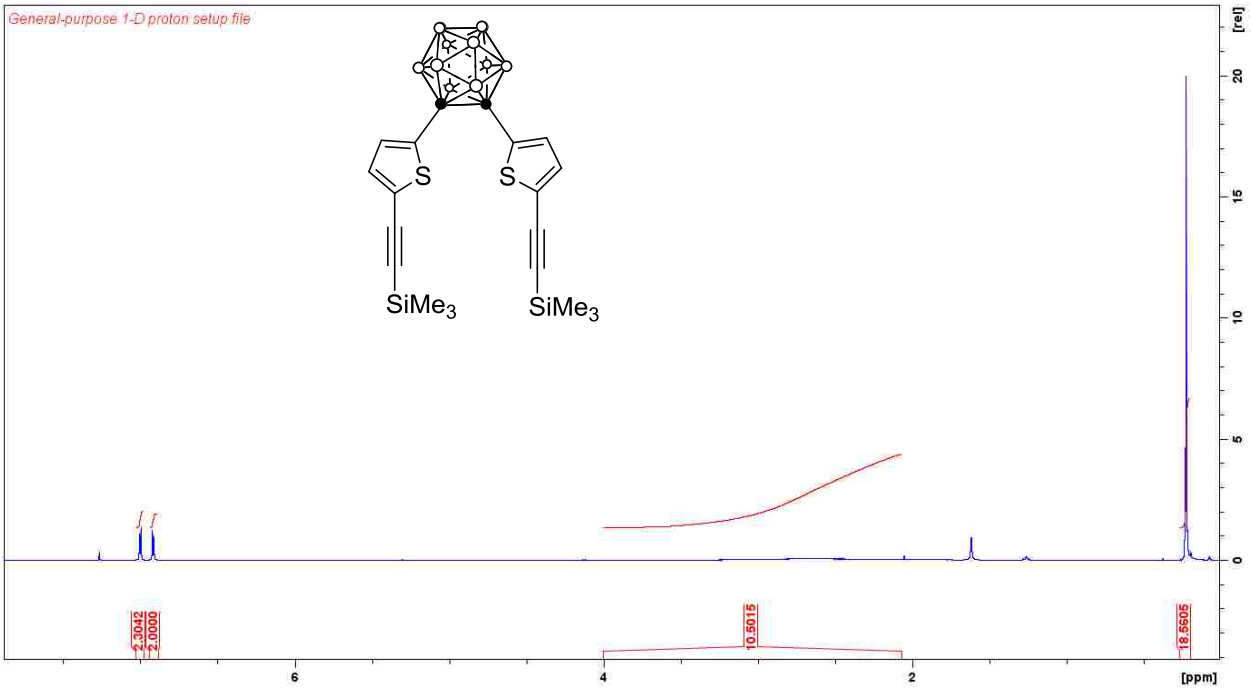

Figure D6: ^{13}C NMR of compound **11**

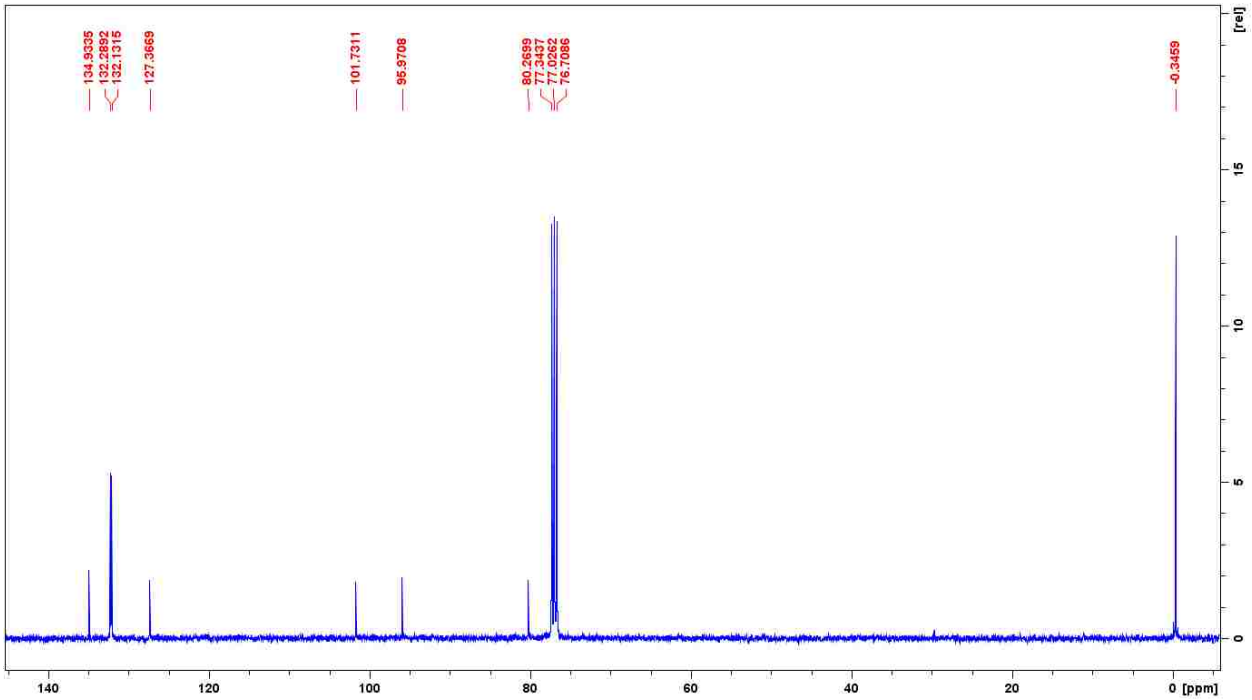

Figure D7: ^{1}H NMR of compound **12a**

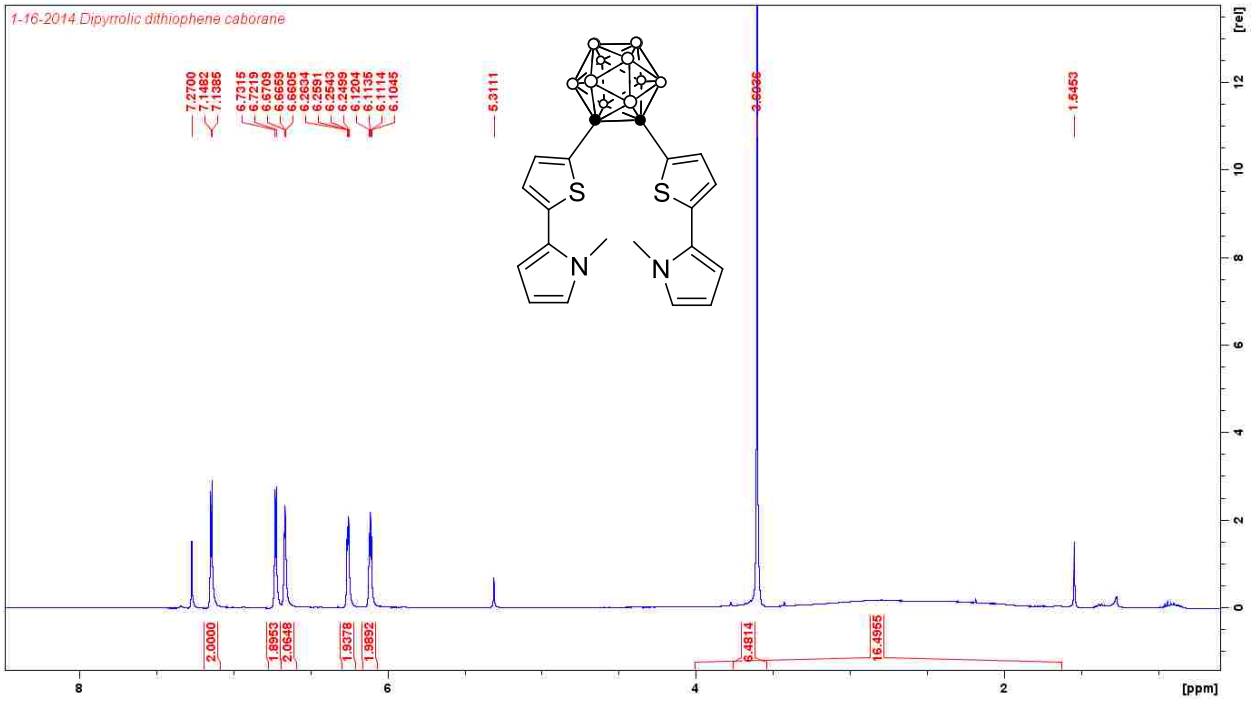

Figure D8: ^{1}H NMR of compound **12a**

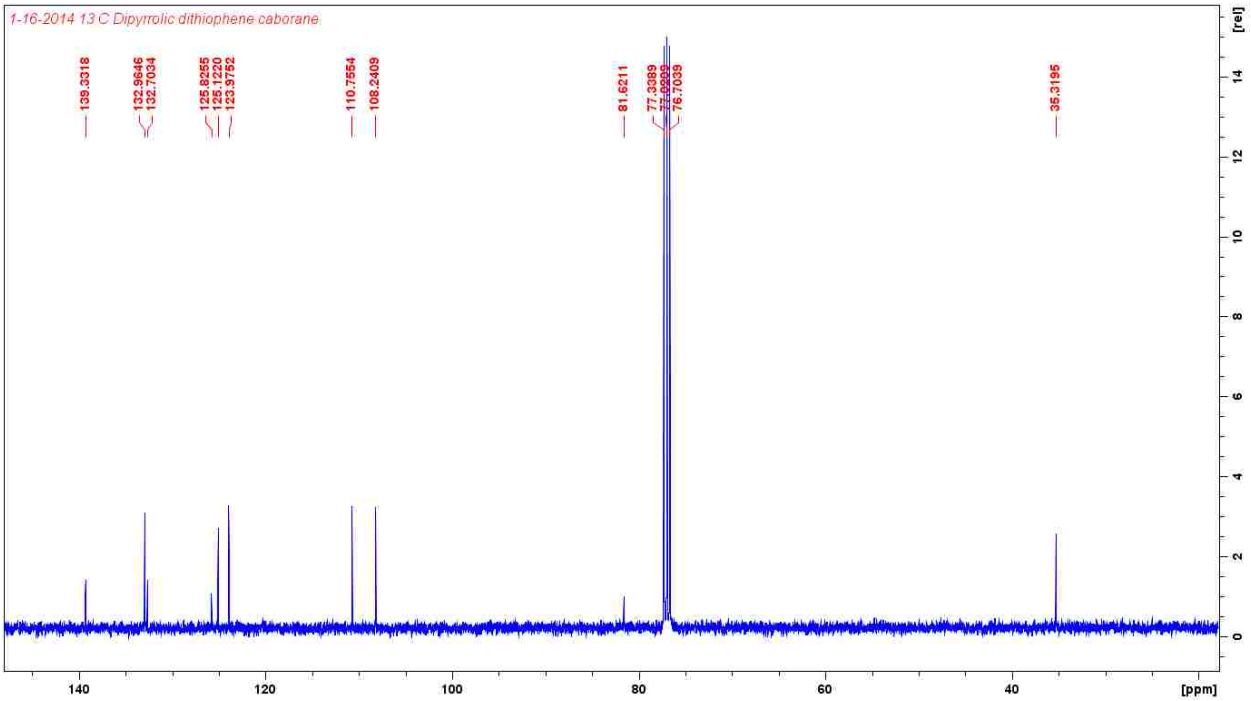

Figure D9: ^{1}H NMR of compound **12b**

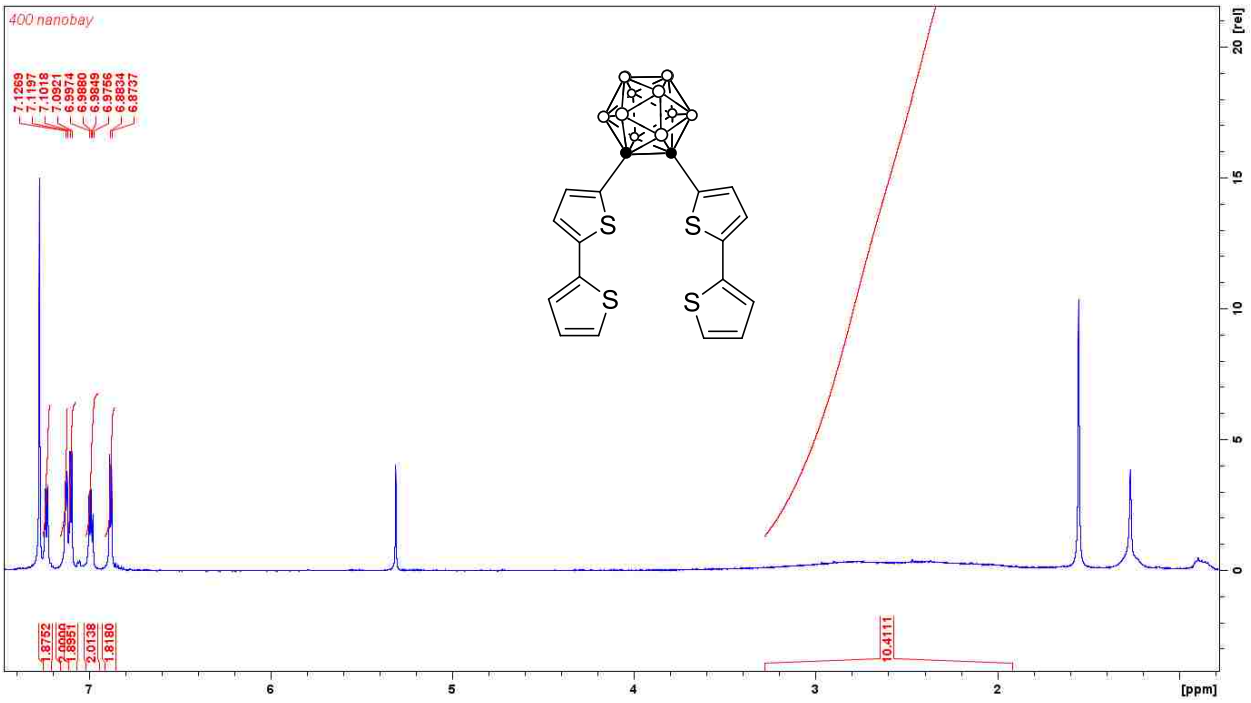

Figure D10: ^{1}H NMR of compound **12b**

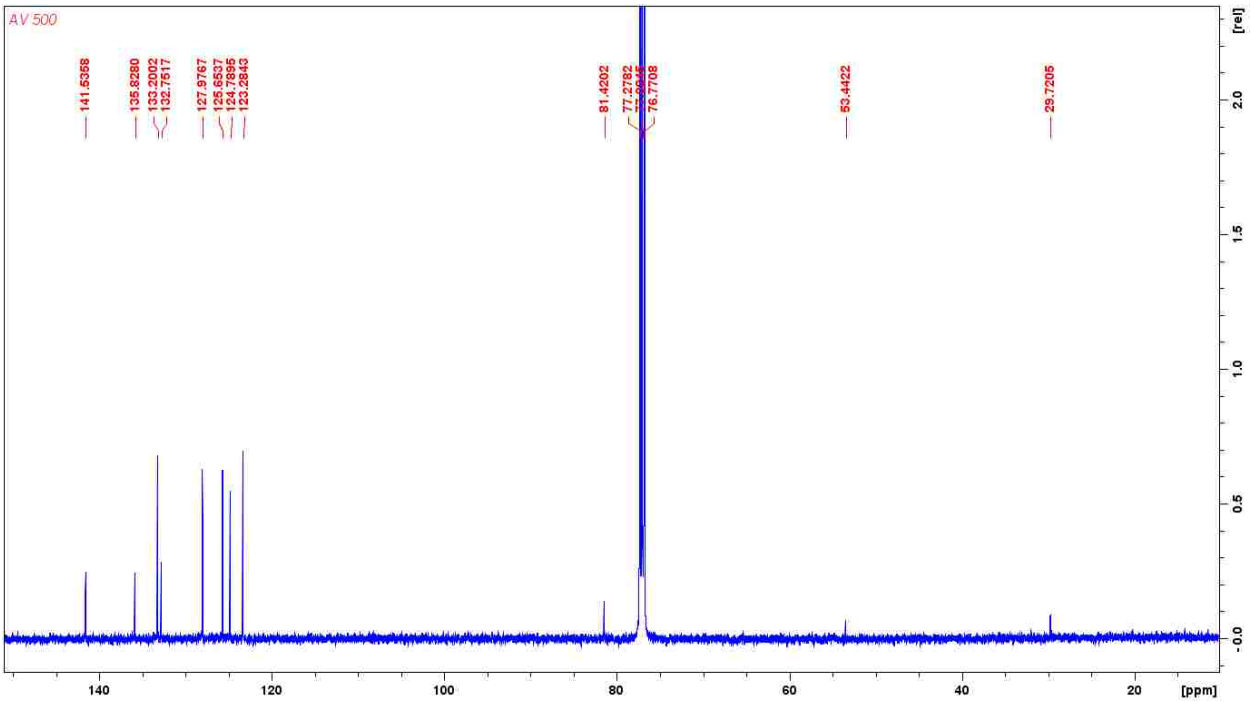

Figure D11: ^{1}H NMR of compound **13a**

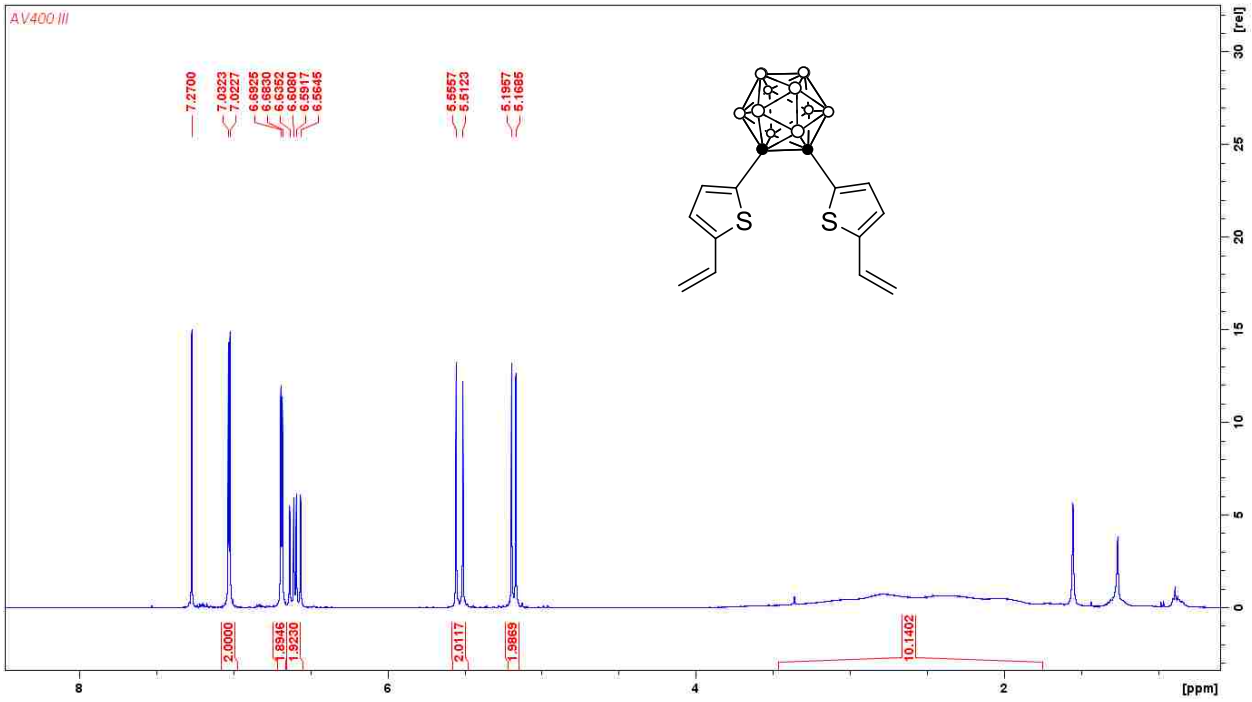

Figure D12: ^{13}C NMR of compound **13a**

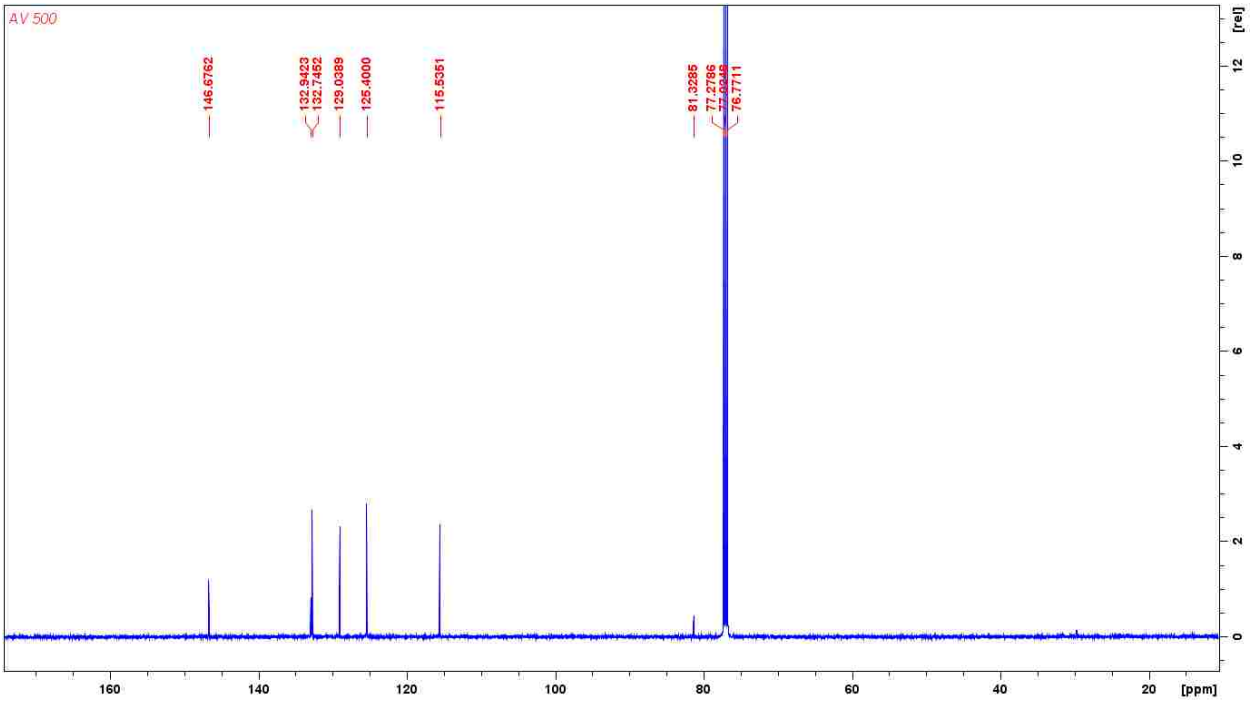

Figure D13: ^{1}H NMR of compound **13b**

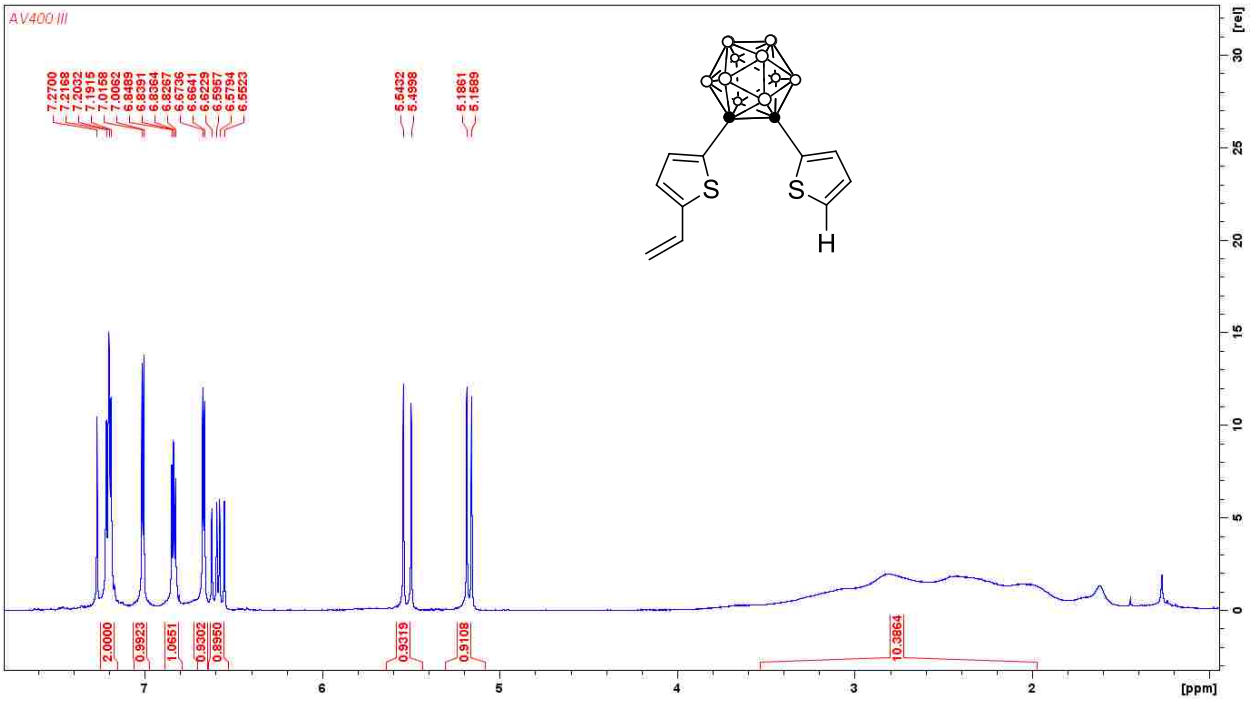

Figure D14: ^{13}C NMR of compound **13b**

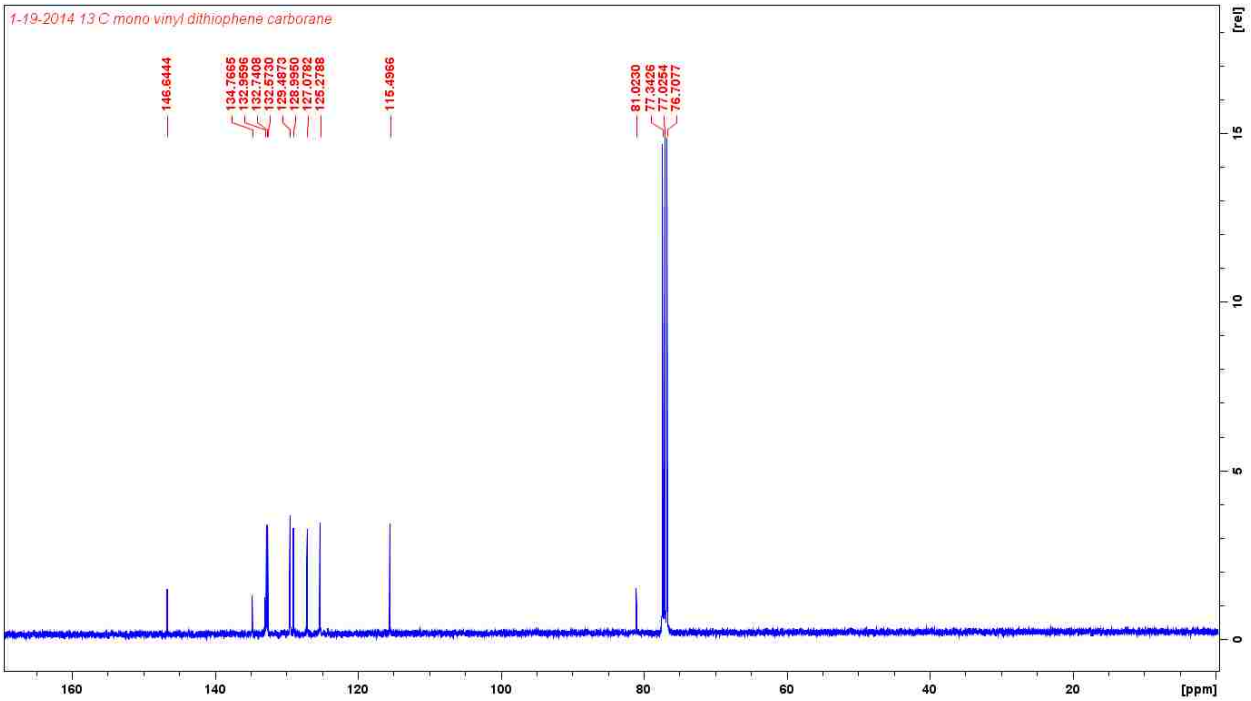

2. Copy of MS spectra

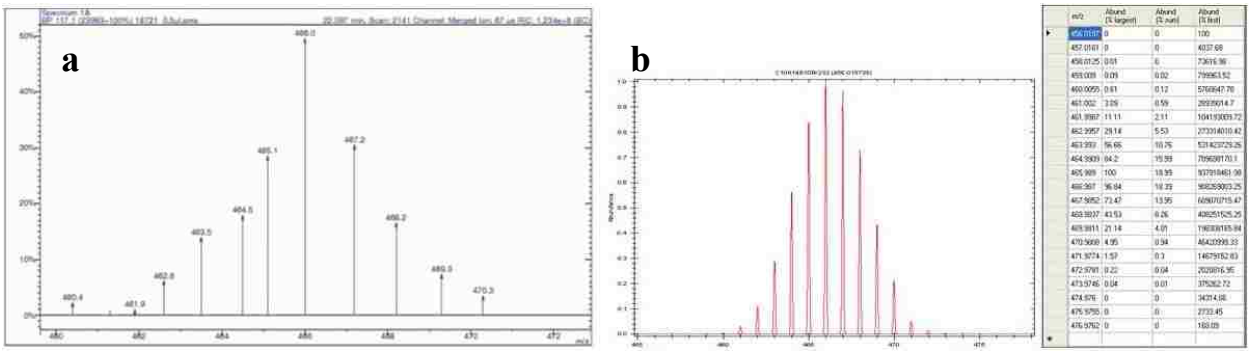

Figure D15: (a) GC-MS copy of Compound **10a;** (b) Predicted mass spectra of Compound of **10a**.

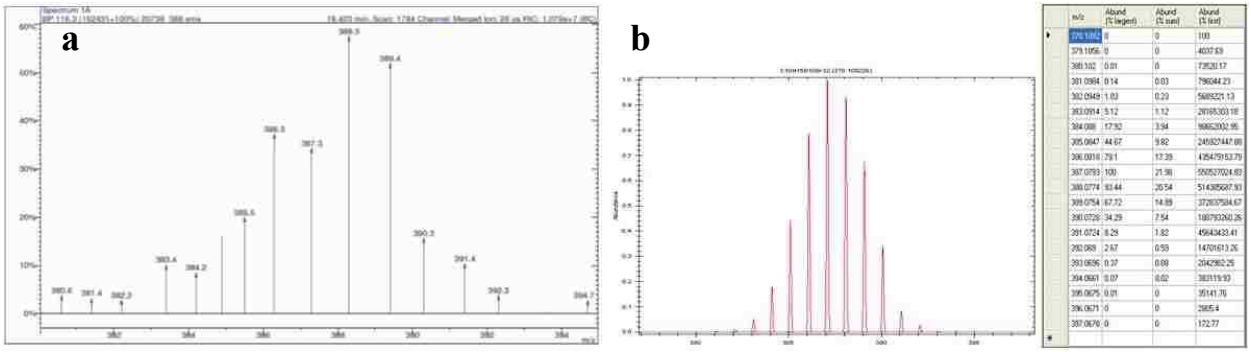

Figure D16: (a) GC-MS copy of Compound **10b;** (b) Predicted mass spectra of Compound of **10b**.

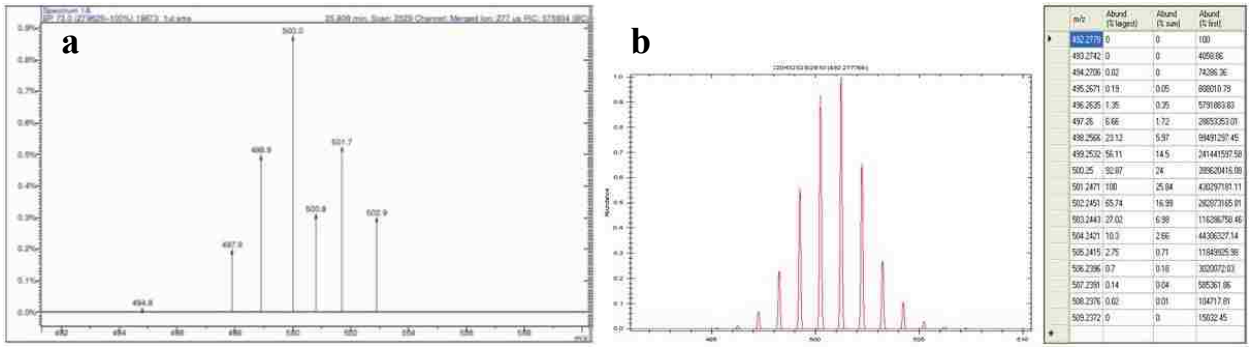

Figure D17: (a) GC-MS copy of Compound **11;** (b) Predicted mass spectra of Compound of **11**.

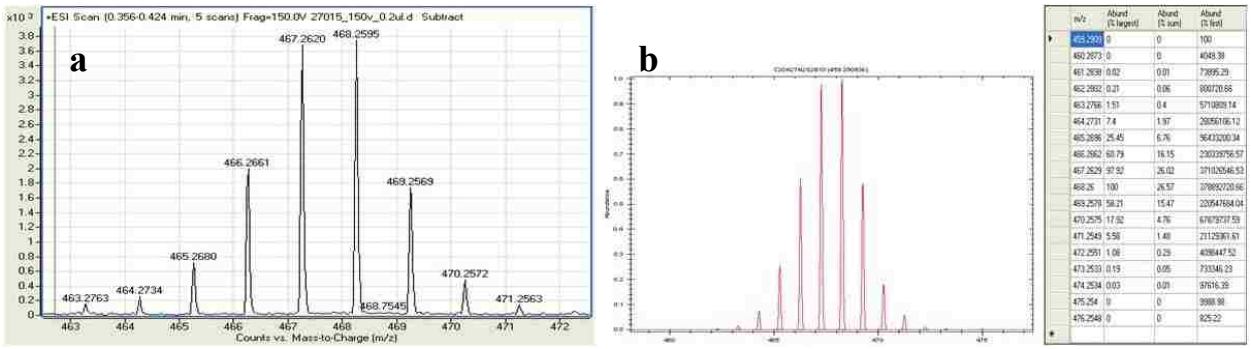

Figure D18: (a) MS(ESI-TOF) copy of Compound **12a;** (b) Predicted mass spectra of Compound of **12a**.

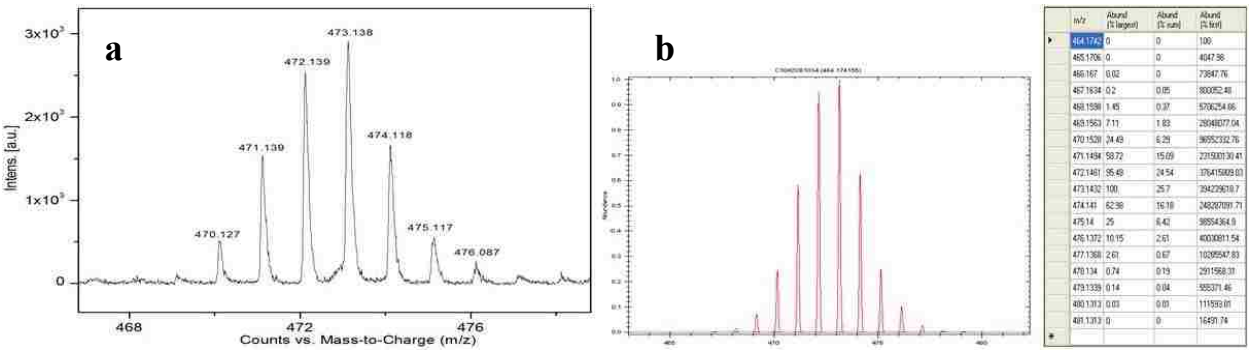

Figure D19: (a) MS(MALDI-TOF) copy of Compound **12b;** (b) Predicted mass spectra of Compound of **12b**.

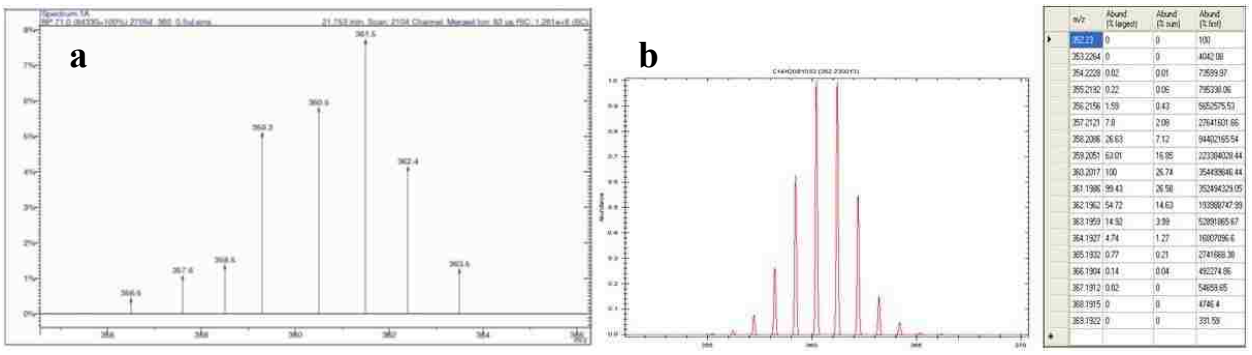

Figure D20: (a) GC-MS copy of Compound **13a;** (b) Predicted mass spectra of Compound of **13a**.

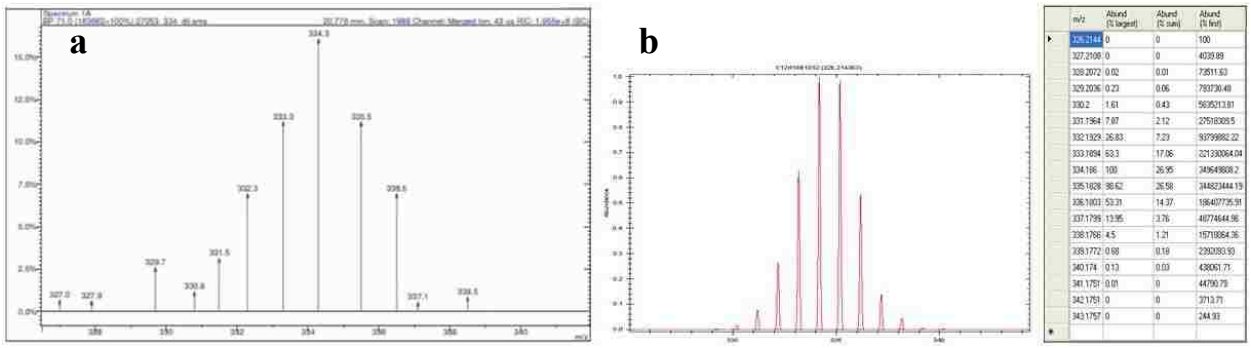

Figure D21: (a) GC-MS copy of Compound **13b;** (b) Predicted mass spectra of Compound of **13b**.

APPENDIX E: LETTERSS OF PERMISSION

ROYAL SOCIETY OF CHEMISTRY LICENSE TERMS AND CONDITIONS

Sep 27, 2016

This Agreement between Ning Zhao ("You") and Royal Society of Chemistry ("Royal Society of Chemistry") consists of your license details and the terms and conditions provided by Royal Society of Chemistry and Copyright Clearance Center.

License Number	3957230879584
License date	Sep 27, 2016
Licensed Content Publisher	Royal Society of Chemistry
Licensed Content Publication	Chemical Society Reviews
Licensed Content Title	Structural modification strategies for the rational design of red/NIR region BODIPYs
Licensed Content Author	Hua Lu,John Mack,Yongchao Yang,Zhen Shen
Licensed Content Date	Apr 15, 2014
Licensed Content Volume Number	43
Licensed Content Issue Number	13
Type of Use	Thesis/Dissertation
Requestor type	academic/educational
Portion	figures/tables/images
Number of figures/tables/images	2
Format	print and electronic
Distribution quantity	5
Will you be translating?	no
Order reference number	19
Title of the thesis/dissertation	Synthesis and Characterization of Polyhalogenated Boron Dipyrromethenes and Carboranylbisthiophene Oligomers
Expected completion date	Dec 2016
Estimated size	250
Requestor Location	Ning Zhao 218 Chemistry and Materials Building Louisiana State University BATON ROUGE, LA 70803 United States Attn: Ning Zhao
Billing Type	Invoice
Billing Address	Ning Zhao 218 Chemistry and Materials Building Louisiana State University BATON ROUGE, LA 70803 United States Attn: Ning Zhao
Total	0.00 USD
Terms and Conditions	

JOHN WILEY AND SONS LICENSE TERMS AND CONDITIONS

Sep 27, 2016

This Agreement between Ning Zhao ("You") and John Wiley and Sons ("John Wiley and Sons") consists of your license details and the terms and conditions provided by John Wiley and Sons and Copyright Clearance Center.

License Number	3957230909916
License date	Sep 27, 2016
Licensed Content Publisher	John Wiley and Sons
Licensed Content Publication	Chemistry - A European Journal
Licensed Content Title	Synthesis of 3,8-Dichloro-6-ethyl-1,2,5,7-tetramethyl–BODIPY from an Asymmetric Dipyrroketone and Reactivity Studies at the 3,5,8-Positions
Licensed Content Author	Ning Zhao,M. Graça H. Vicente,Frank R. Fronczek,Kevin M. Smith
Licensed Content Date	Mar 11, 2015
Licensed Content Pages	12
Type of Use	Dissertation/Thesis
Requestor type	Author of this Wiley article
Format	Print and electronic
Portion	Full article
Will you be translating?	No
Title of your thesis / dissertation	Synthesis and Characterization of Polyhalogenated Boron Dipyrromethenes and Carboranylbisthiophene Oligomers
Expected completion date	Dec 2016
Expected size (number of pages)	250
Requestor Location	Ning Zhao 218 Chemistry and Materials Building Louisiana State University BATON ROUGE, LA 70803 United States Attn: Ning Zhao
Publisher Tax ID	EU826007151
Billing Type	Invoice
Billing Address	Ning Zhao 218 Chemistry and Materials Building Louisiana State University BATON ROUGE, LA 70803 United States Attn: Ning Zhao
Total	**0.00 USD**

Title: Stepwise Polychlorination of 8-Chloro-BODIPY and Regioselective Functionalization of 2,3,5,6,8-Pentachloro-BODIPY

Author: Ning Zhao, Sunting Xuan, Frank R. Fronczek, et al

Publication: The Journal of Organic Chemistry

Publisher: American Chemical Society

Date: Aug 1, 2015

PERMISSION/LICENSE IS GRANTED FOR YOUR ORDER AT NO CHARGE

This type of permission/license, instead of the standard Terms & Conditions, is sent to you because no fee is being charged for your order. Please note the following:

- Permission is granted for your request in both print and electronic formats, and translations.
- If figures and/or tables were requested, they may be adapted or used in part.
- Please print this page for your records and send a copy of it to your publisher/graduate school.
- Appropriate credit for the requested material should be given as follows: "Reprinted (adapted) with permission from (COMPLETE REFERENCE CITATION). Copyright (YEAR) American Chemical Society." Insert appropriate information in place of the capitalized words.
- One-time permission is granted only for the use specified in your request. No additional uses are granted (such as derivative works or other editions). For any other uses, please submit a new request.

BACK CLOSE WINDOW

Gmail Ning Zhao <zhaoning626@gmail.com>

Reuse the paper for the dissertation

CONTRACTS-COPYRIGHT (shared) <Contracts-Copyright@rsc.org> Wed, Sep 28, 2016 at 9:02 AM
To: Ning Zhao <zhaoning626@gmail.com>

The Royal Society of Chemistry (RSC) hereby grants permission for the use of your paper(s) specified below in the printed and microfilm version of your thesis. You may also make available the PDF version of your paper(s) that the RSC sent to the corresponding author(s) of your paper(s) upon publication of the paper(s) in the following ways: in your thesis via any website that your university may have for the deposition of theses, via your university's Intranet or via your own personal website. We are however unable to grant you permission to include the PDF version of the paper(s) on its own in your institutional repository. The Royal Society of Chemistry is a signatory to the STM Guidelines on Permissions (available on request).

Please note that if the material specified below or any part of it appears with credit or acknowledgement to a third party then you must also secure permission from that third party before reproducing that material.

Please ensure that the thesis states the following:

Reproduced by permission of The Royal Society of Chemistry

and include a link to the paper on the Royal Society of Chemistry's website.

Please ensure that your co-authors are aware that you are including the paper in your thesis.

Regards,

Antonella Tesoro

Customer Sales Support

Royal Society of Chemistry

Thomas Graham House,

Science Park, Milton Road,

Cambridge CB4 0WF

Tel. +44 (0) 1223 432 675

tesoroa@rsc.org

Main Reception Tel. +44 (0) 1223 42 0066

VITA

Ning Zhao was born in Yixing, Jiangsu, China, to Junke Zhao (赵君可) and Xihua Hong (洪西华). He received his bachelor's degree in chemistry from Lanzhou University in 2010, In 2011, he was accepted to Graduate School Doctoral program at Louisiana State University in the chemistry department, where he joined Dr. M. Graça. H. Vicente and Dr. Kevin M. Smith's research group. Ning is currently a candidate for the Doctor of Philosophy in organic chemistry, which will be awarded to him at the December 2016 Commencement, Louisiana State University, Baton Rouge, LA.